Departamento de Tecnología y Química Farmacéuticas
Facultad de Farmacia y Nutrición

Universidad de Navarra

Therapeutic potential of zein-based nanoparticles

TESIS DOCTORAL

Cristian Reboredo Fuentes

Pamplona, 2022

Universidad de Navarra

Facultad de Farmacia y Nutrición

Departamento de Tecnología y Química Farmacéuticas

Memoria presentada por D. Cristian Reboredo Fuentes para aspirar al grado de Doctor por la Universidad de Navarra

Fdo. Cristian Reboredo Fuentes

Trabajo realizado en el Departamento de Tecnología y Química Farmacéuticas de la Facultad de Farmacia y Nutrición de la Universidad de Navarra y presentado por Cristian Reboredo Fuentes.

Juan M. Irache

Vº Bº Director de tesis

Juan Manuel Irache Garreta

Vº Bº Codirector de tesis

Carlos Javier González Navarro

“No hay viento favorable para el que no sabe adónde va”

Séneca

A mis padres, mis hermanos, y los más allegados

"Lo que la mente del hombre puede concebir y creer, es lo que la mente puede crear"

Napoleón Hill

Agradecimientos

En primer lugar, me gustaría agradecer a la Universidad de Navarra y al departamento de Tecnología y Química Farmacéuticas por brindarme la posibilidad de realizar este proyecto de tesis. A la Asociación de Amigos de la Universidad de Navarra y a la Obra Social "La Caixa" por la aportación económica recibida durante todo este tiempo.

En segundo lugar, me gustaría agradecer a mis directores de tesis, Juanma y Carlos, por haberme guiado, enseñado y curtido, no sólo en el ámbito científico, sino también en el personal. Gracias por dedicar el tantísimo tiempo que conlleva dirigir una tesis doctoral, por esas ocasiones en las que me hicisteis salir de vuestros despachos más contento y motivado de lo que entré, por haber depositado vuestra confianza en mí.

Gracias a los excelentes científicos, y mejores personas, que me he ido encontrando en los distintos departamentos por los que he pasado durante este tiempo, Tecnología y Química Farmacéuticas, Microbiología, Físico-Química, Farmacología, Nutrición, la Plataforma de Imagen del CIMA y el grupo NTDD del i3S de Oporto. Me gustaría agradecer especialmente a Ana Luisa (AKA Mama Luisa) y a Jorge por ser, aparte de unos magníficos compañeros de trabajo, fuente de sabiduría, de tranquilidad, de intercambio de opiniones, apoyo en las buenas y en las malas y, sobre todo, gracias por esa infinita paciencia que demostrasteis conmigo desde esos comienzos en los que mis rectas de calibrado raramente superaban un R^2 de 0.8. No me olvido en absoluto del resto de gente que me alegraba ver cada día al entrar en el departamento: Inés, Cristina, Alba, Esther, María, Edurne, Raquel, María Luisa, Irati, Souhaila, Silvia, Diego, Aymara, Pablo, Javier…

Por supuesto, mi agradecimiento más personal y sentido es a mis padres y mis hermanos. Gracias por vuestro apoyo incondicional, por vuestra enorme fe en mí, por vuestras palabras de aliento en mis momentos decaído. Por luchar por mí a capa y espada, demostrando en ocasiones más confianza en mí de la que yo mismo depositaba. Pero, sobre todo, por los valores que me habéis inculcado desde pequeño y que me han hecho enorgullecerme de quien soy a día de hoy. Valores como el respeto, la humildad, el compañerismo, la dedicación, y el esfuerzo.

A Claudia, por aguantarme con una sonrisa en mis días de perros en los que yo mismo me daba cuenta de cuan insoportable estaba. Por hacerme reír día tras día y enseñarme que la felicidad se puede encontrar en pequeños detalles cotidianos. Por enseñarme que, la vida, así como las relaciones, pueden ser mucho más fáciles de lo que a veces pensamos. Por tu pasión siempre por progresar y mejorar, la cual me has contagiado durante este tiempo juntos.

A todos vosotros y a los que me pueda dejar en el tintero…

¡GRACIAS!

Table of contents

Chapter 1

General introduction

1. Introduction

1.1. Glucose homeostasis

Glucose homeostasis comprises the action of several metabolic pathways to maintain the blood glucose levels within a normal range (4 – 6 mM) (Röder et al., 2016). When glycemia rises above normal ranges, hypoglycemic mechanisms are triggered to reduce the blood glucose levels and avoid the glucotoxicity phenomenon (Gasa et al., 2016; Stiker, 2001). On the other hand, when glycemic values drop, different counterregulatory hormones and pathways are activated to avoid the state of hypoglycemia (Lang and Hussain, 2014).

The principal hormones involved in the glucose homeostasis are the pancreatic hormones insulin and glucagon. These two hormones have antagonist effects: while insulin is an anabolic hormone that reduces glycemia, glucagon is a catabolic hormone that rises blood glucose levels (Hruby, 1998). However, there are other mechanisms involved in the good maintenance of the glycemic values. These mechanisms include extrapancreatic hormones (cortisol, growth hormone, catecholamines, thyroid hormones or angiotensin II, among others) and neural stimulation through the sympathetic and parasympathetic systems (Tirone and Brunicardi, 2001).

1.2. Insulin

From all the factors mentioned, insulin is the most relevant hormone for glucose homeostasis (Suri and Aurora, 2017). Insulin is a peptide hormone composed by 51 amino acids divided in 2 chains linked by two disulfide bridges: the A chain composed by 21 amino acids, and the B chain composed by 30 amino acids, with a total molecular weight of 5.808 Da (Fu et al., 2012; Vakilian et al., 2019). Insulin is synthetized in the β cells of the pancreas, where it will be stored in granules until the moment of utilization. These β cells are clustered within the pancreas in structures called as islets of Langerhans, which are surrounded by fenestrated capillaries. The structure of these capillaries facilitates the sensing of blood nutrients by the β cells and the diffusion of insulin from the secretory cells to the circulation (Fu et al., 2012).

Insulin is released from the β cells mainly in response to an increase in the blood glucose levels. The β cells themselves act as glycemic sensors; when the glycemia rises, glucose enters the β cells through the glucose transporters (GLUTs) and triggers a signaling cascade that induces an increase in the intracellular Ca^{2+} concentration and, in last term, the exocytosis of the insulin vesicles (Henquin et al., 2006; Röder et al., 2016; Wang and Thurmond, 2009). However, although glucose is the main inductor of insulin release, amino acids, fats and other monosaccharides can also induce its release (Deeney et al., 2000; Fu et al., 2012). Only a few number of amino acids have shown the capacity of inducing insulin release (insulinogogues), being the most effective ones leucine, isoleucine, alanine and arginine (Newsholme et al., 2006). The mechanisms by which amino acids induce insulin release are very variable, depending on their nature and physicochemical properties.

In humans, as in other animals, insulin secretion consists of a biphasic process (Vakilian et al., 2019; Wang and Thurmond, 2009), which has a physiological sense since it has demonstrated a greater hypoglycemic effect than a monophasic, continuous administration of insulin (Matthews et al., 1983). This biphasic release of insulin compresses two steps: a rapid, pulsatile, and ATP-independent secretion of insulin granules, followed by a slow, sustained, and ATP-dependent secretion of the insulin-containing vesicles (Henquin et al., 2002; Rorsman et al., 2000). During the first phase, the already-formed granules that are stored inside the β-cells are released, leading to a rapid increase in the insulinemic levels. These granules are known as the "readily releasable pool" (RRP) and are stored close to the cell membrane, at the apical site. During the second phase, the insulin granules that are stored deeper inside the cell are mobilized closer to the cell membrane, refilling the RRP. These granules that are stored deeper in the cell conform the "storage-granule pool" (Henquin et al., 2002; Wang and Thurmond, 2009). A schematic representation of the signaling pathways that trigger insulin release, as well as the main target cells of the hormone, are shown in Figure 1.

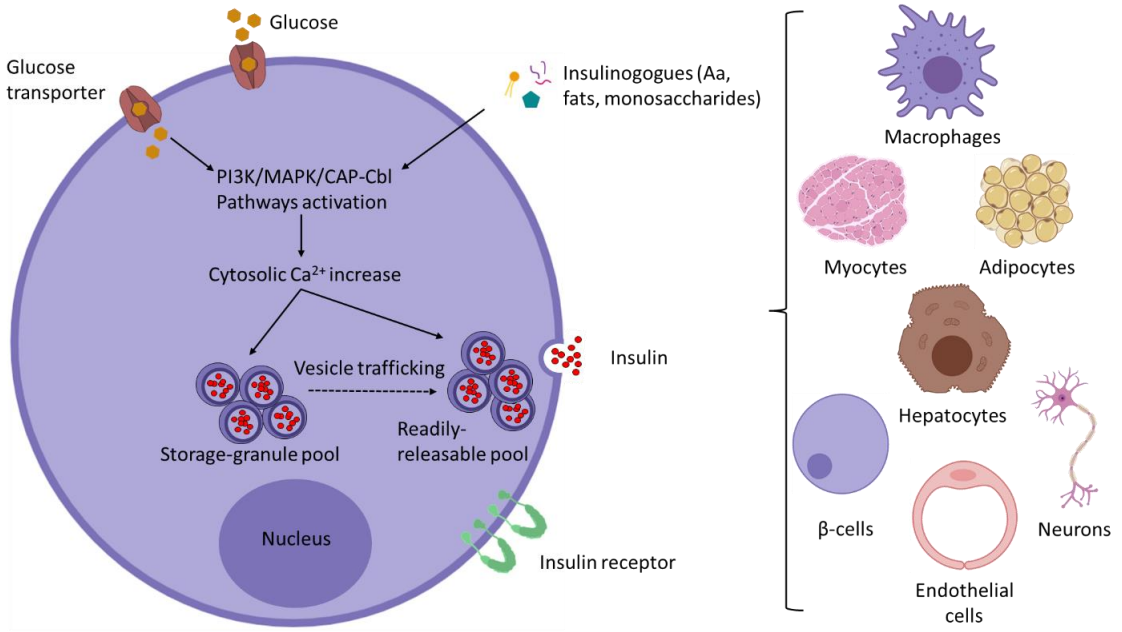

Figure 1. Schematic representation of the signaling pathways involved in the secretion of insulin from a β-cell (left) and the main target cells (right). Figure produced using BioRender's pre-made icons and templates (https://biorender.com)

Although the main function of insulin is the glucose homeostasis, the ways by which this result is achieved involve several tissues and different functions over them. The canonic insulin-sensing tissues are muscle, adipose tissue, and liver.

1.2.1. Insulin in muscle tissue

In muscular tissues, insulin increases the glucose uptake by the myocytes. The signaling pathway triggered by insulin leads to the mobilization of GLUTs to the cell membrane, which allow the influx of glucose from the blood to the cell. In addition, insulin also increases the glycolysis rates of myocytes by upregulating the activity of hexokinase and 6-phosphofructokinase (Dimitriadis et al., 2011). Glycolysis consists on the enzyme-catalyzed degradation of glucose molecules in order to generate useful energy for the cell (ATP) (Pelicano et al., 2006). When the glycogen storage in the muscle cells is fulfilled, lactate is generated by the glycolysis metabolic pathways. Then, lactate molecules are used as intermediators and transported to the liver through the bloodstream. Once in the liver, lactate is transformed back to glucose (gluconeogenesis) and stored as glycogen in the major glycogen-storing organ (Murray and Rosenbloom, 2018). Another function of this anabolic hormone is inducing the synthesis and inhibiting the degradation of proteins in the muscle (Dimitriadis et al., 2011). This is the main reason why diabetic patients show a decrease in the whole-body protein levels (Proud, 2006). Although some mechanisms are still not well understood, insulin has shown the capability of increasing the influx of amino acids from the blood to the myocytes, upregulating the protein biosynthesis and downregulating the protein degradation (Fujita et al., 2006; Proud, 2006).

1.2.2. Insulin in adipose tissue

Adipose tissue is one of the most insulin-sensitive tissues. In preadipocytes, insulin signaling induces the differentiation to adipocytes (Jung and Choi, 2014; Klemm et al., 2001). Meanwhile, in adipocytes, insulin induces an increase in the glucose and fatty acids uptake from blood, which will be used for glycogen synthesis and lipogenesis (Dimitriadis et al., 2011; Jung and Choi, 2014). Glucose can be stored as glycogen, but it can also be transformed to glycerol through the glycolytic pathway (Rotondo et al., 2017) and, then, be used as substrate for the synthesis of the acyl-glycerols that conform the lipid droplets of the adipocytes (Rinia et al., 2008). Moreover, as insulin upregulates lipogenesis, it also downregulates lipolysis (Jung and Choi, 2014).

1.2.3. Insulin in liver

In the liver, insulin binds to the membrane receptors of the hepatocytes and triggers, as in other tissues, the PI3K (phosphatidyl inositol 3-kinase) and MAPK (mitogen-activated protein kinase) signaling pathways that lead to a wide variety of responses (Rahman et al., 2021). First, as in every other insulin-sensitive tissue, it increases the uptake of glucose from blood. Then, on the one hand, it upregulates the glycolysis and the synthesis of proteins, glycogen, and lipids (cholesterol, triglycerides and VLDL). On the other hand, it downregulates the ketogenesis and gluconeogenesis (Cheng et al., 2010; Dimitriadis et al., 2011; Titchenell et al., 2017).

1.2.4. Other insulin-sensing tissues and cells

For decades, it has been thought that the only insulin-sensing tissues were the adipose tissue, muscle, and liver. However, nowadays it is known that insulin receptors are found in other tissues and cellular types. Some of these recently known insulin-sensitive cells are the brain neurons, myeloid cells, endothelial cells from both blood and lymphatic vessels, cardiomyocytes, and the β-cells themselves (Jiang et al., 2019; Rask-Madsen and Kahn, 2012). Therefore, besides the endocrine function of insulin, it also performs auto and paracrine functions.

New research during the last decades has demonstrated that the central nervous system (CNS) is an insulin-sensitive tissue. Both insulin and insulin receptors are found in the neurons and in the glia (Blázquez et al., 2014). Moreover, it has been demonstrated that the insulin present in the brain can be synthesized *in situ* or obtained from circulating insulin molecules (Nakabeppu, 2019; Pomytkin et al., 2018). On the one hand, insulin can reach the CNS by crossing the blood-brain barrier (BBB) through specific transporters (Gabbouj et al., 2019). On the other hand, it has been demonstrated through indirect ways (mRNA detection, C-peptide detection, cell cultures) that insulin can also be produced in the brain itself (Blázquez et al., 2014; Ghasemi et al., 2013; Kyriaki, 2003; Nakabeppu, 2019). However, CNS-produced insulin seems not to be synthesized all over the brain, but in located regions (e.g. hippocampus, olfactory bulb, piriform cortex, and Purkinje cells) (Kyriaki, 2003). The insulin receptors found in the CNS differ from those found in peripheral tissues in molecular size, glycosylation degree, antigenicity, and regulation mechanisms (Blázquez et al., 2014). The main functions that are regulated by insulin in the brain are the food intake, body weight, reproduction, and memory. Moreover, as in other tissues, insulin regulates cell proliferation and differentiation but here it also regulates the neurite growth (Lázár et al., 2018). Nevertheless, insulin also exerts a neuroprotective effect by reducing the apoptosis, the beta amyloid-induced cell death, oxidative stress, and ischemic lesions (Blázquez et al., 2014). All these functions seem to be the reason why insulin resistance is closely related to Alzheimer's disease (Su et al., 2017).

Endothelial cells, from both the blood and lymphatic vessels, express insulin receptors (Jaldin-Fincati et al., 2018). In these tissues, insulin has demonstrated the capability of increasing the angiogenesis by inducing cell proliferation and reducing apoptosis. One of the metabolic pathways triggered by insulin in endothelial cells leads to the overexpression of endothelial nitric oxide synthase (eNOS), what leads to an increase in the production of nitric oxide (Vicent et al., 2003). The nitric oxide (NO) production seems to be one of the main mechanisms through which insulin promotes angiogenesis while inhibits cell apoptosis (Dimmeler and Zeiher, 1999). Moreover, NO is a well-known vasodilator (Ignarro, 1989), so insulin signaling also induces this effect over the vessels (Zeng et al., 2000). The vasodilation induced by insulin-eNOS leads to an increased blood flow and, thus, to an increased glucose uptake from peripheral tissues. Finally, NO has also demonstrated the capability of directly increase the glucose uptake by muscle and adipose tissues (Vicent et al., 2003)

The heart is another insulin-sensitive tissue. It is composed mainly by 3 cellular types: cardiomyocytes, endothelial cells, and fibroblasts, with proportions that vary between animal species. However, there is a consensus claiming that the total amount of cardiomyocytes corresponds to the 30-40% of the total cells of the heart (Pinto et al., 2016; Zhou and Pu, 2016). Nevertheless, in spite of comprising only the 30-40% of the total number of cells, the volume fraction of cardiomyocytes in the hearth reaches the 70-80% (Zhou and Pu, 2016). In this tissue, insulin increases the glucose uptake by the myocardium, leading to a significantly better myocardial function (Klein and Visser, 2010). This improvement in the myocardial function relies on an augmented contractibility/relaxation of the cardiomyocytes, increased biosynthesis of ribosomes and proteins, reduced apoptosis, and greater perfusion of the myocardium (Iliadis et al., 2011).

1.3. Incretins

From the extrapancreatic hormones that regulate glucose homeostasis, incretins are one of the most important ones due to their effect over the synthesis and release of insulin. The term incretin derives from "intestinal secretion of insulin" (Yildirim Simsir et al., 2018), and their influence over insulin release is so high that more than 50% of the total insulin released after food ingestions seems to be caused by the action of Glucagon-like peptide-1 (GLP-1) and glucose-dependent insulinotropic polypeptide (GIP), the two incretin hormones present in humans. (Bugliani et al., 2018; Röhrborn et al., 2015; Vilsbøll and Holst, 2004; Wu et al., 2015). Incretins are rapidly metabolized by an enzyme called dipeptidyl peptidase 4 (DPP-4), also known as CD26, an exopeptidase located in the surface of ubiquitous cells. However, this enzyme can be cleaved from the cell membrane by metalloproteases and, thus, released to circulation, exerting para and endocrine effects (Capuano et al., 2013; Röhrborn et al., 2015). From the total amount of incretins secreted, only 10-15% will reach peripheral circulation without being inactivated by DPP-4 (Wu et al., 2015). Finally, the renal system seems to play a key role in the clearance of incretins (McIntosh et al., 2009). Thus, the combination of enzymatic degradation with the renal clearance leads to the very short half-life of incretins (around 2 minutes) (Stemmer et al., 2020)

1.3.1. GLP-1

From the two incretins present in humans, GLP-1 seems to be the most important one for glucose homeostasis (Holst, 2019). GLP-1 is a peptide hormone composed by 30-to-31 amino acids synthesized and stored in granules within the L cells of the gut, whose abundancy increases from proximal to distal regions of the gut (Mortensen et al., 2003; Pais et al., 2016a). These cells act as sensors and, in response to the presence of nutrients in the lumen, release their GLP-1-containing granules (Chai et al., 2012; Nadkarni et al., 2014; Seino et al., 2010). However, L cells do not only respond to the presence of nutrients in the lumen but also to hormonal and neuronal stimuli. Several hormones can induce GLP-1 production and secretion, such as somatostatin, gastrin releasing polypeptide (GRP), neuromedin C, ghrelin, leptin, GIP, and even insulin (Gagnon et al., 2015; Larsen and Holst, 2005; Lim and Brubaker, 2006). Moreover, a

direct innervation of the L cells by afferent and efferent vagus nerves also potentiate the release of GLP-1 (Rocca and Brubaker, 1999). Some neurotransmitters are also involved in the regulation of GLP-1 secretion, such as GABA, acetylcholine and gastrin-releasing peptide (Lim and Brubaker, 2006). The rise in the GLP-1 levels in blood starts a few minutes after food ingestion (even when the nutrients have not reached the ileum yet) and lasts for several hours (Pais et al., 2016a; Rocca and Brubaker, 1999), following a biphasic pattern (Lim and Brubaker, 2006). The reason for the fast increase in the GLP-1 levels in blood seems to be caused by the effect of GIP, released in the upper regions of the gut, in combination with the neural stimulation through the vagus nerve (Krieger et al., 2016; Rocca and Brubaker, 1999).

As mentioned, L cells secrete their GLP 1-containing granules in response to nutrients present in the lumen of the gastrointestinal tract. Carbohydrates, fats and proteins act as release inductors (Pais et al., 2016a; Yildirim Simsir et al., 2018). Glucose and fats seem to be the most potent GLP-1 release inductors, being glucose the responsible for the first-step release, and lipids for the secondary, long-lasting secretion (Lim and Brubaker, 2006). However, proteins and their metabolites, such as peptones and amino-acids (e.g. L-glutamine, glycine, alanine, phenylalanine and arginine), have shown the capability of directly induce GLP-1 release (Clemmensen et al., 2013; Pais et al., 2016a, 2016b). Moreover, GLP-1 release stimulation seems to be more potent by oligo- or large peptides than by free amino acids (Ishikawa et al., 2015). Finally, bile acids present in the lumen have been demonstrated to also trigger the release of GLP-1 to the bloodstream (Brighton et al., 2015).

1.3.1.1. Targets of GLP-1

A wide variety of cell types express GLP-1 membrane receptors, thus making them sensitive to the effect of this hormone (e.g. pancreas, gut, stomach, skin, lungs, kidneys, muscle, heart, adipose tissue, and the central and peripheral nervous system) (Ayala et al., 2009; Muskiet et al., 2017; Yang et al., 2017). The main effects exerted by the interaction of GLP-1 with GLP-1 receptors (GLP-1R) in different tissues are summarized in Table 1. Independently of the insulinogogue effect of GLP-1, which is always glucose-dependent (Nadkarni et al., 2014; Seino et al., 2010; Thurmond, 2009), it also induces glucose uptake by muscle, adipose tissue, liver and heart (Ayala et al., 2009; Chai et al., 2012; Dardevet et al., 2004; Nikolaidis et al., 2004; Rowlands et al., 2018). Moreover, in the liver, GLP-1 also induces hepatic glucose clearance and glycogen synthesis (Ayala et al., 2009) and reduction in the hepatic glucose production through the inhibition of glucagon release (Jin and Weng, 2016). Nevertheless, it also decreases liver steatosis and fibrosis (Liu et al., 2014). In the brain, GLP-1 signaling has been shown to increase neuronal plasticity and cell survival (Yildirim Simsir et al., 2018), as well as to reduce the appetite, depression, and neurodegeneration (Anderberg et al., 2016; Dorton et al., 2018; Rowlands et al., 2018). These beneficial effects exerted in the brain are translated into an improved memory and learning capacity (Müller et al., 2019), and into a reduced depressive behavior (Anderberg et al., 2016; Guerrero-Hreins et al., 2021). The satiating effect of GLP-1 relies on its direct effect on the brain (Dorton et al., 2018), but also on

its capability to reduce the gastrointestinal motility (MacDonald et al., 2002) and gastric emptying (Nadkarni et al., 2014). GLP-1R are also found in the kidneys, were the hormone triggers cytoprotective and anti-inflammatory pathways as it also regulates the urinary flow rate, renal blood flow, glomerular filtration, and other functions of the organ (Rowlands et al., 2018). Bones are tissues that also display GLP-1R. The action of the hormone over them increases bone formation and improves bone structure (Iepsen et al., 2015; Nuche-Berenguer et al., 2009). Finally, GLP-1R have also been found in the respiratory system, where their activation plays a key role in the lung functions in both biological and pathological conditions, even improving the outcomes of a pulmonary fibrosis (Fandiño et al., 2020).

Apart from the effects exerted by the binding of GLP-1 to the receptors present in the target tissues, this hormone also achieves some effects through neuronal signaling. Enteroendocrine cells have been demonstrated to directly interact with nerve tips of both afferent and efferent nerves through GLP-1, reason why this hormone is also considered as a neurotransmitter (Bohórquez et al., 2015; Larsen and Holst, 2005). The activation of afferent nerves generates a stimulus that is translated to the brain. There, an efferent signal is transmitted through the vagus nerve to the effector organs and, in last term, controls the endocrine function of the pancreas, the gastrointestinal motility or the heart-beating rate (Chai et al., 2012; Larsen and Holst, 2005).

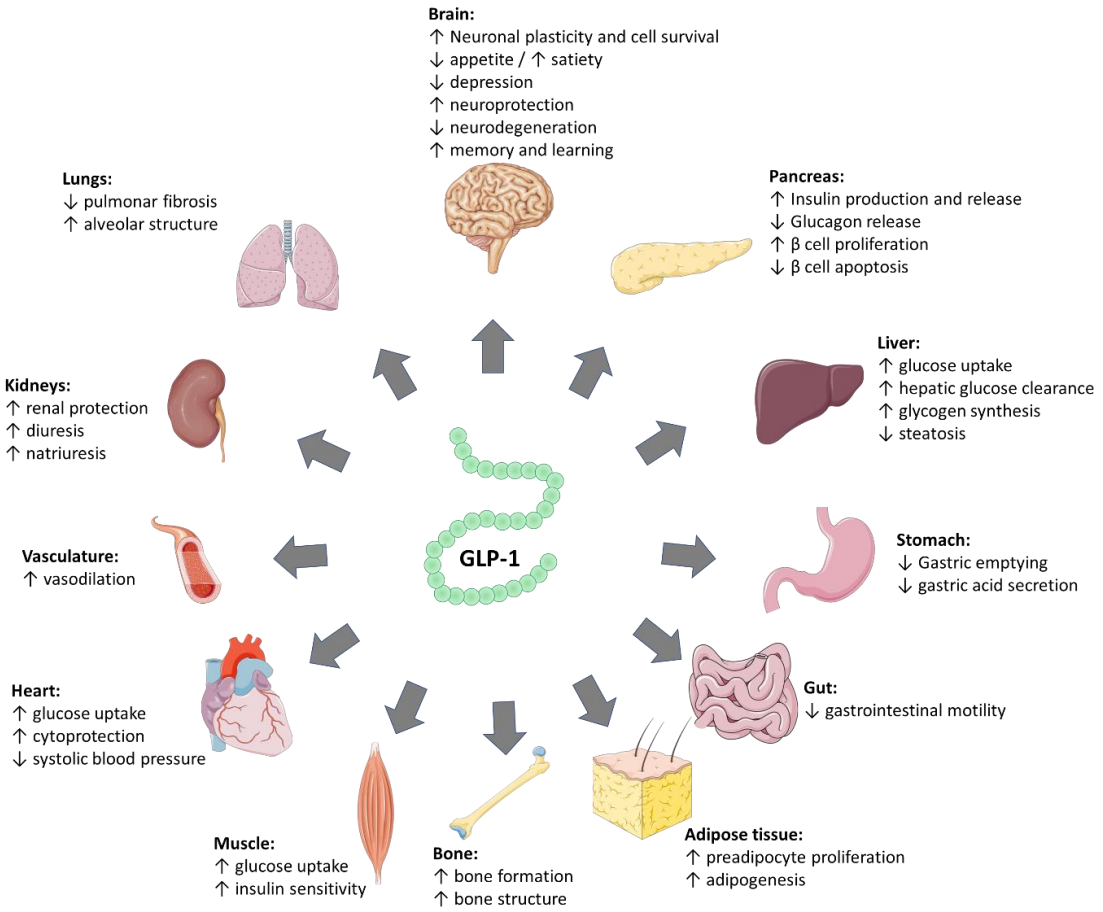

Figure 2. Schematic representation of the main metabolic effects exerted by GLP-1 over different tissues. Figure produced using Servier Medical Art pre-made icons and templates (http://smart.servier.com/).

1.3.2. GIP

The glucose-dependent insulinotropic peptide (GIP), also known as gastric inhibitory polypeptide (Meier et al., 2002), is the other incretin hormone present in humans. It is a 42-amino acid peptide produced and released by the enteroendocrine K cells present in the gut (Kim and Egan, 2008). In contrast to the distribution of L cells, K cells are mainly located in proximal regions of the gut, decreasing in number in further regions (Pais et al., 2016a). As stated for GLP-1, GIP is also secreted in response to the presence of nutrients in the lumen of the intestine, being carbohydrates and fats (long-chain fatty acids) the most potent stimuli (McIntosh et al., 2009). On the contrary, other studies suggest that proteins induce the faster and stronger GIP release (Seino et al., 2010). Moreover, whole proteins have low GIP-inductor activity while individual amino acids seem to be more potent (Marks, 2019). Interestingly, the release patterns seem to differ according to the composition of the meal: carbohydrates lead to a faster and more acute release of GIP while fats lead to a slower and more sustained demeanor (McIntosh et al., 2009). Normally, the peak of GIP release is achieved a few minutes after the meal ingestion (15 – 30 minutes), even before the food reaches the gut, thus a neuronal signaling through the vagus nerve may also be involved in the GIP release (Meier et al., 2002). Finally, GIP is also metabolized by the DPP-4 enzyme, although its affinity seems to be lower than for GLP-1, thus, showing a longer plasma half-life (Baggio and Drucker, 2007).

1.3.2.1. Targets of GIP

The main physiological effects of GIP are summarized in Table 1. GIP is mostly known due to its insulinotropic effect (McIntosh et al., 2009; Meier et al., 2002; Vilsbøll and Holst, 2004), exerting an analogous activity to GLP-1 in the pancreas (Baggio and Drucker, 2007; Kim and Egan, 2008). In this tissue, GIP increases insulin synthesis and secretion and β cell proliferation and differentiation, while reduces β cell apoptosis (Baggio and Drucker, 2007; Hölscher, 2014). Interestingly, in this tissue, GIP also has a stimulatory effect over glucagon release from α cells (El and Campbell, 2020; Stensen et al., 2019). Thus, when glycemic values are low (around 80 mg/dL, as in fasted state), GIP induces glucagon release by targeting α cells. On the other hand, when blood glucose levels rise (postprandial state), it stimulates insulin release by targeting the β cells (El and Campbell, 2020). GIP receptors (GIPR) are found in several extrapancreatic tissues, sharing some but not all, with those targeted by GLP-1 (e.g., trachea, heart, spleen, brain, thymus, testis, or kidneys, among others) (Baggio and Drucker, 2007; Thondam et al., 2020). However, the effects exerted by GIP on them are not all known. Bones are one of those tissues that possess GIP receptors. In the bone, GIP stimulates the activity of osteoblasts and reduces the osteoclastic activity (Helsted et al., 2020; Mieczkowska et al., 2013). These effects are translated into a reduced bone resorption and increased bone formation (Baggio and Drucker, 2007; Helsted et al., 2020). In the adipose tissue,

GIP modulates the synthesis of fatty acids, enhances insulin-stimulated synthesis of triglycerides, increases uptake of glucose and triacylglycerols, and stimulates the activity of the lipoprotein lipase, leading to an increased lipid accumulation within the cells (Asmar et al., 2019; Kim and Egan, 2008; Meier et al., 2002). The ways through which GIP exerts these effects over adipose tissue involve the direct targeting of the adipocytes and an increased blood flow in the tissue, what allows a greater uptake from components from the blood (Asmar et al., 2019; Stensen et al., 2019; Thondam et al., 2020). Apart from increasing the blood flow in the adipose tissue, GIP also regulates the blood flow in other tissues due to its vasoconstrictive and vasodilatory effects, which depend on the vascular bed (Ding et al., 2004; Zhong et al., 2000). Regarding the cardiovascular effects, it has been demonstrated that the administration of GIP reduces the macrophage infiltration, foam cell formation and, in last term, the development of atherosclerotic cardiovascular disease (Greenwell et al., 2020). In addition, the heart myocardium also expresses GIPR, whose signaling seem to be involved in the metabolism of myocardial triglycerides and fatty acids (Greenwell et al., 2020; Heimbürger et al., 2020). Moreover, GIP also increases the heart rate and reduces the mean arterial blood pressure (Heimbürger et al., 2020). The brain is another GIP-sensitive tissue, as demonstrated by the presence of GIPR in different regions of the organ (Kaplan and Vigna, 1994). In this tissue, GIP reduces appetite (Zhang et al., 2021) and acts as neuroprotectant and neuronal stem cells proliferation enhancer, but it also increases the release of synaptic vesicles and improves memory (Hölscher, 2014; Nyberg et al., 2005). Nevertheless, an improvement in the sensorimotor coordination of mice has also been associated with an overexpression of GIPR in the brain (Baggio and Drucker, 2007). Regarding the functions of GIP in the gastrointestinal tract (GIT), it has been demonstrated that GIP diminishes the secretion of acid by the stomach (Gupta et al., 2016). In further regions of the gut, GIP triggers the release of GLP-1 from L cells either by direct targeting or by the activation of the vagus nerve (Rocca and Brubaker, 1999).

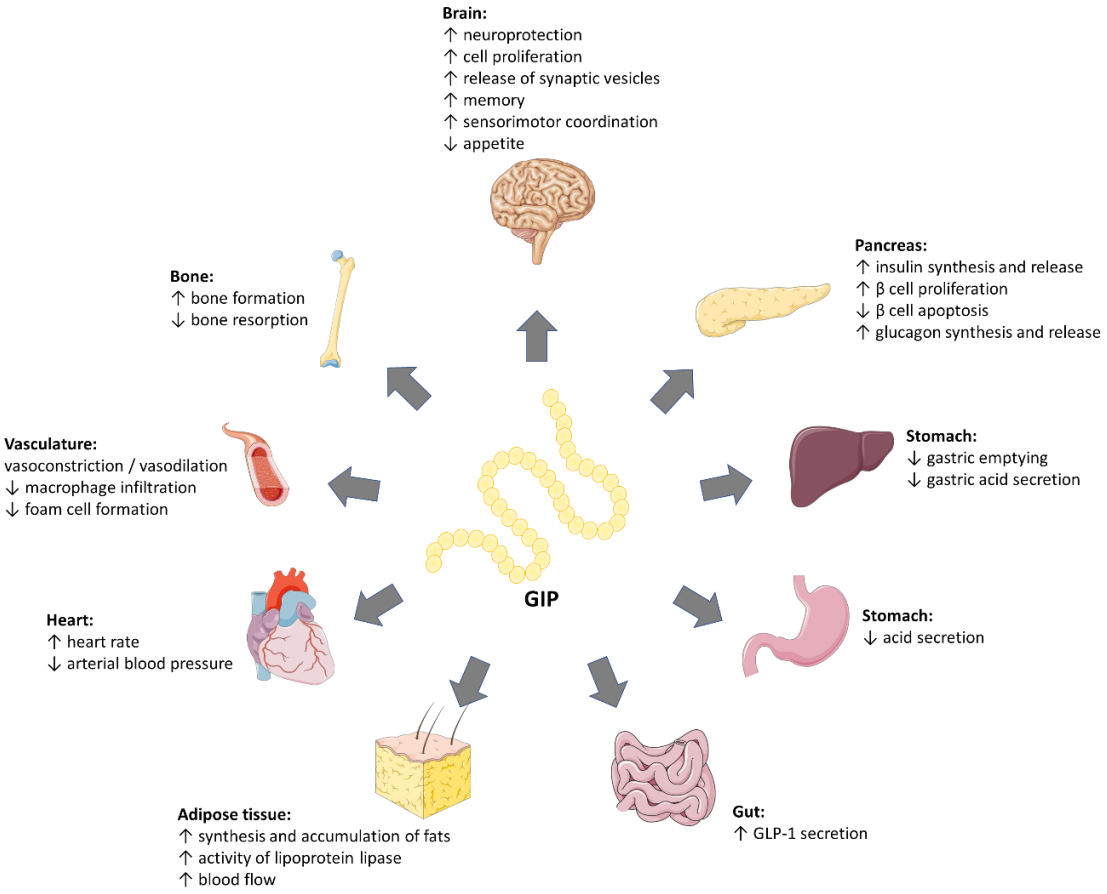

Figure 3. Schematic representation of the main metabolic effects exerted by GIP over different tissues. Figure produced using Servier Medical Art pre-made icons and templates (http://smart.servier.com/).

Table1. Summary of the effects exerted by the incretin hormones (GLP-1 and GIP) over different tissues.

Tissue	Effect	GLP-1	GIP	References
Brain	Appetite	↓	↓	(Dorton et al., 2018) (Rowlands et al., 2018) (Zhang et al., 2021)
	Neuroprotection	↑	↑	(Rowlands et al., 2018) (Hölscher, 2014)
	Neurodegeneration	↓	-	(Rowlands et al., 2018)
	Cell proliferation	↑	↑	(Yildirim Simsir et al., 2018) (Nyberg et al., 2005)
	Neuronal plasticity	↑	-	(Yildirim Simsir et al., 2018)
	Depression	↓	-	(Anderberg et al., 2016)
	Memory	↑	↑	(Müller et al., 2019) (Hölscher, 2014
	Sensorimotor coordination	-	↑	(Baggio and Drucker, 2007)
	Release of synaptic vesicles	-	↑	(Hölscher, 2014)

Pancreas	Insulin production and release	↑	↑	(Nadkarni et al., 2014) (Rowlands et al., 2018) McIntosh et al., 2009)
	β cell proliferation	↑	↑	(Wang et al., 2015) (Baggio and Drucker, 2007) (Kim and Egan, 2008)
	β cell apoptosis	↓	↓	(Wang et al., 2015) (Baggio and Drucker, 2007) (Kim and Egan, 2008)
	Glucagon synthesis and release	↓	↑	(Nadkarni et al., 2014) (Jin and Weng, 2016) (El and Campbell, 2020)
Adipose tissue	Synthesis and accumulation of fats	↑	↑	(Wang et al., 2015) (Asmar et al., 2019)
	Cell proliferation	↑	-	(Rowlands et al., 2018)
	Activity of lipoprotein lipase	-	↑	(Kim and Egan, 2008)
	Blood flow	-	↑	(Stensen et al., 2020)
Stomach	Gastric emptying	↓	-	(Nadkarni et al., 2014) (MacDonald et al., 2002)
	Gastric acid secretion	↓	↓	(MacDonald et al., 2002) (Gupta et al., 2016)
Intestines	Gastrointestinal motility	↓	-	(Wang et al., 2015) (MacDonald et al., 2002)
	GLP-1 secretion	-	↑	(Rocca and Brubaker, 1999)
Heart	Glucose uptake	↑	-	(Nikolaidis et al., 2004)
	Cytoprotection	↑	-	(Rowlands et al., 2018)
	Blood pressure	↓	↓	(Dalsgaard et al., 2018) (Heimbürger et al., 2020)
Vasculature	Heart rate	-	↑	(Heimbürger et al., 2020)
	Vasodilation	↑	↑ / ↓	(Muskiet et al., 2017) (Ding et al., 2004) (Zhong et al., 2000)
	Macrophage infiltration	-	↓	(Greenwell et al., 2020)
	Foam cell formation	-	↓	(Greenwell et al., 2020)
Liver	Glucose uptake	↑	-	(Ayala et al., 2009)
	Hepatic glucose clearance	↑	-	(Ayala et al., 2009)
	Glycogen synthesis	↑	-	(Ayala et al., 2009)
	Steatosis	↓	-	(Muskiet et al., 2017)
Muscle	Glucose uptake	↑	-	(Ayala et al., 2009)
Kidney	Renal protection	↑	-	(Rowlands et al., 2018)
	Diuresis and natriuresis	↑	-	(Muskiet et al., 2017)
Lungs	Pulmonar fibrosis	↓	-	(Fandiño et al., 2020)
	Alveolar structure	↑	-	(Fandiño et al., 2020)

Bone	Bone formation	↑	↑	(Iepsen et al., 2015; Nuche-Berenguer et al., 2009) (Helsted et al., 2020)
	Bone resorption	-	↓	(Helsted et al., 2020)

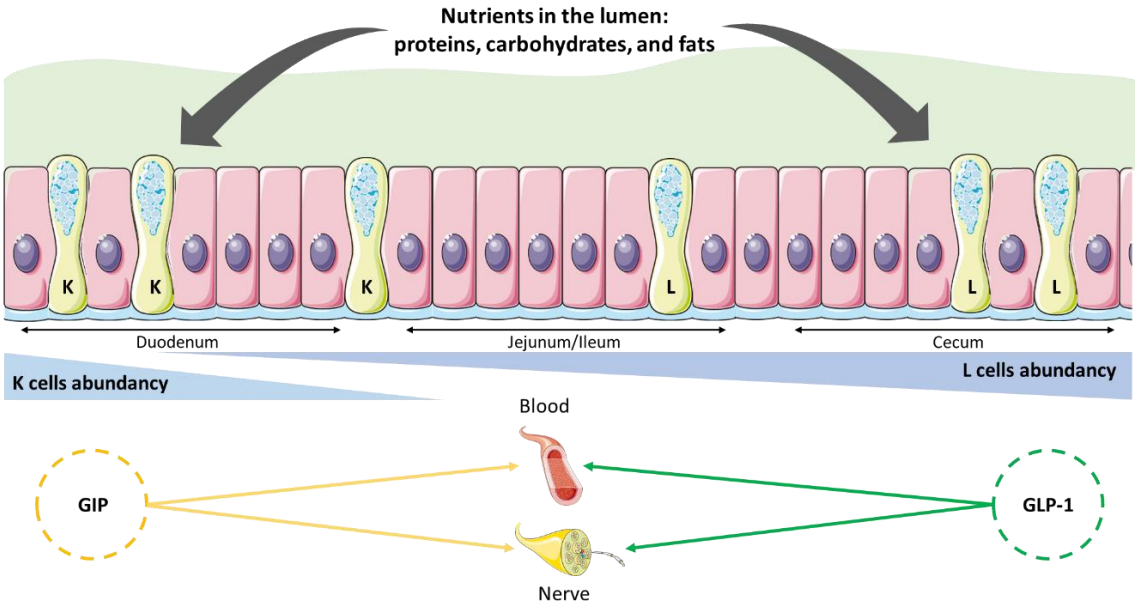

Figure 4. Schematic representation of the distribution of GIP-secreting cells (K cells) and GLP-1-secreting cells (L cells) in the gastrointestinal tract, and the diffusion routes of incretins to reach the target tissues. Figure produced using Servier Medical Art pre-made icons and templates (http://smart.servier.com/).

1.4. Imbalance in glucose homeostasis

An imbalance in the glucose homeostasis can lead to increased or decreased levels of glucose in blood (hyperglycemia and hypoglycemia, respectively). Hypoglycemia is usually associated to a fasting state, although it can also be caused by insulinomas (insulin-secreting tumors), malfunction of liver and kidneys, alcoholism, glucose malabsorption and by medications (Douillard et al., 2020). However, a hypoglycemic state can also be achieved after meal ingestion (reactive or postprandial hypoglycemia) due to an alteration in the biphasic secretion of insulin, leading to a late and excessive release of the hormone (Brun et al., 2000). The complications of this pathological condition range from tremors, palpitations, and anxiety to loss of consciousness, cognitive dysfunction, and even death (Cryer, 1999).

On the other hand, elevated levels of glucose in blood can be caused by a decreased insulin secretion or function, increased synthesis of glucose, reduced glucose utilization, destruction of the pancreas, endocrine disorders, or medication, among others (Suri and Aurora, 2017). A prolonged state of hyperglycemia leads to diabetes and causes microvascular complications, such as damage in the nervous system or dysfunction of

the eyes and kidneys, and macrovascular diseases (coronary, cerebrovascular, and peripheral) (Rahman et al., 2021; Suri and Aurora, 2017).

1.4.1. Diabetes, its epidemiology, economic burden, and prospective

Diabetes mellitus is a group of metabolic disorders characterized by conditions of hyperglycemia caused by an impaired secretion and/or efficacy of insulin (Petersmann et al., 2018; Tan et al., 2019). The toxicity associated to the hyperglycemic conditions is known as glucotoxicity or glucose toxicity. Glucotoxicity refers to the detrimental effects that elevated levels of glucose in blood exert on cells and tissues, but mostly, to its effect over the β cells that lead to a decreased insulin production (Stiker, 2001). Sustained hyperglycemia in the body triggers several metabolic pathways involved in glucose clearance. This increased and continuous activation of the glucose clearance mechanisms lead to an alteration in the redox balance within the cells, increased oxidative stress, protein translational modifications, and generation of advanced glycation end products (AGEs) (Zheng et al., 2016). AGEs are end products generated by the non-enzymatic glycation of proteins or lipids (Goldin et al., 2006), whose normal function and activity is disrupted by the sugar modification (Singh et al., 2014). Glycated haemoglobin (HbA1c) is one of those AGEs and it is considered the hallmark for diabetes diagnosis, setting the cut-off in HbA1c level of ≥6.5% (≥48 mmol/mol) (Gholap et al., 2013). When the hyperglycemic condition is maintained for long periods of time, the accumulation of reactive oxygen species in different tissues leads to oxidative stress and tissue damage that, in last term, causes to disfunction and failure of the organ (Robertson and Harmon, 2006).

This toxicity in the different tissues is the basis of the morbidity and mortality of the disease (Khan et al., 2020; Zheng et al., 2018). Diabetes affects to more than 450 million people worldwide (Cho et al., 2018) and, alone, it belongs to the top 10 diseases with highest mortality, causing more than 1 million deaths per year (Khan et al., 2020). Moreover, it has been estimated that by 2040 more than 640 million people will suffer from diabetes, accounting to 1 out of 10 adults ranging from 20 to 79 years old (Bommer et al., 2018). Age is one of the major risk factors of developing diabetes, and the increasing life expectancy of the population is a reason for the rise in the number of cases nowadays (Halim and Halim, 2019; Kalyani et al., 2017). In spite of being a worldwide issue, the prevalence of diabetes in developed countries is considerably higher, being Western Europe the region with highest prevalence of the pathology (Khan et al., 2020). However, when talking about total number of cases, more than 45% of the total T2D patients are located in three countries: China, India and United States (Zheng et al., 2018). The worldwide distribution of diabetic patients is represented in Figure 5.

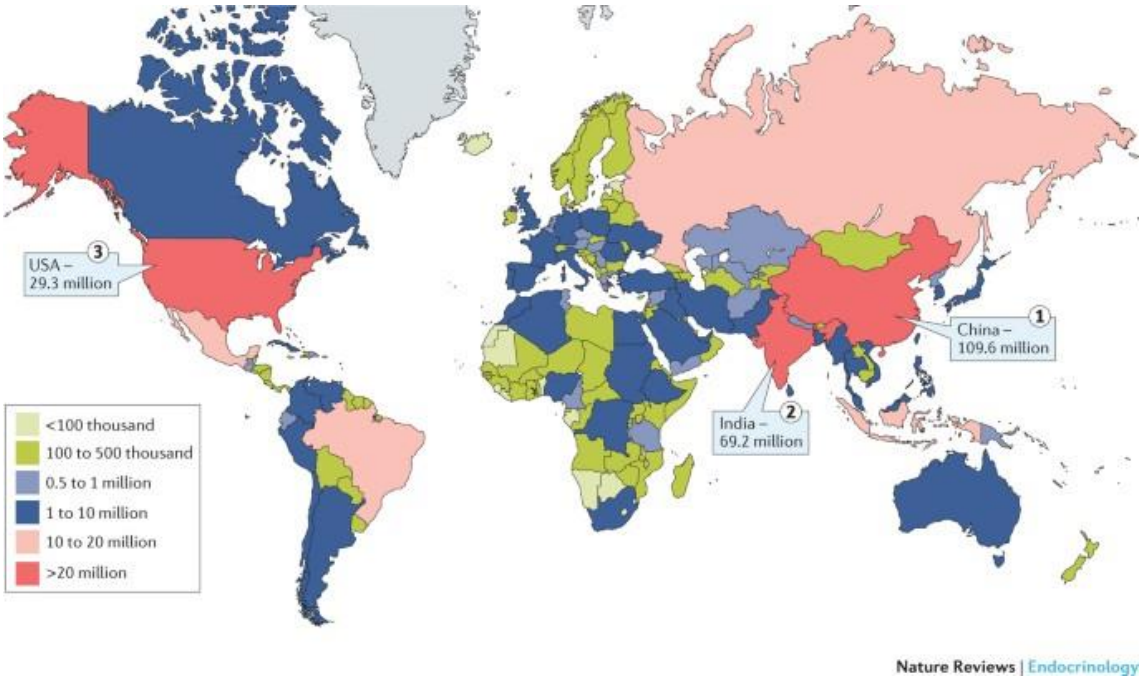

Figure 5. Worldwide distribution of the total cases of diabetic patients, per countries. Image obtained from (Zheng et al., 2018).

In monetary terms, diabetes caused an economic burden of 1.32 trillion dollars by 2015 (considering direct and indirect costs), value that is estimated to pass the 2 trillion dollars by 2030 (Bommer et al., 2018).

Only in Spain, the Di@bet.es study revealed that, by 2012, there were about 5.3 million adults suffering from diabetes, what corresponds to the 13.8 % of the total population. By then, the total costs of this illness in Spain were estimated to be above 23.000 million €, divided in direct costs (5.447 million) and indirect costs (17.630 million). The second phase of this study, carried out during 2016-2017, revealed that almost 400.000 new cases of diabetes are developed every year only in Spain.

1.4.2. Types of diabetes

According to the etiology of the illness, several types of diabetes mellitus can be found, although the bast majority of the cases correspond to type 1 or type 2 diabetes mellitus (Tan et al., 2019). Type 1 diabetes (T1D) is originated by an autoimmune illness that courses with the destruction of the β cells of the pancreas while type 2 diabetes (T2D) is caused by a reduced activity of endogenous insulin, mainly due to insulin resistance by peripheral tissues (Smith and Singleton, 2008; Tan et al., 2019). From the total number or cases of diabetes, T1D comprises only 5 – 10% (Daneman, 2006), while T2D comprises around 90% (Zheng et al., 2018). In the case of T2D, the insulin resistance can occur in different insulin-sensitive tissues, although it does not have to affect all of them at once (De La Monte and Wands, 2008). The most common cause for T2D is an unhealthy lifestyle that causes obesity and its associated metabolic alterations (Czech, 2017; Golay and Ybarra, 2005). Nevertheless, there are also some pathophysiological conditions that lead to the appearance of diabetes, such as a deficient activity of the

exocrine pancreas (e.g., pancreatitis, hemochromatosis, or cystic fibrosis), endocrinopathies (e.g., pheochromocytoma, Cushing syndrome, or acromegaly), chemical induction (e.g., glucocorticoids, interferon, or pentamidine), genetic alterations of the β cells (diabetes types MODY), infections (e.g., rubella), or gestational diabetes (Menser et al., 1978; Petersmann et al., 2018; Suri and Aurora, 2017).

1.4.3. Diabetes mellitus general comorbidities

Table 2 summarizes the main comorbidities associated with diabetes and its concomitant hyperglycemia. The main organs affected are the following: heart and cardiovascular system (Katsiki and Tousoulis, 2020; Suri and Aurora, 2017), lungs (Khateeb et al., 2019), kidneys (Katsiki and Tousoulis, 2020; Rahman et al., 2021; Suri and Aurora, 2017), liver (Katsiki and Tousoulis, 2020), and brain and nervous system (Darwish et al., 2018; Srikanth et al., 2020; Stratton et al., 2000; Tuttolomondo et al., 2015).

Table 2. Main comorbidities associated to diabetes depending on the affected organ or tissue.

Organ	**Associated comorbidities**
Heart	Coronary heart disease, angina, arrhythmias, valvopathies, myocardial infarction, increased epicardial adipose tissue
Lungs	Asthma and chronic obstructive pulmonary disease
Kidney	Nephropathy, chronic kidney disease or any kind of renal disease with exception of kidney stones and urinary tract infections
Liver	Chronic hepatitis, cirrhosis, non-alcoholic fatty liver disease (NAFLD)
Blood	Anemia and hemoglobinopathies
Cardiovascular	Retinopathy, diabetic foot syndrome, stroke, peripheral vasculature disease
Nervous system	Neuropathy, diabetic foot syndrome
Brain	Cognitive dysfunction, dementia, and depression

1.4.4. Diabetes and aging

Other consequence of an improper management of diabetes is an accelerated aging and, thus, to a reduction in the life expectancy (Caspersen et al., 2012; Morley, 2008). The basis for this accelerated aging seems to be the accumulation of oxidative stress in the tissues that leads to a premature senescence of the cells (Liguori et al., 2018; Yegorov et al., 2020). Moreover, as already stated, obesity is the major cause of T2D, and this unhealthy condition is itself a trigger for premature ageing (Burton and Faragher, 2018; Salvestrini et al., 2019). During obesity, the environment in the adipose tissue shows increased oxidative stress, DNA damage and telomerase dysfunction that, in last term, lead to insulin resistance and diabetes (Ahima, 2009). Thus, in most patients with T2D there are two different pathological conditions that lead to a reduction in the life expectancy: expansion of the adipose tissue and increased oxidative stress caused by the hyperglycemic conditions in the whole body.

The effect of diabetes over aging is so huge that a study suggests that the life expectancy of type 1 diabetic patients is reduced by 11 years in men and 13 in women, compared to healthy individuals (Livingstone et al., 2015). In the case of patients with obesity, and its associated T2D, the life expectancy of men was reduced by almost 8.5 years, while for women the years of life lost were up to 6 (Grover et al., 2015). In a communicate from the United Kingdom government, it was stated that the life expectancy of individuals suffering from diabetes was shortened in 20 years for T1D patients and 10 years for T2D patients (Diabetes NSF Team, 2012). However, since all the complications caused by diabetes, including the shortening in the life expectancy, are attributed to the hyperglycemic condition, an effective management reduces the risk of comorbidities and increases the lifespan.

1.4.5. Diabetes and Alzheimer's Disease (AD)

Alzheimer's disease is a deadly neurodegenerative dementia that mostly affects to elderly people and causes a cognitive and functional impairment in the patient (Najafi et al., 2016). This pathology was first described in 1906 by Alois Alzheimer and, since then, this illness has become the most prevalent type of dementia worldwide (Hodson, 2018; Soria Lopez et al., 2019), accounting for the 60-80% of the total cases of dementia (Garre-Olmo, 2018) and affecting to more than 27 million patients in the world (Silva et al., 2019). Moreover, the incidence of AD is expected to increase 3-fold by 2050 due to the increase in the life expectancy of people worldwide (Lane et al., 2018). The first steps in the development of the disease are learning impairments and memory difficulties that, over time, get worse and finally affect to the daily lifestyle of the patient (Lane et al., 2018; Soria Lopez et al., 2019).

Although the etiology of the illness is not well understood yet, the two histopathological hallmarks of the brain of patients suffering from AD are the presence of neurofibrillary tangles (accumulations of hyperphosphorylated tau protein) and β-amyloid plaques, which are thought to lead to neuronal cell death (Silva et al., 2019). Around the 70% of the risk of developing AD is associated to genetic alterations involving different signaling pathways (inflammation, cholesterol metabolism, and recycling of endosomal vesicles). However, there are also several external factors that influence on the generation and development of the pathology, such as obesity, diabetes, hypertension, and dyslipidemia (Lane et al., 2018; Silva et al., 2019). It is thought that the development of AD relies on the combination of several risk factors, from which age is, by far, the greatest of them ("2017 Alzheimer's disease facts and figures," 2017). However, insulin resistance, which can affect exclusively to the brain (De La Monte and Wands, 2008), is gaining a lot of importance due to its huge influence on the development of mild cognitive impairment, dementia, and AD (De la Monte, 2014). During the last decades, new insights regarding the pathogenesis of AD brought to light a relationship between this type of dementia and type 2 diabetes. This relationship is so strong that some authors refer to AD as "diabetes of the brain" or "type 3 diabetes" (De La Monte and Wands, 2008; Kandimalla et al., 2017; Mittal et al., 2016). In fact, poorly controlled blood glucose levels increase the risk of developing dementia (Crane et al., 2013) and a reduced insulin signaling in the brain leads to several pathological conditions: i) reduced

neuronal activity; ii) mitochondrial disfunction and increased oxidative stress; iii) increased levels of proinflammatory cytokine levels (e.g., IL-6, IL-18, TNF-α); iv) increased phosphorylation and cleavage of tau protein that leads to an increased formation of neurofibrillary tangles; v) glutamate-induced excitotoxicity driven by hyperglycemic conditions; and vi) reduced synaptic plasticity (De la Monte, 2014; Kandimalla et al., 2017; Rorbach-Dolata and Piwowar, 2019). All these pathophysiological conditions lead towards an increased accumulation of neurofibrillary tangles, amyloid plaques, inflammation, oxidative stress, and apoptosis (Sims-Robinson et al., 2010). Nevertheless, the relationship between AD and diabetes has also been evidenced by epidemiological studies (Arnold et al., 2014; Sims-Robinson et al., 2010).

1.4.6. Relationship between obesity, diabetes, aging, and Alzheimer's Disease

Taking into account the aforementioned information, a direct relationship between obesity, diabetes, aging and AD can be stablished. First, obesity and its associated metabolic disorders leads to diabetes and to an accelerated aging. Second, type 2 diabetes, which may be caused by obesity, is also a pathological condition causing accelerated aging. Meanwhile, aging is one of the main risk factors of diabetes. Finally, both diabetes and aging are the most important risk factors for developing Alzheimer's Disease. A schematic representation of this relationship is shown in Figure 6.

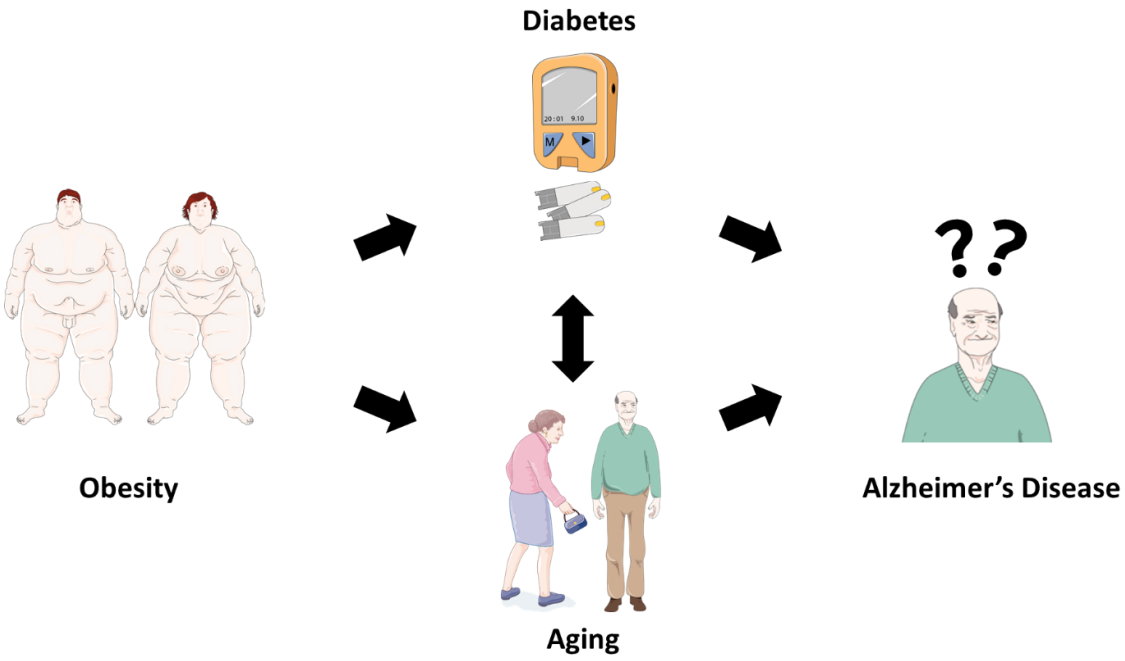

Figure 6. Schematic representation of the relationship between obesity, diabetes, aging and Alzheimer's Disease. Figure produced using Servier Medical Art pre-made icons and templates (http://smart.servier.com/).

1.5. Management of diabetes

1.5.1. Insulin for the management of type 1 diabetes

Since patients suffering from T1D present a destruction of the β cells of the pancreas, their insulin secretion is null or highly deficient. Due to this, in order to diminish the blood glucose levels, they need for an exogenous supply of insulin during their whole lifetime (Atkinson et al., 2014; Tan et al., 2019). The insulin supply is usually administered via subcutaneous injections of the hormone, which can be found as long-acting or rapid-acting insulin analogues. Long-acting analogues provide continuous basal levels during the day while rapid-acting analogues are administered before the meal to control the postprandial glucose levels (Atkinson et al., 2014). However, several insulin and insulin-analogue formulations can be found in the market, with a more varied pharmacokinetic profile and, according to it, can be classified as: rapid-acting: usually with a peak at 0.5 – 2h post-administration and lasting for up to 4 hours (e.g., insulin lispro, aspart and glulisine); fast-acting: usually with a peak at 2 – 5h post-administration and lasting for up to 8 hours (e.g., human regular insulin and soluble insulin); intermediate-acting: usually with a peak at 2 – 5h post-administration and lasting for up to 10 hours (e.g., insulin isophane, lente, Neutral Protamin Hagedorn (NPH), and Insulatard); and long and very-long acting: this type of formulations does not show a clear peak in the pharmacokinetic profile and their effect lasts for up to 24 hours (e.g., ultralente, detemir and glargine) or even 40 h in the case of degludec (Daneman, 2006; Imam, 2015; Kamboj and Henry, 2018; Keegan, 2018).

New technological advances have led to the developments of systems able to continuously track the blood glucose levels (continuous glucose monitoring; CGM) while performing a continuous subcutaneous insulin infusion (CSII), known as closed-loop system or artificial pancreas (Boughton and Hovorka, 2019; Doyle et al., 2014; Schönauer and Thomas, 2010). These insulin pumps with glycemic sensors (sensor-augmented pump therapy) have demonstrated better results in the management of glucose homeostasis than the use conventional devices, as evidenced by lower levels of glycated hemoglobin and a reduction in the time spent in hypoglycemic conditions (Atkinson et al., 2014). Similar to these devices are the predictive low-glucose suspend systems, which are able to monitor blood glucose levels while administering insulin and, before an hypoglycemic event happens, the insulin influx is suspended (Chen et al., 2019). The use of these devices has proven to significantly reduce the nocturnal hypoglycemic events in patients with T1D (Forlenza et al., 2018). These successful results allowed that, in 2016, the first hybrid closed-loop system reached the market in the USA under the name of MiniMed® 670G pump (Medtronic, Northridge, CA, USA) (Boughton

and Hovorka, 2019). A picture showing the different components of the closed-loop insulin pump therapy is shown in Figure 7.

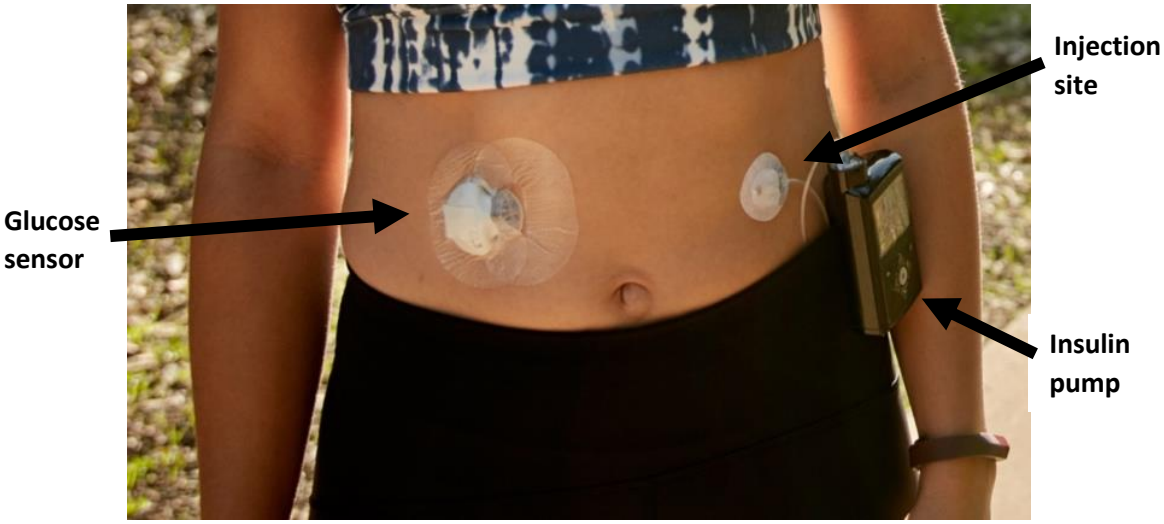

Figure 7. Figure of the different parts of a closed-loop system. CGM: continuous glucose monitor. Picture adapted from the manufacturer's webpage (https://www.medtronic-diabetes.co.uk/).

The use of incretins is also being investigated due to the promising efficacy of the hormones. One of the most important highlights for the use of incretins for the management of diabetes is that their insulinotropic effect is always glucose-mediated, thus, avoiding the possibility of causing hypoglycemia (Farngren and Ahrén, 2019). GLP-1 has been tested in T1D patients and it showed a 45% decrease in the postprandial peak of glucose, independently of a residual β cell function (Kielgast et al., 2011). The administration of exenatide (GLP-1 analog) to patients with T1D has shown to induce a significant reduction in the concentration of glycated hemoglobin and in the total bodyweight (Herold et al., 2020), as well as a reduced glycemic excursion after meal and decreased glucagon release (Ghazi et al., 2014). Liraglutide, another GLP-1 analog, has shown similar results as exenatide when administered in combination with insulin to patients with T1D: reduction in the total body weight, reduction in glycated hemoglobin and reduction in the total dose of insulin needed for the glycemic management (Kuhadiya et al., 2013; Mathieu et al., 2016). Another GLP-1 analog (lixisenatide), which has been widely studied in T2D, has also been evaluated in a cohort of T1D and it showed beneficial effects in glucose management at a postprandial state and a reduced needing of insulin supplementation (Ballav et al., 2020)

1.5.2. Insulin for the management of type 2 diabetes

In the case of T2D patients, since the pathology is caused by unhealthy lifestyles and peripheral insulin resistance, the first-step treatment are lifestyle modifications. When pharmacological treatment is needed, the first-line drug used is metformin (a member of the biguanide family) (Foretz et al., 2019). However, if metformin combined with healthier habits is not enough for the correct management of blood glucose levels, other oral hypoglycemic drugs can be used in mono or combined therapy (e.g., sulfonylureas, meglitinides/glinides, thiazolidinediones/glitazones, α-glucosidase inhibitors, DPP-4

inhibitors, and the oral formulation of a GLP-1 analog: Rybelsus®) (Lorenzati et al., 2010; Moon et al., 2017; Rother, 2007; Scheen, 2004). Furthermore, there are other treatments that are not administered through the oral route and help for the glucose management of diabetic patients, such as amylin analogs (e.g., Pramalitide) or GLP-1 analogs (e.g., exenatide).

Incretins are also being investigated for the management of T2D. It has been reported that the administration of GLP-1 analogues to patients with T2D led to a better glycemic control, reduced glycated hemoglobin, and a facilitated weight loss (Bucheit et al., 2020; Herold et al., 2020). Moreover, this group of drugs have shown better results than conventional hypoglycemic drugs such as sulphonylurea and thiazolidinedione in reducing glycated hemoglobin (Ross and Ballantine, 2013). However, most of the marketed drugs belonging to this group are administered by subcutaneous injection (e.g., exenatide, albiglutide, dulaglutide, semaglutide, liraglutide and lixisenatide), although a new oral formulation of semaglutide (Rybelsus®) was approved by the FDA in 2019 (Blakely and Weaver, 2020). This oral formulation composed by semaglutide and sodium N-[8-(2-hydroxybenzoyl amino]caprylate (SNAC) showed similar results in reducing glycated hemoglobin and weight gain as other GLP-1 analogs administered by subcutaneous injection (Bucheit et al., 2020). Other marketed drugs aiming to increase the incretin effect in diabetic patients are gliptins (DPP-4 inhibitors), such as sitagliptin, vildagliptin or saxagliptin (Richter et al., 2008). These drugs block the degradation of incretins by DPP-4 and, thus, increase their blood half-life and, in last term, their efficacy. The advantages of this type of drugs are their capability to be administered orally, their safety, and their tolerability (Ahrén, 2007).

It is worth noting that in patients with T2D, the incretin effect is altered; although the reasons are still in controversy. Some authors claim that this is caused by a reduction in the levels of incretins (Lim and Brubaker, 2006), which may be caused by a reduced circulating halftime of the hormones (Baggio and Drucker, 2007; Kim and Egan, 2008). On the other hand, other authors believe that the cause is a reduction in the activity rather than in the secretion of the hormones (Ahrén, 2012; Kim and Egan, 2008; Nauck and Meier, 2016). Additionally, some research suggests that T2D patients also show a loss of activity in the GIP receptors of the β cells of the pancreas (El and Campbell, 2020).

In some T2D patients, the administration of hypoglycemic drugs is still not enough for the correct management of diabetes and, when this happens, insulin formulations can be used in combination with them or even as monotherapy (Moon et al., 2017; Tan et al., 2019).

1.5.3. Insulin for the management of "type 3 diabetes"

Due to the last insights regarding the pathogenesis of Alzheimer's Disease, which demonstrated a close relationship between this illness and diabetes mellitus, insulin has been being studied as treatment for this type of dementia (Hallschmid, 2021; Mao et al., 2016). In experiments carried out to evaluate the potential of insulin for the treatment of AD, the administration route is usually intranasal because, by this way, the hormone bypasses the blood-brain barrier (BBB) via the trigeminal perivascular channels and

olfactory nerve channels (Craft et al., 2012; Kellar and Craft, 2020). Trials performed in different cognitive-impaired animal models have demonstrated that the administration of insulin leads to a reduced state of anxiety and to a memory improvement (Mao et al., 2016; Salameh et al., 2015; Vandal et al., 2014). In an animal model of T2D, intranasal but not subcutaneous administration of insulin, led to a reduced hyperphosphorylation of tau protein (Yang et al., 2013), which is one of the hallmarks of AD. In a clinical study carried out in humans (clinicaltrials.gov; NCT00438568), intranasal administration of insulin has shown to improve cognition in patients suffering from dementia (Claxton et al., 2015; Srikanth et al., 2020).

Since AD is considered as a central nervous system (CNS) affection of T2D, insulin sensitizers have also been studied to improve the outcomes of the neurodegenerative disorder. Metformin has shown to improve insulin signaling in the brain and, as consequence, the memory of a mouse model of AD (Ou et al., 2018). Other hypoglycemic agents used for the treatment of T2D that have shown a beneficial effect on the management of AD are sulfonylureas, which reduced the formation of β-amyloid plaques (Macauley et al., 2021). Due to the effects of GLP-1 on insulin secretion and sensitivity, as well as in neuroprotection and increased neuronal plasticity, analogs from this hormone have also been tested as treatments for AD. For instance, SAMP8 mice (senescence accelerated prone mouse 8; used as model for AD) treated with liraglutide, showed a cognitive improvement and increased hippocampal neuronal density (Hansen et al., 2015). In another study, memory deficit and depressive-like behavior was chemically induced to Swiss mice through the injection of Aβ oligomers (AβOs). However, previous administration of liraglutide prevented the memory impairment caused by the injection of AβOs (Batista et al., 2018). In that study, the same chemically induced memory deficit was inducted to non-human primates (NHP) and, the administration of liraglutide, reduced the AβO-triggered insulin receptors loss and the synapse mislaying in the primates' brain. Again, the inhibition of the DPP-4 is an interesting strategy to increase the levels and half-life of circulating GLP-1. Thus, gliptins have demonstrated to significantly improve the cognitive and learning capabilities of both mouse and rat models of AD (Chalichem et al., 2017).

1.6. New challenges for oral insulin delivery

The oral route is the most desirable one due to its advantages for the patient and for the provider. From the point of view of the manufacturer, drugs intended for oral administration have less sterility requirements, what is associated to reduced production costs (Mahmood and Bernkop-Schnürch, 2019). On the other hand, for the patient, the oral route is painless and allows self-administration, what results in a better compliance to the treatment (Ahmad et al., 2012; Mahmood and Bernkop-Schnürch, 2019).

However, the oral route presents several drawbacks that hamper the capability of the administered drug to reach the bloodstream. This is the reason why peptide and protein treatments are usually administered through a parenteral route (Gedawy et al., 2018), by which the presence of physiological barriers is minimum. The physiological barriers that hinder the absorption of orally administered drugs can be divided in those found

before the absorptive epithelium, and the epithelium itself. Thus, before reaching the enterocytes that compose the absorptive epithelium, the administered drug must cope with the chemical and enzymatic barriers, as well as with the mucus layer that covers the epithelium. The chemical barrier refers to the shifting acidic conditions all along the gastrointestinal tract, being highly acidic (pH ≈ 1.5) in the stomach and slightly basic (pH ≈ 7.5) in colon (Yilmaz and Li, 2018). Under these conditions, many proteins may experience pH-induced oxidation, hydrolysis or deamination phenomena that lead to a loss of function (Ahmad et al., 2012; Chen et al., 2011). The enzymatic barrier comprises the presence of degrading enzymes that can be found secreted into the lumen or membrane-bound onto the brush border of the enterocytes (e.g., trypsin, chymotrypsin, pepsin, elastase, aminopeptidases, carboxypeptidases) (Ahmad et al., 2012; Chen et al., 2011; Sonia and Sharma, 2012). The mucus layer is a gel-like structure that cover the epithelium of the whole gastrointestinal tract, protecting it from external pathogenic agents but also acting as scaffold for the host microbiota and for the digesting enzymes (Morishita et al., 2004). It is secreted by goblet cells (Elderman et al., 2017) and its principal components are mucins (highly O-glycosylated proteins). The chemical properties of mucins confer them a negative charge (Li et al., 2013; Morishita et al., 2004) and presence of hydrophobic domains where proteins may bind (Johansson et al., 2011). Moreover, the mucus layer is continuously secreted and renewed, with turnover rates that differ between animal species (Ahmad et al., 2012; Chen et al., 2011).

Once all these barriers are overcome, the drugs must deal with the absorption barrier, which is mainly composed by enterocytes (absorptive brush-bordered cells) and goblet cells (mucus-secretory cells) (Chen et al., 2011). Absorption through the epithelium can occur by two different pathways: the paracellular or the transcellular route (Hwang and Byun, 2014). The former consists on the passive diffusion through the spaces between neighbor cells, spaces that are filled by the tight junctions that bind both cells and act as discriminatory barrier (Lee et al., 2018; Suzuki, 2020). Regarding the passage of peptides through this route, only those with low molecular weight and hydrophilic properties can pass (Xu et al., 2019). Hence, molecules with a molecular weight greater than 700 Da must enter the cell via active transport through the transcellular route (Hwang and Byun, 2014). The latter implies the cellular absorption of the elements from the lumen, which is driven mainly by enterocytes, although M cells have also shown to be involved in this process (Shakweh et al., 2004). This cell-mediated uptake of compounds can be performed by active or passive transport, depending on the physicochemical properties of the molecule and the gut (molecular weight, lipophilicity, binding site, specific transporters, etc.) (Constantinescu et al., 2019; Nielsen et al., 2017). The cellular uptake of large molecules (such as peptides and proteins) from the medium is mainly driven by vesicle-mediated transcytosis. It consists on the endocytosis at the apical site, transport of the vesicle within the cell, and basolateral excretion of the vesicle content (Li et al., 2021). The high molecular weight of insulin (5,808 Da) (Vakilian et al., 2019) makes it impossible to be absorbed through the paracellular route without the presence of compounds able to open the tight junctions. Thus, its pass from the intestinal lumen to the bloodstream occurs, mostly, via the transcellular route (McGinn and Morrison, 2016). Moreover, the endocytosis of insulin is receptor-mediated (Hall et al., 2020), and enterocytes have been demonstrated to possess insulin receptors in the apical membrane (Ben Lulu et al., 2010). Nevertheless, the absorption of insulin is not the last barrier to overcome because, upon internalization of the insulin-receptor complexes,

most part of the internalized insulin is degraded in the cytoplasm (McClain, 1992; Najjar and Perdomo, 2019). All these drawbacks, summarized in Figure 8, lead towards an almost null bioavailability of orally administered insulin (Niu et al., 2012; Pérez et al., 2016).

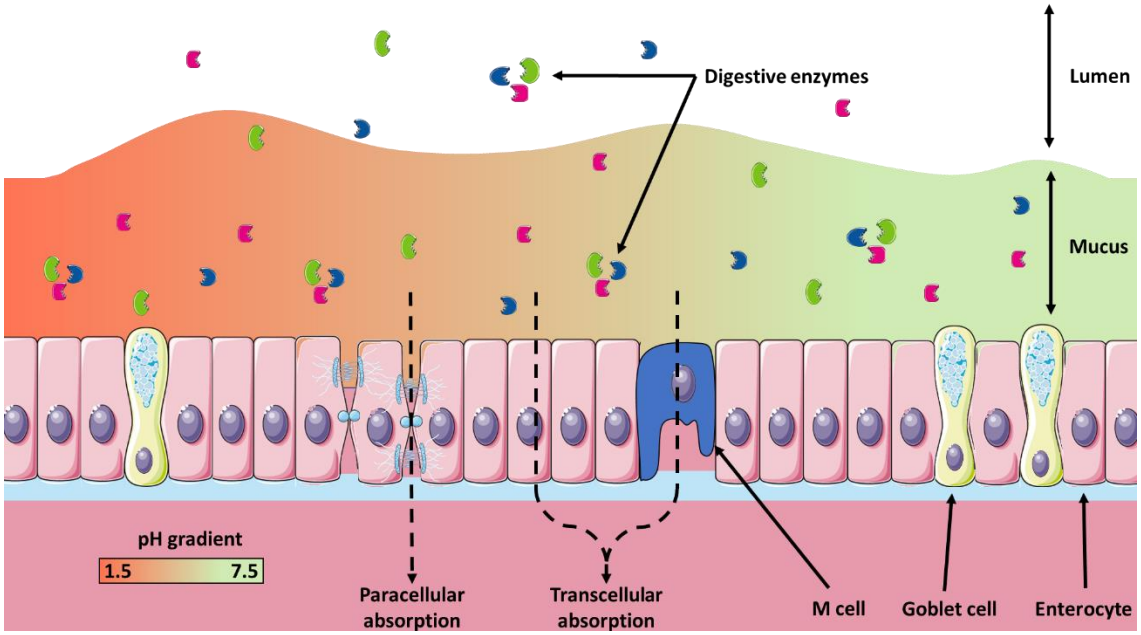

Figure 8. Schematic representation of the different barriers that hamper the oral bioavailability of drugs, including the variable pH conditions, the presence of digestive enzymes, the mucus layer, and the absorptive epithelium. Figure produced using Servier Medical Art pre-made icons and templates (http://smart.servier.com/).

During the last decades, several strategies based on the use of nanotechnology have been evaluated to develop a system that enables oral administration of insulin. The use of nanosized formulations is useful to improve the characteristics of a drug in terms of targeting, controlled release, absorption, solubility, biodistribution, or to decrease the toxicity and side-effects associated to a drug (Irache et al., 2011; Vinogradov and Wei, 2012). Some of the most studied nanosystems for the oral delivery of insulin are insulin conjugates, liposomes, solid lipid nanoparticles, self-nanoemulsifying drug delivery system (SNEDDS), and polymeric nanoparticles.

1.6.1. Polymer-insulin conjugates

Polymer-insulin conjugates are complexes formed by the union of insulin with other molecules such as carbohydrates, PEG, Brownlee's polymer, or albumin, in order to confer better pharmacokinetic profiles or stimuli-responsive effects (Hoeg-Jensen, 2021; Xie et al., 2017). Insulin can be attached to polymers that are already bound to molecules with protease inhibitor activity (e.g., Bowman-Birk inhibitor, aprotinin, soybean trypsin inhibitor, or elastatinal (Bernkop-Schnürch, 1998; Marschütz and Bernkop-Schnürch, 2000)), or to molecules that increase the absoprtion through the intestinal epitehlium (e.g., transferrin, penetratin) (He et al., 2018; Kavimandan et al., 2006). However, the disadvantages of this systems is that they do not increase the stability of insulin in the harsh conditions of the gut. Moreover, the conjugation usually leads to a reduction in the bioactivity of the therapeutic agent (Xie et al., 2017). The

administration of insulin conjugated with cell penetrating peptides (CPP) directly into the ileum of rats has demonstrated to increase the bioavailability of the hormone, achieving a 5.5 ± 0.9%. In another study, the oral administration of insulin-transferrin conjugates induced a significant decrease in the glycemia of diabetic rats in a dose-dependent manner (Xia et al., 2000). Nevertheless, 11 hours post-adminsitration, the glycemia of the animals was reduced by 70%.

1.6.2. Liposomes

Liposomes are lipid vesicles formed by one or several phospholipid bilayers (unilamellar or multilamellar respectively) that generate an aqueous cavity in which hydrophilic molecules can be hosted. Moreover, hydrophobic molecules can be incorporated in the bilayer as well (Irache et al., 2011). Liposomes can interact with the target cell in several ways: i) they can get internalized (specifically or nonspecifically), and after cytosolic degradation, their cargo is released and passed to the bloodstream (Kim et al., 2013; Zhang et al., 2014); ii) they can fuse with the cell membrane and directly release their content into the cytosol; iii) they can just adhere to the cell membrane and release their cargo, which will enter into the cell via micropinocytosis (Torchilin, 2005). In spite of showing low stability in the gastrointestinal tract and poor encapsulation efficiencies, liposomes have good permeation properties due to their similar structure to cell membranes and, moreover, their surface can be modified with proteins, polysaccharides or polymers to improve their properties (Kaklotar et al., 2016; Kim et al., 2013; Lopes et al., 2015; Yazdi et al., 2020). Insulin-loaded liposomes are usually combined with bile salts (e.g. sodium deoxycholate, sodium taurocholate and sodium deoxycholate) because they give protection against enzymatic degradation and increase the pass through epithelial membranes (Kaklotar et al., 2016; Luo et al., 2016; Niu et al., 2014). Some disadvantages of liposomes are that they tend to aggregate and to release the entrapped drugs, specially highly hydrophilic ones, so their storage is a challenge (Irache et al., 2011; Keller, 2001). Insulin-loaded liposomes have demonstrated the capability of increase the oral bioavailability of the loaded drugs, reaching values of 11% compared to subcutaneous administration. Moreover, the hypoglycemic effect exerted by their administration to diabetic rats lasted a minimum period of time of 15 hours (Niu et al., 2012). In another study, surface-functionalized liposomes with PEG and folate acid increased the oral bioavailability of insulin to a 19.08%, compared to subcutaneous injection. Furthermore, in this study, the hypoglycemic effect following oral administration to diabetic was also increased, lasting 25 hours.

1.6.3. Solid lipid nanoparticles (SLNs)

SLNs are colloidal carriers composed by physiological GRAS (generally recognized as safe) solid lipids. These lipids are solid at room or body temperature and stabilized by surfactants. Compared to liposomes and other lipid carriers, they present several advantages: narrow size distribution, controlled drug release over time, protection of the cargo against chemical degradation, lack of organic solvents during the formulation, lower toxicity, ease to scale up and ease to freeze/spray dry (Gaba et al., 2015; Hirlekar et al., 2017; Irache et al., 2011). However, they present poor loading capacity and they aggregate during incubation in gastric fluid (Irache et al., 2011; Kaklotar et al., 2016). The surface of SLNs can also be modified with polymers or other molecules to modify

their physicochemical properties (Anchan and Koland, 2021; Koland et al., 2021; Zhang et al., 2006). SLNs have also been used for oral delivery of insulin, as they protect the hormone against the harsh conditions of the gastrointestinal tract. However, the high temperatures needed to melt the lipids and form the nanoparticles can affect the integrity of insulin, and thus, its activity (Lopes et al., 2015). SLNs can get internalized into the enterocyte through endocytosis but they are summited to lyso-endosomal degradation (Xu et al., 2018). They also present bioadhesive properties, so they can stick to the enterocytes and, through gradient diffusion, insulin leaves the SLN and gets absorbed by the enterocyte. When evaluated *in vivo*, insulin-loaded SLN showed worse results than liposomes, displaying an oral bioavailability of 7.11%, reaching the highest hypoglycemic effect 3h after the oral administration (Zhang et al., 2006). In another study, insulin-loaded SLN were coated with alginate, what increased the relative oral bioavailability to 15.7%, with a maximum hypoglycemic effect achieved 10 h post-administration (Koland et al., 2021).

Cationic solid lipid nanoparticles (cSLNs) are SLNs produced using at least one cationic lipid (Doktorovova et al., 2011). The main advantage of cSLNs compared to SLNs is that the electrostatic repulsion between the positively-charged nanoparticles avoids their aggregation. Moreover, cSLNs are more mucoadhesive due to the interaction of their positive surface charges with the negative charges of the mucus mucins (Hecq et al., 2016). However, despite there are no in vivo pharmacological studies for insulin-loaded cSLN, their efficacy for oral delivery purposes is expected to be worse than for neutral or negatively-charged SLN, as they demonstrated the lowest rates of oral absorption (Yu et al., 2019).

1.6.4. Self-nanoemulsifying drug delivery system (SNEDDS)

SNEDDS are isotropic mixtures of oil, surfactants, co-surfactants and the drug. This mixture spontaneously forms a nanoemulsion (O/W) in the GI tract or in aqueous solution (Irache et al., 2011; Li et al., 2014). SNEDDS can be used to entrap both hydrophilic and lipophilic molecules and they can pass through the intestinal mucus layer (depending on size, shape and surface modifications) (Friedl et al., 2013). For oral insulin delivery, SNEDDS have shown great encapsulation efficiency (100%) and very low release after incubation in bulk buffer during 24h. Encapsulated insulin into SNEDDS showed less proteolysis than free insulin and a sustained release profile (Ma et al., 2006). Moreover, insulin-loaded SNEDDS showed stable storage up to 6 months at 4ºC. When evaluated *in vivo*, insulin-loaded SNEDDS showed low relative oral bioavailability (1.8%), with the highest hypoglycemic effect achieved 4 h post-administration (Bravo-Alfaro et al., 2020). In another study, the relative bioavailability of insulin-loaded SNEDDS was slightly increased (7.15%), although this value is still very low. In this study, the hypoglycemic effect lasted for 4 hours, reaching its maximum effect 2 h after the oral administration (Zhang et al., 2012).

1.6.5 Polymeric nanoparticles

Nanoparticles can be classified in 2 groups: nanospheres, where the drug is dispersed into the polymer matrix, or nanocapsules where the polymer generates a film with an

empty core where the drug is entrapped (Hirlekar et al., 2017). Although there are several polymers that may be used for the formulation of nanoparticles, the most used devices are built of a combination of them. Some of the molecules used to prepare polymeric nanoparticles are: i) poly (lactic-co-glycolic acid) (PLGA): synthetic aliphatic polyester approved by the FDA. That displays high insulin entrapment efficiencies (up to 90%) (Hirlekar et al., 2017; Sharma et al., 2015). When evaluated in vivo, insulin-loaded PLGA nanoparticles showed an hypoglycemic effect that lasted more than 15 hours, with the maximum effect achieved 7.5 h post-administration, although no values for the oral bioavailability were provided (X. Zhang et al., 2012). Moreover, in the same study, the coating of PLGA nanoparticles with the mucoadhesive polymer chitosan increased the hypoglycemic effect of the formulation. In another study, the coating of PLGA nanoparticles with 5β-cholanic acid conjugated glycol chitosan, lead to an increased oral bioavailability of insulin, reaching the surprising value of 30.43% (Wang et al., 2021); ii) poly (acrylic acid) (PAA): mucoadhesive polymers based on acrylic and methacrylic acid with pH-dependent release of insulin. One of the most interesting properties of this polymer is its intrinsic capability to inhibit luminal proteolytic enzymes (Perera et al., 2009). However, although the encapsulation of insulin into PAA nanoparticles showed promising results *in vitro*, no experiments have been carried out in animal models; iii) dextran: bacterial polysaccharide with pH-sensitive properties that decreases blood viscosity. Its commonly used as coating for other nanoparticles in order to increase their biocompatibility and reduce the opsonization processes over them (Alhareth et al., 2012), although it can form nanoparticles by itself (Wasiak et al., 2016). Moreover, the surface of dextran nanoparticles can also be modified. For instance, vitamin B12-coated dextran nanoparticles have been evaluated in animal models, showing a biphasic hypoglycemic effect that lasted for a minimum period of time of 54 h (Chalasani et al., 2007); iv) alginate: anionic algae polysaccharide with mucoadhesive properties, biocompatible and non-immunogenic. Despite alginate nanoparticles have low drug encapsulation efficacy by themselves, it can be increased by combination with other polymers (Sonia and Sharma, 2012). In an animal of diabetic rats, oral administration of alginate nanoparticles loaded with insulin induced an significant hypoglycemic effect that lasted 5 h and whose maximum effect was found to be 3-to-4 h post-administration (Li et al., 2021). In the same study, the modification of the nanoparticles with octaarginine increased the efficacy of the formulation, leading to a more potent and long-lasting hypoglycemic effect; v) chitosan: polycationic polymer with mucoadhesive and absorption enhancer properties that can entrap both hydrophilic and hydrophobic drugs. It is the most widely studied polymer for the oral administration of insulin because of its promising results so far. The main problem of chitosan nanoparticles is their sensitivity to acidic conditions, in which it gets dissolved (Van Der Merwe et al., 2004), resulting in a burst release during its pass through the stomach. Following oral administration to diabetic animals, insulin-loaded chitosan nanoparticles induced an hypoglycemic effect that lasted for 10 hours, showing the maximum effect 6 h after the administration (Mukhopadhyay et al., 2013). In another study in which chitosan nanoparticles were modified by thiolation, the hypoglycemic effect induced by insulin-loaded nanoparticles showed the highest effect 2 h post-administration, although the

total effect lasted for 6 hours (Sudhakar et al., 2020); vi) zein: vegetal protein obtained from maize, widely used in the pharmaceutical as well as in other industries (Martínez-López et al., 2020). Zein nanoparticles have shown high stability in simulated gastric fluid, as well as a sustained release of the loaded drug. When evaluated in animals, insulin-loaded zein nanoparticles showed a potent hypoglycemic effect that lasted for more than 17 h, with the maximum effect observed 10 h post-administration (Inchaurraga et al., 2020). Moreover, in that study, the oral bioavailability achieved with insulin nanoparticles was found to be 5.2%.

In summary, although there are several nanoformulations aiming the oral administration of insulin, and, despite some of them showed promising results in animal models, there is not currently any available drug in the market for the oral administration of insulin.

1.7. References

2017 Alzheimer's disease facts and figures, 2017. . Alzheimer's Dement. 13, 325–373. https://doi.org/10.1016/j.jalz.2017.02.001

Ahima, R.S., 2009. Connecting obesity, aging and diabetes. Nat. Med. 15, 996–997. https://doi.org/10.1038/nm0909-996

Ahmad, A., Othman, I., Zaini, A., Chowdhury, E.H., 2012. Oral Nano-Insulin Therapy: Current Progress on Nanoparticle-Based Devices for Intestinal Epithelium-Targeted Insulin Delivery. J. Nanomed. Nanotechnol. s4. https://doi.org/10.4172/2157-7439.s4-007

Ahrén, B., 2012. Incretin hormones and the up-regulation of insulin secretion in insulin resistance. J. Clin. Endocrinol. Metab. 97, 1173–1175. https://doi.org/10.1210/jc.2012-1420

Ahrén, B., 2007. DPP-4 inhibitors. Best Pract. Res. Clin. Endocrinol. Metab. 21, 517–533. https://doi.org/10.1016/j.beem.2007.07.005

Alhareth, K., Vauthier, C., Bourasset, F., Gueutin, C., Ponchel, G., Moussa, F., 2012. Conformation of surface-decorating dextran chains affects the pharmacokinetics and biodistribution of doxorubicin-loaded nanoparticles. Eur. J. Pharm. Biopharm. 81, 453–457. https://doi.org/10.1016/j.ejpb.2012.03.009

Anchan, R.B., Koland, M., 2021. Oral Insulin Delivery by Chitosan Coated Solid Lipid Nanoparticles: Ex vivo and in vivo Studies. J. Young Pharm. 13, 43–48. https://doi.org/10.5530/jyp.2021.13.10

Anderberg, R.H., Richard, J.E., Hansson, C., Nissbrandt, H., Bergquist, F., Skibicka, K.P., 2016. GLP-1 is both anxiogenic and antidepressant; divergent effects of acute and chronic GLP-1 on emotionality. Psychoneuroendocrinology 65, 54–66. https://doi.org/10.1016/j.psyneuen.2015.11.021

Arnold, S.E., Lucki, I., Brookshire, B.R., Carlson, G.C., Browne, C.A., Kazi, H., Bang, S., Choi, B.R., Chen, Y., McMullen, M.F., Kim, S.F., 2014. High fat diet produces brain insulin resistance, synaptodendritic abnormalities and altered behavior in mice. Neurobiol. Dis. 67, 79–87. https://doi.org/10.1016/j.nbd.2014.03.011

Asmar, M., Asmar, A., Simonsen, L., Dela, F., Holst, J.J., Bülow, J., 2019. GIP-induced vasodilation in human adipose tissue involves capillary recruitment. Endocr. Connect. 8, 806–813. https://doi.org/10.1530/EC-19-0144

Atkinson, M.A., Eisenbarth, G.S., Michels, A.W., 2014. Type 1 diabetes. Lancet 383, 69–82. https://doi.org/10.1016/S0140-6736(13)60591-7

Ayala, J.E., Bracy, D.P., James, F.D., Julien, B.M., Wasserman, D.H., Drucker, D.J., 2009. The glucagon-like peptide-1 receptor regulates endogenous glucose production and muscle glucose uptake independent of its incretin action. Endocrinology 150, 1155–1164. https://doi.org/10.1210/en.2008-0945

Baggio, L.L., Drucker, D.J., 2007. Biology of Incretins: GLP-1 and GIP. Gastroenterology 132, 2131–2157. https://doi.org/10.1053/j.gastro.2007.03.054

Ballav, C., Dhere, A., Kennedy, I., Agbaje, O.F., White, S., Franklin, R., Hartmann, B., Holst, J.J., Holman, R.R., Owen, K.R., 2020. Lixisenatide in type 1 diabetes: A randomised control trial of the effect of lixisenatide on post-meal glucose excursions and glucagon in type 1 diabetes patients. Endocrinol. Diabetes Metab. 3, e00130. https://doi.org/10.1002/edm2.130

Batista, A.F., Forny-Germano, L., Clarke, J.R., Lyra e Silva, N.M., Brito-Moreira, J., Boehnke, S.E., Winterborn, A., Coe, B.C., Lablans, A., Vital, J.F., Marques, S.A., Martinez, A.M.B., Gralle, M., Holscher, C., Klein, W.L., Houzel, J.C., Ferreira, S.T., Munoz, D.P., De Felice, F.G., 2018. The diabetes drug liraglutide reverses cognitive impairment in mice and attenuates insulin receptor and synaptic pathology in a non-human primate model of Alzheimer's disease. J. Pathol. 245, 85–100. https://doi.org/10.1002/path.5056

Ben Lulu, S., Coran, A.G., Mogilner, J.G., Shaoul, R., Shamir, R., Shehadeh, N., Sukhotnik, I., 2010. Oral insulin stimulates intestinal epithelial cell turnover in correlation with insulin-receptor expression along the villus-crypt axis in a rat model of short bowel syndrome. Pediatr. Surg. Int. 26, 37–44. https://doi.org/10.1007/s00383-009-2520-x

Bernkop-Schnürch, A., 1998. The use of inhibitory agents to overcome the enzymatic barrier to perorally administered therapeutic peptides and proteins. J. Control. Release 52, 1–16. https://doi.org/10.1016/S0168-3659(97)00204-6

Blakely, K.K., Weaver, K., 2020. Semaglutide Is a New Once-Daily Oral Medication to Treat Type 2 Diabetes. Nurs. Womens. Health 24, 370–376. https://doi.org/10.1016/j.nwh.2020.07.005

Blázquez, E., Velázquez, E., Hurtado-Carneiro, V., Ruiz-Albusac, J.M., 2014. Insulin in the brain: Its pathophysiological implications for states related with central insulin resistance, type 2 diabetes and alzheimer's disease. Front. Endocrinol. (Lausanne). https://doi.org/10.3389/fendo.2014.00161

Bohórquez, D. V., Shahid, R.A., Erdmann, A., Kreger, A.M., Wang, Y., Calakos, N., Wang, F., Liddle, R.A., 2015. Neuroepithelial circuit formed by innervation of sensory enteroendocrine cells. J. Clin. Invest. 125, 782–786. https://doi.org/10.1172/JCI78361

Bommer, C., Sagalova, V., Heesemann, E., Manne-Goehler, J., Atun, R., Bärnighausen, T., Davies, J., Vollmer, S., 2018. Global Economic Burden of Diabetes in Adults: Projections From 2015 to 2030. Diabetes Care 41, 963–970. https://doi.org/10.2337/dc17-1962

Boughton, C.K., Hovorka, R., 2019. Is an artificial pancreas (closed-loop system) for Type 1 diabetes effective? Diabet. Med. 36, 279–286. https://doi.org/10.1111/dme.13816

Bravo-Alfaro, D.A., Muñoz-Correa, M.O.F., Santos-Luna, D., Toro-Vazquez, J.F., Cano-Sarmiento, C., García-Varela, R., García, H.S., 2020. Encapsulation of an insulin-modified phosphatidylcholine complex in a self-nanoemulsifying drug delivery system (SNEDDS) for oral insulin delivery. J. Drug Deliv. Sci. Technol. 57, 101622.

https://doi.org/10.1016/j.jddst.2020.101622

Brighton, C.A., Rievaj, J., Kuhre, R.E., Glass, L.L., Schoonjans, K., Holst, J.J., Gribble, F.M., Reimann, F., 2015. Bile acids trigger GLP-1 release predominantly by accessing basolaterally located G protein-coupled bile acid receptors. Endocrinology 156, 3961–3970. https://doi.org/10.1210/en.2015-1321

Brun, J.F., Fedou, C., Mercier, J., 2000. Postprandial reactive hypoglycemia. Diabetes Metab. 26, 337–351. https://doi.org/10.14744/semb.2019.59455

Bucheit, J.D., Pamulapati, L.G., Carter, N., Malloy, K., Dixon, D.L., Sisson, E.M., 2020. Oral Semaglutide: A Review of the First Oral Glucagon-Like Peptide 1 Receptor Agonist. Diabetes Technol. Ther. 22, 10–18. https://doi.org/10.1089/dia.2019.0185

Bugliani, M., Syed, F., Paula, F.M.M., Omar, B.A., Suleiman, M., Mossuto, S., Grano, F., Cardarelli, F., Boggi, U., Vistoli, F., Filipponi, F., De Simone, P., Marselli, L., De Tata, V., Ahren, B., Eizirik, D.L., Marchetti, P., 2018. DPP-4 is expressed in human pancreatic beta cells and its direct inhibition improves beta cell function and survival in type 2 diabetes. Mol. Cell. Endocrinol. 473, 186–193. https://doi.org/10.1016/j.mce.2018.01.019

Burton, D.G.A., Faragher, R.G.A., 2018. Obesity and type-2 diabetes as inducers of premature cellular senescence and ageing. Biogerontology 19, 447–459. https://doi.org/10.1007/s10522-018-9763-7

Capuano, A., Sportiello, L., Maiorino, M.I., Rossi, F., Giugliano, D., Esposito, K., 2013. Dipeptidyl peptidase-4 inhibitors in type 2 diabetes therapy - Focus on alogliptin. Drug Des. Devel. Ther. 7, 989–1001. https://doi.org/10.2147/DDDT.S37647

Caspersen, C.J., Thomas, G.D., Boseman, L.A., Beckles, G.L.A., Albright, A.L., 2012. Aging, diabetes, and the public health system in the United States. Am. J. Public Health 102, 1482–1497. https://doi.org/10.2105/AJPH.2011.300616

Chai, W., Dong, Z., Wang, N., Wang, W., Tao, L., Cao, W., Liu, Z., 2012. Glucagon-like peptide 1 recruits microvasculature and increases glucose use in muscle via a nitric oxide-dependent mechanism. Diabetes 61, 888–896. https://doi.org/10.2337/db11-1073

Chalasani, K.B., Russell-Jones, G.J., Jain, A.K., Diwan, P. V., Jain, S.K., 2007. Effective oral delivery of insulin in animal models using vitamin B12-coated dextran nanoparticles. J. Control. Release 122, 141–150. https://doi.org/10.1016/j.jconrel.2007.05.019

Chalichem, N.S.S., Gonugunta, C., Krishnamurthy, P.T., Duraiswamy, B., 2017. DPP4 Inhibitors Can Be a Drug of Choice for Type 3 Diabetes: A Mini Review. Am. J. Alzheimers. Dis. Other Demen. 32, 444–451. https://doi.org/10.1177/1533317517722005

Chen, E., King, F., Kohn, M.A., Spanakis, E.K., Breton, M., Klonoff, D.C., 2019. A Review of predictive low glucose suspend and its effectiveness in preventing nocturnal hypoglycemia. Diabetes Technol. Ther. 21, 589–601. https://doi.org/10.1089/dia.2019.0119

Chen, M.C., Sonaje, K., Chen, K.J., Sung, H.W., 2011. A review of the prospects for polymeric nanoparticle platforms in oral insulin delivery. Biomaterials 32, 9826–9838. https://doi.org/10.1016/j.biomaterials.2011.08.087

Cheng, Z., Tseng, Y., White, M.F., 2010. Insulin signaling meets mitochondria in metabolism. Trends Endocrinol. Metab. https://doi.org/10.1016/j.tem.2010.06.005

Cho, N.H., Shaw, J.E., Karuranga, S., Huang, Y., da Rocha Fernandes, J.D., Ohlrogge, A.W., Malanda, B., 2018. IDF Diabetes Atlas: Global estimates of diabetes prevalence for 2017 and projections for 2045. Diabetes Res. Clin. Pract. 138, 271–281. https://doi.org/10.1016/j.diabres.2018.02.023

Claxton, A., Baker, L.D., Hanson, A., Trittschuh, E.H., Cholerton, B., Morgan, A., Callaghan, M., Arbuckle, M., Behl, C., Craft, S., 2015. Long-acting intranasal insulin detemir improves cognition for adults with mild cognitive impairment or early-stage Alzheimer's Disease dementia. J. Alzheimer's Dis. 44, 897–906. https://doi.org/10.3233/JAD-141791

Clemmensen, C., Smajilovic, S., Smith, E.P., Woods, S.C., Bräuner-Osborne, H., Seeley, R.J., D'Alessio, D.A., Ryan, K.K., 2013. Oral L-arginine stimulates GLP-1 secretion to improve glucose tolerance in male mice. Endocrinology 154, 3978–3983. https://doi.org/10.1210/en.2013-1529

Constantinescu, T., Lungu, C.N., Lung, I., 2019. Lipophilicity as a central component of drug-like properties of chalchones and flavonoid derivatives. Molecules 24, 1505. https://doi.org/10.3390/molecules24081505

Craft, S., Baker, L.D., Montine, T.J., Minoshima, S., Watson, G.S., Claxton, A., Arbuckle, M., Callaghan, M., Tsai, E., Plymate, S.R., Green, P.S., Leverenz, J., Cross, D., Gerton, B., 2012. Intranasal insulin therapy for Alzheimer disease and amnestic mild cognitive impairment: A pilot clinical trial. Arch. Neurol. 69, 29–38. https://doi.org/10.1001/archneurol.2011.233

Crane, P.K., Walker, R., Hubbard, R.A., Li, G., Nathan, D.M., Zheng, H., Haneuse, S., Craft, S., Montine, T.J., Kahn, S.E., McCormick, W., McCurry, S.M., Bowen, J.D., Larson, E.B., 2013. Glucose levels and risk of dementia. Forsch. Komplementarmed. 20, 386–387. https://doi.org/10.1056/nejmoa1215740

Cryer, P.E., 1999. Symptoms of hypoglycemia, thresholds for their occurrence, and hypoglycemia unawareness. Endocrinol. Metab. Clin. North Am. 28, 495–500. https://doi.org/10.1016/S0889-8529(05)70084-0

Czech, M.P., 2017. Insulin action and resistance in obesity and type 2 diabetes. Nat. Med. 23, 804–814. https://doi.org/10.1038/nm.4350

Daneman, D., 2006. Type 1 diabetes. Lancet 367, 847–858. https://doi.org/10.1016/S0140-6736(06)68341-4

Dardevet, D., Moore, M.C., Neal, D., DiCostanzo, C.A., Snead, W., Cherrington, A.D., 2004. Insulin-independent effects of GLP-1 on canine liver glucose metabolism: Duration of infusion and involvement of hepatoportal region. Am. J. Physiol. -

Endocrinol. Metab. 287, E75–E81. https://doi.org/10.1152/ajpendo.00035.2004

Darwish, L., Beroncal, E., Sison, M.V., Swardfager, W., 2018. Depression in people with type 2 diabetes: Current perspectives. Diabetes, Metab. Syndr. Obes. Targets Ther. 11, 333–343. https://doi.org/10.2147/DMSO.S106797

De la Monte, S.M., 2014. Type 3 diabetes is sporadic Alzheimer-s disease: Mini-review. Eur. Neuropsychopharmacol. 24, 1954–1960. https://doi.org/10.1016/j.euroneuro.2014.06.008

De La Monte, S.M., Wands, J.R., 2008. Alzheimer's disease is type 3 diabetes-evidence reviewed. J. Diabetes Sci. Technol. https://doi.org/10.1177/193229680800200619

Deeney, J.T., Prentki, M., Corkey, B.E., 2000. Metabolic control of β-cell function. Semin. Cell Dev. Biol. 11, 267–275. https://doi.org/10.1006/scdb.2000.0175

Diabetes NSF Team, 2012. National Service Framework for Diabetes: Standards, Department of Health and Social Care.

Dimitriadis, G., Mitron, P., Lambadiari, V., Maratou, E., Raptis, S.A., 2011. Insulin effects in muscle and adipose tissue, Diabetes Research and Clinical Practice. https://doi.org/10.1016/S0168-8227(11)70014-6

Dimmeler, S., Zeiher, A.M., 1999. Nitric oxide - An endothelial cell survival factor. Cell Death Differ. 6, 964–968. https://doi.org/10.1038/sj.cdd.4400581

Ding, K.H., Zhong, Q., Xu, J., Isales, C.M., 2004. Glucose-dependent insulinotropic peptide: Differential effects on hepatic artery vs. portal vein endothelial cells. Am. J. Physiol. - Endocrinol. Metab. 286. https://doi.org/10.1152/ajpendo.00507.2003

Doktorovova, S., Shegokar, R., Rakovsky, E., Gonzalez-Mira, E., Lopes, C.M., Silva, A.M., Martins-Lopes, P., Muller, R.H., Souto, E.B., 2011. Cationic solid lipid nanoparticles (cSLN): Structure, stability and DNA binding capacity correlation studies. Int. J. Pharm. 420, 341–349. https://doi.org/10.1016/j.ijpharm.2011.08.042

Dorton, H.M., Luo, S., Monterosso, J.R., Page, K.A., 2018. Influences of Dietary Added Sugar Consumption on Striatal Food-Cue Reactivity and Postprandial GLP-1 Response. Front. Psychiatry 0, 297. https://doi.org/10.3389/FPSYT.2017.00297

Douillard, C., Jannin, A., Vantyghem, M.C., 2020. Rare causes of hypoglycemia in adults. Ann. Endocrinol. (Paris). 81, 110–117. https://doi.org/10.1016/j.ando.2020.04.003

Doyle, F.J., Huyett, L.M., Lee, J.B., Zisser, H.C., Dassau, E., 2014. Closed-loop artificial pancreas systems: Engineering the algorithms. Diabetes Care 37, 1191–1197. https://doi.org/10.2337/dc13-2108

El, K., Campbell, J.E., 2020. The role of GIP in α-cells and glucagon secretion. Peptides. https://doi.org/10.1016/j.peptides.2019.170213

Elderman, M., Sovran, B., Hugenholtz, F., Graversen, K., Huijskes, M., Houtsma, E., Belzer, C., Boekschoten, M., De Vos, P., Dekker, J., Wells, J., Faas, M., 2017. The effect of age on the intestinal mucus thickness, microbiota composition and immunity in relation to sex in mice. PLoS One 12, e0184274. https://doi.org/10.1371/journal.pone.0184274

Fandiño, J., Toba, L., González-Matías, L.C., Diz-Chaves, Y., Mallo, F., 2020. GLP-1 receptor agonist ameliorates experimental lung fibrosis. Sci. Rep. 10, 1–15. https://doi.org/10.1038/s41598-020-74912-1

Farngren, J., Ahrén, B., 2019. Incretin-based medications (GLP-1 receptor agonists, DPP-4 inhibitors) as a means to avoid hypoglycaemic episodes. Metabolism. 99, 25–31. https://doi.org/10.1016/j.metabol.2019.06.016

Foretz, M., Guigas, B., Viollet, B., 2019. Understanding the glucoregulatory mechanisms of metformin in type 2 diabetes mellitus. Nat. Rev. Endocrinol. 15, 569–589. https://doi.org/10.1038/s41574-019-0242-2

Forlenza, G.P., Li, Z., Buckingham, B.A., Pinsker, J.E., Cengiz, E., Paul Wadwa, R., Ekhlaspour, L., Church, M.M., Weinzimer, S.A., Jost, E., Marcal, T., Andre, C., Carria, L., Swanson, V., Lum, J.W., Kollman, C., Woodall, W., Beck, R.W., 2018. Predictive low-glucose suspend reduces hypoglycemia in adults, adolescents, and children with type 1 diabetes in an at-home randomized crossover study: Results of the PROLOG trial. Diabetes Care 41, 2155–2161. https://doi.org/10.2337/dc18-0771

Friedl, H., Dünnhaupt, S., Hintzen, F., Waldner, C., Parikh, S., Pearson, J.P., Wilcox, M.D., Bernkop-Schnürch, A., 2013. Development and evaluation of a novel mucus diffusion test system approved by self-nanoemulsifying drug delivery Systems. J. Pharm. Sci. 102, 4406–4413. https://doi.org/10.1002/jps.23757

Fu, Z., R. Gilbert, E., Liu, D., 2012. Regulation of Insulin Synthesis and Secretion and Pancreatic Beta-Cell Dysfunction in Diabetes. Curr. Diabetes Rev. 9, 25–53. https://doi.org/10.2174/15733998130104

Fujita, S., Rasmussen, B.B., Cadenas, J.G., Grady, J.J., Volpi, E., 2006. Effect of insulin on human skeletal muscle protein synthesis is modulated by insulin-induced changes in muscle blood flow and amino acid availability. Am. J. Physiol. - Endocrinol. Metab. 291. https://doi.org/10.1152/ajpendo.00271.2005

Gaba, B., Fazil, M., Ali, A., Baboota, S., Sahni, J.K., Ali, J., 2015. Nanostructured lipid (NLCs) carriers as a bioavailability enhancement tool for oral administration. Drug Deliv. 22, 691–700. https://doi.org/10.3109/10717544.2014.898110

Gabbouj, S., Ryhänen, S., Marttinen, M., Wittrahm, R., Takalo, M., Kemppainen, S., Martiskaine, H., Tanila, H., Haapasalo, A., Hiltunen, M., Natunen, T., 2019. Altered insulin signaling in Alzheimer's disease brain-special emphasis on pi3k-akt pathway. Front. Neurosci. 13, 629. https://doi.org/10.3389/fnins.2019.00629

Gagnon, J., Baggio, L.L., Drucker, D.J., Brubaker, P.L., 2015. Ghrelin is a novel regulator of GLP-1 secretion. Diabetes 64, 1513–1521. https://doi.org/10.2337/db14-1176

Garre-Olmo, J., 2018. Epidemiology of alzheimer's disease and other dementias. Rev. Neurol. https://doi.org/10.33588/rn.6611.2017519

Gasa, R., Gomis, R., Novials, A., Servitja, J.M., 2016. Molecular Aspects of Glucose Regulation of Pancreatic β Cells. Mol. Nutr. Diabetes A Vol. Mol. Nutr. Ser. 155–168. https://doi.org/10.1016/B978-0-12-801585-8.00013-0

Gedawy, A., Martinez, J., Al-Salami, H., Dass, C.R., 2018. Oral insulin delivery: existing

barriers and current counter-strategies. J. Pharm. Pharmacol. 70, 197–213. https://doi.org/10.1111/jphp.12852

Ghasemi, R., Haeri, A., Dargahi, L., Mohamed, Z., Ahmadiani, A., 2013. Insulin in the brain: Sources, localization and functions. Mol. Neurobiol. https://doi.org/10.1007/s12035-012-8339-9

Ghazi, T., Rink, L., Sherr, J.L., Herold, K.C., 2014. Acute metabolic effects of exenatide in patients with type 1 diabetes with and without residual insulin to oral and intravenous glucose challenges. Diabetes Care 37, 210–216. https://doi.org/10.2337/dc13-1169

Gholap, N.N., Davies, M.J., Mostafa, S.A., Khunti, K., 2013. Diagnosing type 2 diabetes and identifying high-risk individuals using the new glycated haemoglobin (HbA1c) criteria. Br. J. Gen. Pract. 63, e165–e167. https://doi.org/10.3399/bjgp13X663244

Golay, A., Ybarra, J., 2005. Link between obesity and type 2 diabetes. Best Pract. Res. Clin. Endocrinol. Metab. 19, 649–663. https://doi.org/10.1016/j.beem.2005.07.010

Goldin, A., Beckman, J.A., Schmidt, A.M., Creager, M.A., 2006. Advanced glycation end products: Sparking the development of diabetic vascular injury. Circulation 114, 597–605. https://doi.org/10.1161/CIRCULATIONAHA.106.621854

Greenwell, A.A., Chahade, J.J., Ussher, J.R., 2020. Cardiovascular biology of the GIP receptor. Peptides 125, 170228. https://doi.org/10.1016/j.peptides.2019.170228

Grover, S.A., Kaouache, M., Rempel, P., Joseph, L., Dawes, M., Lau, D.C.W., Lowensteyn, I., 2015. Years of life lost and healthy life-years lost from diabetes and cardiovascular disease in overweight and obese people: A modelling study. Lancet Diabetes Endocrinol. 3, 114–122. https://doi.org/10.1016/S2213-8587(14)70229-3

Guerrero-Hreins, E., Goldstone, A.P., Brown, R.M., Sumithran, P., 2021. The therapeutic potential of GLP-1 analogues for stress-related eating and role of GLP-1 in stress, emotion and mood: a review. Prog. Neuro-Psychopharmacology Biol. Psychiatry 110, 110303. https://doi.org/10.1016/j.pnpbp.2021.110303

Gupta, A., Al-Aubaidy, H.A., Mohammad, B., 2016. Glucose dependent insulinotropic polypeptide and dipeptidyl peptidase inhibitors: Their roles in management of type 2 diabetes mellitus. Diabetes Metab. Syndr. Clin. Res. Rev. 10, S170–S175. https://doi.org/10.1016/j.dsx.2016.03.013

Halim, M., Halim, A., 2019. The effects of inflammation, aging and oxidative stress on the pathogenesis of diabetes mellitus (type 2 diabetes). Diabetes Metab. Syndr. Clin. Res. Rev. 13, 1165–1172. https://doi.org/10.1016/j.dsx.2019.01.040

Hall, C., Yu, H., Choi, E., 2020. Insulin receptor endocytosis in the pathophysiology of insulin resistance. Exp. Mol. Med. 52, 911–920. https://doi.org/10.1038/s12276-020-0456-3

Hallschmid, M., 2021. Intranasal Insulin for Alzheimer's Disease. CNS Drugs 35, 21–37. https://doi.org/10.1007/s40263-020-00781-x

Hansen, H.H., Fabricius, K., Barkholt, P., Niehoff, M.L., Morley, J.E., Jelsing, J., Pyke, C., Knudsen, L.B., Farr, S.A., Vrang, N., 2015. The GLP-1 Receptor Agonist Liraglutide Improves Memory Function and Increases Hippocampal CA1 Neuronal Numbers in a Senescence-Accelerated Mouse Model of Alzheimer's Disease. J. Alzheimer's Dis. 46, 877–888. https://doi.org/10.3233/JAD-143090

He, Z., Liu, Z., Tian, H., Hu, Y., Liu, L., Leong, K.W., Mao, H.Q., Chen, Y., 2018. Scalable production of core-shell nanoparticles by flash nanocomplexation to enhance mucosal transport for oral delivery of insulin. Nanoscale 10, 3307–3319. https://doi.org/10.1039/c7nr08047f

Hecq, J., Amighi, K., Goole, J., 2016. Development and evaluation of insulin-loaded cationic solid lipid nanoparticles for oral delivery. J. Drug Deliv. Sci. Technol. 36, 192–200. https://doi.org/10.1016/j.jddst.2016.10.012

Heimbürger, S.M., Bergmann, N.C., Augustin, R., Gasbjerg, L.S., Christensen, M.B., Knop, F.K., 2020. Glucose-dependent insulinotropic polypeptide (GIP) and cardiovascular disease. Peptides 125, 170174. https://doi.org/10.1016/j.peptides.2019.170174

Helsted, M.M., Gasbjerg, L.S., Lanng, A.R., Bergmann, N.C., Stensen, S., Hartmann, B., Christensen, M.B., Holst, J.J., Vilsbøll, T., Rosenkilde, M.M., Knop, F.K., 2020. The role of endogenous GIP and GLP-1 in postprandial bone homeostasis. Bone 140, 115553. https://doi.org/10.1016/j.bone.2020.115553

Henquin, J.C., Dufrane, D., Nenquin, M., 2006. Nutrient control of insulin secretion in isolated normal human islets. Diabetes 55, 3470–3477. https://doi.org/10.2337/db06-0868

Henquin, J.C., Ishiyama, N., Nenquin, M., Ravier, M.A., Jonas, J.C., 2002. Signals and pools underlying biphasic insulin secretion, in: Diabetes. American Diabetes Association, pp. S60–S67. https://doi.org/10.2337/diabetes.51.2007.s60

Herold, K.C., Reynolds, J., Dziura, J., Baidal, D., Gaglia, J., Gitelman, S.E., Gottlieb, P.A., Marks, J., Philipson, L.H., Pop-Busui, R., Weinstock, R.S., 2020. Exenatide extended release in patients with type 1 diabetes with and without residual insulin production. Diabetes, Obes. Metab. 22, 2045–2054. https://doi.org/10.1111/dom.14121

Hirlekar, R.S., Patil, E.J., Bhairy, S.R., 2017. Oral insulin delivery: Novel strategies. Asian J. Pharm. 11, S434–S443.

Hodson, R., 2018. Alzheimer's disease. Nature. https://doi.org/10.1038/d41586-018-05717-6

Hoeg-Jensen, T., 2021. Review: Glucose-sensitive insulin. Mol. Metab. 46, 101107. https://doi.org/10.1016/j.molmet.2020.101107

Hölscher, C., 2014. The incretin hormones glucagonlike peptide 1 and glucose-dependent insulinotropic polypeptide are neuroprotective in mouse models of Alzheimer's disease. Alzheimer's Dement. 10. https://doi.org/10.1016/j.jalz.2013.12.009

Holst, J.J., 2019. The incretin system in healthy humans: The role of GIP and GLP-1.

Metabolism. 96, 46–55. https://doi.org/10.1016/j.metabol.2019.04.014

Hruby, V.J., 1998. Chapter 16 Glucagon: Molecular biology and structure-activity. Princ. Med. Biol. 10, 387–401. https://doi.org/10.1016/S1569-2582(97)80161-4

Hwang, S.R., Byun, Y., 2014. Advances in oral macromolecular drug delivery. Expert Opin. Drug Deliv. 11, 1955–1967. https://doi.org/10.1517/17425247.2014.945420

Iepsen, E.W., Lundgren, J.R., Hartmann, B., Pedersen, O., Hansen, T., Jørgensen, N.R., Jensen, J.E.B., Holst, J.J., Madsbad, S., Torekov, S.S., 2015. GLP-1 receptor agonist treatment increases bone formation and prevents bone loss in weight-reduced obese women. J. Clin. Endocrinol. Metab. 100, 2909–2917. https://doi.org/10.1210/jc.2015-1176

Ignarro, L.J., 1989. Endothelium-derived nitric oxide: actions and properties. FASEB J. 3, 31–36. https://doi.org/10.1096/fasebj.3.1.2642868

Iliadis, F., Kadoglou, N., Didangelos, T., 2011. Insulin and the heart. Diabetes Res. Clin. Pract. 93. https://doi.org/10.1016/S0168-8227(11)70019-5

Imam, S.K., 2015. Diabetes: A New Horizon and Approach to Management. Glucose Intake Util. Pre-Diabetes Diabetes Implic. Cardiovasc. Dis. 29–44. https://doi.org/10.1016/B978-0-12-800093-9.00003-X

Inchaurraga, L., Martínez-López, A.L., Martin-Arbella, N., Irache, J.M., 2020. Zein-based nanoparticles for the oral delivery of insulin. Drug Deliv. Transl. Res. 10, 1601–1611. https://doi.org/10.1007/s13346-020-00796-3

Irache, J.M., Esparza, I., Gamazo, C., Agüeros, M., Espuelas, S., 2011. Nanomedicine: Novel approaches in human and veterinary therapeutics. Vet. Parasitol. 180, 47–71. https://doi.org/10.1016/j.vetpar.2011.05.028

Ishikawa, Y., Hira, T., Inoue, D., Harada, Y., Hashimoto, H., Fujii, M., Kadowaki, M., Hara, H., 2015. Rice protein hydrolysates stimulate GLP-1 secretion, reduce GLP-1 degradation, and lower the glycemic response in rats. Food Funct. 6, 2525–2534. https://doi.org/10.1039/c4fo01054j

Jaldin-Fincati, J.R., Pereira, R.V.S., Bilan, P.J., Klip, A., 2018. Insulin uptake and action in microvascular endothelial cells of lymphatic and blood origin. Am. J. Physiol. - Endocrinol. Metab. 315, E204–E217. https://doi.org/10.1152/ajpendo.00008.2018

Jiang, X., Tian, W., Nicolls, M.R., Rockson, S.G., 2019. The Lymphatic System in Obesity, Insulin Resistance, and Cardiovascular Diseases. Front. Physiol. https://doi.org/10.3389/fphys.2019.01402

Jin, T., Weng, J., 2016. Hepatic functions of GLP-1 and its based drugs: Current disputes and perspectives. Am. J. Physiol. - Endocrinol. Metab. 311, E620–E627. https://doi.org/10.1152/ajpendo.00069.2016

Johansson, M.E.V., Ambort, D., Pelaseyed, T., Schütte, A., Gustafsson, J.K., Ermund, A., Subramani, D.B., Holmén-Larsson, J.M., Thomsson, K.A., Bergström, J.H., Van Der Post, S., Rodriguez-Piñeiro, A.M., Sjövall, H., Bäckström, M., Hansson, G.C., 2011. Composition and functional role of the mucus layers in the intestine. Cell. Mol. Life

Sci. 68, 3635–3641. https://doi.org/10.1007/s00018-011-0822-3

Jung, U.J., Choi, M.S., 2014. Obesity and its metabolic complications: The role of adipokines and the relationship between obesity, inflammation, insulin resistance, dyslipidemia and nonalcoholic fatty liver disease. Int. J. Mol. Sci. https://doi.org/10.3390/ijms15046184

Kaklotar, D., Agrawal, P., Abdulla, A., Singh, R.P., Sonali, Mehata, A.K., Singh, S., Mishra, B., Pandey, B.L., Trigunayat, A., Muthu, M.S., 2016. Transition from passive to active targeting of oral insulin nanomedicines: Enhancement in bioavailability and glycemic control in diabetes. Nanomedicine 11, 1465–1486. https://doi.org/10.2217/nnm.16.43

Kalyani, R.R., Golden, S.H., Cefalu, W.T., 2017. Diabetes and aging: Unique considerations and goals of care. Diabetes Care 40, 440–443. https://doi.org/10.2337/dci17-0005

Kamboj, M.K., Henry, R.K., 2018. Diabetes in children and adolescents. Chronic Dis. Disabil. Pediatr. Gastrointest. Tract 223–239. https://doi.org/10.1016/b978-0-12-407822-2.00012-8

Kandimalla, R., Thirumala, V., Reddy, P.H., 2017. Is Alzheimer's disease a Type 3 Diabetes? A critical appraisal. Biochim. Biophys. Acta - Mol. Basis Dis. https://doi.org/10.1016/j.bbadis.2016.08.018

Kaplan, A.M., Vigna, S.R., 1994. Gastric inhibitory polypeptide (GIP) binding sites in rat brain. Peptides 15, 297–302. https://doi.org/10.1016/0196-9781(94)90016-7

Katsiki, N., Tousoulis, D., 2020. Diabetes mellitus and comorbidities: A bad romance. Hell. J. Cardiol. 61, 23–25. https://doi.org/10.1016/j.hjc.2020.02.009

Kavimandan, N.J., Losi, E., Peppas, N.A., 2006. Novel delivery system based on complexation hydrogels as delivery vehicles for insulin-transferrin conjugates. Biomaterials 27, 3846–3854. https://doi.org/10.1016/j.biomaterials.2006.02.026

Keegan, M.T., 2018. Endocrine pharmacology. Pharmacol. Physiol. Anesth. Found. Clin. Appl. 708–731. https://doi.org/10.1016/B978-0-323-48110-6.00036-3

Kellar, D., Craft, S., 2020. Brain insulin resistance in Alzheimer's disease and related disorders: mechanisms and therapeutic approaches. Lancet Neurol. 19, 758–766. https://doi.org/10.1016/S1474-4422(20)30231-3

Keller, B.C., 2001. Liposomes in nutrition. Trends Food Sci. Technol. 12, 25–31. https://doi.org/10.1016/S0924-2244(01)00044-9

Khan, M.A.B., Hashim, M.J., King, J.K., Govender, R.D., Mustafa, H., Kaabi, J. Al, 2020. Epidemiology of Type 2 diabetes - Global burden of disease and forecasted trends. J. Epidemiol. Glob. Health 10, 107–111. https://doi.org/10.2991/JEGH.K.191028.001

Khateeb, J., Fuchs, E., Khamaisi, M., 2019. Diabetes and lung disease: An underestimated relationship. Rev. Diabet. Stud. 15, 1–15. https://doi.org/10.1900/RDS.2019.15.1

Kielgast, U., Holst, J.J., Madsbad, S., 2011. Antidiabetic actions of endogenous and

exogenous GLP-1 in type 1 diabetic patients with and without residual β-cell function. Diabetes 60, 1599–1607. https://doi.org/10.2337/db10-1790

Kim, H., Kim, Y., Lee, J., 2013. Liposomal formulations for enhanced lymphatic drug delivery. Asian J. Pharm. Sci. 8, 96–103. https://doi.org/10.1016/j.ajps.2013.07.012

Kim, W., Egan, J.M., 2008. The role of incretins in glucose homeostasis and diabetes treatment. Pharmacol. Rev. 60, 470–512. https://doi.org/10.1124/pr.108.000604

Klein, L.J., Visser, F.C., 2010. The effect of insulin on the heart: Part 1: Effects on metabolism and function. Netherlands Hear. J. 18, 197–201. https://doi.org/10.1007/BF03091761

Klemm, D.J., Leitner, J.W., Watson, P., Nesterova, A., Reusch, J.E.B., Goalstone, M.L., Draznin, B., 2001. Insulin-induced adipocyte differentiation: Activation of CREB rescues adipogenesis from the arrest caused by inhibition of prenylation. J. Biol. Chem. 276, 28430–28435. https://doi.org/10.1074/jbc.M103382200

Koland, M., Anchan, R.B., Mukund, S.G., Sindhoor, S.M., 2021. Design and investigation of alginate coated solid lipid nanoparticles for oral insulin delivery. Indian J. Pharm. Educ. Res. 55, 383–394. https://doi.org/10.5530/ijper.55.2.76

Krieger, J.P., Arnold, M., Pettersen, K.G., Lossel, P., Langhans, W., Lee, S.J., 2016. Knockdown of GLP-1 receptors in vagal afferents affects normal food intake and glycemia. Diabetes 65, 34–43. https://doi.org/10.2337/db15-0973

Kuhadiya, N., Malik, R., Bellini, N., Patterson, J., Traina, A., Makdissi, A., Dandona, P., 2013. Liraglutide as additional treatment to insulin in obese patients with type 1 diabetes mellitus. Endocr. Pract. 19, 963–967. https://doi.org/10.4158/EP13065.OR

Kyriaki, G., 2003. Brain insulin: Regulation, mechanisms of action and functions. Cell. Mol. Neurobiol. https://doi.org/10.1023/A:1022598900246

Lane, C.A., Hardy, J., Schott, J.M., 2018. Alzheimer's disease. Eur. J. Neurol. 25, 59–70. https://doi.org/10.1111/ene.13439

Lang, T.F., Hussain, K., 2014. Pediatric hypoglycemia. Adv. Clin. Chem. 63, 211–245. https://doi.org/10.1016/B978-0-12-800094-6.00006-6

Larsen, P.J., Holst, J.J., 2005. Glucagon-related peptide 1 (GLP-1): Hormone and neurotransmitter. Regul. Pept. https://doi.org/10.1016/j.regpep.2004.08.026

Lázár, B.A., Jancsó, G., Pálvölgyi, L., Dobos, I., Nagy, I., Sántha, P., 2018. Insulin confers differing effects on neurite outgrowth in separate populations of cultured dorsal root ganglion neurons: The role of the insulin receptor. Front. Neurosci. 12, 732. https://doi.org/10.3389/fnins.2018.00732

Lee, B., Moon, K.M., Kim, C.Y., 2018. Tight junction in the intestinal epithelium: Its association with diseases and regulation by phytochemicals. J. Immunol. Res. 2018, 2645465. https://doi.org/10.1155/2018/2645465

Li, L.D., Crouzier, T., Sarkar, A., Dunphy, L., Han, J., Ribbeck, K., 2013. Spatial configuration and composition of charge modulates transport into a mucin

hydrogel barrier. Biophys. J. 105, 1357–1365. https://doi.org/10.1016/j.bpj.2013.07.050

Li, M., Sun, Y., Ma, C., Hua, Y., Zhang, L., Shen, J., 2021. Design and Investigation of Penetrating Mechanism of Octaarginine-Modified Alginate Nanoparticles for Improving Intestinal Insulin Delivery. J. Pharm. Sci. 110, 268–279. https://doi.org/10.1016/j.xphs.2020.07.004

Li, P., Tan, A., Prestidge, C.A., Nielsen, H.M., Müllertz, A., 2014. Self-nanoemulsifying drug delivery systems for oral insulin delivery: In vitro and in vivo evaluations of enteric coating and drug loading. Int. J. Pharm. 477, 390–398. https://doi.org/10.1016/j.ijpharm.2014.10.039

Li, R., Laurent, F., Taverner, A., Mackay, J., De Bank, P.A., Mrsny, R.J., 2021. Intestinal transcytosis of a protein cargo and nanoparticles mediated by a non-toxic form of pseudomonas aeruginosa exotoxin a. Pharmaceutics 13, 1171. https://doi.org/10.3390/pharmaceutics13081171

Liguori, I., Russo, G., Curcio, F., Bulli, G., Aran, L., Della-Morte, D., Gargiulo, G., Testa, G., Cacciatore, F., Bonaduce, D., Abete, P., 2018. Oxidative stress, aging, and diseases. Clin. Interv. Aging 13, 757–772. https://doi.org/10.2147/CIA.S158513

Lim, G.E., Brubaker, P.L., 2006. Glucagon-like peptide 1 secretion by the L-cell: The view from within. Diabetes 55, S70–S77. https://doi.org/10.2337/db06-S020

Liu, Y., Wei, R., Hong, T.P., 2014. Potential roles of glucagon-like peptide-1-based therapies in treating non-alcoholic fatty liver disease. World J. Gastroenterol. 20, 9090–9097. https://doi.org/10.3748/wjg.v20.i27.9090

Livingstone, S.J., Levin, D., Looker, H.C., Lindsay, R.S., Wild, S.H., Joss, N., Leese, G., Leslie, P., McCrimmon, R.J., Metcalfe, W., McKnight, J.A., Morris, A.D., Pearson, D.W.M., Petrie, J.R., Philip, S., Sattar, N.A., Traynor, J.P., Colhoun, H.M., 2015. Estimated life expectancy in a scottish cohort with type 1 diabetes, 2008-2010. JAMA - J. Am. Med. Assoc. 313, 37–44. https://doi.org/10.1001/jama.2014.16425

Lopes, M., Simões, S., Veiga, F., Seiça, R., Ribeiro, A., 2015. Why most oral insulin formulations do not reach clinical trials. Ther. Deliv. 6, 973–987. https://doi.org/10.4155/TDE.15.47

Lorenzati, B., Zucco, C., Miglietta, S., Lamberti, F., Bruno, G., 2010. Oral hypoglycemic drugs: Pathophysiological basis of their mechanism of action. Pharmaceuticals 3, 3005–3020. https://doi.org/10.3390/ph3093005

Luo, Y.Y., Xiong, X.Y., Tian, Y., Li, Z.L., Gong, Y.C., Li, Y.P., 2016. A review of biodegradable polymeric systems for oral insulin delivery. Drug Deliv. 23, 1882–1891. https://doi.org/10.3109/10717544.2015.1052863

Ma, E.L., Ma, H., Liu, Z., Zheng, C.X., Duan, M.X., 2006. In vitro and in vivo evaluation of a novel oral insulin formulation. Acta Pharmacol. Sin. 27, 1382–1388. https://doi.org/10.1111/j.1745-7254.2006.00424.x

Macauley, S.L., Stanley, M.S., Caesar, E.E., Moritz, W.R., Bice, A.R., Cruz-Diaz, N., Carroll, C.M., Day, S.M., Grizzanti, J., Mahan, T.E., Snipes, J.A., Orr, T.E., Culver, J.P., Remedi,

M.S., Nichols, C.G., Karch, C.M., Cox, L.A., Diz, D.I., Bauer, A.Q., Holtzman, D.M., 2021. Sulfonylureas target the neurovascular response to decrease Alzheimer's pathology. bioRxiv 2021.08.11.455969. https://doi.org/10.1101/2021.08.11.455969

MacDonald, P.E., El-kholy, W., Riedel, M.J., Salapatek, A.M.F., Light, P.E., Wheeler, M.B., 2002. The multiple actions of GLP-1 on the process of glucose-stimulated insulin secretion. Diabetes 51, S434–S442. https://doi.org/10.2337/diabetes.51.2007.s434

Mahmood, A., Bernkop-Schnürch, A., 2019. SEDDS: A game changing approach for the oral administration of hydrophilic macromolecular drugs. Adv. Drug Deliv. Rev. 142, 91–101. https://doi.org/10.1016/j.addr.2018.07.001

Mao, Y.F., Guo, Z., Zheng, T., Jiang, Y., Yan, Y., Yin, X., Chen, Y., Zhang, B., 2016. Intranasal insulin alleviates cognitive deficits and amyloid pathology in young adult APPswe/PS1dE9 mice. Aging Cell 15, 893–902. https://doi.org/10.1111/acel.12498

Marks, V., 2019. The early history of GIP 1969–2000: From enterogastrone to major metabolic hormone. Peptides. https://doi.org/10.1016/j.peptides.2019.170155

Marschütz, M.K., Bernkop-Schnürch, A., 2000. Oral peptide drug delivery: Polymer-inhibitor conjugates protecting insulin from enzymatic degradation in vitro. Biomaterials 21, 1499–1507. https://doi.org/10.1016/S0142-9612(00)00039-9

Martínez-López, A.L., Pangua, C., Reboredo, C., Campión, R., Morales-Gracia, J., Irache, J.M., 2020. Protein-based nanoparticles for drug delivery purposes. Int. J. Pharm. 581, 119289. https://doi.org/10.1016/j.ijpharm.2020.119289

Mathieu, C., Zinman, B., Hemmingsson, J.U., Woo, V., Colman, P., Christiansen, E., Linder, M., Bode, B., 2016. Efficacy and safety of liraglutide added to insulin treatment in type 1 diabetes: The adjunct one treat-to-target randomized trial. Diabetes Care 39, 1702–1710. https://doi.org/10.2337/dc16-0691

Matthews, D.R., Naylor, B.A., Jones, R.G., 1983. Pulsatile insulin has greater hypoglycemic effect than continuous delivery. Diabetes 37, 617–621. https://doi.org/10.2337/diab.32.7.617

McClain, D.A., 1992. Mechanism and role of insulin receptor endocytosis. Am. J. Med. Sci. 304, 192–201. https://doi.org/10.1097/00000441-199209000-00009

McGinn, B.J., Morrison, J.D., 2016. Investigations into the absorption of insulin and insulin derivatives from the small intestine of the anaesthetised rat. J. Control. Release 232, 120–130. https://doi.org/10.1016/j.jconrel.2016.04.002

McIntosh, C.H.S., Widenmaier, S., Kim, S.J., 2009. Chapter 15 Glucose-Dependent Insulinotropic Polypeptide (Gastric Inhibitory Polypeptide; GIP). Vitam. Horm. 80, 409–471. https://doi.org/10.1016/S0083-6729(08)00615-8

Meier, J.J., Nauck, M.A., Schmidt, W.E., Gallwitz, B., 2002. Gastric inhibitory polypeptide: The neglected incretin revisited. Regul. Pept. 107, 1–13. https://doi.org/10.1016/S0167-0115(02)00039-3

Menser, M.A., Forrest, J.M., Bransby, R.D., 1978. Rubella Infection and Diabetes Mellitus. Lancet 311, 57–60. https://doi.org/10.1016/S0140-6736(78)90001-6

Mieczkowska, A., Irwin, N., Flatt, P.R., Chappard, D., Mabilleau, G., 2013. Glucose-dependent insulinotropic polypeptide (GIP) receptor deletion leads to reduced bone strength and quality. Bone 56, 337–342. https://doi.org/10.1016/j.bone.2013.07.003

Mittal, K., Mani, R.J., Katare, D.P., 2016. Type 3 Diabetes: Cross Talk between Differentially Regulated Proteins of Type 2 Diabetes Mellitus and Alzheimer's Disease. Sci. Rep. 6. https://doi.org/10.1038/srep25589

Moon, M.K., Hur, K.Y., Ko, S.H., Park, S.O., Lee, B.W., Kim, J.H., Rhee, S.Y., Kim, H.J., Choi, K.M., Kim, N.H., Kim, T.N., Lee, Y.H., Kim, J.H., Hong, E.G., Kim, J., Lee, W.Y., Song, B., Kim, J.Y., Yang, D.H., Taeyoung Yang, Hyeongjin Kim, 2017. Combination therapy of oral hypoglycemic agents in patients with type 2 diabetes mellitus. Diabetes Metab. J. 41, 357–366. https://doi.org/10.4093/dmj.2017.41.5.357

Morishita, M., Aoki, Y., Sakagami, M., Nagai, T., Takayama, K., 2004. In Situ Ileal Absorption of Insulin in Rats: Effects of Hyaluronidase Pretreatment Diminishing the Mucous/Glycocalyx Layers. Pharm. Res. 21, 309–316. https://doi.org/10.1023/B:PHAM.0000016244.88820.28

Morley, J.E., 2008. Diabetes and Aging: Epidemiologic Overview. Clin. Geriatr. Med. 24, 395–405. https://doi.org/10.1016/j.cger.2008.03.005

Mortensen, K., Christensen, L.L., Holst, J.J., Orskov, C., 2003. GLP-1 and GIP are colocalized in a subset of endocrine cells in the small intestine. Regul. Pept. 114, 189–196. https://doi.org/10.1016/S0167-0115(03)00125-3

Mukhopadhyay, P., Sarkar, K., Chakraborty, M., Bhattacharya, S., Mishra, R., Kundu, P.P., 2013. Oral insulin delivery by self-assembled chitosan nanoparticles: In vitro and in vivo studies in diabetic animal model. Mater. Sci. Eng. C 33, 376–382. https://doi.org/10.1016/j.msec.2012.09.001

Müller, T.D., Finan, B., Bloom, S.R., D'Alessio, D., Drucker, D.J., Flatt, P.R., Fritsche, A., Gribble, F., Grill, H.J., Habener, J.F., Holst, J.J., Langhans, W., Meier, J.J., Nauck, M.A., Perez-Tilve, D., Pocai, A., Reimann, F., Sandoval, D.A., Schwartz, T.W., Seeley, R.J., Stemmer, K., Tang-Christensen, M., Woods, S.C., DiMarchi, R.D., Tschöp, M.H., 2019. Glucagon-like peptide 1 (GLP-1). Mol. Metab. https://doi.org/10.1016/j.molmet.2019.09.010

Murray, B., Rosenbloom, C., 2018. Fundamentals of glycogen metabolism for coaches and athletes. Nutr. Rev. 76, 243–259. https://doi.org/10.1093/NUTRIT/NUY001

Muskiet, M.H.A., Tonneijck, L., Smits, M.M., Van Baar, M.J.B., Kramer, M.H.H., Hoorn, E.J., Joles, J.A., Van Raalte, D.H., 2017. GLP-1 and the kidney: From physiology to pharmacology and outcomes in diabetes. Nat. Rev. Nephrol. 13, 605–628. https://doi.org/10.1038/nrneph.2017.123

Nadkarni, P., Chepurny, O.G., Holz, G.G., 2014. Regulation of glucose homeostasis by GLP-1, in: Progress in Molecular Biology and Translational Science. Elsevier B.V., pp.

23–65. https://doi.org/10.1016/B978-0-12-800101-1.00002-8

Najafi, Z., Saeedi, M., Mahdavi, M., Sabourian, R., Khanavi, M., Tehrani, M.B., Moghadam, F.H., Edraki, N., Karimpor-Razkenari, E., Sharifzadeh, M., Foroumadi, A., Shafiee, A., Akbarzadeh, T., 2016. Design and synthesis of novel anti-Alzheimer's agents: Acridine-chromenone and quinoline-chromenone hybrids. Bioorg. Chem. 67, 84–94. https://doi.org/10.1016/j.bioorg.2016.06.001

Najjar, S.M., Perdomo, G., 2019. Hepatic Insulin Clearance: Mechanism and Physiology. Physiology (Bethesda). 34, 198–215. https://doi.org/10.1152/physiol.00048.2018

Nakabeppu, Y., 2019. Origins of brain insulin and its function. Adv. Exp. Med. Biol. 1128, 1–11. https://doi.org/10.1007/978-981-13-3540-2_1

Nauck, M.A., Meier, J.J., 2016. The incretin effect in healthy individuals and those with type 2 diabetes: Physiology, pathophysiology, and response to therapeutic interventions. Lancet Diabetes Endocrinol. https://doi.org/10.1016/S2213-8587(15)00482-9

Newsholme, P., Brennan, L., Bender, K., 2006. Amino acid metabolism, β-cell function, and diabetes. Diabetes 55, S39–S47. https://doi.org/10.2337/db06-S006

Nielsen, D.S., Shepherd, N.E., Xu, W., Lucke, A.J., Stoermer, M.J., Fairlie, D.P., 2017. Orally Absorbed Cyclic Peptides. Chem. Rev. 117, 8094–8128. https://doi.org/10.1021/acs.chemrev.6b00838

Nikolaidis, L.A., Elahi, D., Hentosz, T., Doverspike, A., Huerbin, R., Zourelias, L., Stolarski, C., Shen, Y.T., Shannon, R.P., 2004. Recombinant glucagon-like peptide-1 increases myocardial glucose uptake and improves left ventricular performance in conscious dogs with pacing-induced dilated cardiomyopathy. Circulation 110, 955–961. https://doi.org/10.1161/01.CIR.0000139339.85840.DD

Niu, M., Lu, Y., Hovgaard, L., Guan, P., Tan, Y., Lian, R., Qi, J., Wu, W., 2012. Hypoglycemic activity and oral bioavailability of insulin-loaded liposomes containing bile salts in rats: The effect of cholate type, particle size and administered dose. Eur. J. Pharm. Biopharm. 81, 265–272. https://doi.org/10.1016/j.ejpb.2012.02.009

Niu, M., Tan, Y., Guan, P., Hovgaard, L., Lu, Y., Qi, J., Lian, R., Li, X., Wu, W., 2014. Enhanced oral absorption of insulin-loaded liposomes containing bile salts: A mechanistic study. Int. J. Pharm. 460, 119–130. https://doi.org/10.1016/j.ijpharm.2013.11.028

Nuche-Berenguer, B., Moreno, P., Esbrit, P., Dapía, S., Caeiro, J.R., Cancelas, J., Haro-Mora, J.J., Villanueva-Peñacarrillo, M.L., 2009. Effect of GLP-1 treatment on bone turnover in normal, type 2 diabetic, and insulin-resistant states. Calcif. Tissue Int. 84, 453–461. https://doi.org/10.1007/s00223-009-9220-3

Nyberg, J., Anderson, M.F., Meister, B., Alborn, A.M., Ström, A.K., Brederlau, A., Illerskog, A.C., Nilsson, O., Kieffer, T.J., Hietala, M.A., Ricksten, A., Eriksson, P.S., 2005. Glucose-dependent insulinotropic polypeptide is expressed in adult hippocampus and induces progenitor cell proliferation. J. Neurosci. 25, 1816–1825. https://doi.org/10.1523/JNEUROSCI.4920-04.2005

Ou, Z., Kong, X., Sun, X., He, X., Zhang, L., Gong, Z., Huang, J., Xu, B., Long, D., Li, J., Li, Q., Xu, L., Xuan, A., 2018. Metformin treatment prevents amyloid plaque deposition and memory impairment in APP/PS1 mice. Brain. Behav. Immun. 69, 351–363. https://doi.org/10.1016/j.bbi.2017.12.009

Pais, R., Gribble, F.M., Reimann, F., 2016a. Stimulation of incretin secreting cells. Ther. Adv. Endocrinol. Metab. https://doi.org/10.1177/2042018815618177

Pais, R., Gribble, F.M., Reimann, F., 2016b. Signalling pathways involved in the detection of peptones by murine small intestinal enteroendocrine L-cells. Peptides 77, 9–15. https://doi.org/10.1016/j.peptides.2015.07.019

Pelicano, H., Martin, D.S., Xu, R.H., Huang, P., 2006. Glycolysis inhibition for anticancer treatment. Oncogene. https://doi.org/10.1038/sj.onc.1209597

Perera, G., Greindl, M., Palmberger, T.F., Bernkop-Schnrch, A., 2009. Insulin-loaded poly(acrylic acid)-cysteine nanoparticles: Stability studies towards digestive enzymes of the intestine Insulin-loaded poly(acrylic acid)-cysteine nanoparticles Glen Perera et al. Drug Deliv. 16, 254–260. https://doi.org/10.1080/10717540902937471

Pérez, Y.A., Urista, C.M., Martínez, J.I., Nava, M.D.C.D., Rodríguez, F.A.R., 2016. Functionalized polymers for enhance oral bioavailability of sensitive molecules. Polymers (Basel). 8, 214. https://doi.org/10.3390/polym8060214

Petersmann, A., Nauck, M., Müller-Wieland, D., Kerner, W., Müller, U.A., Landgraf, R., Freckmann, G., Heinemann, L., 2018. Definition, Classification and Diagnosis of Diabetes Mellitus. Exp. Clin. Endocrinol. Diabetes 126, 406–410. https://doi.org/10.1055/a-0584-6223

Pinto, A.R., Ilinykh, A., Ivey, M.J., Kuwabara, J.T., D'antoni, M.L., Debuque, R., Chandran, A., Wang, L., Arora, K., Rosenthal, N.A., Tallquist, M.D., 2016. Revisiting cardiac cellular composition. Circ. Res. 118, 400–409. https://doi.org/10.1161/CIRCRESAHA.115.307778

Pomytkin, I., Costa-Nunes, J.P., Kasatkin, V., Veniaminova, E., Demchenko, A., Lyundup, A., Lesch, K.P., Ponomarev, E.D., Strekalova, T., 2018. Insulin receptor in the brain: Mechanisms of activation and the role in the CNS pathology and treatment. CNS Neurosci. Ther. 24, 763–774. https://doi.org/10.1111/cns.12866

Proud, C.G., 2006. Regulation of protein synthesis by insulin. Biochem. Soc. Trans. 34, 213–216. https://doi.org/10.1042/bst0340213

Rahman, M.S., Hossain, K.S., Das, S., Kundu, S., Adegoke, E.O., Rahman, M.A., Hannan, M.A., Uddin, M.J., Pang, M.G., 2021. Role of insulin in health and disease: An update. Int. J. Mol. Sci. 22. https://doi.org/10.3390/ijms22126403

Rask-Madsen, C., Kahn, C.R., 2012. Tissue-specific insulin signaling, metabolic syndrome, and cardiovascular disease. Arterioscler. Thromb. Vasc. Biol. 32, 2052–2059. https://doi.org/10.1161/ATVBAHA.111.241919

Richter, B., Bandeira-Echtler, E., Bergerhoff, K., Lerch, C.L., 2008. Dipeptidyl peptidase-4 (DPP-4) inhibitors for type 2 diabetes mellitus. Cochrane Database Syst. Rev.

https://doi.org/10.1002/14651858.CD006739.pub2

Rinia, H.A., Burger, K.N.J., Bonn, M., Müller, M., 2008. Quantitative label-free imaging of lipid composition and packing of individual cellular lipid droplets using multiplex CARS microscopy. Biophys. J. 95, 4908–4914. https://doi.org/10.1529/biophysj.108.137737

Robertson, R.P., Harmon, J.S., 2006. Diabetes, glucose toxicity, and oxidative stress: A case of double jeopardy for the pancreatic islet β cell. Free Radic. Biol. Med. 41, 177–184. https://doi.org/10.1016/j.freeradbiomed.2005.04.030

Rocca, A.S., Brubaker, P.L., 1999. Role of the vagus nerve in mediating proximal nutrient-induced glucagon- like peptide-1 secretion. Endocrinology 140, 1687–1694. https://doi.org/10.1210/endo.140.4.6643

Röder, P. V., Wu, B., Liu, Y., Han, W., 2016. Pancreatic regulation of glucose homeostasis. Exp. Mol. Med. 48, e219. https://doi.org/10.1038/emm.2016.6

Röhrborn, D., Wronkowitz, N., Eckel, J., 2015. DPP4 in diabetes. Front. Immunol. 6, 386. https://doi.org/10.3389/fimmu.2015.00386

Rorbach-Dolata, A., Piwowar, A., 2019. Neurometabolic Evidence Supporting the Hypothesis of Increased Incidence of Type 3 Diabetes Mellitus in the 21st Century. Biomed Res. Int. https://doi.org/10.1155/2019/1435276

Rorsman, P., Eliasson, L., Renström, E., Gromada, J., Barg, S., Göpel, S., 2000. The cell physiology of biphasic insulin secretion. News Physiol. Sci. 15, 72–77. https://doi.org/10.1152/physiologyonline.2000.15.2.72

Ross, S.A., Ballantine, J., 2013. Early use of glucagon-like peptide-1 receptor agonists (GLP-1 RAs) in Type 2 diabetes. Curr. Med. Res. Opin. https://doi.org/10.1185/03007995.2013.837817

Rother, K.I., 2007. Diabetes Treatment — Bridging the Divide. N. Engl. J. Med. 356, 1499–1501. https://doi.org/10.1056/nejmp078030

Rotondo, F., Ho-Palma, A.C., Remesar, X., Fernández-López, J.A., Romero, M.D.M., Alemany, M., 2017. Glycerol is synthesized and secreted by adipocytes to dispose of excess glucose, via glycerogenesis and increased acyl-glycerol turnover. Sci. Rep. 7, 1–14. https://doi.org/10.1038/s41598-017-09450-4

Rowlands, J., Heng, J., Newsholme, P., Carlessi, R., 2018. Pleiotropic Effects of GLP-1 and Analogs on Cell Signaling, Metabolism, and Function. Front. Endocrinol. (Lausanne). 9, 672. https://doi.org/10.3389/fendo.2018.00672

Salameh, T.S., Bullock, K.M., Hujoel, I.A., Niehoff, M.L., Wolden-Hanson, T., Kim, J., Morley, J.E., Farr, S.A., Banks, W.A., 2015. Central Nervous System Delivery of Intranasal Insulin: Mechanisms of Uptake and Effects on Cognition. J. Alzheimer's Dis. 47, 715–728. https://doi.org/10.3233/JAD-150307

Salvestrini, V., Sell, C., Lorenzini, A., 2019. Obesity may accelerate the aging process. Front. Endocrinol. (Lausanne). 10, 266. https://doi.org/10.3389/fendo.2019.00266

Scheen, A.J., 2004. Combined thiazolidinedione-insulin therapy: Should we be

concerned about safety? Drug Saf. 27, 841–856. https://doi.org/10.2165/00002018-200427120-00002

Schönauer, M., Thomas, A., 2010. Sensor-augmented pump therapy - On the way to artificial pancreas. Av. en Diabetol. 26, 143–146. https://doi.org/10.1016/S1134-3230(10)63002-5

Seino, Y., Fukushima, M., Yabe, D., 2010. GIP and GLP-1, the two incretin hormones: Similarities and differences. J. Diabetes Investig. https://doi.org/10.1111/j.2040-1124.2010.00022.x

Shakweh, M., Ponchel, G., Fattal, E., 2004. Particle uptake by Peyer's patches: A pathway for drug and vaccine delivery. Expert Opin. Drug Deliv. 1, 141–163. https://doi.org/10.1517/17425247.1.1.141

Sharma, G., Sharma, A.R., Nam, J.S., Doss, G.P.C., Lee, S.S., Chakraborty, C., 2015. Nanoparticle based insulin delivery system: The next generation efficient therapy for Type 1 diabetes. J. Nanobiotechnology 13, 74. https://doi.org/10.1186/s12951-015-0136-y

Silva, M.V.F., Loures, C.D.M.G., Alves, L.C.V., De Souza, L.C., Borges, K.B.G., Carvalho, M.D.G., 2019. Alzheimer's disease: Risk factors and potentially protective measures. J. Biomed. Sci. 26, 1–11. https://doi.org/10.1186/s12929-019-0524-y

Sims-Robinson, C., Kim, B., Rosko, A., Feldman, E.L., 2010. How does diabetes accelerate Alzheimer disease pathology? Nat. Rev. Neurol. https://doi.org/10.1038/nrneurol.2010.130

Singh, V.P., Bali, A., Singh, N., Jaggi, A.S., 2014. Advanced glycation end products and diabetic complications. Korean J. Physiol. Pharmacol. 18, 1–14. https://doi.org/10.4196/kjpp.2014.18.1.1

Smith, A.G., Singleton, J.R., 2008. Impaired glucose tolerance and neuropathy. Neurologist 14, 23–29. https://doi.org/10.1097/NRL.0b013e31815a3956

Sonia, T.A., Sharma, C.P., 2012. An overview of natural polymers for oral insulin delivery. Drug Discov. Today 17, 784–792. https://doi.org/10.1016/j.drudis.2012.03.019

Soria Lopez, J.A., González, H.M., Léger, G.C., 2019. Alzheimer's disease, in: Handbook of Clinical Neurology. Elsevier B.V., pp. 231–255. https://doi.org/10.1016/B978-0-12-804766-8.00013-3

Srikanth, V., Sinclair, A.J., Hill-Briggs, F., Moran, C., Biessels, G.J., 2020. Type 2 diabetes and cognitive dysfunction—towards effective management of both comorbidities. Lancet Diabetes Endocrinol. 8, 535–545. https://doi.org/10.1016/S2213-8587(20)30118-2

Stemmer, K., Finan, B., DiMarchi, R.D., Tschöp, M.H., Müller, T.D., 2020. Insights into incretin-based therapies for treatment of diabetic dyslipidemia. Adv. Drug Deliv. Rev. 159, 34–53. https://doi.org/10.1016/j.addr.2020.05.008

Stensen, S., Gasbjerg, L.S., Helsted, M.M., Hartmann, B., Christensen, M.B., Knop, F.K., 2019. GIP and the gut-bone axis – Physiological, pathophysiological and potential

therapeutic implications. Peptides 125, 170197. https://doi.org/10.1016/j.peptides.2019.170197

Stiker, G., 2001. Glucose toxicity. Kidney Int. 59, 799–800. https://doi.org/10.1046/j.1523-1755.2001.059002799.x

Stratton, I.M., Adler, A.I., Neil, H.A.W., Matthews, D.R., Manley, S.E., Cull, C.A., Hadden, D., Turner, R.C., Holman, R.R., 2000. Association of glycaemia with macrovascular and microvascular complications of type 2 diabetes (UKPDS 35): Prospective observational study. Br. Med. J. 321, 405–412. https://doi.org/10.1136/bmj.321.7258.405

Su, F., Shu, H., Ye, Q., Wang, Z., Xie, C., Yuan, B., Zhang, Z., Bai, F., 2017. Brain insulin resistance deteriorates cognition by altering the topological features of brain networks. NeuroImage Clin. 13, 280–287. https://doi.org/10.1016/j.nicl.2016.12.009

Sudhakar, S., Chandran, S.V., Selvamurugan, N., Nazeer, R.A., 2020. Biodistribution and pharmacokinetics of thiolated chitosan nanoparticles for oral delivery of insulin in vivo. Int. J. Biol. Macromol. 150, 281–288. https://doi.org/10.1016/j.ijbiomac.2020.02.079

Suri, P., Aurora, T., 2017. Hyperglycemia. Obs. Med. Princ. Protoc. 225–230. https://doi.org/10.1017/9781139136365.043

Suzuki, T., 2020. Regulation of the intestinal barrier by nutrients: The role of tight junctions. Anim. Sci. J. 91, e13357. https://doi.org/10.1111/asj.13357

Tan, S.Y., Mei Wong, J.L., Sim, Y.J., Wong, S.S., Mohamed Elhassan, S.A., Tan, S.H., Ling Lim, G.P., Rong Tay, N.W., Annan, N.C., Bhattamisra, S.K., Candasamy, M., 2019. Type 1 and 2 diabetes mellitus: A review on current treatment approach and gene therapy as potential intervention. Diabetes Metab. Syndr. Clin. Res. Rev. 13, 364–372. https://doi.org/10.1016/j.dsx.2018.10.008

Thondam, S.K., Cuthbertson, D.J., Wilding, J.P.H., 2020. The influence of Glucose-dependent Insulinotropic Polypeptide (GIP) on human adipose tissue and fat metabolism: Implications for obesity, type 2 diabetes and Non-Alcoholic Fatty Liver Disease (NAFLD). Peptides 125, 170208. https://doi.org/10.1016/j.peptides.2019.170208

Thurmond, D.C., 2009. Insulin-regulated glucagon-like peptide-1 release from l cells: Actin' out. Endocrinology. https://doi.org/10.1210/en.2009-1178

Tirone, T.A., Brunicardi, F.C., 2001. Overview of glucose regulation. World J. Surg. 25, 461–467. https://doi.org/10.1007/s002680020338

Titchenell, P.M., Lazar, M.A., Birnbaum, M.J., 2017. Unraveling the Regulation of Hepatic Metabolism by Insulin. Trends Endocrinol. Metab. https://doi.org/10.1016/j.tem.2017.03.003

Torchilin, V.P., 2005. Recent advances with liposomes as pharmaceutical carriers. Nat. Rev. Drug Discov. 4, 145–160. https://doi.org/10.1038/nrd1632

Tuttolomondo, A., Maida, C., Pinto, A., 2015. Diabetic foot syndrome: Immune-inflammatory features as possible cardiovascular markers in diabetes. World J. Orthop. 6, 62–76. https://doi.org/10.5312/wjo.v6.i1.62

Vakilian, M., Tahamtani, Y., Ghaedi, K., 2019. A review on insulin trafficking and exocytosis. Gene. https://doi.org/10.1016/j.gene.2019.04.063

Van Der Merwe, S.M., Verhoef, J.C., Verheijden, J.H.M., Kotzé, A.F., Junginger, H.E., 2004. Trimethylated chitosan as polymeric absorption enhancer for improved peroral delivery of peptide drugs. Eur. J. Pharm. Biopharm. 58, 225–235. https://doi.org/10.1016/j.ejpb.2004.03.023

Vandal, M., White, P.J., Tremblay, C., St-Amour, I., Chevrier, G., Emond, V., Lefrançois, D., Virgili, J., Planel, E., Giguere, Y., Marette, A., Calon, F., 2014. Insulin reverses the high-fat diet-induced increase in brain Aβ and improves memory in an animal model of Alzheimer disease. Diabetes 63, 4291–4301. https://doi.org/10.2337/db14-0375

Vicent, D., Ilany, J., Kondo, T., Naruse, K., Fisher, S.J., Kisanuki, Y.Y., Bursell, S., Yanagisawa, M., King, G.L., Kahn, C.R., 2003. The role of endothelial insulin signaling in the regulation of vascular tone and insulin resistance. J. Clin. Invest. 111, 1373–1380. https://doi.org/10.1172/JCI15211

Vilsbøll, T., Holst, J.J., 2004. Incretins, insulin secretion and Type 2 diabetes mellitus. Diabetologia 47, 357–366. https://doi.org/10.1007/s00125-004-1342-6

Vinogradov, S., Wei, X., 2012. Cancer stem cells and drug resistance: The potential of nanomedicine. Nanomedicine 7, 597–615. https://doi.org/10.2217/nnm.12.22

Wang, W., Yu, C., Zhang, F., Li, Y., Zhang, B., Huang, J., Zhang, Z., Jin, L., 2021. Improved oral delivery of insulin by PLGA nanoparticles coated with 5β-cholanic acid conjugated glycol chitosan. Biomed. Mater. 16, 064103. https://doi.org/10.1088/1748-605x/ac2a8c

Wang, Z., Thurmond, D.C., 2009. Mechanisms of biphasic insulin-granule exocytosis - Roles of the cytoskeleton, small GTPases and SNARE proteins. J. Cell Sci. 122, 893–903. https://doi.org/10.1242/jcs.034355

Wasiak, I., Kulikowska, A., Janczewska, M., Michalak, M., Cymerman, I.A., Nagalski, A., Kallinger, P., Szymanski, W.W., Ciach, T., 2016. Dextran nanoparticle synthesis and properties. PLoS One 11, e0146237. https://doi.org/10.1371/journal.pone.0146237

Wu, T., Rayner, C.K., Horowitz, M., 2015. Incretins. Handb. Exp. Pharmacol. 233, 137–171. https://doi.org/10.1007/164_2015_9

Xia, C.Q., Wang, J., Shen, W.C., 2000. Hypoglycemic effect of insulin-transferrin conjugate in streptozotocin-induced diabetic rats. J. Pharmacol. Exp. Ther. 295, 594–600.

Xie, J., Lu, Y., Wang, W., Zhu, H., Wang, Z., Cao, Z., 2017. Simple Protein Modification Using Zwitterionic Polymer to Mitigate the Bioactivity Loss of Conjugated Insulin. Adv. Healthc. Mater. 6, 1601428. https://doi.org/10.1002/adhm.201601428

Xu, Q., Hong, H., Wu, J., Yan, X., 2019. Bioavailability of bioactive peptides derived from food proteins across the intestinal epithelial membrane: A review. Trends Food Sci. Technol. 86, 399–411. https://doi.org/10.1016/j.tifs.2019.02.050

Xu, Y., Zheng, Y., Wu, L., Zhu, X., Zhang, Z., Huang, Y., 2018. Novel Solid Lipid Nanoparticle with Endosomal Escape Function for Oral Delivery of Insulin. ACS Appl. Mater. Interfaces 10, 9315–9324. https://doi.org/10.1021/acsami.8b00507

Yang, M., Wang, J., Wu, S., Yuan, L., Zhao, X., Liu, C., Xie, J., Jia, Y., Lai, Y., Zhao, A.Z., Boden, G., Li, L., Yang, G., 2017. Duodenal GLP-1 signaling regulates hepatic glucose production through a PKC-δ-dependent neurocircuitry. Cell Death Dis. 8, e2609–e2609. https://doi.org/10.1038/cddis.2017.28

Yang, Y., Ma, D., Wang, Y., Jiang, T., Hu, S., Zhang, M., Yu, X., Gongb, C.X., 2013. Intranasal insulin ameliorates tau hyperphosphorylation in a rat model of type 2 diabetes. J. Alzheimer's Dis. 33, 329–338. https://doi.org/10.3233/JAD-2012-121294

Yazdi, J.R., Tafaghodi, M., Sadri, K., Mashreghi, M., Nikpoor, A.R., Nikoofal-Sahlabadi, S., Chamani, J., Vakili, R., Moosavian, S.A., Jaafari, M.R., 2020. Folate targeted PEGylated liposomes for the oral delivery of insulin: In vitro and in vivo studies. Colloids Surfaces B Biointerfaces 194, 111203. https://doi.org/10.1016/j.colsurfb.2020.111203

Yegorov, Y.E., Poznyak, A. V., Nikiforov, N.G., Sobenin, I.A., Orekhov, A.N., 2020. The link between chronic stress and accelerated aging. Biomedicines 8. https://doi.org/10.3390/BIOMEDICINES8070198

Yildirim Simsir, I., Soyaltin, U.E., Cetinkalp, S., 2018. Glucagon like peptide-1 (GLP-1) likes Alzheimer's disease. Diabetes Metab. Syndr. Clin. Res. Rev. 12, 469–475. https://doi.org/10.1016/j.dsx.2018.03.002

Yilmaz, B., Li, H., 2018. Gut microbiota and iron: The crucial actors in health and disease. Pharmaceuticals 11. https://doi.org/10.3390/ph11040098

Yu, Z., Fan, W., Wang, L., Qi, J., Lu, Y., Wu, W., 2019. Effect of Surface Charges on Oral Absorption of Intact Solid Lipid Nanoparticles. Mol. Pharm. https://doi.org/10.1021/acs.molpharmaceut.9b00861

Zeng, G., Nystrom, F.H., Ravichandran, L. V., Cong, L.N., Kirby, M., Mostowski, H., Quon, M.J., 2000. Roles for insulin receptor, PI3-kinase, and Akt in insulin-signaling pathways related to production of nitric oxide in human vascular endothelial cells. Circulation 101, 1539–1545. https://doi.org/10.1161/01.CIR.101.13.1539

Zhang, N., Ping, Q., Huang, G., Xu, W., Cheng, Y., Han, X., 2006. Lectin-modified solid lipid nanoparticles as carriers for oral administration of insulin. Int. J. Pharm. 327, 153–159. https://doi.org/10.1016/j.ijpharm.2006.07.026

Zhang, Q., Delessa, C.T., Augustin, R., Bakhti, M., Colldén, G., Drucker, D.J., Feuchtinger, A., Caceres, C.G., Grandl, G., Harger, A., Herzig, S., Hofmann, S., Holleman, C.L., Jastroch, M., Keipert, S., Kleinert, M., Knerr, P.J., Kulaj, K., Legutko, B., Lickert, H., Liu, X., Luippold, G., Lutter, D., Malogajski, E., Medina, M.T., Mowery, S.A., Blutke, A., Perez-Tilve, D., Salinno, C., Sehrer, L., DiMarchi, R.D., Tschöp, M.H., Stemmer,

K., Finan, B., Wolfrum, C., Müller, T.D., 2021. The glucose-dependent insulinotropic polypeptide (GIP) regulates body weight and food intake via CNS-GIPR signaling. Cell Metab. 33, 833-844.e5. https://doi.org/10.1016/j.cmet.2021.01.015

Zhang, Q., He, N., Zhang, L., Zhu, F., Chen, Q., Qin, Y., Zhang, Z., Zhang, Qiang, Wang, S., He, Q., 2012. The in vitro and in vivo study on Self-Nanoemulsifying Drug Delivery System (SNEDDS) based on insulin-phospholipid complex. J. Biomed. Nanotechnol. 8, 90–97. https://doi.org/10.1166/jbn.2012.1371

Zhang, X., Qi, J., Lu, Y., He, W., Li, X., Wu, W., 2014. Biotinylated liposomes as potential carriers for the oral delivery of insulin. Nanomedicine Nanotechnology, Biol. Med. 10, 167–176. https://doi.org/10.1016/j.nano.2013.07.011

Zhang, X., Sun, M., Zheng, A., Cao, D., Bi, Y., Sun, J., 2012. Preparation and characterization of insulin-loaded bioadhesive PLGA nanoparticles for oral administration. Eur. J. Pharm. Sci. 45, 632–638. https://doi.org/10.1016/j.ejps.2012.01.002

Zheng, H., Wu, J., Jin, Z., Yan, L.-J., 2016. Protein Modifications as Manifestations of Hyperglycemic Glucotoxicity in Diabetes and Its Complications. Biochem. Insights 9, BCI.S36141. https://doi.org/10.4137/bci.s36141

Zheng, Y., Ley, S.H., Hu, F.B., 2018. Global aetiology and epidemiology of type 2 diabetes mellitus and its complications. Nat. Rev. Endocrinol. 14, 88–98. https://doi.org/10.1038/nrendo.2017.151

Zhong, Q., Bollag, R.J., Dransfield, D.T., Gasalla-Herraiz, J., Ding, K.H., Min, L., Isales, C.M., 2000. Glucose-dependent insulinotropic peptide signaling pathways in endothelial cells. Peptides 21, 1427–1432. https://doi.org/10.1016/S0196-9781(00)00287-4

Zhou, P., Pu, W.T., 2016. Recounting cardiac cellular composition. Circ. Res. https://doi.org/10.1161/CIRCRESAHA.116.308139

Chapter 2

Objectives

2. Objectives

The general objective of this project was to evaluate the potential of zein-based nanoparticles in therapeutics, as well as carriers for oral delivery of biomacromolecules, using insulin as a model.

Zein was chosen as polymer to form the nanoparticles due to its ease to form stable and reproducible nanoparticles with high insulin encapsulation efficiencies. In addition, zein hydrolysates have been demonstrated to induce hypoglycemic effects driven by an increase in the secretion of incretins and an inhibitory effect over DPP-4 (Higuchi et al., 2013; Mochida et al., 2010).

In this context, the general objective was divided into 4 partial objectives:

1. To optimize the preparation of oral nanocarriers with mucus-permeating properties, based on the coating of zein nanoparticles with PEG.

2. To evaluate the hypoglycemic effect of empty zein-based nanoparticles, when orally administered, in laboratory animals.

3. To evaluate the effect of zein-based nanoparticles, orally administered, in two animal models cursing with hyperglycemia: *C. elegans* and the Alzheimer's Disease animal model of SAMP8 mice.

4. To evaluate and compare the capability of both "naked" (mucoadhesive) and PEG-coated (mucus-permeating) zein nanoparticles as oral carriers for insulin delivery.

Chapter 3

Preparation and evaluation of PEG-coated zein nanoparticles for oral drug delivery purposes

3. Preparation and evaluation of PEG-coated zein nanoparticles for oral drug delivery purposes

Reboredo C.[1], González-Navarro C.J.[2], Martínez-Oharriz C.[3], Martínez-López A.L.[1], Irache J.M.[1]

[1]Department of Chemistry and Pharmaceutical Technology, University of Navarra; C/ Irunlarrea 1, 31008 Pamplona, Spain.
[2]Centre for Nutrition Research, University of Navarra; C/ Irunlarrea 1, 31008 Pamplona, Spain.
[3]Department of Chemistry, University of Navarra; C/ Irunlarrea 1, 31008 Pamplona, Spain.

Corresponding author:
Prof. Juan M. Irache
Dep. Chemistry and Pharmaceutical Technology
University of Navarra
C/ Irunlarrea, 1
31008 – Pamplona Spain
Phone: +34948425600
Fax: +34948425619
E-mail: jmirache@unav.es

International Journal of Pharmaceutics (2021) 597: 120287

DOI: https://doi.org/10.1016/j.ijpharm.2021.120287

Abstract

The aim was to produce PEG-coated nanoparticles (NP-PEG), with mucus-permeating properties, for oral drug delivery purposes by using simple procedures and regulatory-approved compounds in order to facilitate a potential clinical development. For this purpose, zein nanoparticles were prepared by desolvation and, then, coated by incubation with PEG 35,000. The resulting nanocarriers displayed a mean size of about 200 nm and a negative zeta potential. The presence of PEG on the surface of nanoparticles was evidenced by electron microscopy and confirmed by FTIR analysis. Likely, the hydrophobic surface of zein nanoparticles (NP) was significantly reduce by their coating with PEG. This increase of the hydrophilicity of PEG-coated nanoparticles was associated with an important increase of their mobility in pig intestinal mucus. In laboratory animals, NP-PEG (fluorescently labelled with Lumogen® Red 305) displayed a different behavior when compared with bare nanoparticles. After oral administration, NP appeared to be trapped in the mucus mesh, whereas NP-PEG were capable of crossing the protective mucus layer and reach the epithelium. Finally, PEG-coated zein nanoparticles, prepared by a simple and reproducible method without employing reactive reagents, may be adequate carriers for promoting the oral bioavailability of biomacromolecules and other biologically active compounds with low permeability properties.

3.1. Introduction

In the last decades, numerous efforts have been performed in order to develop new and effective treatments for a multitude of diseases based on the use of nanodevices (e.g., liposomes, nanoparticles, micelles, dendrimers, etc.) as drug delivery systems. Many of these developments have clearly demonstrated (in preclinical studies) multiple benefits in treating chronic diseases, including important improvements in the therapeutic index of antimicrobials (Pison et al., 2006; Singh and Nalwa, 2011) or anticancer drugs (Gurunathan et al., 2018; Ma and Mumper, 2013). These improvements are directly related to the capabilities of these nanodevices to protect the loaded drug against a premature degradation in the body, improving its bioavailability, or/and to increase the therapeutic agent in its site of action (Irache et al., 2011; Vinogradov and Wei, 2012). Nevertheless, the number of these nanoparticles that have reached commercialization after a successful clinical trial is extremely low. At this moment, there would be around 20 commercial nano-based drugs approved by Regulatory Agencies (Bhardwaj et al., 2019), particularly based on the use of liposomes and polymers to encapsulate drugs inside their core and intended for cancer therapy (Hua et al., 2018). In addition, an estimated 100 nanoparticle-based products are in clinical trials, from which 18 started in the past 3 years (Martins et al., 2020); although, only six would be intended for oral administration (ClinicalTrials.gov, 2021).

This relatively low number of “successful” developments is (at least in part) related with a long and challenging regulatory pathway (Bremer-Hoffmann et al., 2018; Gaspani, 2013); surely influenced by a vague definition of the term “nanoparticle” and a certain negative state of public opinion (Bhardwaj et al., 2019) with everything that the term "nano" means or includes. Other barriers that importantly hamper the clinical development of nanoparticles for drug delivery purposes include the use of “innovative” materials rather than the approved excipients, and the difficulties to scale-up and transfer the whole preparative process to an industrial environment. In this way, the formulation of nanoparticles with a compound without a regulatory status (i.e., excipient or GRAS) makes the development process more challenging, longer, and therefore, more expensive (Cicha et al., 2018). This would be the case when nanoparticles are prepared with a new synthetic polymer, where additional information is required to demonstrate its safety with respect to the currently proposed level of exposure or administration route. Moreover, the employment of toxic reagents or organic solvents for the synthesis of nanoparticles, as well as the complexity and reproducibility of the preparative method, are also important aspects that will hinder the continuity of the project towards clinical phases. Nevertheless, the robustness of the process has to be evaluated as a whole, including all the steps and procedures involved in the manufacture of the final product (i.e., purification, concentration and drying steps).

In this context, the aim of this work was to produce mucus-permeating nanocarriers for oral drug delivery purposes by using simple procedures and regulatory-approved compounds in order to facilitate a potential clinical development. Mucus-permeating nanocarriers have the capability of minimizing the interaction with the mucus mesh (Netsomboon and Bernkop-Schnürch, 2016) and, thus, promoting diffusion through its protective layer lining the epithelium (Maisel et al., 2016; Netsomboon and Bernkop-Schnürch, 2016). The use of this type of nanocarriers may be of interest to improve the

oral bioavailability of biomacromolecules (Ensign et al., 2012) and other biologically active compounds with low permeability properties. For this purpose, zein-based nanoparticles prepared by a desolvation procedure and coated by simple adsorption with poly(ethylene glycol) (PEG) were prepared and evaluated. Zein is the main protein from corn with a hydrophobic character and insoluble in water that possesses a GRAS regulatory status (Irache and González-Navarro, 2017; Penalva et al., 2015). PEGs are hydrophilic neutral polymers approved as excipients and widely employed in several cosmetic and pharmacological products due to its safeness (D'souza and Shegokar, 2016).

3.2. Materials and methods

3.2.1. Materials

Zein, lysine, poly(ethylene glycol) 35,000 Da (PEG35), and Rose Bengal sodium salt were purchased from Sigma-Aldrich (Steinheim, Germany). Ethanol absolut was obtained from Scharlab (Sentmenat, Spain). Lumogen® Red 305 was provided by BASF (Ludwigshafen am Rhein, Germany). Mannitol was purchased from Guinama (La Pobla de Vallbona, Spain). O.C.T.™ Compound Tissue-Tek was obtained from Sakura Finetek Europe (Alphen aan Der Rijn, The Netherlands).

3.2.2. Preparation of nanoparticles

3.2.2.1. Preparation of bare nanoparticles (NP)

Zein nanoparticles were prepared by a desolvation procedure previously described (Penalva et al., 2015), with minor modifications. Briefly, 200 mg zein and 30 mg lysine were dissolved in 20 mL ethanol 55% with magnetic stirring for 10 minutes at room temperature. Nanoparticles were obtained by the addition of 20 mL purified water. The ethanol was removed in a rotatory evaporator under reduced pressure (Büchi Rotavapor R-144; Büchi, Postfach, Switzerland) and the resulting suspension of nanoparticles was concentrated and purified by tangential flow filtration through a polysulfone membrane with a molecular weight cut off (MWCO) of 500 kDa (Spectrumlabs, California, USA) in order to remove the excess of "free" reagents that were not part of the nanoparticles (e.g., zein, PEG and lysine). Finally, 2 mL of a mannitol aqueous solution (200 mg/mL) was added to the suspension of nanoparticles and the mixture was dried in a Büchi Mini Spray Dryer B-290 apparatus (Büchi Labortechnik AG, Switzerland) under the following experimental conditions: (i) inlet temperature, 90 °C; (ii) outlet temperature, 45−50 °C; (iii) air pressure, 4−6 bar; (iv) pumping rate, 5 mL/min; (v) aspirator, 80%; and (vi) airflow, 400− 500 L/h.

3.2.2.2. Preparation of PEG-coated nanoparticles

The coating of nanoparticles with PEG was performed by simple incubation between the just formed nanoparticles (before the purification step) and PEG 35,000 at different PEG-to-zein ratios. For this purpose, a stock solution of PEG 35,000 was prepared by dissolving the polymer in water to a final concentration of 100 mg/mL. Then, different volumes of this stock solution were added to the suspension of fresh nanoparticles. The mixture was maintained under magnetic agitation for 30 minutes at room temperature. After this time, nanoparticles were concentrated and purified by tangential filtration and dried as described above.

3.2.2.3. Preparation of fluorescently labelled nanoparticles

Nanoparticles were fluorescently labelled by the encapsulation of Lumogen® F Red 305. For this purpose, 2.6 mL of a Lumogen® red solution (concentration of 0.4 mg/mL) in ethanol was added to the solution of zein and lysine, prior to the formation of the nanoparticles. Then, nanoparticles were formed, and dried as described above.

3.2.3. Physico-chemical characterization of nanoparticles

3.2.3.1. Size, polydispersity index and zeta potential

Particle size and polydispersity index (PDI) were measured after dispersion in ultrapure water, at 25 °C, by dynamic light scattering (DLS) (angle of 90°). Zeta-potential was determined by electrophoretic laser Doppler anemometry after the dispersion of nanoparticles in purified water. All of these measurements were carried out in a Zetasizer analyzer system (Brookhaven Instruments Corporation, Holtsville, USA).

3.2.3.2. Morphology analysis

The shape and surface morphology of the dried nanoparticles were examined by scanning electron microscopy (SEM) and transmission electron microscopy (TEM). For SEM, 1.5 mg of nanoparticles were dispersed in 1 mL deionized water and centrifuged at 9,500 x g for 5 min in order to remove the mannitol. Then, the obtained pellet was re-dispersed in 1 mL water, mounted on SEM grids, dried and coated with a gold layer using a Quorum Technologies Q150R S sputter-coated (Ontario, Canada) and analyzed using a ZEISS Sigma 500 VP FE-SEM apparatus. For TEM, a drop of a suspension of nanoparticles was placed over a Holey Carbon film on Cu 300 mesh + thick C + SH grid (EM Resolutions, Sheffield, UK). The grid with the nanoparticle's suspension was allowed to dry and, then, images were taken using a Tecnai F30 microscope (Thermo Fischer Scientific, Oregon, USA).

3.2.3.3. Fourier Transform Infrared Resonance (FTIR) analysis

The analysis of the nanoparticle's surface was carried out by infrared spectroscopy (FTIR), using a Fourier transform spectrophotometer IR Affinity-1S (Shimadzu, Japan) coupled to a Specac Golden Gate ATR. The samples analyzed were placed directly on the diamond and the spectra were collected in the mode reflectance under the following conditions: wavenumber from 600 to 4000 cm^{-1} at 2 cm^{-1} of resolution and 50 scans per spectrum. Spectra were analyzed employing the Labsolution IR software.

Finally, the yield of the total preparative process of nanoparticles was calculated by gravimetry (Arbós et al., 2002).

3.2.3.4. Amount of protein transformed into nanoparticles and total process yield

The amount of zein forming nanoparticles was estimated by the quantification of the protein in the eluents obtained during the purification/concentration step by UV-vis molecular absorption spectroscopy at 300 nm wavelength, using a PowerWave XS Microplate reader (BioTek Instruments, Inc; Vermont, USA). The standard curve was prepared by dissolving increasing concentrations of pure zein in ethanol 70%. The amount of protein forming nanoparticles in the formulation was estimated as the ratio

between the amount of the protein quantified in the elute and the total amount of protein used for the preparation of nanoparticles, and, expressed as a percentage.
Finally, the yield of the whole preparative process of nanoparticles was calculated by gravimetry (Arbós et al., 2002).

3.2.3.5. Surface hydrophobicity evaluation

The surface hydrophobicity of the different nanoparticles was evaluated by the Rose Bengal method (Doktorovova et al., 2012). Briefly, 500 µL of nanoparticle suspensions (from 0.03 to 3 mg/mL) was mixed with 1 mL of a Rose Bengal aqueous solution (100 µg/mL). All samples were incubated under constant shaking at 1500 rpm, for 30 min at 25 °C (Labnet VorTemp 56 EVC, Labnet International, Inc. New Jersey, USA). Afterwards, the samples were centrifuged at 13,500 x g for 30 min (centrifuge MIKRO 220, Hettich, Germany) to remove the nanoparticles. The amount of Rose Bengal in the supernatants (Rose Bengal unbound) was calculated by measuring the absorbance at 548 nm, using a PowerWave XS Microplate reader (BioTek Instruments, Inc., Vermont, USA).
For calculations, the total surface area (TSA) of nanoparticles (calculated using Equation 1) was determined by assuming that the nanoparticles were spherical in shape and monodisperse, with a diameter equal to the mean size determined by DLS.

$$\mathrm{TSA} = (\mathrm{SA_{NP}})\ \mathrm{x}\ (\mathrm{NT_{NP}}) \qquad \text{[Equation 1]}$$

where SA_{NP} is the surface of one individual nanoparticle ($4\pi r^2$), and NT_{NP} is the total number of nanoparticles in each dilution, calculated using the Equation 2:

$$\mathrm{NT_{NP}} = \mathrm{m_{NP}}/(\rho\mathrm{zein}\ \mathrm{X}\ \mathrm{V_{NP}}) \qquad \text{[Equation 2]}$$

where m_{NP} is the weight of the nanoparticles in each dilution, ρzein is the density of zein (1.41 g/mL calculated by pycnometry) and V_{NP} is the volume ($4/3\pi r^3$) of an individual nanoparticle.
On the other hand, the partitioning quotient (PQ) was calculated as the quotient between the amount of the Rose bengal bound and unbound. The slope of the line of the chart represents the hydrophobicity of the formulation. The higher the slope, the higher the hydrophobicity.

3.2.4. Ex vivo mucus diffusion studies in porcine intestinal mucus

3.2.4.1. Collection and preparation of porcine mucus

The native porcine mucus was harvested from small intestine. The intestines were collected from a slaughterhouse and kept in ice-cold PBS (for a maximum period of 2 h) prior to the mucus collection. Intestine was cut into small portions that were opened to expose the lumen. Then, the exposed lumen was cleaned with PBS and the mucus collected using a spatula. The scraping was very gently in order not to drag epithelial tissue. A single pool of mucus was obtained, which was then distributed in 0.5 g-aliquots in microtubes that were stored at -80 ºC until the moment of use.

3.2.4.2. Evaluation of the diffusion of nanoparticles in mucus by Multiple Particle tracking (MPT)

The diffusion of the nanoparticles through pig intestinal mucus, as an in vitro measurement of their mucus-permeating properties, was assessed by the Multiple Particle Tracking (MPT) technique (Abdulkarim et al., 2015; Rohrer et al., 2016).

MPT involves video capturing and post-acquisition analysis for the individual movement of hundreds of fluorescently labelled particles within a mucus matrix (Grießinger et al., 2015). 25 µL of a suspension of fluorescently labelled nanoparticles (4 mg/mL in water) were inoculated into approximately 0.5 g of mucus aliquots. Then, each sample was incubated in gently agitation for 2 h at 37 ºC in order to ensure effective particle distribution before the video recording. 2-dimensional videos were captured in a Leica DM IRB wide-field epifluorescence microscope (×63 magnification oil immersion lens) using a high-speed camera (Allied Vision Technologies, UK) and capturing 30 frames/second; 10 s videos (i.e., complete video comprised 300 frames). At least 100 individual trajectories were tracked and analyzed from each mucus inoculated with fluorescent nanoparticles. Examples of videos, for bare (NP) and PEG-coated nanoparticles (NP-PEG50), are included in the Supplementary Material section. The MPT of each formulation was carried out in triplicates, leading to a minimum of 300 individual trajectories assessed. Videos were analyzed using Fiji (Image J). Only trajectories longer than 30 frames were considered, in order to ensure a continuous presence of the individual nanoparticles in the X-Y plane. The trajectory of each nanoparticle was then converted into numeric pixel data and, finally, into metric distances (based on the recording settings). The displacement of each nanoparticle overtime was expressed as the squared displacement (SD), and the mean square displacement (MSD) was calculated as the geometric mean of that nanoparticle's squared displacement along its entire trajectory. MSD was determined as follows:

$$MSD = (X\Delta t)^2 + (Y\Delta t)^2 \qquad \text{[Equation 3]}$$

For each nanoparticle formulation studied, the "ensemble mean square displacement" (<MSD>) was determined for each of the replicates by calculating the geometric mean of 100 individual trajectories. Then, the effective diffusion coefficient (Deff) of each formulation was calculated by:

$$Deff = \frac{<MSD>}{4\times\Delta t} \qquad \text{[Equation 4]}$$

Where 4 is a constant relating to the 2-dimensional mode of video capturing and Δt is the selected time interval.

In parallel, the diffusion of the nanoparticles in water ($D^{º}$) was calculated by the Stokes–Einstein equation at 37ºC:

$$D^{º} = kT6\pi\eta r \qquad \text{[Equation 5]}$$

In which k is the Boltzmann constant, T is absolute temperature, η is water viscosity and r is the mean radius of nanoparticles.

Finally, the diffusion of all the formulations was expressed as the ratio (%) between their Deff and their $D^{º}$ (diffusions in mucus and in water, respectively). This ratio provides a measure of the relative diffusion of the nanoparticles in mucus when considering their Brownian motion in water. For the graphical representation and for each formulation, these ratios were normalized to the ratio obtained for bare nanoparticles.

3.2.5. In vivo biodistribution evaluation of nanoparticles in healthy rats

The biodistribution of the nanoparticles in the gastrointestinal tract of male Wistar rats (weight 180-220 g; Envigo, Indianapolis, USA) was visualized by fluorescence microscopy (Inchaurraga et al., 2015). Animals were housed under controlled temperature (23 ± 2 ºC) with 12-hour light/dark cycles and with free access to normal chow and water. All experiments were performed after a minimum acclimation period of 7 days. Prior to any procedure, animals were fasted overnight. During the procedures, animals were kept fasted but with free access to water. All the procedures were performed following a protocol previously approved by the "Ethical and Biosafety Committee for Research on Animals" at the University of Navarra in line with the European legislation on animal experiments (protocol 045-18). For the study, 10 mg of fluorescently labelled nanoparticles dispersed in 1 mL purified water were orally administered to fasted animals. Two hours post-administration, animals were sacrificed by cervical dislocation and the guts were removed. Tissue portions of 1 cm were collected, washed with PBS, and frozen at -80 °C after inclusion in the tissue proceeding medium O.C.T.™. Each portion was then cut into 5 µm sections on a cryostat and attached to glass slides. Finally, the slices were fixed with formaldehyde and stained with DAPI for 15 min. before the cover assembly. The presence of fluorescently loaded zein nanoparticles in the intestinal mucosa and the cell nuclei of intestinal cells, dyed with DAPI, were visualized in a fluorescence microscope (Axioimager M1, Zeiss; Oberkochen, Germany) with a coupled camera (Axiocam ICc3, Zeiss) and fluorescent source (HBO 100, Zeiss). The images were captured with the software ZEN (Zeiss). The post-acquisition processing of the images was carried out with the software Fiji (Image J).
As control, an aqueous suspension of Lumogen® F Red 305 was administered.

3.2.6. Statistical analysis

The means and standard errors were calculated for every data set. All the group comparisons and statistical analyses were performed using a one-way ANOVA test followed by a Tukey-Kramer multicomparison test. In all cases, $p < 0.05$ was considered as a statistically significant difference. All calculations were performed using Graphpad Prism v6 (California, USA) and the curves were plotted with the Origin 8 software from Origin Lab (Massachusetts, USA).

3.3. Results

3.3.1. Nanoparticles characterization

The main physico-chemical characteristics of bare nanoparticles and nanoparticles coated at different PEG-to-zein ratios are shown in Table 1. The coating with PEG did not significantly modify the mean size of the resulting nanoparticles, with a typical diameter close to 200 nm and a polydispersity index (PDI) lower than 0.15. The morphological analysis by scanning electron microscopy (SEM) showed that all the formulations consisted of a homogeneous population of spherical-shaped nanoparticles (Figure 1), with no apparent differences between bare and PEG-coated nanoparticles. Likely, the size values obtained by this technique were similar to those obtained by dynamic light scattering. By TEM (Figure 1C), the presence of a less dense substance (corresponding to the PEG-coating) on the surface of zein nanoparticles was observed. Moreover, the coating with PEG slightly decreased the negative zeta potential of the resulting nanoparticles. In addition, the amount of zein transformed into nanoparticles was, in all cases, close to 80%. This value was not affected by the coating with PEG. Finally, the total preparative process yield (after the drying step) was calculated to be around 60%, without differences between formulations.

Table 1. Physico-chemical characteristics of bare (NP) and PEG-coated nanoparticles at different PEG-to-zein ratios (5%, 25%, 50% and 75%; w/w). Data expressed as mean ± SD, $n \geq 3$.

	Size (nm)	PDI	Zeta potential (mv)	Amount of protein (%)	Total process yield (%)
NP	200 ± 15	0.04 ± 0.03	-54 ± 4	82.8 ± 1.7	61.3 ± 5.6
NP-PEG5	203 ± 8	0.05 ± 0.02	-51 ± 3	80.8 ± 1.6	58.5 ± 1.8
NP-PEG25	202 ± 9	0.06 ± 0.02	-49 ± 2	77.4 ± 3.7	57.9 ± 3.9
NP-PEG50	201 ± 14	0.08 ± 0.01	-50 ± 2	81.5 ± 2.4	61.6 ± 9.8
NP-PEG75	213 ± 18	0.07 ± 0.02	-51 ± 2	82.8 ± 1.3	60.5 ± 1.8

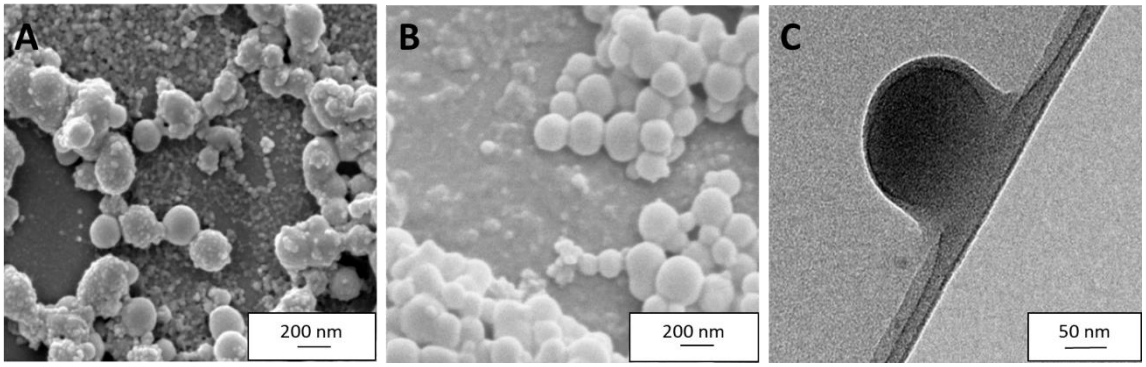

Figure 1. Microphotographs of bare nanoparticles (NP) and PEG-coated nanoparticles (NP-PEG50). A: NP obtained by SEM; B: NP-PEG50 obtained by SEM; C: NP-PEG50 obtained by TEM.

Figure 2 shows the FTIR spectra of the different nanoparticles and the raw materials employed in their preparation. The FTIR analysis demonstrated the presence of PEG in the nanoparticles after their formulation and drying. For all the formulations and for the free zein, two characteristic stretching vibration bands of amide I and amide II groups (at 1637 and 1521 cm^{-1}, respectively) were observed. The amide I band is associated with the C=O stretching and the amide II absorption peak is associated to C-N and N-H stretching vibrations. Regarding the FTIR spectrum of PEG, among others, the following typical signals were found: the vibration of CH_2 groups (1465 cm^{-1}), the stretching vibration of C-O-C (1143 cm^{-1}) or the C-O vibration of the OH end group of PEG (1093 cm^{-1}). The spectra of nanoparticles showed a displacement in the amide I stretching vibration band, which may be consequence of a conformational change when the nanoparticles are formed. Furthermore, in the spectra of PEG-coated nanoparticles obtained at a PEG-to-zein ratio higher than 0.05, some of the polymer vibration bands were clearly detected (1465, 1143 and 1058 cm^{-1}); confirming the presence of PEG on the surface of the nanoparticles. In addition, it is worth noting the shift of the vibration band corresponding to the alcoholic group of PEG (1093 to 1101 cm^{-1}) as well as that associated to the amide II of zein. This finding would indicate a possible interaction between the protein and the polymer through the formation of hydrogen bonds. Finally, absorption peaks corresponding to lysine (1577, 1408, 1358 cm^{-1}) were also detected in all the nanoparticle formulations.

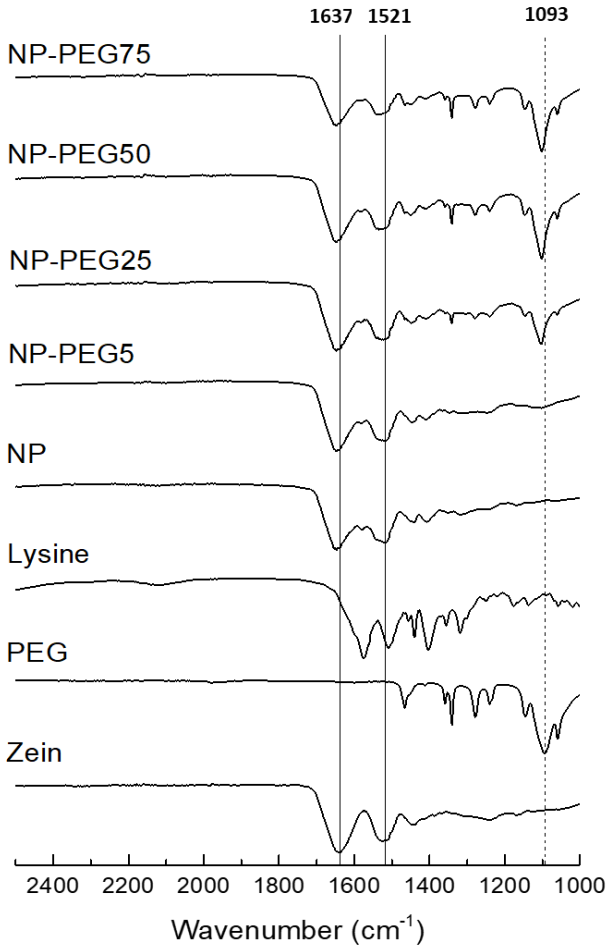

Figure 2. FTIR spectra of zein, PEG 35,000, lysine, bare zein nanoparticles and PEG-coated zein nanoparticles. Straight lines correspond to 1637 and 1521 cm^{-1} stretching vibration bands. Dashed line corresponds to 1093 cm^{-1} band.

Figure 3 shows the surface hydrophobicity of nanoparticles, calculated by means of the Rose Bengal test, as a function of the PEG-to-zein ratio employed in the preparation of nanoparticles. The coating of nanoparticles with PEG 35,000 significantly reduced the surface hydrophobicity, and this effect was found to be dependent on the amount of PEG employed during the coating process. Thus, the surface hydrophobicity of NP-PEG5 was calculated to be about 60% of the value determined for bare nanoparticles, whereas for NP-PEG75, the hydrophobicity was 4-times lower than for NP.

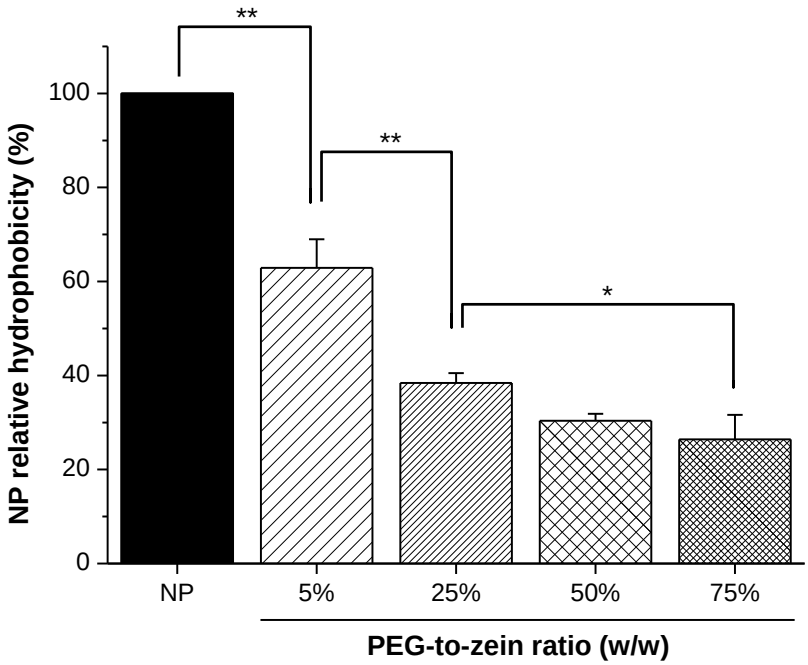

Figure 3. Surface hydrophobicity of the different formulations. Values are normalized to the hydrophobicity of bare nanoparticles (NP). Data expressed as mean ± SD (*n* = 3). *: $p < 0.05$; **: $p < 0.01$.

3.3.2. Ex vivo mucus diffusion studies in porcine intestinal mucus

Table 2 summarizes the main parameters defining the diffusivity of the nanoparticles and Figure 4 shows the capability of the different formulations to diffuse through pig intestinal mucus. Again, the coating of zein nanoparticles with PEG 35,000 significantly increased their ability to move and diffuse within mucus. Thus, for nanoparticles prepared at a PEG-to-zein ratio similar or higher than 0.25, their diffusivity in pig intestinal mucus was about 8-times higher than for bare nanoparticles.

Table 2. Diffusion behavior of the different formulations tested. < D_{eff}>: diffusion coefficient in mucus; D°: theoretical diffusion coefficient in water; <D_{eff}>/ D°: quotient between the diffusion coefficients of nanoparticles in mucus and water, respectively (expressed in percentage). Data expressed as mean ± SD, n = 3.

	<Deff> (mucus) $cm^2 \times S^{-1} \times 10^{-9}$	D° (water) $cm^2 \times S^{-1} \times 10^{-9}$	<Deff>/D° (%)
NP	0.054 ± 0.038	23.47	0.23 ± 0.11
NP-PEG5	0.169 ± 0.085	24.85	0.68 ± 0.03
NP-PEG25	0.473 ± 0.237	24.76	1.91 ± 0.07
NP-PEG50	0.447 ± 0.226	22.35	2.00 ± 0.15
NP-PEG75	0.479 ± 0.244	23.02	2.08 ± 0.15

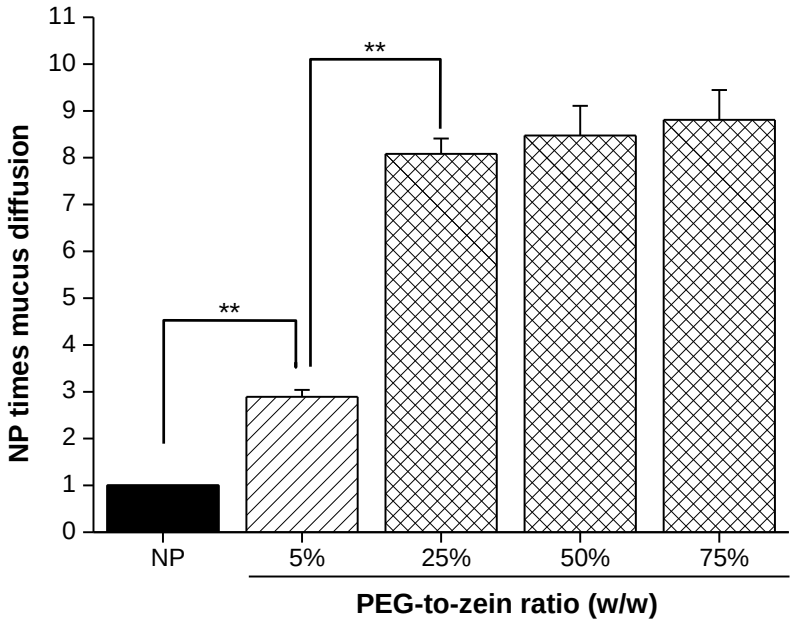

Figure 4. Comparative of the capability of nanoparticles (bare and PEG-coated) to diffuse through pig intestinal mucus. Values are normalized to the diffusion of bare nanoparticles (NP diffusion in intestinal mucus = 1). Data expressed as mean ± SD (*n* = 3). **: $p < 0.01$.

3.3.3. In vivo evaluation of the mucus-permeating properties of nanoparticles in healthy rats

Figure 5 shows fluorescence micrographs of duodenum slices obtained 2 hours post-administration of different Lumogen®-loaded formulations to animals. On the one hand, both bare and PEG-coated nanoparticles at a PEG-to-zein ratio of 0.05 displayed a localization that seemed to be restricted to the mucus layer covering the epithelium, without presence between intestinal villi. On the other hand, PEG-coated nanoparticles prepared at a PEG-to-zein ratio higher than 0.05 were clearly seen in close contact with the intestinal epithelium, occupying the inter-villi spaces and, even reaching the intestinal crypts. Afterwards, the biodistribution of mucoadhesive and mucus-permeating formulations (NP and NP-PEG50, respectively) along the gastrointestinal tract were evaluated (Figure 6). In the small intestine (Figures 6C-6F), mucus-permeating nanocarriers were able to diffuse through the protective mucus layer and reach the

epithelium surface. Finally, in the cecum of animals, only fluorescence associated to NP-PEG50 was visualized, suggesting the capability of these nanoparticles to reach this region of the gut 2 hours post-administration.

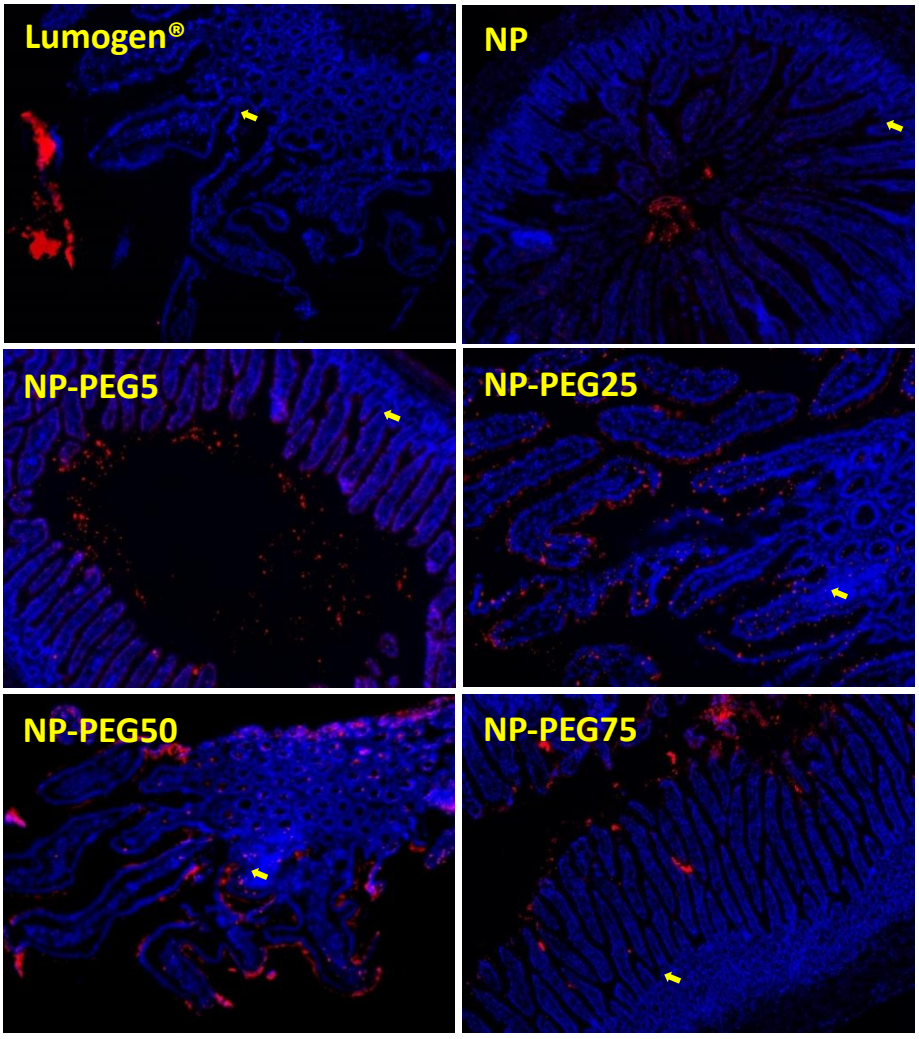

Figure 5. Fluorescence microscopic visualization of a lumogen® aqueous suspension, bare nanoparticles (NP), and PEG-coated nanoparticles in sections of rat duodenums 2 h after oral administration. Yellow arrows point to intestinal crypts. Nuclei of cells, stained with DAPI, are seen in blue.

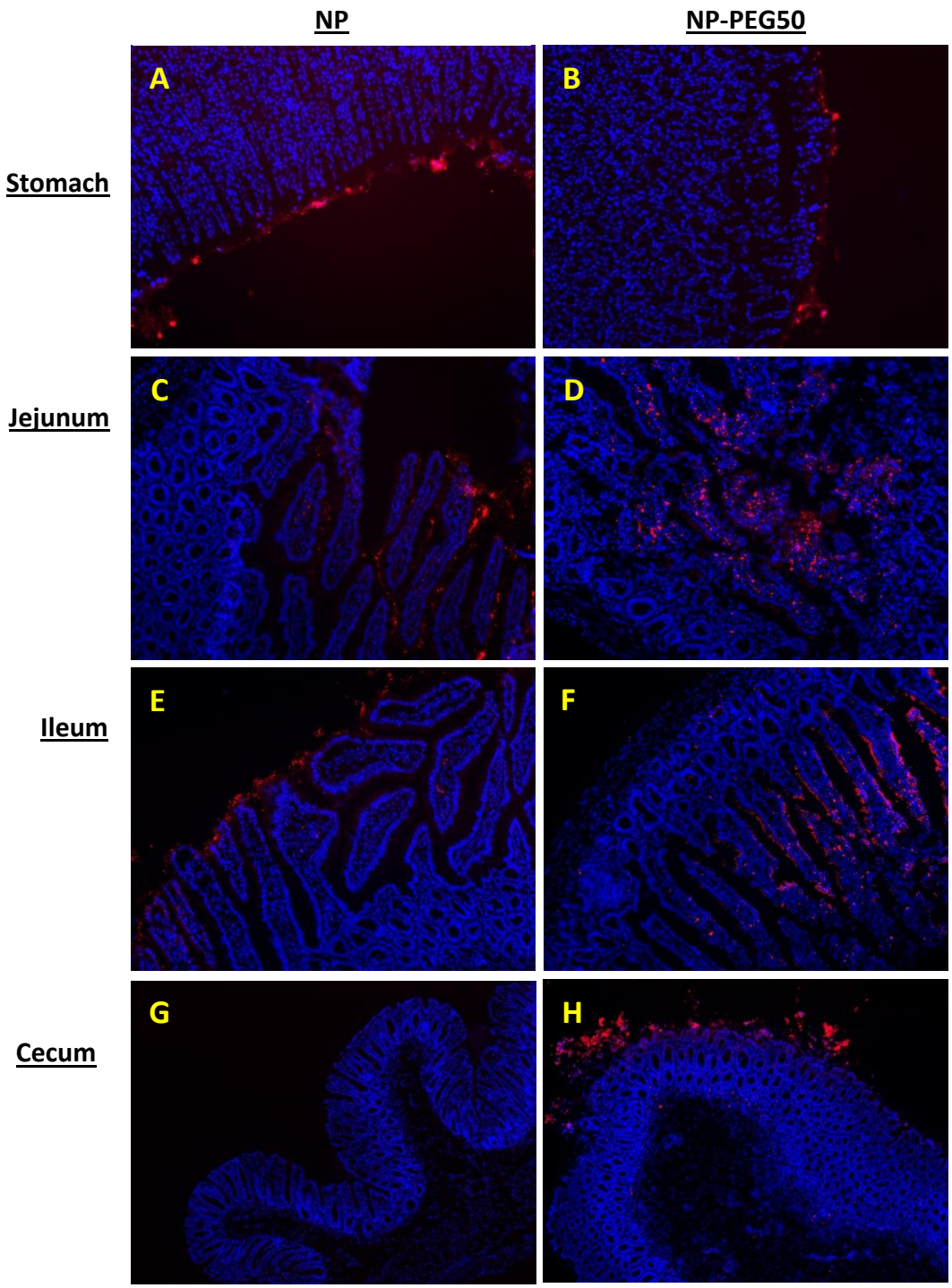

Figure 6. Fluorescence microscopic visualization of bare nanoparticles (NP) and nanoparticles coated with PEG at a PEG-to-zein ratio of 0.5 (NP-PEG50) in slices of the different portions of the gastrointestinal tract of animals, 2 h post-administration. A and B show slices from the stomachs of animals, C and D from jejunums, E and F from ileums, and G and H from cecums. Nuclei of cells, stained with DAPI, are seen in blue.

3.4. Discussion

This study aimed to develop suitable oral nanocarriers with mucus-permeating properties based on GRAS material and produced by a simple, cheap and reliable procedure. For that purpose, zein (GRAS protein) was chosen to generate the nanoparticles. These nanoparticles have shown (as other nanocarriers based on proteins) an interesting ability to encapsulate both hydrophobic small molecules (i.e., glibenclamide (Lucio et al., 2017)) and hydrophilic biomacromolecules (e,g., insulin (Inchaurraga et al., 2020)). However, and particularly for the oral delivery of therapeutic proteins, conventional zein nanoparticles (NP) do not provide the required increases in bioavailability necessary for a clinical application. In order to minimize this problem, one alternative would be the use of zein nanoparticles with mucus-permeating properties. For this purpose, zein nanoparticles were coated with a hydrophilic polymer (PEG) at different PEG-to-zein ratios. This coating would reduce the interactions between the nanoparticle and the mucus matrix, conferring mucus-penetrating nanoparticles. The capability of PEG to confer mucus-permeating properties relies on its molecular weight and grafting density, which, in last term, will determine its conformation (Inchaurraga et al., 2015; Xu et al., 2015). In fact, PEG with MW as high as 40 kDa, if densely grafted to the surface of nanoparticles, would prevent their interactions with mucus, conferring a mucoinert surface (Maisel et al., 2016). Since the coating occurs by physical adsorption, no new chemical entities are generated during the formulation of PEG-coated zein nanoparticles. Thus, this method leads to the formation of mucus-permeating nanoparticles composed only by GRAS materials, what would facilitate a faster clinical development (Ensign et al., 2012; Yu et al., 2012).

All the formulations were prepared by a desolvation method and the coating of the just formed nanoparticles with PEG was carried out by simple incubation. During the preparative process of nanoparticles, no type of organic solvent (apart from ethanol) was used. In addition, during the evaporation step, the ethanol used can be recovered and, later, reused. All of the resulting nanoparticles displayed a mean size of about 200 nm, independently of the PEG-to-zein ratio, and a negative zeta potential. Likely, under the experimental conditions tested, the amount of protein transformed into nanoparticles was high (about 80%), whereas the total yield of the process was calculated to be close to 60%. This last result may be considered low but it is in line with previous results using similar lab-scale Spray-dryer apparatus and might be improved during scale-up (Li et al., 2010; Ngan et al., 2014). In fact, it is well known that, in the particular case of Spray-drying, the yield of the process increases by increasing the size of batches (Draheim et al., 2015). The scanning electron microscopy confirmed the size, shape, and the homogeneity of the formulations measured by DLS. Nanoparticles were round-shaped with a smooth surface (Figure 1A and 1B). Interestingly, the incubation of nanoparticles with PEG produced a homogeneous layer around the surface of nanoparticles of about 10 nm (Figure 1C). This finding was corroborated by FTIR analysis (Figure 2) which not only showed the presence of the most characteristic PEG bands but also that the size of these signals increased by increasing the PEG-to-zein ratio. Considering all these data, it is possible to hypothesize an intermolecular interaction between PEG and zein. This interaction could be driven by a combination of hydrogen bonds (as predicted by the FTIR results) with other weak PEG-protein interactions (e.g., Van der Waals forces) (Wu et al., 2014).

The hydrophobic surface of zein nanoparticles was significantly reduced by their coating with PEG (Figure 3). This increase of the hydrophilicity of nanoparticles was associated with an important increase of their mobility in pig intestinal mucus (Figure 4), in line with previous results demonstrating that the PEGylation of polymer nanoparticles produced important improvements in their diffusive properties in mucus (Laffleur et al., 2014; Xu et al., 2015). In addition, in our case, a good correlation between hydrophobicity and mucus diffusivity was obtained ($R^2 > 0.93$; Figure 7).

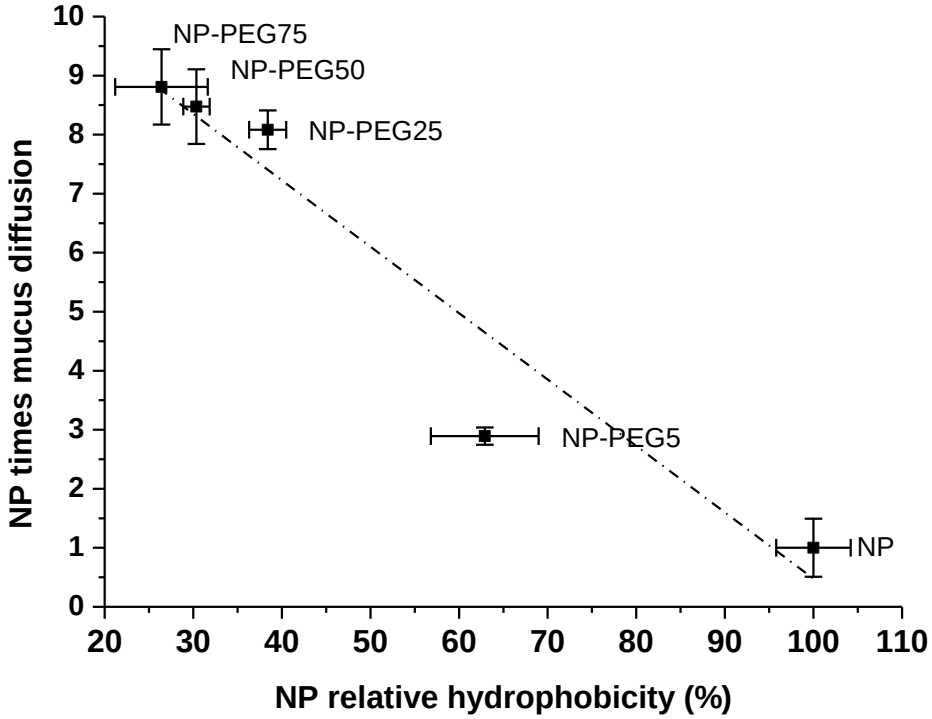

Figure 7. Correlation between the capability of PEG-coated zein nanoparticles (prepared at different PEG-to-zein ratios) to diffuse in pig intestinal mucus and their surface hydrophobicity. Both parameters are normalized to the values of bare nanoparticles. Data expressed as mean ± SD (n = 3).

The biodistribution assays carried out in rats revealed that, 2 hours post-administration of fluorescently labelled nanoparticles, bare zein nanoparticles and NP-PEG5 were found mainly entangled into the mucus layer of the duodenum, far away from the absorptive epithelium (Figure 5). Likely, this finding agreed well with a higher hydrophobicity and lower diffusivity in pig intestinal mucus (as measured by MPT). On the contrary, under the same conditions, nanoparticles prepared at a PEG-to-zein ratio similar or higher than 0.25 (with lower hydrophobicity and higher diffusivity in mucus than bare nanoparticles) were localized in close contact with the epithelium (Figure 5). In a similar way, NP-PEG50 were found in the cecum 2 hours post-administration, while bare nanoparticles did not reach this portion of the gastrointestinal tract (figure 6H and G, respectively). This, once again, reinforces the mucus-permeating properties of the PEG coating. The fact that NP-PEG50 reached the cecum might be because their increased diffusivity is applied not only for a transversal flow through the mucus gel, what allows them to reach the epithelium, but also for longitudinal flowing all along the gastrointestinal tract.

In summary, PEG-coated zein nanoparticles may be prepared by a desolvation procedure, subsequent purification by tangential flow filtration, and drying in a spray-drier. The preparative process is simple and reproducible, without employing reactive reagents. The PEG layer on the surface of zein nanoparticles conferred a hydrophilic corona and a superior capability to diffuse in pig intestinal mucus than bare nanoparticles. *In vivo*, PEG-coated nanoparticles showed mucus-permeating properties with an important ability to reach the gut epithelium and appeared to move more rapidly along the gut, reaching the cecum two-hours post-administration.

3.5. References

Abdulkarim, M., Agulló, N., Cattoz, B., Griffiths, P., Bernkop-Schnürch, A., Gómez Borros, S., Gumbleton, M., 2015. Nanoparticle diffusion within intestinal mucus: Three-dimensional response analysis dissecting the impact of particle surface charge, size and heterogeneity across polyelectrolyte, pegylated and viral particles. Eur. J. Pharm. Biopharm. 97, 230–238. https://doi.org/10.1016/j.ejpb.2015.01.023

Arbós, P., Arangoa, M.A., Campanero, M.A., Irache, J.M., 2002. Quantification of the bioadhesive properties of protein-coated PVM/MA nanoparticles. Int. J. Pharm. 242, 129–136. https://doi.org/10.1016/S0378-5173(02)00182-5

Bhardwaj, V., Kaushik, A., Khatib, Z.M., Nair, M., McGoron, A.J., 2019. Recalcitrant issues and new frontiers in nano-pharmacology. Front. Pharmacol. 10, 1369. https://doi.org/10.3389/fphar.2019.01369

Bremer-Hoffmann, S., Halamoda-Kenzaoui, B., Borgos, S.E., 2018. Identification of regulatory needs for nanomedicines. J. Interdiscip. Nanomedicine 3, 4–15. https://doi.org/10.1002/jin2.34

Cicha, I., Chauvierre, C., Texier, I., Cabella, C., Metselaar, J.M., Szebeni, J., Dézsi, L., Alexiou, C., Rouzet, F., Storm, G., Stroes, E., Bruce, D., MacRitchie, N., Maffia, P., Letourneur, D., 2018. From design to the clinic: Practical guidelines for translating cardiovascular nanomedicine. Cardiovasc. Res. 114, 1714–1727. https://doi.org/10.1093/cvr/cvy219

D'souza, A.A., Shegokar, R., 2016. Polyethylene glycol (PEG): a versatile polymer for pharmaceutical applications. Expert Opin. Drug Deliv. 13, 1257–1275. https://doi.org/10.1080/17425247.2016.1182485

Doktorovova, S., Shegokar, R., Martins-Lopes, P., Silva, A.M., Lopes, C.M., Müller, R.H., Souto, E.B., 2012. Modified Rose Bengal assay for surface hydrophobicity evaluation of cationic solid lipid nanoparticles (cSLN). Eur. J. Pharm. Sci. 45, 606–612. https://doi.org/10.1016/j.ejps.2011.12.016

Draheim, C., De Crécy, F., Hansen, S., Collnot, E.M., Lehr, C.M., 2015. A design of experiment study of nanoprecipitation and nano spray drying as processes to prepare plga nano-and microparticles with defined sizes and size distributions. Pharm. Res. 32, 2609–2624. https://doi.org/10.1007/s11095-015-1647-9

Ensign, L.M., Schneider, C., Suk, J.S., Cone, R., Hanes, J., 2012. Mucus penetrating nanoparticles: Biophysical tool and method of drug and gene delivery. Adv. Mater. 24, 3887–3894. https://doi.org/10.1002/adma.201201800

Gaspani, S., 2013. Access to liposomal generic formulations: beyond AmBisome and Doxil/Caelyx. Generics Biosimilars Initiat. J. 2, 60–62. https://doi.org/10.5639/gabij.2013.0202.022

Grießinger, J., Dünnhaupt, S., Cattoz, B., Griffiths, P., Oh, S., Gómez, S.B.I., Wilcox, M., Pearson, J., Gumbleton, M., Abdulkarim, M., Pereira De Sousa, I., Bernkop-Schnürch, A., 2015. Methods to determine the interactions of micro- and nanoparticles with mucus. Eur. J. Pharm. Biopharm. 96, 464–476. https://doi.org/10.1016/j.ejpb.2015.01.005

Gurunathan, S., Kang, M.H., Qasim, M., Kim, J.H., 2018. Nanoparticle-mediated combination therapy: Two-in-one approach for cancer. Int. J. Mol. Sci. 19, 3264. https://doi.org/10.3390/ijms19103264

Hua, S., de Matos, M.B.C., Metselaar, J.M., Storm, G., 2018. Current trends and challenges in the clinical translation of nanoparticulate nanomedicines: Pathways for translational development and commercialization. Front. Pharmacol. 9, 790. https://doi.org/10.3389/fphar.2018.00790

Inchaurraga, L., Martín-Arbella, N., Zabaleta, V., Quincoces, G., Peñuelas, I., Irache, J.M., 2015. In vivo study of the mucus-permeating properties of PEG-coated nanoparticles following oral administration. Eur. J. Pharm. Biopharm. 97, 280–289. https://doi.org/10.1016/j.ejpb.2014.12.021

Irache, J.M., Esparza, I., Gamazo, C., Agüeros, M., Espuelas, S., 2011. Nanomedicine: Novel approaches in human and veterinary therapeutics. Vet. Parasitol. 180, 47–71. https://doi.org/10.1016/j.vetpar.2011.05.028

Irache, J.M., González-Navarro, C.J., 2017. Zein nanoparticles as vehicles for oral delivery purposes. Nanomedicine 12, 1209–1211. https://doi.org/10.2217/nnm-2017-0075

Laffleur, F., Hintzen, F., Shahnaz, G., Rahmat, D., Leithner, K., Bernkop-Schnürch, A., 2014. Development and in vitro evaluation of slippery nanoparticles for enhanced diffusion through native mucus. Nanomedicine 9, 387–396. https://doi.org/10.2217/nnm.13.26

Li, X., Anton, N., Arpagaus, C., Belleteix, F., Vandamme, T.F., 2010. Nanoparticles by spray drying using innovative new technology: The Büchi Nano Spray Dryer B-90. J. Control. Release 147, 304–310. https://doi.org/10.1016/j.jconrel.2010.07.113

Ma, P., Mumper, R.J., 2013. Paclitaxel nano-delivery systems: A comprehensive review. J. Nanomedicine Nanotechnol. 4, 6. https://doi.org/10.4172/2157-7439.1000164

Maisel, K., Reddy, M., Xu, Q., Chattopadhyay, S., Cone, R., Ensign, L.M., Hanes, J., 2016. Nanoparticles coated with high molecular weight PEG penetrate mucus and provide uniform vaginal and colorectal distribution in vivo. Nanomedicine 11, 1337–1343. https://doi.org/10.2217/nnm-2016-0047

Netsomboon, K., Bernkop-Schnürch, A., 2016. Mucoadhesive vs. mucopenetrating particulate drug delivery. Eur. J. Pharm. Biopharm. 98, 76–89. https://doi.org/10.1016/j.ejpb.2015.11.003

Ngan, L.T.K., Wang, S.L., Hiep, I.M., Luong, P.M., Vui, N.T., Crossed D Signinh, T.M., Dzung, N.A., 2014. Preparation of chitosan nanoparticles by spray drying, and their antibacterial activity. Res. Chem. Intermed. 40, 2165–2175. https://doi.org/10.1007/s11164-014-1594-9

Penalva, R., Esparza, I., Larraneta, E., González-Navarro, C.J., Gamazo, C., Irache, J.M., 2015. Zein-Based Nanoparticles Improve the Oral Bioavailability of Resveratrol and Its Anti-inflammatory Effects in a Mouse Model of Endotoxic Shock. J. Agric. Food Chem. 63, 5603–5611. https://doi.org/10.1021/jf505694e

Pison, U., Welte, T., Giersig, M., Groneberg, D.A., 2006. Nanomedicine for respiratory

diseases. Eur. J. Pharmacol. 533, 341–350. https://doi.org/10.1016/j.ejphar.2005.12.068

Rohrer, J., Partenhauser, A., Hauptstein, S., Gallati, C.M., Matuszczak, B., Abdulkarim, M., Gumbleton, M., Bernkop-Schnürch, A., 2016. Mucus permeating thiolated self-emulsifying drug delivery systems. Eur. J. Pharm. Biopharm. 98, 90–97. https://doi.org/10.1016/j.ejpb.2015.11.004

Singh, R., Nalwa, H.S., 2011. Medical applications of nanoparticles in biological imaging, cell labeling, antimicrobial agents, and anticancer nanodrugs. J. Biomed. Nanotechnol. 7, 489–503. https://doi.org/10.1166/jbn.2011.1324

Vinogradov, S., Wei, X., 2012. Cancer stem cells and drug resistance: The potential of nanomedicine. Nanomedicine 7, 597–615. https://doi.org/10.2217/nnm.12.22

Wu, J., Zhao, C., Lin, W., Hu, R., Wang, Q., Chen, H., Li, L., Chen, S., Zheng, J., 2014. Binding characteristics between polyethylene glycol (PEG) and proteins in aqueous solution. J. Mater. Chem. B 2, 2983–2992. https://doi.org/10.1039/c4tb00253a

Xu, Q., Ensign, L.M., Boylan, N.J., Schön, A., Gong, X., Yang, J.C., Lamb, N.W., Cai, S., Yu, T., Freire, E., Hanes, J., 2015. Impact of Surface Polyethylene Glycol (PEG) Density on Biodegradable Nanoparticle Transport in Mucus ex Vivo and Distribution in Vivo. ACS Nano 9, 9217–9227. https://doi.org/10.1021/acsnano.5b03876

Yu, T., Wang, Y.Y., Yang, M., Schneider, C., Zhong, W., Pulicare, S., Choi, W.J., Mert, O., Fu, J., Lai, S.K., Hanes, J., 2012. Biodegradable mucus-penetrating nanoparticles composed of diblock copolymers of polyethylene glycol and poly(lactic-co-glycolic acid). Drug Deliv. Transl. Res. 2, 124–128. https://doi.org/10.1007/s13346-011-0048-9

Chapter 4

Effect of orally administered zein nanoparticles on the glucose homeostasis of *C. elegans* and healthy rats

4. Effect of orally administered zein nanoparticles on the glucose homeostasis of *C. elegans* and healthy rats

Reboredo C.[1], González-Navarro C.J.[2], Martínez-López A.L.[1], Irache J.M.[1]

[1]Department of Chemistry and Pharmaceutical Technology, University of Navarra; C/ Irunlarrea 1, 31008 Pamplona, Spain.
[2]Centre for Nutrition Research, University of Navarra; C/ Irunlarrea 1, 31008 Pamplona, Spain.

Abstract

The objective of this work was to evaluate the potential hypoglycemic effect of orally administered zein-based nanoparticles. For this purpose, two different formulations, a mucoadhesive (NP) and a mucus-diffusive (NP-PEG50), were supplemented into the growth medium of *C. elegans* cultured under high glucose conditions. Under these conditions, the addition of nanoparticles to the medium induced a significant decrease in the fat accumulation within the body of the worms, which is closely related to the glucose metabolism. Moreover, NP-PEG50 displayed a more potent effect than NP on reducing the lipid tissue. Afterwards, the effect of the formulations, as well as the free protein, was assessed in a murine laboratory animal. Treatments were administered to healthy rats by oral gavage and changes in the blood glucose levels, insulinemia, and in the plasma values of incretins (glucose-dependent insulinotropic polypeptide (GIP) and glucagon-like peptide-1 (GLP-1)) were assessed. All the treatments induced an insulinotropic effect that started 1.5 h post-administration, being free zein the most potent one. On the other hand, only nanoparticulated zein was able of reducing the glycemia of the animals and increasing the secretion of GLP-1, effects observed from 1.5 h after the oral administration and that lasted a minimum period of time of 6 hours. Regarding GIP values, all three treatments displayed the same effect, inducing no changes during the first 3 hours followed by a significant increase in the circulating levels of the hormone 6 h post-administration. Finally, the capability of the treatments to modulate the glycemic control of animals facing an intraperitoneal glucose tolerance test (ipGTT; 2 g/kg) was also evaluated. Only NP-PEG50 treatment was able of modulating the glycemic response to the intraperitoneal injection of glucose, displaying a more delayed glycemic peak and a reduction in the total exposure to the sugar (measured as the area under the curve).

4.1. Introduction

Glucose homeostasis is a complex phenomenon involving a wide variety of hormones whose objective is to keep the blood glucose levels within the normal range (4 – 6 mM), avoiding the conditions of hyper and hypoglycemia (Röder et al., 2016). Insulin is the principal hypoglycemic hormone, and it is produced and stored in the β cells of pancreas, cells that are found forming clusters called islets of Langerhans (Fu et al., 2012). These β cells themselves act as glycemic sensors. When the glycemia rises, glucose enters the β cells through the GLUT transporters and triggers a signaling cascade that induces an increase in the intracellular calcium concentration and, in last term, leads to the exocytosis of the insulin vesicles (Henquin et al., 2006; Röder et al., 2016; Wang and Thurmond, 2009). After its release, insulin reaches, through the bloodstream, different insulin-sensitive tissues (e.g., liver, muscle, adipose tissue, brain or heart among others) and stimulate the glucose uptake by the cells, leading to a reduction in the circulating levels of glucose (Cheng et al., 2010; Dimitriadis et al., 2011; Jung and Choi, 2014; Klein and Visser, 2010; Kleinridders et al., 2014; Lázár et al., 2018).

Although glucose is the main inductor for insulin release, other types of stimuli can also exert this effect. The presence in blood of some amino acids, fats and other monosaccharides different from glucose have also demonstrated to act as insulinogogues (Deeney et al., 2000; Fu et al., 2012). Interestingly, not all the amino acids have the same potency on triggering insulin release, and the most potent ones would be leucine, isoleucine, alanine, and arginine (Henquin et al., 2006; Newsholme et al., 2006; Newsholme and Krause, 2012). However, the mechanisms by which amino acids induce secretion of insulin are very variable, depending on their nature and physicochemical properties (McClenaghan et al., 1996). After food ingestion, the rise in the blood insulin levels has been shown to be more potent than during an isoglycemic intravenous glucose infusion. This phenomenon is known as the incretin effect and it happens because the food present in the lumen of the gastrointestinal tract stimulates the production of hormones by the enteroendocrine cells present in the gut (Kazafeos, 2011; Mortensen et al., 2003). The hormones involved in this response are the incretins GLP-1 and GIP, from which GLP-1 has been shown to play a more important role in glucose homeostasis (Holst, 2019).

GLP-1 is stored in granules within the L cells of the gut, whose abundancy increases from proximal to distal regions of the intestine (Pais et al., 2016a). These cells act as sensors and, in response to the presence of nutrients in the lumen, release their GLP-1-containing granules (Chai et al., 2012; Nadkarni et al., 2014; Seino et al., 2010). The release of GLP-1 starts a few minutes after the ingestion of the meal and lasts for several hours (Pais et al., 2016a; Rocca and Brubaker, 1999). Carbohydrates, fats, and proteins present in the lumen act as GLP-1 release inductors. Regarding the secretagogue effect of proteins and their metabolites, several peptones and amino-acids (e.g. glutamine, glycine, alanine, phenylalanine and arginine) have shown the capability of directly induce GLP-1 release (Clemmensen et al., 2013; Pais et al., 2016a, 2016b), although oligo- or large peptides seem to be more potent than free amino acids (Ishikawa et al., 2015). Independently of the insulinogogue effect of GLP-1, which is always glucose-dependent (Nadkarni et al., 2014; Seino et al., 2010; Thurmond, 2009), it also induces

glucose uptake by muscle, adipose tissue and liver (Ayala et al., 2009; Chai et al., 2012; Dardevet et al., 2004; Rowlands et al., 2018). Moreover, in the liver, GLP-1 also induces hepatic glucose clearance and glycogen synthesis (Ayala et al., 2009) while reducing the hepatic glucose production through the inhibition of glucagon release (Jin and Weng, 2016).

GIP is another incretin produced and secreted by the enteroendocrine K cells present in the gut in response to food intake. In contrast to the distribution of L cells, K cells are mainly located in proximal regions of the gut, decreasing in number in further sections (Pais et al., 2016a). Although K cells are sensitive to all type of nutrients (sugars, fats and proteins), it has been observed that proteins are the most potent inductors of GIP release (Seino et al., 2010). GIP exerts its function mainly over the pancreas, the bone, the adipose tissue, and the brain. However, in contrast to the effect exerted by GLP-1 in the pancreas, GIP can stimulate both the production of insulin and glucagon (Seino et al., 2010). When glycemia is low (around 80 mg/dL, as in fasted state), GIP induces glucagon release by targeting α cells. However, when blood glucose levels rise (postprandial state), it stimulates insulin release by targeting the β cells (El and Campbell, 2020)

Zein, the main storage protein found in the seeds of maize, is a prolamin insoluble in water but soluble in hydro-alcoholic solutions with high ethanol contents (between 60 and 80%). For drug delivery purposes, zein presents two major advantages. The former is its regulatory status as a GRAS material (Weissmueller et al., 2016). The latter is the capability of this material to be transformed into nanoparticles by simple preparative methods and without the need of using toxic chemical reagents as cross-linkers (Martínez-López et al., 2020). Moreover, zein nanoparticles may be also easily "decorated" with PEG, yielding nanocarriers with similar physicochemical properties but with an increased mucus-diffusive behavior (Inchaurraga et al., 2015; Reboredo et al., 2021). Zein hydrolysates have shown the capability of inducing the release of incretins and inhibit the action of DPP-4 (the enzyme responsible for the degradation of both GLP-1 and GIP) (Mochida et al., 2010). Thus, zein and its nanoparticulated form could also keep this incretin-inducing properties and, therefore, exert a hypoglycemic activity in healthy individuals.

The objective of this work was to evaluate the effect of two different types of zein-based nanoparticles over the glucose homeostasis of two different animal models, following oral administration. One of the formulations consist of bare zein nanoparticles (NP), which display a mucoadhesive behavior (Inchaurraga et al., 2019). The other formulation consists of PEG-coated zein nanoparticles (NP-PEG50), which have a more mucus-diffusive demeanor (Reboredo et al., 2021). The effect of both formulations, as well as the native protein, over the glucose homeostasis of two different animal models (*C. elegans* and healthy male Wistar rats) was assessed. Moreover, the hormonal mechanisms involved for the improved glycemic control were also evaluated.

4.2. Material and methods

4.2.1. Materials

Zein, L-lysine, poly(ethylene glycol) 35,000 Da (PEG35), Orlistat®, Nile red, isopropanol, glucose, sodium azide, agarose, and Triton X-100 were purchased from Sigma-Aldrich (Steinheim, Germany). Ethanol absolute was obtained from Scharlab (Sentmenat, Spain). DPPIV inhibitor, aprotinin, insulin ELISA kit (EZRMI-13K) and GIP ELISA kit (EZRMGIP-55K) were obtained from Merck (Darmstadt, Germany). GLP-1 ELISA kit (YK160 GLP-1 EIA) was purchased from Yanaihara Institute Inc. (Awakura, Japan). Rat somatostatin ELISA kit (E-EL-R0914) was purchased from Elabscience (Houston, USS)

4.2.2. Preparation of nanoparticles

4.2.2.1. Preparation of bare nanoparticles (NP)

Zein nanoparticles were prepared by a desolvation procedure previously described (Penalva et al., 2015), with minor modifications. Briefly, 200 mg zein and 30 mg lysine were dissolved in 20 mL ethanol 55% with magnetic stirring for 10 minutes at room temperature. Nanoparticles were obtained by the addition of 20 mL purified water. The ethanol was removed in a rotatory evaporator under reduced pressure (Büchi Rotavapor R-144; Büchi, Postfach, Switzerland) and the resulting suspension of nanoparticles was concentrated and purified by tangential flow filtration through a polysulfone membrane with a molecular weight cut off (MWCO) of 500 kDa (Spectrumlabs, CA, USA). Finally, nanoparticles were dried in a Büchi Mini Spray Dryer B-290 apparatus (Büchi Labortechnik AG, Switzerland) under the following experimental conditions: (i) inlet temperature, 90 °C; (ii) outlet temperature, 45−50 °C; (iii) air pressure, 4−6 bar; (iv) pumping rate, 5 mL/min; (v) aspirator, 80%; and (vi) airflow, 400− 500 L/h.

4.2.2.2. Preparation of PEG-coated nanoparticles (NP-PEG50)

The coating of nanoparticles with PEG was performed by simple incubation of the just formed nanoparticles (before the purification step) and PEG 35,000 at a PEG-to-zein ratio of 0.5. For this purpose, the adequate volume of a solution of PEG 35,000 in water (100 mg/mL) was added to the suspension of nanoparticles. The mixture was maintained under magnetic agitation for 30 minutes at room temperature. After this time, nanoparticles were concentrated and purified by tangential flow filtration and dried as described above.

4.2.3. Physico-chemical characterization of nanoparticles

4.2.3.1. Size, polydispersity index and zeta potential

Particle size and polydispersity index (PDI) were measured after dispersion in ultrapure water, at 25 °C, by dynamic light scattering (DLS) (angle of 90°). Zeta-potential was determined by electrophoretic laser Doppler anemometry after the dispersion of nanoparticles in purified water. All these measurements were carried out in a Zetasizer analyzer system (Brookhaven Instruments Corporation, Holtsville, NY, USA).

4.2.3.2. Morphology analysis

The shape and surface morphology of the dried nanoparticles were examined by scanning electron microscopy (SEM). 1.5 mg of nanoparticles were dispersed in 1 mL

purified water, mounted on SEM grids, dried, and coated with a gold layer using a Quorum Technologies Q150R S sputter-coated (Ontario, Canada). Images from were taken using a ZEISS Sigma 500 VP FE-SEM (Oberkochen, Germany) apparatus.

4.2.4. In vivo evaluation of nanoparticles in C. elegans

4.2.4.1. Strain and culture conditions

Caernoharbditis elegans (*C. elegans*) was maintained and cultured as described previously (Lazzaro and Schneider, 2014). Wild-type N2 Bristol strain was obtained from the Caenorhabditis Genetics Center (CGC, University of Minnesota, MN, USA), and were cultured at 20 ºC on NGM (Nematode Growth Medium) agar with *Escherichia coli* OP50 as normal nematode diet. For all experiments, age-synchronized worms were used. Synchronization was performed by hypochlorite treatment, a condition in which only eggs can survive, and eggs were let hatch overnight in M9 buffer solution (Porta-de-la-Riva et al., 2012).

4.2.4.2. Treatment with nanoparticles and fat content quantification

The quantification of the fat content within the body of the worms was performed by the Nile Red staining method (Navarro-Herrera et al., 2018). For that purpose, worms (L1 larvae stage) were cultured under high glucose conditions (0.5% w/v). Under these conditions, worms show an expansion of the fat tissue due to an increase in the ammount of lipidic droplets (Martínez-López et al., 2021). All the assays were performed in triplicates using 6-well plates. In each well, 4 mL of the glucose-suplemented medium were added, with or without treatments. Moreover, 3 wells with NGM without glucose suplementation were added to confirm the fattening effect of the glucose. Treatments were added to the wells at a concentration of 1.6 mg/mL nanoparticles. Finally, a positive control of Orlistat® (6 µg/mL), as a fat reducing agent, was also added (Martorell et al., 2012). All the treatments were added, after resuspension/dissolution in purified water, to the wells containing liquid NGM. After the addition, plates were let solidify in a dark environment. Once solidified, 100 µL of a culture of *E. coli* (OP50 strain) were added to each well and let dry in darkness. Finally, the L1-synchronized worms were placed into the wells and incubated for 46 h at 20 ºC. After the incubation period, worms were picked up and stained by a Nile Red staining method (Pino et al., 2013). Stained worms were fixed in agarose (2%) over glass slides and observed on a Nikon's SMZ18 stereomicroscope (Nikon Instruments Inc., Japan) coupled to an epi-fluorescence system and a DS-FI1C refrigerated color digital camera. Pictures were acquired under a GFP filter (Ex 480-500; DM 505; BA 535-550). Post-acquisition processing and fat quantification was performed with the FIJI (image J) software.

4.2.5. In vivo evaluation of nanoparticles in healthy rats

4.2.5.1. Strain and housing conditions

Male Wistar rats weighing 180-220 g were purchased from Envigo (Indianapolis, IN, USA). Animals were housed under controlled temperature (23 ± 2 ºC) with 12-hour light/dark cycles and with free access to normal chow and water. All experiments were performed after a minimum acclimation period of 7 days. Prior to any procedure, animals were fasted overnight. During the procedures, animals were kept fasted but with free access to water.

All the procedures were performed following a protocol previously approved by the "Ethical and Biosafety Committee for Research on Animals" at the University of Navarra in line with the European legislation on animal experiments (protocol 071-19).

4.2.5.2. Evaluation of the hypoglycemic effect of nanoparticles

For this experiment, healthy rats were divided in different groups of at least 6 animals. Each group received orally one of the following treatments: (i) free zein in water (50 mg/kg), (ii) bare zein nanoparticles in water (NP; 50 mg/kg), (iii) PEG-coated zein nanoparticles (NP-PEG50; 50 mg/kg). All these formulations were dispersed in 1 mL water prior administration to animals through oral gavage, using a stainless-steel cannula. As controls, one group received orally 1 mL water. At different times, 300 µL of blood samples were collected, from the tail vein, into K_3EDTA tubes at. Protease inhibitors (DPP-4 inhibitor, 50 µM; aprotinin 500 KIU) were added to the tubes just after the collection of the blood. At each extraction, glucose levels in blood were quantified using an Accu-Check® Aviva glucometer (Roche Diagnostics, Basel, Switzerland). The blood-containing tubes were centrifuged at 2500 g for 10 minutes at 4 ºC. The plasma was withdrawn, placed into new microtubes and stored at -80 ºC until use. Finally, insulin, GIP, GLP-1 and somatostatin levels in the blood of rats were quantified by ELISA, following the indications of the kit's manufacturers.

4.2.5.3. Intraperitoneal Glucose Tolerance Test (ipGTT) in healthy rats

The ipGTT was performed to evaluate the change in the glycemic control of rats receiving the different treatments (50 mg/kg) when facing an intraperitoneal injection of glucose (2 g/kg). Animals were fasted overnight prior to any procedure and treatments were administered by oral gavage 2 hours before the intraperitoneal injection of glucose. For this purpose, rats were divided into 4 different groups ($n \geq 6$): (i) untreated control (1 mL of purified water), (ii) free zein dispersed in 1 mL water; (iii) 1 mL of a suspension of bare nanoparticles in purified water (NP), (iv) 1 mL of a suspension of PEG-coated nanoparticles (NP-PEG50). Blood glucose levels were measured at several times, before and after the intraperitoneal injection of glucose: -120 minutes (just before oral administration of nanoparticles), T_0 (prior to the intraperitoneal injection of glucose) and 15, 30, 60 and 120 minutes after the glucose overload. Blood samples (50 µL) were collected from the tail vein and the glycemia was measured using an Accu-Check® Aviva glucometer (Roche Diagnostics, Basel, Switzerland).

4.2.6. Statistical analysis

Means and standard errors were calculated for every data set. All the group comparisons and statistical analyses were performed using a one-way ANOVA test followed by a Tukey-Kramer multiple comparisons test, except for the data obtained from the efficacy studies in rats, where the statistical analysis performed was a two-way ANOVA. Significant differences with respect to control group are marked as follows: *$p < 0.05$, **$p < 0.01$ or ***$p < 0.001$. All calculations were performed using GraphPad Prism v6 (GraphPad Software, San Diego, CA, USA) and the curves were plotted with the Origin 8 software (OriginLab Corp, Northampton, MA, USA).

4.3. Results

4.3.1. Nanoparticles characterization

The main physico-chemical properties of both formulations are summarized in Table 1. Both formulations displayed an average size of around 200 nm, with very low PDI indexes (less than 0.1). Regarding the zeta potential, both formulations showed a negative zeta potential, without differences between bare and PEG-coated nanoparticles.

Table 1. Physico-chemical characteristics of empty zein nanoparticles without coating (NP) or coated with PEG at a PEG-to-zein ratio of 0.5 (NP-PEG50). Data expressed as mean ± SD, n ≥ 3.

Formulation	Size (nm)	PDI	Zeta potential (mv)
NP	199 ± 28	0.04 ± 0.03	-52 ± 4
NP-PEG50	203 ± 13	0.08 ± 0.01	-50 ± 1

The images obtained by SEM showed that the resulting nanoparticles consisted of homogenous populations of around 200 nm, confirming the results found by DLS. Moreover, the nanoparticles display a spherical shape and a smooth surface, without apparent differences between bare and PEG-coated nanoparticles (Figures 1A and B respectively).

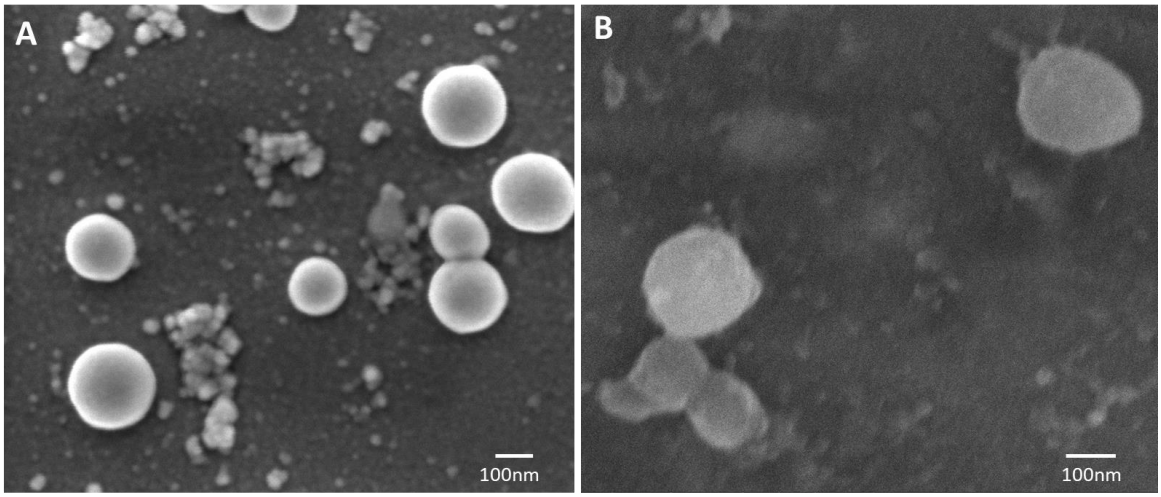

Figure 1. SEM microphotographs of NP (A) and NP-PEG50 (B).

4.3.2. In vivo evaluation of nanoparticles in C. elegans

The effect of the formulations over the fat accumulation of the worms, as an indirect measurement of the hypoglycemic effect, is shown in Figure 2A. The values of the fat content in the worms are normalized to the content of those cultured under high glucose conditions without treatment. Worms cultured in normal NGM medium showed a fat content equal to 62% of the content displayed by those cultured under high glucose conditions. In worms cultured in a medium supplemented with glucose, orlistat®-treated worms (positive control) displayed a fat content equal to the 58% of the fat

content of those receiving no treatment. On the other hand, worms receiving NP and NP-PEG50 showed, respectively, a fat content of 89% and 86% compared to the control worms. These reductions in the fat accumulation observed in animals treated with nanoparticles were, in both cases, statistically significant ($p < 0.01$) when compared with control worms. On the other hand, no significant differences were found between worms receiving bare or PEG-coated nanoparticles. Representative images of the worms are displayed in Figure 2B, where the brightness in green represents the amount of lipid droplets within the body of the nematode.

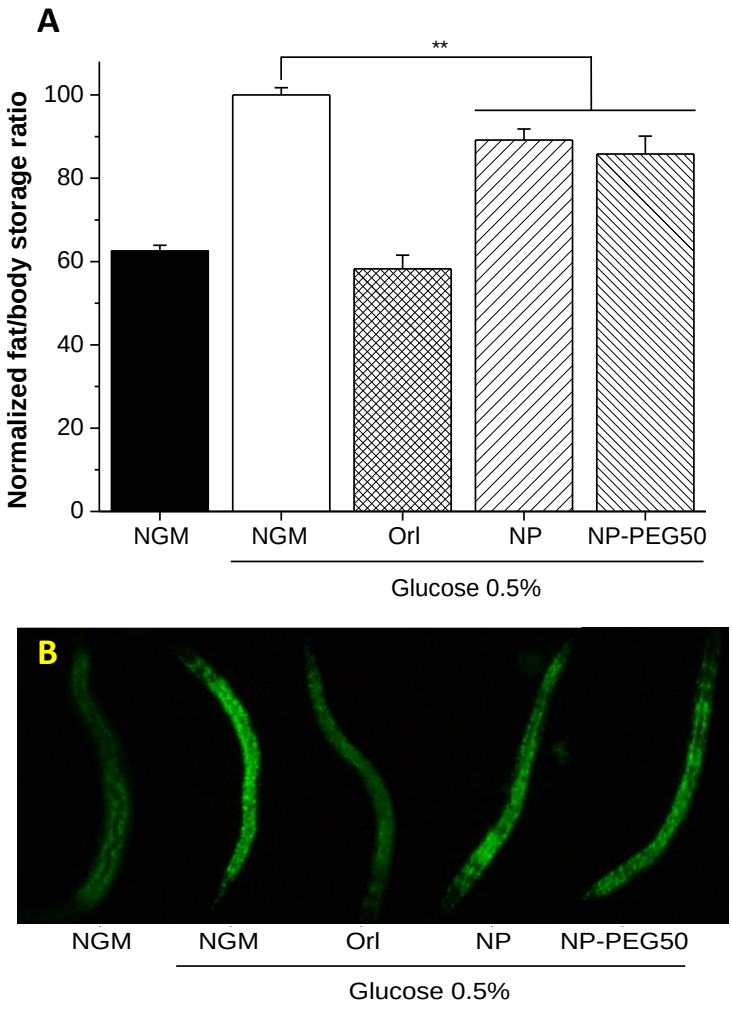

Figure 2. A: Quantified fat content in the worms, values are normalized to the fat content of worms cultured under high glucose conditions and receiving no treatment; B: Pictures of worms cultured with the different treatments. Orl: orlistat®; NP: bare zein nanoparticles; NP-PEG50: PEG-coated zein nanoparticles. Data expressed as mean ± SD (n = 3 wells with at least 25 worms/well). **: $p < 0.01$.

4.3.3. Evaluation of the hypoglycemic effect of nanoparticles

The effect of the oral administration of the different treatments on the glycemia of rats is shown in Figure 3. The administration of an aqueous suspension of free zein at a dose of 50 mg/kg did not induce any relevant effect in glycemia of rats. However, the same dose of both nanoparticle formulations (NP and NP-PEG50) induced a significant

decrease in the blood glucose levels of the animals, that lasted for at least 6 hours. The hypoglycemic effect of zein nanoparticles was clearly observed three hours post-administration. At this time point, for both formulations, the decrease in the initial levels of glucose in blood was about 25%. Nevertheless, NP-PEG50 appeared to offer a more intense and lasted hypoglycemic effect than NP. Thus, 6 h after administration, the hypoglycemic effect induced by the oral administration of NP-PEG50 was significantly higher than for bare nanoparticles ($p < 0.01$).

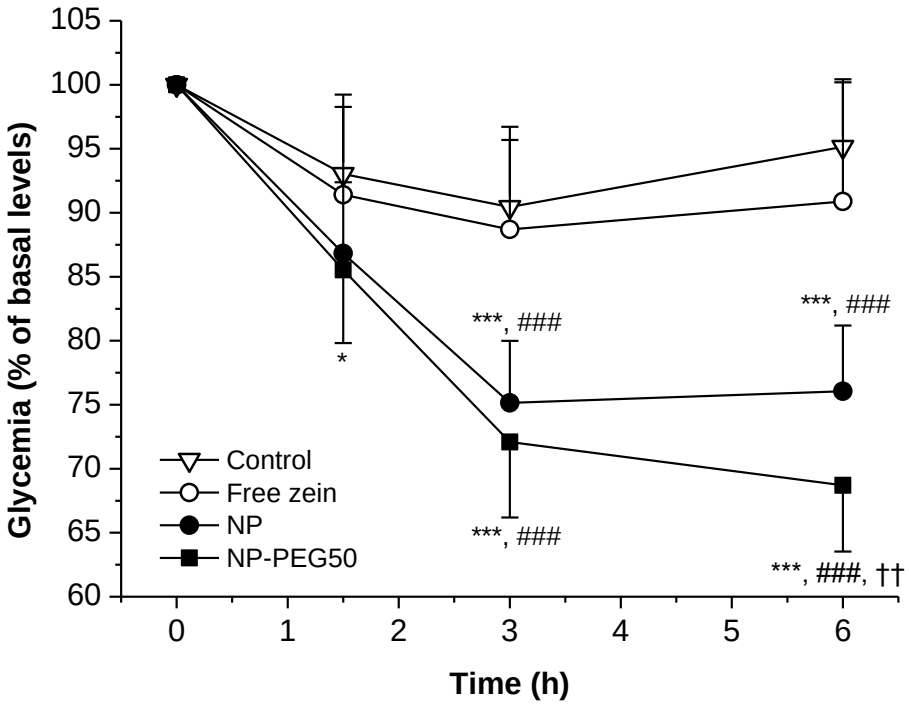

Figure 3. Blood glucose levels of animals treated orally with zein nanoparticles (NP; NP-PEG50) or an aqueous suspension of free zein. All the treatments were administered at a dose of 50 mg/kg. Data expressed as mean ± SD ($n \geq 6$). *: $p < 0.05$; ***: $p < 0.001$ compared to control. ###: $p < 0.001$ compared to free zein. ††: $p < 0.01$ compared to NP.

The effect of the oral administration of the treatments on different hormones involved in the glucose homeostasis was also assessed. At the same extraction points at which blood glucose levels were measured, the following hormones were quantified: insulin, GLP-1, and GIP. Figure 4 shows the changes in the blood levels of insulin. In fasted control animals, insulinemia drastically decreased to values below 10% of the basal levels 3 h after the beginning of the experiment. On the contrary, animals receiving a suspension of the free protein showed a fast increase in the insulinemic values, increasing more than 50% of the basal levels 3 hours post-administration. These high levels of insulin in blood were maintained for at least 3 hours. Animals treated with either NP or NP-PEG50 displayed an insulinemic profile different to that observed for animals receiving the free protein. Thus, during the first 3 h after the oral administration of nanoparticles, no apparent modification of insulin levels in blood were observed.

However, after these first 3 h, the levels of insulin clearly increased, reaching those observed for animals treated with the aqueous suspension of the protein.

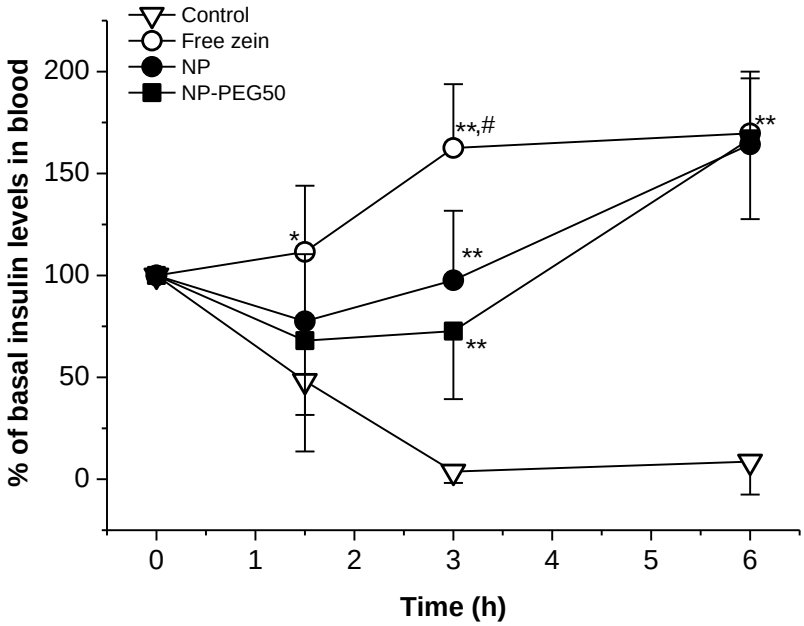

Figure 4. Blood insulin levels of healthy rats treated orally with zein nanoparticles (NP; NP-PEG50) or an aqueous suspension of free zein. All the treatments were administered at a dose of 50 mg/kg. Data expressed as mean ± SD ($n \geq 6$). *: $p < 0.05$; **: $p < 0.01$ compared to control. #: $p < 0.05$ compared to NP-PEG50.

The effect of the treatments on the blood levels of GLP-1 in healthy rats is shown in Figure 5. Control animals and animals treated with the suspension of free zein displayed similar GLP-1 values, without significant differences, during the 6 h post-administration. However, animals receiving either NP or NP-PEG50 presented a significant increase in the levels of GLP-1. This increase, which started 1.5 h after the beginning of the experiment, reached its maximum at the last extraction point, 6 h post-administration. At this extraction point, NP induced a 39% increase (over the initial levels) while NP-PEG50 led to a 59% rise of the GLP-1 levels, compared to basal values.

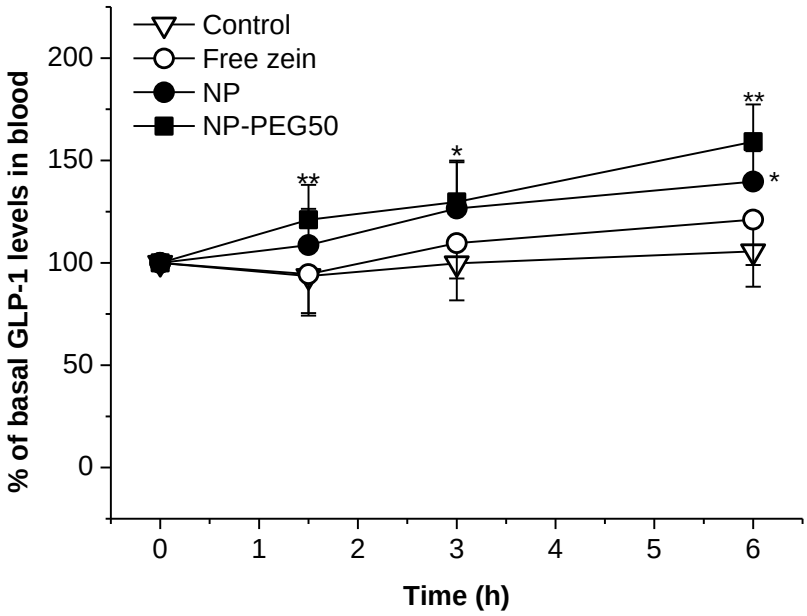

Figure 5. Blood GLP-1 levels of healthy rats treated orally with zein nanoparticles (NP; NP-PEG50) or an aqueous suspension of free zein. All the treatments were administered at a dose of 50 mg/kg. Data expressed as mean ± SD (n ≥ 6). *: $p < 0.05$; **: $p < 0.01$ compared to control.

The effect of the treatments on the blood levels of GIP are shown in Figure 6. For animals treated with either zein nanoparticles or the aqueous suspension of the protein, during the first 3 h post-administration, a slight decrease in the blood levels of this hormone was observed. At 6 h post-administration, for all the zein treatments, the levels of GIP were significantly higher than for control animals ($p < 0.01$).

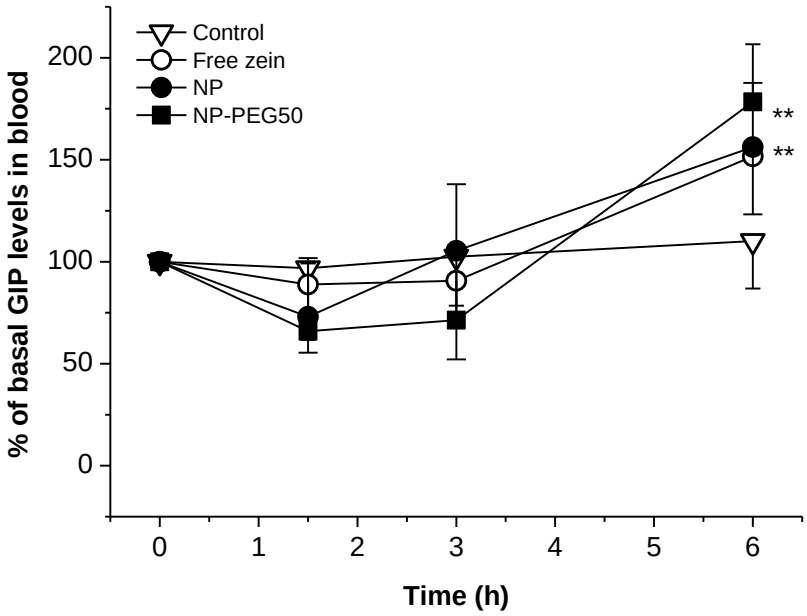

Figure 6. Blood GIP levels of healthy rats treated orally with zein nanoparticles (NP; NP-PEG50) or an aqueous suspension of free zein. All the treatments were administered at a dose of 50 mg/kg. Data expressed as mean ± SD (n ≥ 6). **: $p < 0.01$ compared to control.

Figure 7 illustrates the somatostatin levels during the first 3 h post-administration for animals treated with either NP or NP-PEG50. Both types of treatment induced an important secretion of this hormone, particularly in animals treated with NP-PEG50. Thus, 3 h post-administration, the levels of somatostatin in blood of control animals were reduced by half while, in NP-PEG50 treated animals, they increased by approximately 45%.

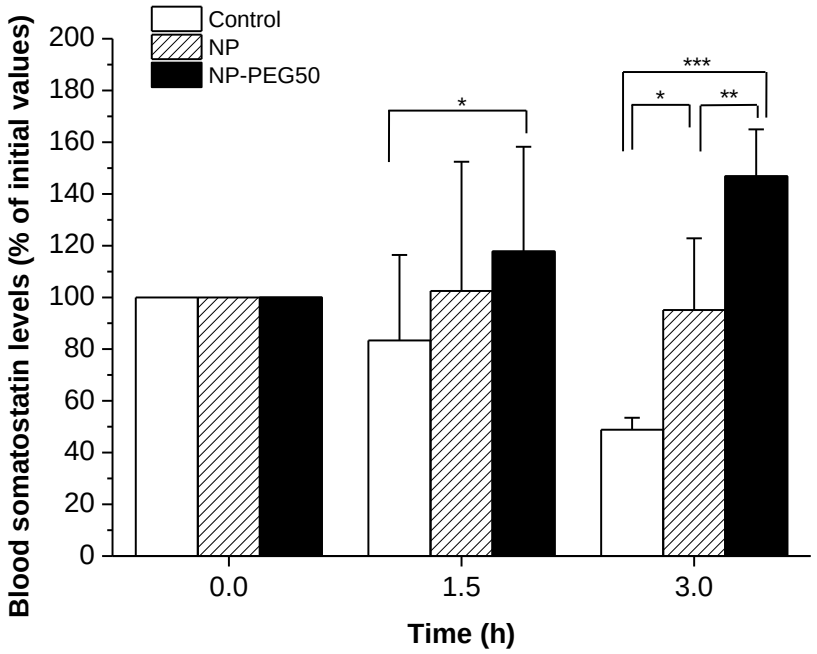

Figure 7. Somatostatin blood levels of healthy rats receiving water (control), NP and NP-PEG50. All the treatments were administered at a dose of 50 mg/kg. Data expressed as mean ± SD ($n \geq 6$). *: $p < 0.05$; **: $p < 0.01$ compared to control.

4.3.4. Intraperitoneal Glucose Tolerance Test (ipGTT) in healthy rats

The response to a glucose overload in rats was evaluated through an intraperitoneal glucose tolerance test. Figure 8A shows the changes in the glycemia of rats during the 2 hours after the intraperitoneal challenge with a glucose injection. All the treatments significantly reduced the glycemic increase 15 minutes after the challenge, compared to the controls ($p < 0.001$). However, this reduction in the glycemic increase was significantly higher in the group of animals treated with NP-PEG50 than in animals receiving either free zein or NP ($p < 0.05$). Only the group treated with NP-PEG50 showed a relevant reduction in the glucose rise 30 minutes after the glucose injection, leading to a significant decrease ($p < 0.05$) compared to naked nanoparticles, and a very significant decrease ($p < 0.001$) compared to control and free zein groups. From this point on, no differences were found between all 4 treatments.

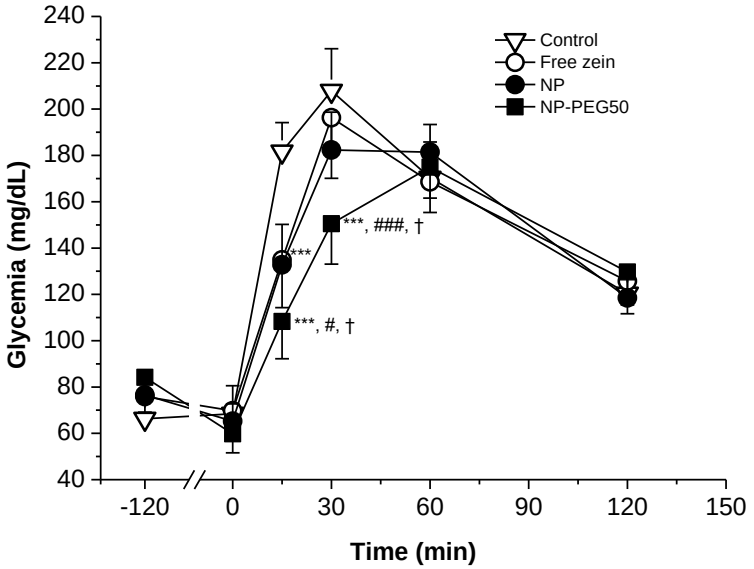

Figure 8. Effect of the different treatments over the blood glucose levels of healthy male Wistar rats after an intraperitoneal injection of glucose (2 g/kg). All the treatments were orally administered 2 h prior to the glucose injection, at a dose of 50 mg/kg. Control: animals receiving water; Free zein: zein in purified water; NP: bare zein nanoparticles dispersed in 1 mL purified water; NP-PEG50: PEG-coated zein nanoparticles dispersed in 1 mL purified water. Data expressed as mean ± SD ($n \geq 6$). *: $p < 0.05$; **: $p < 0.01$; ***: $p < 0.001$ compared to control. #: $p < 0.05$; ###: $p < 0.001$ compared to free zein. †: $p < 0.05$ compared to NP.

The main pharmacodynamic parameters of the ipGTT are summarized in Table 2. Control animals showed the highest glycemic values (T_{max}) 30 minutes after the intraperitoneal injection of glucose, with a mean value above 200 mg/dL (C_{max}). Animals previously treated with an oral administration of free zein or NP did not significantly modify the C_{max}, or the total exposure to glucose (AUC), although NP-treated rats showed a slight delay in the T_{max}. On the contrary, animals that received NP-PEG50 not only shifted the T_{max} from 0.5 h to almost 1 h, but also showed a statistically relevant decrease in the total exposure to glucose ($p < 0.05$).

Table 2. Main pharmacodynamic parameters of rats receiving an oral administration of water (control); free zein; bare nanoparticles (NP); or PEG-coated nanoparticles (NP-PEG50). All the treatments were administered at a 50 mg/kg dose and 2 h prior to the ipGTT (2 g/kg). Data expressed as mean ± SD ($n \geq 6$). *: $p < 0.05$ compared to control.

Treatment	Dose (mg/kg)	C_{max} (mg/dL)	T_{max} (h)	AUC	AUC quotient
Control	-	207 ± 18	0.50 ± 0.00	18952 ± 1528	1.00 ± 0.08
Free zein	50	196 ± 26	0.57 ± 0.17	18319 ± 821	0.96 ± 0.04
NP	50	182 ± 16	0.71 ± 0.24	18225 ± 815	0.96 ± 0.04
NP-PEG50	50	174 ± 13*	0.93 ± 0.17*	16885 ± 868*	0.89 ± 0.04*

4.4. Discussion

In this work, the objective was, in a first step, to evaluate the real hypoglycemic potential of zein-based nanoparticles in rats and, in a second step, if their distribution within the gut may modulate and determine the intensity of this effect. For this purpose, bare and PEG-coated nanoparticles were selected. Conventional zein nanoparticles display mucoadhesive properties and their localization within the gut appear to be restricted to the mucus layer of the upper regions of the gastrointestinal tract (Inchaurraga et al., 2019). On the contrary, the "decoration" of the nanoparticles with PEG 35,000 at a PEG-to-zein ratio of 0.5 (NP-PEG50) yields nanocarriers with mucus-permeating properties capable of targeting the epithelium of the distal region of the small intestine and the cecum (Reboredo et al., 2021).

The evaluation of the effect of zein nanoparticles over the fat accumulation of *C. elegans* was performed by culturing the worms under high glucose conditions. Under these conditions, resembling the hyperglycemic condition in diabetics (Zhu et al., 2016), worms experience (among other effects) an expansion of the adipose tissue, which is, in part, caused by the toxicity exerted by the hyperglycemic conditions (Alcántar-Fernández et al., 2018; Lu and Qiu, 2017; Nomura et al., 2010).

However, this increase in the fatty tissue accumulation was partially countered by the supplementation of zein nanoparticles into the growth medium (Figure 2). This could be caused by a hypoglycemic/glucotoxicity reducing effect of the nanoparticles, combined with an increased uptake of amino acids and oligopeptides through the PEPT-1 receptor present in the enterocytes of the worm. Similar to what happens in mammalians, *C. elegans* intestinal cells act as nutrient sensors that, depending on the composition of the chyme, trigger different metabolic pathways. This sensing of the nutrients present in the lumen is carried out through different transporters present in the surface of the enterocytes. Actually, the gastrointestinal tract of the worms presents several peptide and amino acid transporter systems (Miguel-Aliaga, 2012). PEPT-1 is an amino acid and oligopeptide transporter present in the enterocytes of *C. elegans* whose activation trigger biological responses that lead to a decreased fat accumulation in the worm (Spanier et al., 2009; Xiao et al., 2015).

In a similar way, mammalian intestinal cells are also sensitive to the presence of nutrients in the lumen and, according to it, different physiological responses are triggered. Some protein metabolites are sensed by the L cells of the gastrointestinal tract through the PEPT1 transporter (Diakogiannaki et al., 2013), which is the mammalian counterpart of the PEPT-1 expressed in *C. elegans* (Spanier et al., 2009). In response to the presence of oligopeptides and amino acids in the lumen, L cells secrete GLP-1, a hormone of the incretin family (Clemmensen et al., 2013; Pais et al., 2016a) with hypoglycemic, antidiabetic, and antiobesity effects (Nadkarni et al., 2014; Rowlands et al., 2018; Vilsbøll et al., 2012).

Regarding the insulin levels in blood, on the one hand, control animals showed a huge decrease during the development of the experiment. This phenomenon may be associated to the effect of inhaled anesthesia (isoflurane), which has been

demonstrated to diminish the insulinemic values (Zardooz et al., 2010), combined with the fasting state, in which the circulating levels of the hormone are also diminished (Jørgensen et al., 2021). On the other hand, oral administration of either nanoparticulated or free zein induced an insulinotropic effect that countered the effect of the anesthesia. While free zein induced an insulinemic increase from the beginning of the experiment, nanoparticulated zein displayed a delayed effect. The cause for this may be the high stability of the nanoparticles in the gastric medium (Brotons-Canto et al., 2018) combined with the slow digestibility of zein nanoparticles (Irache and González-Navarro, 2017) that would delay the release of the insulinogogue peptides and amino acids. It is worth noting that lysine (used as stabilizer for the formulation of our nanoparticles) has an inductor effect over insulin secretion (Kalogeropoulou et al., 2009; Sener et al., 1989). Regarding the free protein, its insolubility in aqueous medium facilitates its aggregation and the formation of a highly hydrophobic sticky mass that would be retained in the stomach and upper regions of the intestine. There, the protein will be degraded, releasing peptones and amino acids (some of which with insulinogogue activity) that would be absorbed by the enterocytes. The action of these amino acids would lead to the increased levels of insulin in blood (Figure 4). Moreover, zein is particularly rich in leucine (around 19% of the total amino acid residues) (Gianazza et al., 1977; Rosentrater and Evers, 2018) and this amino acid acutely stimulates insulin secretion (Yang et al., 2010). Nevertheless, when the blood levels of these amino acid rise, the glucose uptake by peripheral tissues is inhibited (even in conditions of hyperinsulinemia (Pisters et al., 1991)) and the protein anabolism is potentiated (James et al., 2017). These would lead to the apparently contradictory results found in animals receiving the oral suspension of zein: highest values of insulin in blood without a reduction in the blood glucose levels. In the case of animals receiving NP, since nanoparticulated zein does not form such sticky aggregates, the nanoparticles would transit through the stomach and reach the intestines probably faster than the free protein conglomerates. However, these nanoparticles display a mucoadhesive behavior that makes them get retained in the mucus gel, far away from the absorptive epithelium. This, combined with the distribution of the L cells (which are more abundant in distal regions of the gut), leads to a slower and less potent stimulation of the GLP-1 release. Moreover, the digestion of the nanoparticles in the upper regions of the gut would lead to the absorption of amino acids and peptones that, as with the free protein, would act as insulinogogues. The increased mucus-diffusivity of NP-PEG50 allows the nanoparticles to freely move through the mucus gel and reach further regions of the gut. Hence, following oral administration, NP-PEG50 will rapidly transit through the stomach, move to the intestines and the cecum, and cross the mucus layer to reach the surface of the intestinal epithelium. There, they will be digested and, the peptones and amino acids released, will stimulate GLP-1 secretion from L cells. Likely, the capability of PEG-coated nanoparticles to reach further regions of the gut in a more rapid way than bare nanoparticles, is the reason for their more potent GLP-1 releasing effect.

A previous report has demonstrated that the oral administration of zein hydrolysates also confer a better glycemic control of animals facing an intraperitoneal glucose

tolerance test due to an increased GLP-1 secretion (Higuchi et al., 2013). Thus, the increased GLP-1 levels in blood of animals receiving NP or NP-PEG50 could be translated into a better glycemic control when facing an ipGTT. In animals receiving NP or free zein, despite they showed a significant decrease in the glycemic rise 15 minutes after the intraperitoneal injection, no relevant differences were found in the T_{max}, C_{max} nor in the AUC. On the contrary, animals treated with NP-PEG50 showed significantly lower glycemic values until 30 minutes after the glucose injection. Moreover, the T_{max} was delayed from 30 to 60 minutes and the total exposure to glucose (measured as the AUC) was significantly lower ($p < 0.05$). Again, the reason for the differences found between NP and NP-PEG50 regarding the glucose management during an ipGTT may be the increased GLP-1 secretion induced by PEG-coated nanoparticles, based on their better mucus-diffusivity. Moreover, it is worth noting that in the mentioned study, the dose of zein hydrolysates was 2 g/kg while, in our case, the dose of the treatments was 50 mg/kg (40 times lower). This reinforces the evidence that orally administered NP-PEG50 may be more effective for the glucose management than zein hydrolysates.

Concerning GIP, an increase on its levels in blood would be expectable after the administration of the different treatments since this incretin is also released in response to food intake and, mostly, in response to proteins (Seino et al., 2010). However, during the first 3 hours after the administration, no increase in the GIP levels in blood was observed. Interestingly, although the differences were not statistically significant, NP and NP-PEG50 induced a slight decrease on the GIP levels. One reason for this finding would be the secretion of somatostatin from the D cells of the stomach (Mani and Zigman, 2015), which has a potent inhibitory effect over the GIP synthesis and release (Kumar and Singh, 2020). It has been demonstrated that, 2 h post-administration, nanoparticles of both types of formulations (NP and NP-PEG50) are still found in stomach and proximal regions of the gut (Reboredo et al., 2021). Therefore, the presence of the nanoparticles in the stomach would keep stimulating somatostatin release and, thus, inhibiting GIP secretion. This was evidenced by the quantification of somatostatin levels in blood of animals treated with either NP or NP-PEG50. While control animals showed decreasing levels of somatostatin along time, caused by fasting (Verrillo et al., 1988), animals receiving nanoparticulated zein showed sustained or even increased levels of the hormone during the experiment. Finally, 6 h post-administration, the GIP levels in blood of every group of animals receiving a zein formulations (either free or as nanoparticles) increased very significantly caused by the flow of the remaining traces of zein from the stomach to the intestine.

In summary, herein we demonstrated that zein in a nanoparticulated form can induce a hypoglycemic response and improve the glycemic control against an ipGTT in healthy animals. Moreover, the main differences found in the effects exerted by the different forms of the administered zein rely on the biodistribution of the zein molecules along the gastrointestinal tract. The free protein, which is the most sticky and hydrophobic, had no effect over the glucose homeostasis while NP-PEG50, the most hydrophilic and mucus-diffusive, had the greatest values. NP, which has intermediate values of mucoadhesiveness and hydrophobicity, showed greater results than the free protein but

worse than NP-PEG50. Nevertheless, we demonstrated that the mechanisms involved in these responses are incretin mediated.

4.5. References

Alcántar-Fernández, J., Navarro, R.E., Salazar-Martínez, A.M., Pérez-Andrade, M.E., Miranda-Ríos, J., 2018. Caenorhabditis elegans respond to high-glucose diets through a network of stress-responsive transcription factors. PLoS One 13. https://doi.org/10.1371/journal.pone.0199888

Ayala, J.E., Bracy, D.P., James, F.D., Julien, B.M., Wasserman, D.H., Drucker, D.J., 2009. The glucagon-like peptide-1 receptor regulates endogenous glucose production and muscle glucose uptake independent of its incretin action. Endocrinology 150, 1155–1164. https://doi.org/10.1210/en.2008-0945

Brotons-Canto, A., Gamazo, C., Martín-Arbella, N., Abdulkarim, M., Matías, J., Gumbleton, M., Irache, J.M., 2018. Evaluation of nanoparticles as oral vehicles for immunotherapy against experimental peanut allergy. Int. J. Biol. Macromol. 110, 328–335. https://doi.org/10.1016/j.ijbiomac.2017.09.109

Chai, W., Dong, Z., Wang, N., Wang, W., Tao, L., Cao, W., Liu, Z., 2012. Glucagon-like peptide 1 recruits microvasculature and increases glucose use in muscle via a nitric oxide-dependent mechanism. Diabetes 61, 888–896. https://doi.org/10.2337/db11-1073

Cheng, Z., Tseng, Y., White, M.F., 2010. Insulin signaling meets mitochondria in metabolism. Trends Endocrinol. Metab. https://doi.org/10.1016/j.tem.2010.06.005

Clemmensen, C., Smajilovic, S., Smith, E.P., Woods, S.C., Bräuner-Osborne, H., Seeley, R.J., D'Alessio, D.A., Ryan, K.K., 2013. Oral L-arginine stimulates GLP-1 secretion to improve glucose tolerance in male mice. Endocrinology 154, 3978–3983. https://doi.org/10.1210/en.2013-1529

Dardevet, D., Moore, M.C., Neal, D., DiCostanzo, C.A., Snead, W., Cherrington, A.D., 2004. Insulin-independent effects of GLP-1 on canine liver glucose metabolism: Duration of infusion and involvement of hepatoportal region. Am. J. Physiol. - Endocrinol. Metab. 287, E75–E81. https://doi.org/10.1152/ajpendo.00035.2004

Deeney, J.T., Prentki, M., Corkey, B.E., 2000. Metabolic control of β-cell function. Semin. Cell Dev. Biol. 11, 267–275. https://doi.org/10.1006/scdb.2000.0175

Diakogiannaki, E., Pais, R., Tolhurst, G., Parker, H.E., Horscroft, J., Rauscher, B., Zietek, T., Daniel, H., Gribble, F.M., Reimann, F., 2013. Oligopeptides stimulate glucagon-like peptide-1 secretion in mice through proton-coupled uptake and the calcium-sensing receptor. Diabetologia 56, 2688–2696. https://doi.org/10.1007/s00125-013-3037-3

Dimitriadis, G., Mitron, P., Lambadiari, V., Maratou, E., Raptis, S.A., 2011. Insulin effects in muscle and adipose tissue, Diabetes Research and Clinical Practice. https://doi.org/10.1016/S0168-8227(11)70014-6

El, K., Campbell, J.E., 2020. The role of GIP in α-cells and glucagon secretion. Peptides 125, 170213. https://doi.org/10.1016/j.peptides.2019.170213

Fu, Z., R. Gilbert, E., Liu, D., 2012. Regulation of Insulin Synthesis and Secretion and

Pancreatic Beta-Cell Dysfunction in Diabetes. Curr. Diabetes Rev. 9, 25–53. https://doi.org/10.2174/15733998130104

Gianazza, E., Viglienghi, V., Righetti, P.G., Salamini, F., Soave, C., 1977. Amino acid composition of zein molecular components. Phytochemistry 16, 315–317. https://doi.org/10.1016/0031-9422(77)80054-X

Henquin, J.C., Dufrane, D., Nenquin, M., 2006. Nutrient control of insulin secretion in isolated normal human islets. Diabetes 55, 3470–3477. https://doi.org/10.2337/db06-0868

Higuchi, N., Hira, T., Yamada, N., Hara, H., 2013. Oral administration of corn zein hydrolysate stimulates GLP-1 and GIP secretion and improves glucose tolerance in male normal rats and Goto-Kakizaki rats. Endocrinology 154, 3089–3098. https://doi.org/10.1210/en.2012-2275

Holst, J.J., 2019. The incretin system in healthy humans: The role of GIP and GLP-1. Metabolism. 96, 46–55. https://doi.org/10.1016/j.metabol.2019.04.014

Inchaurraga, L., Martín-Arbella, N., Zabaleta, V., Quincoces, G., Peñuelas, I., Irache, J.M., 2015. In vivo study of the mucus-permeating properties of PEG-coated nanoparticles following oral administration. Eur. J. Pharm. Biopharm. 97, 280–289. https://doi.org/10.1016/j.ejpb.2014.12.021

Inchaurraga, L., Martínez-López, A.L., Abdulkarim, M., Gumbleton, M., Quincoces, G., Peñuelas, I., Martin-Arbella, N., Irache, J.M., 2019. Modulation of the fate of zein nanoparticles by their coating with a Gantrez® AN-thiamine polymer conjugate. Int. J. Pharm. X 1, 100006. https://doi.org/10.1016/j.ijpx.2019.100006

Irache, J.M., González-Navarro, C.J., 2017. Zein nanoparticles as vehicles for oral delivery purposes. Nanomedicine 12, 1209–1211. https://doi.org/10.2217/nnm-2017-0075

Ishikawa, Y., Hira, T., Inoue, D., Harada, Y., Hashimoto, H., Fujii, M., Kadowaki, M., Hara, H., 2015. Rice protein hydrolysates stimulate GLP-1 secretion, reduce GLP-1 degradation, and lower the glycemic response in rats. Food Funct. 6, 2525–2534. https://doi.org/10.1039/c4fo01054j

James, H.A., O'Neill, B.T., Nair, K.S., 2017. Insulin Regulation of Proteostasis and Clinical Implications. Cell Metab. https://doi.org/10.1016/j.cmet.2017.06.010

Jin, T., Weng, J., 2016. Hepatic functions of GLP-1 and its based drugs: Current disputes and perspectives. Am. J. Physiol. - Endocrinol. Metab. 311, E620–E627. https://doi.org/10.1152/ajpendo.00069.2016

Jørgensen, S.W., Hjort, L., Gillberg, L., Justesen, L., Madsbad, S., Brøns, C., Vaag, A.A., 2021. Impact of prolonged fasting on insulin secretion, insulin action, and hepatic versus whole body insulin secretion disposition indices in healthy young males. Am. J. Physiol. - Endocrinol. Metab. 320, E281–E290. https://doi.org/10.1152/AJPENDO.00433.2020

Jung, U.J., Choi, M.S., 2014. Obesity and its metabolic complications: The role of adipokines and the relationship between obesity, inflammation, insulin resistance, dyslipidemia and nonalcoholic fatty liver disease. Int. J. Mol. Sci.

https://doi.org/10.3390/ijms15046184

Kalogeropoulou, D., LaFave, L., Schweim, K., Gannon, M.C., Nuttall, F.Q., 2009. Lysine ingestion markedly attenuates the glucose response to ingested glucose without a change in insulin response. Am. J. Clin. Nutr. 90, 314–320. https://doi.org/10.3945/ajcn.2008.27381

Kazafeos, K., 2011. Incretin effect: GLP-1, GIP, DPP4. Diabetes Res. Clin. Pract. 93, S32–S36. https://doi.org/10.1016/S0168-8227(11)70011-0

Klein, L.J., Visser, F.C., 2010. The effect of insulin on the heart: Part 1: Effects on metabolism and function. Netherlands Hear. J. 18, 197–201. https://doi.org/10.1007/BF03091761

Kleinridders, A., Ferris, H.A., Cai, W., Kahn, C.R., 2014. Insulin action in brain regulates systemic metabolism and brain function, in: Diabetes. American Diabetes Association Inc., pp. 2232–2243. https://doi.org/10.2337/db14-0568

Kumar, U., Singh, S., 2020. Role of somatostatin in the regulation of central and peripheral factors of satiety and obesity. Int. J. Mol. Sci. 21, 2568. https://doi.org/10.3390/ijms21072568

Lázár, B.A., Jancsó, G., Pálvölgyi, L., Dobos, I., Nagy, I., Sántha, P., 2018. Insulin confers differing effects on neurite outgrowth in separate populations of cultured dorsal root ganglion neurons: The role of the insulin receptor. Front. Neurosci. 12, 732. https://doi.org/10.3389/fnins.2018.00732

Lazzaro, B.P., Schneider, D.S., 2014. The genetics of immunity. Genetics 197, 467–470. https://doi.org/10.1534/genetics.114.165449

Lu, Z., Qiu, Z., 2017. High glucose concentration restricts fat consumption in Caenorhabditis elegans. Int. J. Clin. Exp. Med. 10, 10554–10559.

Mani, B.K., Zigman, J.M., 2015. A strong stomach for somatostatin. Endocrinology 156, 3876–3879. https://doi.org/10.1210/en.2015-1756

Martínez-López, A.L., González-Navarro, C.J., Vizmanos, J.L., Irache, J.M., 2021. Zein-based nanocarriers for the oral delivery of insulin. In vivo evaluation in Caenorhabditis elegans. Drug Deliv. Transl. Res. 11, 647–658. https://doi.org/10.1007/s13346-021-00919-4

Martínez-López, A.L., Pangua, C., Reboredo, C., Campión, R., Morales-Gracia, J., Irache, J.M., 2020. Protein-based nanoparticles for drug delivery purposes. Int. J. Pharm. 581. https://doi.org/10.1016/j.ijpharm.2020.119289

Martorell, P., Llopis, S., González, N., Montón, F., Ortiz, P., Genovés, S., Ramón, D., 2012. Caenorhabditis elegans as a model to study the effectiveness and metabolic targets of dietary supplements used for obesity treatment: The specific case of a conjugated linoleic acid mixture (Tonalin). J. Agric. Food Chem. 60, 11071–11079. https://doi.org/10.1021/jf3031138

McClenaghan, N.H., Barnett, C.R., O'Harte, F.P.M., Flatt, P.R., 1996. Mechanisms of amino acid-induced insulin secretion from the glucose-responsive BRIN-BD11

pancreatic B-cell line. J. Endocrinol. 151, 349–357. https://doi.org/10.1677/joe.0.1510349

Miguel-Aliaga, I., 2012. Nerveless and gutsy: Intestinal nutrient sensing from invertebrates to humans. Semin. Cell Dev. Biol. 23, 614–620. https://doi.org/10.1016/j.semcdb.2012.01.002

Mochida, T., Hira, T., Hara, H., 2010. The corn protein, zein hydrolysate, administered into the ileum attenuates hyperglycemia via its dual action on glucagon-like peptide-1 secretion and dipeptidyl peptidase-IV activity in rats. Endocrinology 151, 3095–3104. https://doi.org/10.1210/en.2009-1510

Mortensen, K., Christensen, L.L., Holst, J.J., Orskov, C., 2003. GLP-1 and GIP are colocalized in a subset of endocrine cells in the small intestine. Regul. Pept. 114, 189–196. https://doi.org/10.1016/S0167-0115(03)00125-3

Nadkarni, P., Chepurny, O.G., Holz, G.G., 2014. Regulation of glucose homeostasis by GLP-1, in: Progress in Molecular Biology and Translational Science. Elsevier B.V., pp. 23–65. https://doi.org/10.1016/B978-0-12-800101-1.00002-8

Navarro-Herrera, D., Aranaz, P., Eder-Azanza, L., Zabala, M., Hurtado, C., Romo-Hualde, A., Martínez, J.A., González-Navarro, C.J., Vizmanos, J.L., 2018. Dihomo-gamma-linolenic acid induces fat loss in: C. Elegans in an omega-3-independent manner by promoting peroxisomal fatty acid β-oxidation. Food Funct. 9, 1621–1637. https://doi.org/10.1039/c7fo01625e

Newsholme, P., Brennan, L., Bender, K., 2006. Amino acid metabolism, β-cell function, and diabetes. Diabetes 55, S39–S47. https://doi.org/10.2337/db06-S006

Newsholme, P., Krause, M., 2012. Nutritional Regulation of Insulin Secretion: Implications for Diabetes. Clin. Biochem. Rev. 33, 35–47.

Nomura, T., Horikawa, M., Shimamura, S., Hashimoto, T., Sakamoto, K., 2010. Fat accumulation in Caenorhabditis elegans is mediated by SREBP homolog SBP-1. Genes Nutr. 5, 17–27. https://doi.org/10.1007/s12263-009-0157-y

Pais, R., Gribble, F.M., Reimann, F., 2016a. Stimulation of incretin secreting cells. Ther. Adv. Endocrinol. Metab. https://doi.org/10.1177/2042018815618177

Pais, R., Gribble, F.M., Reimann, F., 2016b. Signalling pathways involved in the detection of peptones by murine small intestinal enteroendocrine L-cells. Peptides 77, 9–15. https://doi.org/10.1016/j.peptides.2015.07.019

Penalva, R., Esparza, I., Larraneta, E., González-Navarro, C.J., Gamazo, C., Irache, J.M., 2015. Zein-Based Nanoparticles Improve the Oral Bioavailability of Resveratrol and Its Anti-inflammatory Effects in a Mouse Model of Endotoxic Shock. J. Agric. Food Chem. 63, 5603–5611. https://doi.org/10.1021/jf505694e

Pino, E.C., Webster, C.M., Carr, C.E., Soukas, A.A., 2013. Biochemical and high throughput microscopic assessment of fat mass in Caenorhabditis elegans. J. Vis. Exp. https://doi.org/10.3791/50180

Pisters, P.W.T., Restifo, N.P., Cersosimo, E., Brennan, M.F., 1991. The effects of

euglycemic hyperinsulinemia and amino acid infusion on regional and whole body glucose disposal in man. Metabolism 40, 59–65. https://doi.org/10.1016/0026-0495(91)90193-Z

Porta-de-la-Riva, M., Fontrodona, L., Villanueva, A., Cerón, J., 2012. Basic Caenorhabditis elegans methods: Synchronization and observation. J. Vis. Exp. https://doi.org/10.3791/4019

Reboredo, C., González-Navarro, C.J., Martínez-Oharriz, C., Martínez-López, A.L., Irache, J.M., 2021. Preparation and evaluation of PEG-coated zein nanoparticles for oral drug delivery purposes. Int. J. Pharm. 597. https://doi.org/10.1016/j.ijpharm.2021.120287

Rocca, A.S., Brubaker, P.L., 1999. Role of the vagus nerve in mediating proximal nutrient-induced glucagon- like peptide-1 secretion. Endocrinology 140, 1687–1694. https://doi.org/10.1210/endo.140.4.6643

Röder, P. V., Wu, B., Liu, Y., Han, W., 2016. Pancreatic regulation of glucose homeostasis. Exp. Mol. Med. 48, e219. https://doi.org/10.1038/emm.2016.6

Rosentrater, K.A., Evers, A.D., 2018. Chemical components and nutrition. Kent's Technol. Cereal. 267–368. https://doi.org/10.1016/b978-0-08-100529-3.00004-9

Rowlands, J., Heng, J., Newsholme, P., Carlessi, R., 2018. Pleiotropic Effects of GLP-1 and Analogs on Cell Signaling, Metabolism, and Function. Front. Endocrinol. (Lausanne). 9, 672. https://doi.org/10.3389/fendo.2018.00672

Seino, Y., Fukushima, M., Yabe, D., 2010. GIP and GLP-1, the two incretin hormones: Similarities and differences. J. Diabetes Investig. https://doi.org/10.1111/j.2040-1124.2010.00022.x

Sener, A., Blachier, F., Rasschaert, J., Mourtada, A., Malaisse-Lagae, F., Malaisse, W.J., 1989. Stimulus-secretion coupling of arginine-induced insulin release: Comparison with lysine-induced insulin secretion. Endocrinology 124, 2558–2567. https://doi.org/10.1210/endo-124-5-2558

Spanier, B., Lasch, K., Marsch, S., Benner, J., Liao, W., Hu, H., Kienberger, H., Eisenreich, W., Daniel, H., 2009. How the intestinal peptide transporter PEPT-1 contributes to an obesity phenotype in Caenorhabditits elegans. PLoS One 4. https://doi.org/10.1371/journal.pone.0006279

Thurmond, D.C., 2009. Insulin-regulated glucagon-like peptide-1 release from l cells: Actin' out. Endocrinology. https://doi.org/10.1210/en.2009-1178

Verrillo, A., de Teresa, A., Martino, C., di Chiara, G., Verrillo, L., 1988. Somatostatin response to glucose before and after prolonged fasting in lean and obese non-diabetic subjects. Regul. Pept. 21, 185–195. https://doi.org/10.1016/0167-0115(88)90001-8

Vilsbøll, T., Christensen, M., Junker, A.E., Knop, F.K., Gluud, L.L., 2012. Effects of glucagon-like peptide-1 receptor agonists on weight loss: Systematic review and meta-analyses of randomised controlled trials. BMJ 344. https://doi.org/10.1136/bmj.d7771

Wang, Z., Thurmond, D.C., 2009. Mechanisms of biphasic insulin-granule exocytosis - Roles of the cytoskeleton, small GTPases and SNARE proteins. J. Cell Sci. 122, 893–903. https://doi.org/10.1242/jcs.034355

Weissmueller, N.T., Lu, H.D., Hurley, A., Prud'Homme, R.K., 2016. Nanocarriers from GRAS Zein Proteins to Encapsulate Hydrophobic Actives. Biomacromolecules 17, 3828–3837. https://doi.org/10.1021/acs.biomac.6b01440

Xiao, R., Chun, L., Ronan, E.A., Friedman, D.I., Liu, J., Shawn Xu, X.Z., 2015. RNAi Interrogation of Dietary Modulation of Development, Metabolism, Behavior, and Aging in C.elegans. Cell Rep. 11, 1123–1133. https://doi.org/10.1016/j.celrep.2015.04.024

Yang, J., Chi, Y., Burkhardt, B.R., Guan, Y., Wolf, B.A., 2010. Leucine metabolism in regulation of insulin secretion from pancreatic beta cells. Nutr. Rev. 68, 270–279. https://doi.org/10.1111/j.1753-4887.2010.00282.x

Zardooz, H., Rostamkhani, F., Zaringhalam, J., Shahrivar, F.F., 2010. Plasma corticosterone, insulin and glucose changes induced by brief exposure to isoflurane, diethyl ether and CO2 in male rats. Physiol. Res. 59, 973–978. https://doi.org/10.33549/physiolres.931896

Zhu, G., Yin, F., Wang, L., Wei, W., Jiang, L., Qin, J., 2016. Modeling type 2 diabetes-like hyperglycemia in C. elegans on a microdevice. Integr. Biol. (United Kingdom) 8, 30–38. https://doi.org/10.1039/c5ib00243e

Chapter 5

Evaluation of the biological effects of oral zein-based nanoparticles in *C. elegans* and SAMP8 mice

5. Evaluation of biological effects of oral zein-based nanoparticles in *C. elegans* and SAMP8 mice

Reboredo C.[1], González-Navarro C.J.[2], Martínez-López A.L.[1], Irache J.M.[1]

[1]Department of Chemistry and Pharmaceutical Technology, University of Navarra; C/ Irunlarrea 1, 31008 Pamplona, Spain.
[2]Centre for Nutrition Research, University of Navarra; C/ Irunlarrea 1, 31008 Pamplona, Spain.

Abstract

The aim of this study was to evaluate the beneficial outcomes that the hypoglycemic effect of empty nanoparticles could induce, when orally administered, in two different animal models: *C. elegans* and the senescence accelerated mouse prone-8 (SAMP8). For this purpose, the lifespan of hyperglycemic worms was evaluated. The growth medium of the worms was supplemented with two different zein-based nanoparticle formulations: bare nanoparticles (NP), which display a mucoadhesive behavior, and PEG-coated nanoparticles (NP-PEG50) with a more mucus-diffusive demeanor. In addition, a solution of PEG was also added as treatment to assess the effect of the polymer alone. Both formulations, but not the solution of PEG, induced a very significant increase in the lifespan of the worms, thus, evidencing the beneficial hypoglycemic effect of zein nanoparticles in the lifespan of the worms. Subsequently, the efficacy of the nanoparticles was evaluated in a mouse model of Alzheimer's Disease, the SAMP8 mice. This animal model shows a continuous hyperglycemic state, as well as insulin resistance and impaired cognitive and memory functions. The oral administration of either NP or NP-PEG50 did not improve the memory decline in the animals. On the other hand, the oral administration of NP significantly increased the lifespan of the mice, while NP-PEG50 had no effect.

5.1. Introduction

Diabetes is a well-known pathological condition that courses with elevated blood glucose levels caused by a null production of insulin (type 1 diabetes), or insulin resistance by peripheral tissues combined with low production of the hormone (type 2 diabetes) (Bullard et al., 2018). The metabolic alterations caused by diabetes lead to an accelerated aging and, thus, to a reduced life expectancy of the individual (Caspersen et al., 2012; Morley, 2008). The major cause of diabetes type 2 is obesity and its associated metabolic alterations (Czech, 2017; Golay and Ybarra, 2005). During obesity, the environment in the adipose tissue shows increased oxidative stress, DNA damage and telomerase dysfunction that, in last term, lead to insulin resistance and diabetes (Ahima, 2009). Moreover, the metabolic dysregulation caused by obesity alone also induces premature ageing, leading to a reduced lifespan (Burton and Faragher, 2018; Salvestrini et al., 2019). For instance, *C. elegans* cultured under high glucose conditions present an expansion in the adipose tissue and a reduction in the life expectancy (Alcántar-Fernández et al., 2018; Martínez-López et al., 2021b). Another example is the SAMP8 (senescence accelerated mouse prone-8) mouse strain. This type of mice, characterized by a short life span and fast aging process, has been proposed as model for studying age-related metabolic alterations, as well as learning and memory deficits and AD-like dementia (Diaz-Perdigon et al., 2020; Pallas et al., 2008). Furthermore, these mice have been reported to exhibit several features of insulin resistance (including hyperglycemia) and high levels of free fatty acids (Cuesta et al., 2013; Liu et al., 2017).

It is thought that the development of AD relies on the combination of several risk factors, from which age is, by far, the greatest of them ("2017 Alzheimer's disease facts and figures," 2017). Moreover, during the last decades, new insights regarding the pathogenesis of AD brought to light a relationship between this type of dementia and type 2 diabetes. This relationship is so strong that some authors refer to AD as "diabetes of the brain" or "type 3 diabetes" (De La Monte and Wands, 2008; Kandimalla et al., 2017; Mittal et al., 2016) and insulin is being studied as a treatment to slow the progression of the disease (Hallschmid, 2021; Mao et al., 2016).

In previous works, it has been demonstrated the capability of empty zein nanoparticles to reduce the fat accumulation in *C. elegans* cultured under high glucose conditions (type 2 diabetes-like hyperglycemia model; chapter 2). This reduced expansion in the adipose tissue of nematodes has been related with important reductions in the formation of reactive oxygen species (ROS), as well as with increased life expectancy (Martínez-López et al., 2021a; Schulz et al., 2007). Moreover, in Wistar rats, the oral administration of zein-based nanoparticles induced an important improvement of glucose homeostasis mediated by GLP-1 (Chapter 2). Likely, GLP-1 and other GLP-1R agonists (i.e., exendin-4, liraglutide) appear to have a neuroprotective effect over the cholinergic neurons in the hippocampus, preventing the development of learning and memory deficits (Müller et al., 2019; Qi et al., 2016).

Within this context, the first step of the work was to evaluate the capability of zein nanoparticles to increase the lifespan of *C. elegans* when supplemented into the growth

medium. The following step was to assess the efficacy of orally administered zein nanoparticles to reduce the cognitive and locomotor impairment of SAMP8 mice, as well as their effect over the lifespan of the animals.

5.2. Material and methods

5.2.1. Materials

Zein, L-lysine, poly(ethylene glycol) 35,000 Da, Orlistat®, glucose, sodium hypochlorite and 5-fluoro-2'-deoxyuridine were purchased from Sigma-Aldrich (Steinheim, Germany). Ethanol absolut was obtained from Scharlab (Sentmenat, Spain). Mannitol was purchased from Guinama (La Pobla de Vallbona, Spain). Deionized water was prepared by a water purification system (Wasserlab, Pamplona, Spain).

5.2.2. Preparation of nanoparticles

5.2.2.1 Preparation of bare nanoparticles (NP)

Zein nanoparticles were prepared by a desolvation procedure previously described (Reboredo et al., 2021), with minor modifications. Briefly, 200 mg zein and 30 mg lysine were dissolved in 20 mL ethanol 55% with magnetic stirring for 10 minutes at room temperature. Nanoparticles were obtained by the addition of 20 mL purified water. The ethanol was removed in a rotatory evaporator under reduced pressure (Büchi Rotavapor R-144; Büchi, Postfach, Switzerland) and the resulting suspension of nanoparticles was concentrated and purified by ultrafiltration through a polysulfone membrane cartridge of 500 kDa pore size (Medica SPA, Medolla, Italy). Finally, 1 mL of a mannitol aqueous solution (200 mg/mL) was added to the suspension of nanoparticles and the mixture was dried in a Büchi Mini Spray Dryer B-290 apparatus (Büchi Labortechnik AG, Switzerland) under the following experimental conditions: (i) inlet temperature, 90 °C; (ii) outlet temperature, 45−50 °C; (iii) air pressure, 4−6 bar; (iv) pumping rate, 5 mL/min; (v) aspirator, 80%; and (vi) airflow, 400− 500 L/h.

5.2.2.2. Preparation of PEG-coated nanoparticles (NP-PEG50)

The coating of nanoparticles with PEG was performed by simple incubation between the just formed nanoparticles (before the purification step) and PEG 35,000 at a PEG-to-zein ratio of 0.5. For this purpose, a stock solution of PEG 35,000 was prepared by dissolving the polymer in water to a final concentration of 100 mg/mL. Then, the needed volume of this stock solution was added to the suspension of fresh nanoparticles. The mixture was maintained under magnetic agitation for 30 minutes at room temperature. After this time, nanoparticles were concentrated and purified by tangential filtration and dried as described above.

5.2.3. Physico-chemical characterization of the formulations

The size and polydispersity index (PDI) of the nanoparticles were determined, after the dispersion of the dry powder in ultrapure water at 25 ºC, by dynamic light scattering (DLS). The zeta potential was measured by electrophoretic laser Doppler anemometry of aqueous suspensions of nanoparticles. All these measurements were performed in a Zetasizer (Brookhaven Instruments Corporation, Holtsville, NY, USA). The yield of the

total process of production of nanoparticles was calculated by gravimetry (Arbós et al., 2002).

5.2.4. Evaluation of zein nanoparticles on the lifespan of C. elegans

5.2.4.1. Strain and culture conditions

Wild type N2 Bristol *Caenorhabditis elegans* strain was used for the experiments. The strain was obtained from the Caenorhabditis Genetics Center (CGC, University of Minnesota, MN, USA) and cultured as previously described (Lazzaro and Schneider, 2014). Worms were cultured at 20 ºC on Nematode Growth Medium (NGM) agar plates with *Escherichia coli* OP50 as normal diet. Before any experiment, worms were age-synchronized by bleach (sodium hypochlorite) treatment, where only eggs can survive. Then, eggs were maintained in M9 buffer solution until hatching (L1 larvae stage).

5.2.4.2. Treatment with nanoparticles and lifespan follow-up

The lifespan assay was conducted at 20 ºC in 6-well plates filled with 4 mL NGM containing 5-Fluoro-2'-deoxyuridine (40 mM), compound that avoids the growth of new worms. Orlistat® (Orl) was used as positive control at a concentration of 6 µg/mL. Both formulations (NP and NP-PEG50) were resuspended in purified water and added to the NGM plates at a final concentration of 5 mg/mL of nanoparticles. An aqueous solution of PEG (1.65 mg/mL) was also added to assess the effect of the polymer alone. The same volume of water was added to the control wells. All the treatments were added to the wells with liquid NGM and plates were allowed to solidify in a dark environment. Afterwards, a suspension of *E. coli* OP50 was added over the NGM agar and let dry. 3 wells were used for each treatment, with about 25 worms per well.

L1 age-synchronized worms were grown in NGM supplemented with glucose (0.5%; w/w) until L4 larvae stage (46 h). Afterwards, they were harvested and passed to the 6-well plates containing NGM supplemented with the treatments and kept at 20 ºC. Worms were counted every 2-to-3 days and dead ones were removed from the plates. Worms were considered as dead if they did not move and did not react to physical stimuli.

5.2.5. Evaluation of zein nanoparticles on the cognitive impairment of SAMP8 mice

Experiments were carried out in male SAMP8 and SAMR1 mice (28-30 g; 7-month-old) obtained from an inbreed colony. SAMR1 (Senescence-Accelerated Mouse Resistant-1) animals were used as control. Animals were housed in constant conditions of humidity and temperature (22 ± 1 °C), with 12-hour/12-hour light-dark cycle (lights on at 7:00 h). Food and water were available *ad libitum*. All the procedures followed in this work were in compliance with the European Community Council Directive of 20 November 1986 (86/609/EEC) and were approved by the Ethical Committee of the University of Navarra (protocol 026-18).

Animals from both strains were divided in three groups (n = 10). The first group received, by oral gavage, a dose of 200 mg/kg of bare nanoparticles (dispersed in approximately

300 µL water) every two days. The second group received, by the same route and posology, PEG-coated nanoparticles. Finally, the animals of the third group received water (control).

5.2.6. Behavioral and cognitive tests

After two months of treatment, the following behavioral and cognitive tests were conducted: (i) open field, (ii) rotarod, and the (iii) Morris water maze.

5.2.6.1. Open field test (OFT)

Animals were placed into square-shaped boxes (35 cm length × 35 cm width × 30 cm height) for 30 minutes and allowed to move at will. A virtually generated 20 cm x 20 cm square region in the center of the arena represented the center, while the outer region was defined as the peripheral area. During those 30 minutes, animals were being recorded with a video tracking system (Ethovision XT 11.5 plus multiple body point module) (Ethovision XT 11.5; Noldus Information Technology B.V, Wageningen, The Netherlands). The total distance walked (cm), its proportion in the central area (%), and their velocity (cm/s) were calculated.

5.2.6.2. Rotarod

The motor coordination and balance of the mice were evaluated in a rotarod device (LE8200 Panlab, Harvard Apparatus, Holliston, MA, USA). First, mice were taught to stay on the rod. For that purpose, animals were placed over the rod, which was rotating at a constant speed of 5 rpm, until they could stay longer than one minute. If any mouse dropped during the learning phase without reaching one minute, it was placed again over the rod and the countdown was restarted. After all the animals learned to stay on the rod, the motor coordination evaluation was performed three times per mice. For the evaluation, the mice were placed on the rod that was scheduled to gradually accelerate from 4 to 40 rpm in a 5-minute time lapse. The time that every mouse took to fall was scored and the mean of the three trials calculated.

5.2.6.3. Cognitive evaluation: Morris water maze (MWM)

The spatial, working and reference memories evaluation was carried out by the Morris water maze test (Diaz-Perdigon et al., 2020). The water maze consists of a circular pool (145 cm diameter) filled with water at 21-22 ºC and virtually divided into four quadrants. The procedure involves 3 phases. In the first phase, or habituation phase, animals were dropped into the pool 6 times in one day (day 1), each time from a different quadrant and always facing the wall. During this phase, there was a platform that raises above the water. If animals did not reach the platform within the first minute, they were manually placed and let there for 15 seconds.

In the second phase, or acquisition phase, animals were dropped into the pool 4 times per day for 6 consecutive days (days 2 to 7). At each trial, animals were dropped from a different quadrant but always facing the wall. In this case, the platform was completely sunk, so it could not be visible by the mice. However, some visual clues were placed in the walls of the room to help the mice reaching the platform. Again, as during the habituation phase, each trial lasted for 1 minute or until the mouse reached the platform, what happened first. If animals did not reach the platform in one minute, they

were manually placed and let there for 15 seconds. The time that it takes for each mouse to reach the platform is known as the scape latency, and it was used to assess the spatial learning and memory of the mice.

Finally, in the third phase or retention phase, the memory of the animals was evaluated. This evaluation was performed at days 4 and 7, prior to the daily acquisitions. The platform was removed from the pool and then, each mouse was dropped once and allowed to swim for one minute. The percentage of time swum in the target quadrant was quantified and used as a memory parameter.

Every trial was monitored and recorded with a camera placed over the center of the pool and connected to a video tracking system (Ethovision XT 11.5; Noldus Information Technology B.V., The Netherlands). Moreover, as an indirect measurement of the locomotor activity of the mice, their swimming velocities were also quantified.

5.2.7. Study of the longevity of SAMP8 mice receiving zein nanoparticles

After performing the cognitive and behavioral tests, SAMR1 mice were sacrificed and SAMP8 mice were kept to evaluate the influence of the oral administration of nanoparticles over their lifespan. Animals received the same dose of nanoparticles, by the same route and posology, until their death. To gather maximum life span data, animals were allowed to get old and die naturally. Moribund animals were immediately euthanized by cervical dislocation. Animals were considered as moribund if they fail to eat or drink, did not respond to touch stimuli, became completely blind (due to the degeneration of typical periophthalmic lesions (Nomura and Okuma, 1999)) or developed tumors. The weight of the mice was followed up during the experiment.

5.2.8. Statistical analysis

Means and standard errors were calculated for every data set except for the MWM in which the mean ± standard error of the mean (SEM) was used. All the group comparisons and statistical analyses were performed using a one-way or two-way ANOVA test followed by a Tukey's multiple comparisons test. Two-way ANOVA analysis was performed to assess the main effect and the interaction of the treatment and the strain. Statistical differences in survival plots were calculated using Log-rank (Mantel-Cox) test. Significant differences with respect to control group are marked as follows: *p < 0.05, **p < 0.01 or ***p < 0.001. All calculations were performed using GraphPad Prism v6 (GraphPad Software, San Diego, CA, USA) and the curves were plotted with the Origin 8 software (OriginLab Corp, Northampton, MA, USA).

5.3. Results

5.3.1. Nanoparticles characterization

The main physico-chemical characteristics of bare nanoparticles (NP) and PEG-coated nanoparticles (NP-PEG50) are shown in Table 1. The coating with PEG did not significantly modify the mean size of the resulting nanoparticles, with a typical diameter close to 190 nm and a polydispersity index (PDI) lower than 0.15. Moreover, the coating with PEG slightly decreased the negative zeta potential of the resulting nanoparticles. Finally, the total preparative process yield (after the drying step) was calculated to be around 60%, without differences between formulations.

Table 1. Physico-chemical characteristics of NP and NP-PEG50. Data expressed as mean ± SD (n ≥ 3).

Formulation	Size (nm)	PDI	Zeta potential (mv)	Yield (%)
NP	189 ± 18	0.11 ± 0.08	-53 ± 4	62.6 ± 3.5
NP-PEG50	194 ± 8	0.09 ± 0.02	-50 ± 1	64.5 ± 5.9

5.3.2. Effect of nanoparticles over the lifespan of C. elegans

The supplementation of the NGM medium with nanoparticles induced a very significant increase in the lifespan of the worms (Figure 1). Both types of nanoparticles, bare and PEG-coated, showed to have the same effect on expanding the life expectancy of the worms, without differences between them. Table 2 summarizes the main results of the influence of the treatments over the lifespan. The supplementation with nanoparticles increased not only the mean lifespan but also the median and the maximum life expectancy of the worms. In worms treated with bare nanoparticles, a 55% increase in the mean and the median lifespan were observed, while for the maximum lifespan the increase was of 32%. Regarding the worms treated with PEG-coated nanoparticles, a 50% increase in the mean, 55% in the median and 32% in the maximum lifespan were observed. Moreover, no effect over the life expectancy was observed for the worms treated with a solution of PEG 35,000, meaning that the increased longevity is due to the presence of nanoparticles.

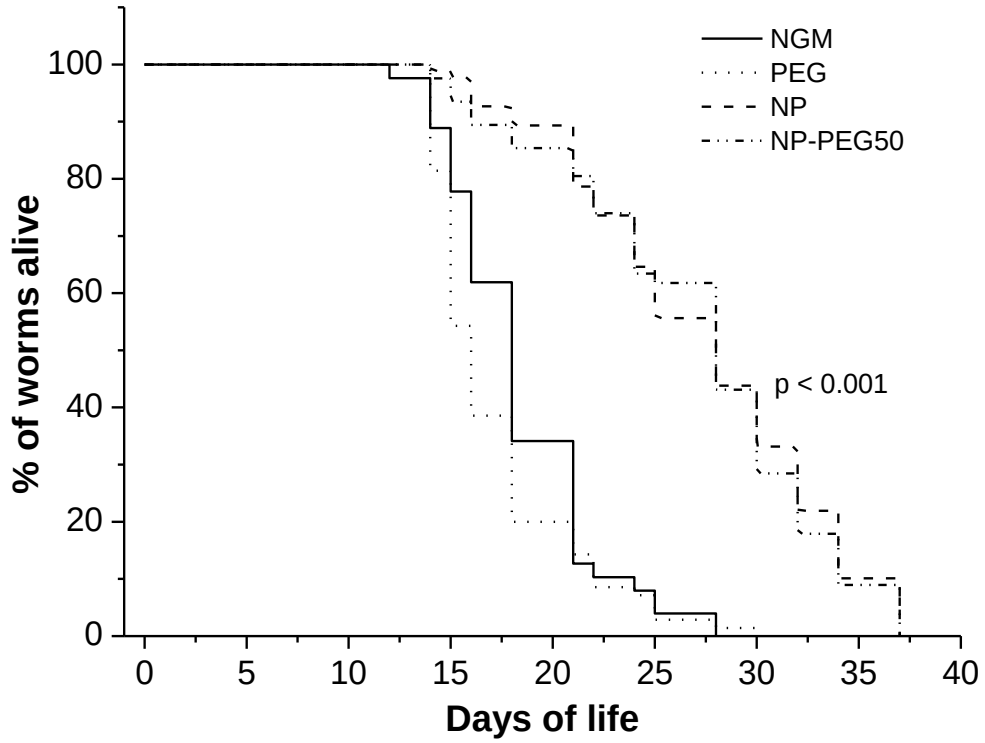

Figure 1. Effect of NP, NP-PEG50, and a solution of PEG 35,000 over the lifespan of *C. elegans*. Kaplan-Meier representation of the percentage of worms alive over time (n ≥ 70 worms). NGM: control medium supplemented with water; PEG: medium

supplemented with a solution of poly(ethylene glycol) 35,000 (1.65 mg/mL); NP: medium supplemented with bare nanoparticles (5 mg/mL); NP-PEG50: medium supplemented with PEG-coated nanoparticles (5 mg/mL). The statistical difference shown is compared to NGM (control), using the Log-rank (Mantel-Cox) test.

Table 2. Summary of the main lifespan data of *C. elegans* without treatment (NGM), treated with two different nanoparticles (bare and PEG-coated), and treated with a solution of PEG (n ≥ 70 worms). ***: P < 0.001 compared to NGM.

	Lifespan		
Treatment	**Mean (days)**	**Median (days)**	**Maximum (days)**
NGM	18 ± 4	18	28
PEG	17 ± 4	16	30
NP	28 ± 5***	28	37
NP-PEG50	27 ± 6***	28	37

5.3.3. In vivo evaluation of nanoparticles in mice.

5.3.3.1 Behavioral and cognitive tests

The results obtained from the open field test showed no differences in the total distance travelled (Figure 2A) or in the velocity (Figure 2B) between treatments and strains. However, the results of their exploratory behavior, measured as the percentage of the travelled distance in the central zone, clearly demonstrated a significant difference between the SAMR1 and the SAMP8 strains (50 vs 30% approximately; Figure 2C). This reduction in the percentage walked in the zone by SAMP8 mice is a demonstration of their increased anxiety. However, no differences were found between mice receiving nanoparticles and the control ones, neither in the SAMR1 nor SAMP8 strains.

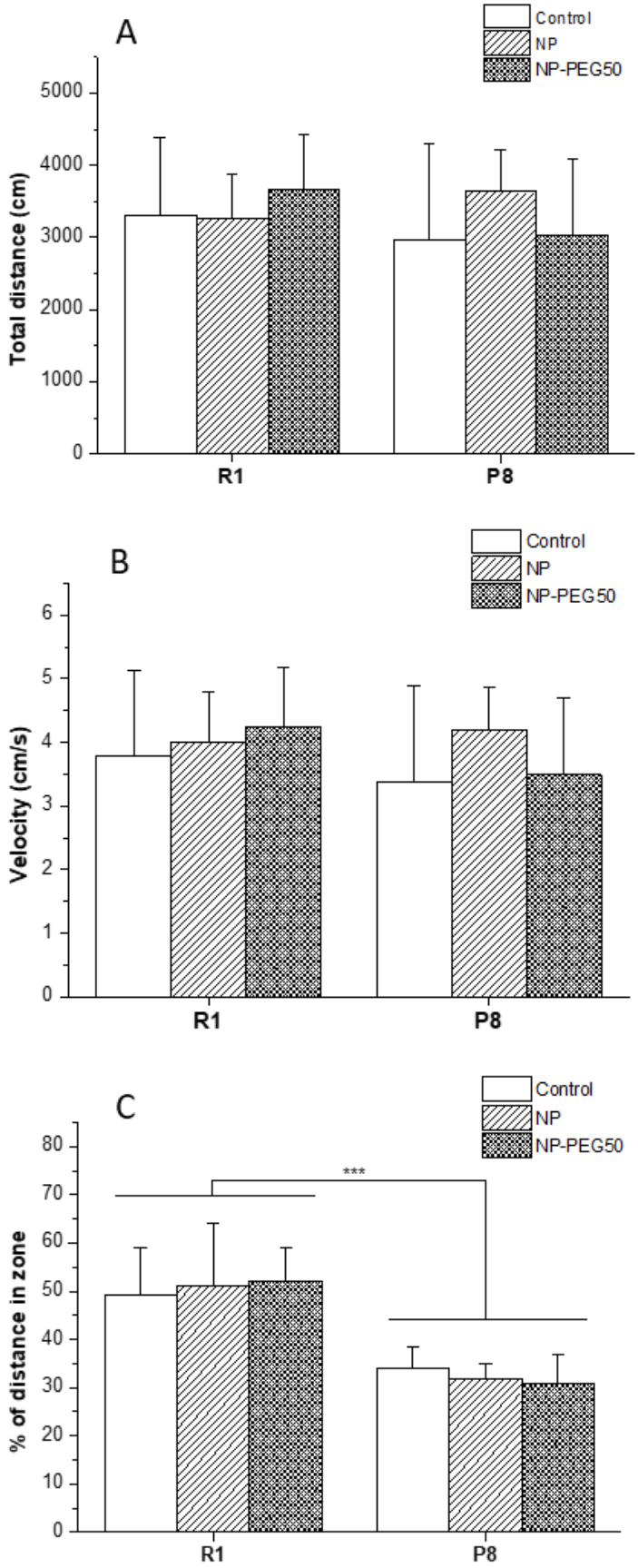

Figure 2. Effect of the oral administration of NP and NP-PEG50 over the motor performance and the exploratory behavior. R1 corresponds to SAMR1 mice, used as control. P8 corresponds to SAMP8 mice. Control: animals receiving water; NP: animals

receiving bare nanoparticles (200 mg/kg); NP-PEG50: animals receiving PEG-coated nanoparticles (200 mg/kg). Three different parameters were evaluated: the total distance walked (A), the movement velocity (B), and the % of distance walked in the center, as a measurement of the exploratory behavior (C). Data expressed as mean ± SD ($n \geq 8$). ***: $p < 0.001$.

The results of the spontaneous motor activity and coordination, evaluated by the rotarod test, are shown in Figure 3. In this case, SAMR1 displayed a superior motor coordination and balance than SAMP8 mice ($p < 0.001$). Nevertheless, the administration of formulations did not show any effect on improving the coordination of the mice.

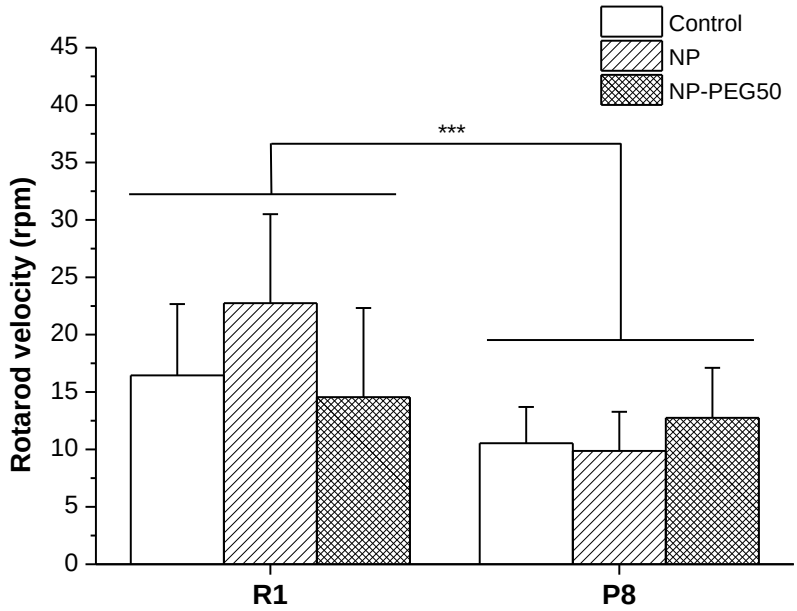

Figure 3. Mean rotarod speeds achieved by the animals. R1 corresponds to the SAMR1 strain, used as control. P8 corresponds to the SAMP8 strain. Control: animals receiving water; NP: animals receiving bare nanoparticles (200 mg/kg); NP-PEG50: animals receiving PEG-coated nanoparticles (200 mg/kg). Data expressed as mean ± SD ($n \geq 8$). ***: $p < 0.001$.

Figure 4 summarizes the results of the acquisition phase of the Morris water maze (MWM). During the 6 days of the acquisition phase, SAMR1 mice showed a decreasing tendency of the time needed to reach the platform (escape latency), showing a learning capacity (Figure 4A). On the contrary, SAMP8 mice did not show any improvement over days of the acquisition phase, confirming their learning impairment (Figure 4B). Nevertheless, no differences were found in the learning capacity of the mice treated with nanoparticles, neither in the SAMP8 nor in the SAMR1 strains.

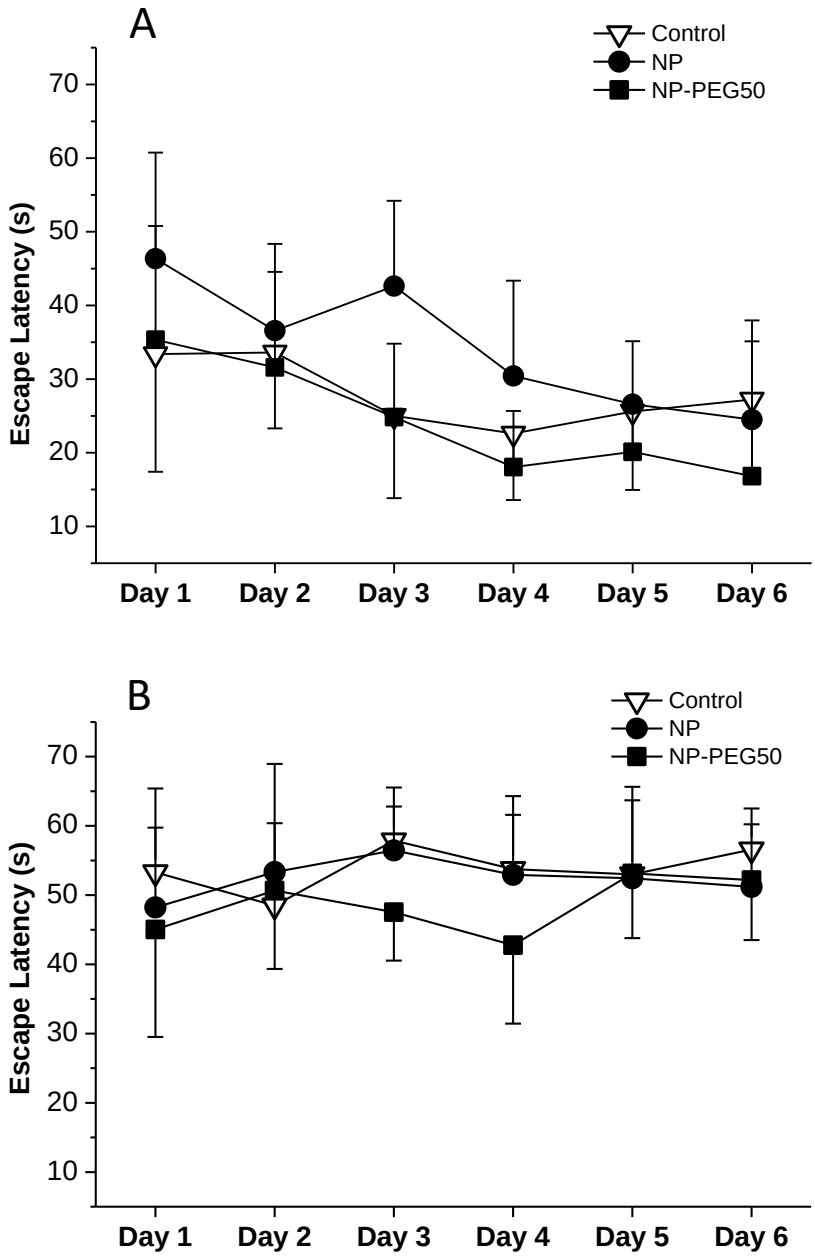

Figure 4. Escape latencies of A: SAMR1 mice; and B: SAMP8 mice during the acquisition phase. Control: animals receiving water; NP: animals receiving bare nanoparticles (200 mg/kg); NP-PEG50: animals receiving PEG-coated nanoparticles (200 mg/kg). Data expressed as mean ± SD ($n \geq 8$).

At the beginning of the fourth and seventh day, the memory retention of the mice was evaluated. The results of the retention test are shown in Figure 5. On the one hand, SAMR1 mice showed an increase in the time spent at the target quadrant from day 4 to day 7 (Figure 5A), what demonstrates their capacity to learn and to remember. On the other hand, SAMP8 mice did not show any increase in the time spent at the correct quadrant (Figure 5B), thus, demonstrating their lack of learning and memory capacities. For day 7, The retention values of SAMP8 mice were very significantly lower than those for SAMR1 mice ($p < 0.001$). However, no differences were observed between animals

receiving water, NP, or NP-PEG50, independently of the strain or the day of the retention evaluation.

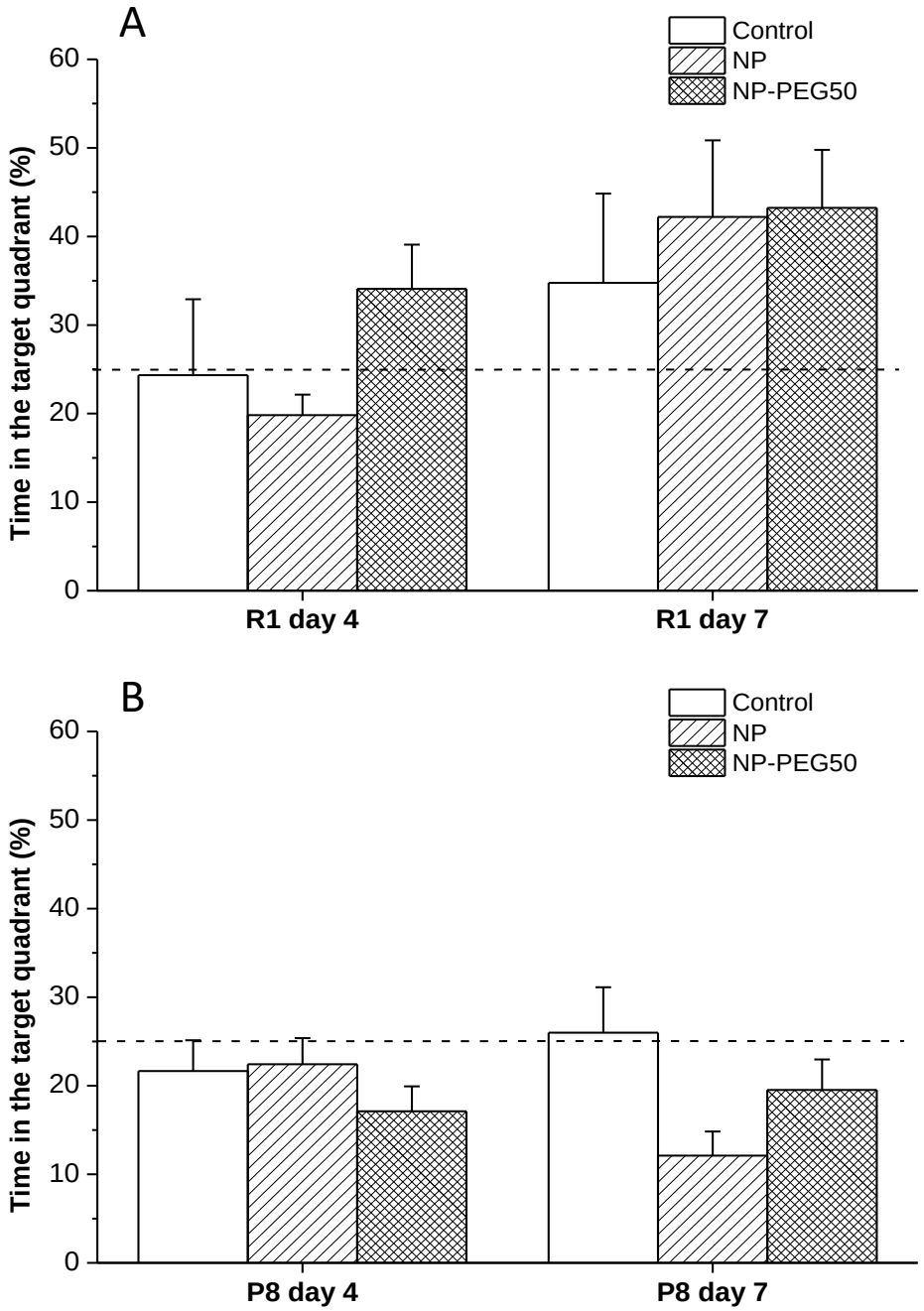

Figure 5. Times spent in the correct quadrant by mice during the two retention evaluations (days 4 and 7). R1 corresponds to SAMR1 mice, used as control. P8 corresponds to SAMP8 mice. Control: animals receiving water; NP: animals receiving bare nanoparticles (200 mg/kg); NP-PEG50: animals receiving PEG-coated nanoparticles (200 mg/kg). Dashed line stablishes the 25% threshold, considered as the value randomly reachable. Data expressed as mean ± SEM (n ≥ 8).

During the seventh day retention test, the swimming velocity of every mouse was tracked and analyzed, as an indirect measurement of their locomotor activity. As shown in Figure 6, no differences were found between animals receiving water, NP or NP-PEG50 in the SAMR1 mice. However, in the SAMP8 mice, animals treated with NP-PEG50 showed a higher swimming velocity compared to control and NP-treated mice ($p < 0.01$).

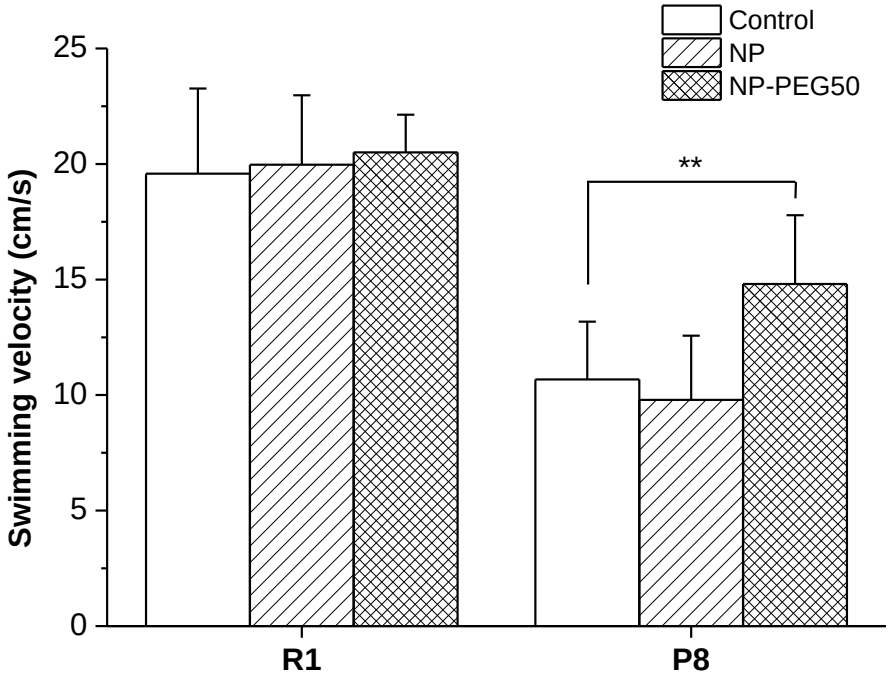

Figure 6. Swimming velocities of the mice during the evaluation of the 7th day retention. R1 corresponds to SAMR1 mice, used as control. P8 corresponds to SAMP8 mice. Control: animals receiving water; NP: animals receiving bare nanoparticles (200 mg/kg); NP-PEG50: animals receiving PEG-coated nanoparticles (200 mg/kg). Data expressed as mean ± SD ($n \geq 8$). **: $p < 0.01$ compared to control.

5.3.3.2. Effect of nanoparticles over the lifespan of SAMP8 mice

The lifespans of SAMP8 mice receiving the different treatments are shown in Figure 7. Oral administration of PEG-coated nanoparticles showed no effect over the lifespan of the animals, with a curve overlapping the one of control animals. On the other hand, animals treated with bare nanoparticles showed a significant increase in their life expectancy, compared to controls.

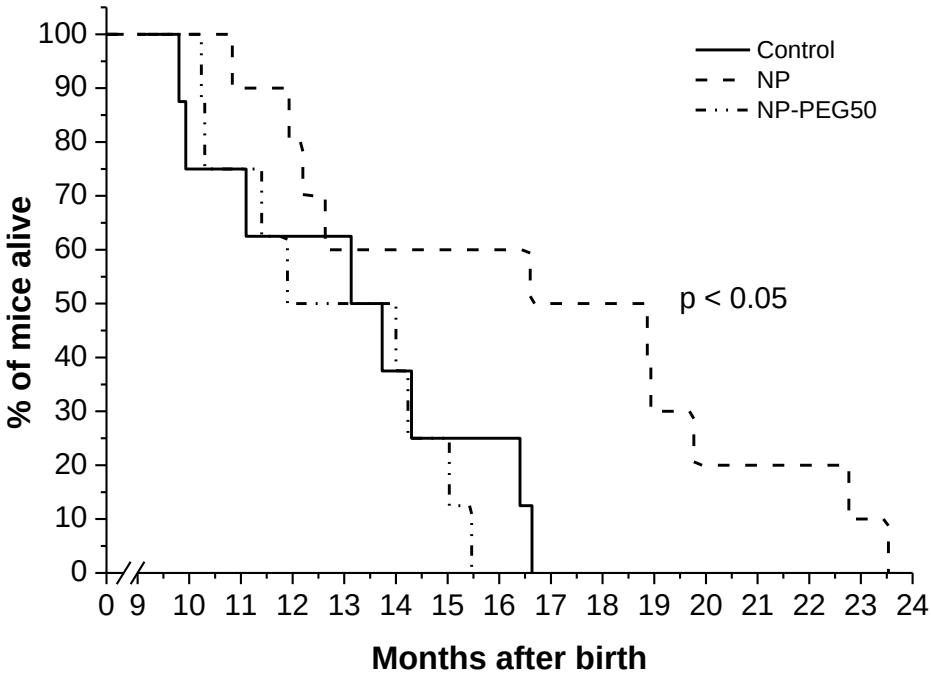

Figure 7. Effect of oral administration of bare nanoparticles (NP) and PEG-coated nanoparticles (NP-PEG50) on the lifespan of SAMP8 mice. Kaplan-Meier representation of the percentage of mice alive during time (n ≥ 8). Control: animals receiving water; NP: animals receiving bare nanoparticles (200 mg/kg); NP-PEG50: animals receiving PEG-coated nanoparticles (200 mg/kg). The statistical difference shown is compared to control group, using the Log-rank (Mantel-Cox) test.

The main results of the influence of the treatments over the lifespan of SAMP8 mice are summarized in Table 3. The oral administration of NP increased not only the mean lifespan (28%) but also the median and the maximum (32% and 41%, respectively). On the other hand, animals receiving NP-PEG50 did not show any relevant difference in the lifespan, compared to control animals.

Table 3. Summary of the main lifespan data of SAMP8 mice receiving water (control), bare nanoparticles (NP) or PEG-coated nanoparticles (NP-PEG50) (n ≥ 8). *: p < 0.05 compared to control.

	Lifespan		
Treatment	**Mean (months)**	**Median (months)**	**Maximum (months)**
Control	13.13 ± 2.50	13.43	16.63
NP	16.81 ± 4.43*	17.73	23.50
NP-PEG	12.82 ± 1.97	12.95	15.50

Finally, the weights of the animals during the whole experiment are summarized in Figure 8. No differences were observed in the weight gain/loss of the animals receiving different treatments during the 13 months that lasted the experiment.

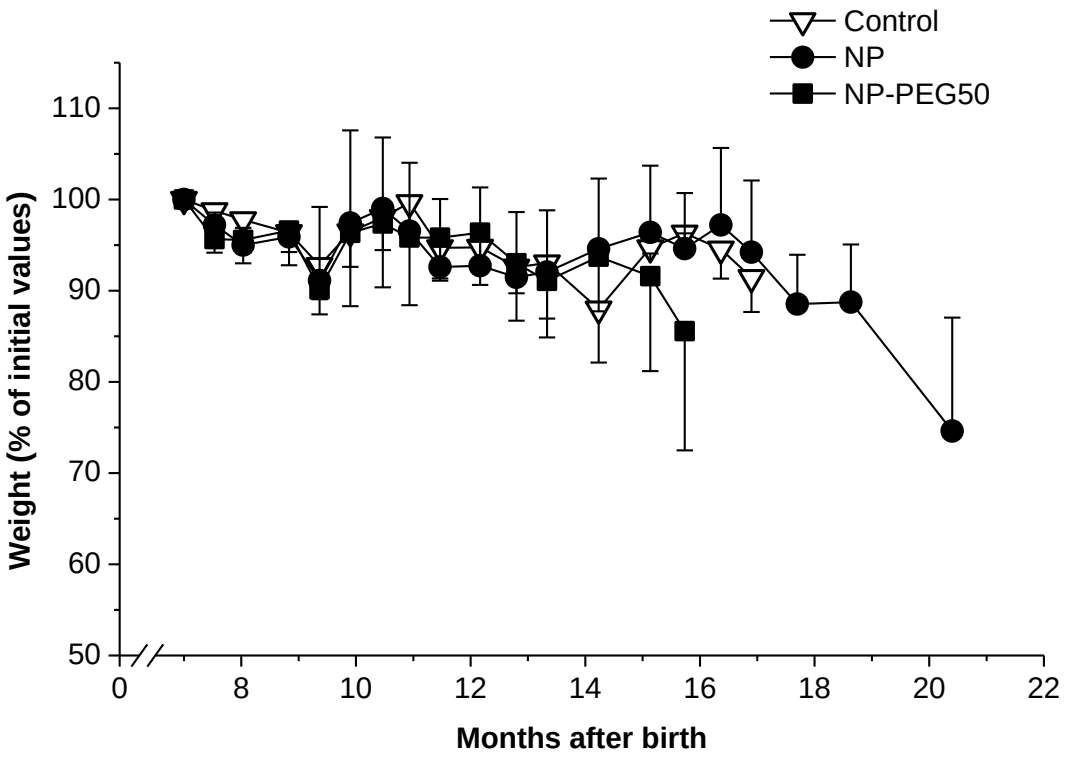

Figure 8. Effect of the oral administration of bare nanoparticles (NP) and PEG-coated nanoparticles (NP-PEG50) on the bodyweight of SAMP8 mice. Control: animals receiving water; NP: animals receiving bare nanoparticles (200 mg/kg); NP-PEG50: animals receiving PEG-coated nanoparticles (200 mg/kg). Data expressed as mean ± SD (n ≥ 8).

5.4. Discussion

The senescence-accelerated mouse prone-8 (SAMP8) is a widely used murine model for AD (Morley et al., 2012; Su et al., 2018). SAMP8 is characterized by the deposition of amyloid-beta (Aβ) protein in cerebral cortex and hippocampus areas, similar to those observed in AD, leading to rapid development of learning impairments and memory disorders (at about 6 months of age) (B. Liu et al., 2020; Moreno et al., 2017). In addition of these features of pathogenesis of AD, SAMP8 mice also exhibit an abnormal expression of antiaging factors and several characteristics of insulin resistance including hyperglycemia, and high levels of free fatty acids, as compared to SAMR1 (Cuesta et al., 2013; Liu et al., 2015)

Zein is the major storage protein present in maize and is considered as a GRAS material by the FDA (Reboredo et al., 2021). Moreover, in addition to its biocompatibility, biodegradability, and safety, peptides derived from the hydrolysis of this protein possess several interesting properties, including antioxidant (Shukla and Cheryan, 2001; Tang et al., 2010), immunomodulatory (Liang et al., 2020; P. Liu et al., 2020), and hypoglycemic (Higuchi et al., 2013; Mochida et al., 2010) effects. These three properties of zein hydrolysates could induce some benefit in the management of AD since the pathology runs with increased oxidative stress (Wang et al., 2014), inflammation (Kinney et al., 2018), and decreased insulin sensitivity, which is usually caused by sustained hyperglycemia (Shieh et al., 2020). Moreover, the capability of zein nanoparticles to

induce insulin secretion, as well as to improve the glycemic control in healthy animals, by triggering incretins secretion has also been demonstrated (Chapter 2). Both incretins (GLP-1 and GIP) exert some beneficial neuroprotective effects over the brain, such as improved memory and sensorimotor coordination, and reduced neurodegeneration (Anderberg et al., 2016; Baggio and Drucker, 2007; Hölscher, 2014; Nyberg et al., 2005; Rowlands et al., 2018). In a similar way, insulin receptors are also found in the central nervous system, where the union with the ligand trigger several metabolic pathways with neuroprotective and neuromodulatory effects that are involved in the control of cognition and memory (Blázquez et al., 2014; Hallschmid, 2021). Hence, oral administration of zein nanoparticles could improve the outcomes of AD via the increased secretion of incretins and insulin.

In the study carried out in a murine model of AD, 7-month-old SAMP8 mice showed the typical behavioral and cognitive alterations of this strain. SAMP8 mice were significantly more anxious than their healthy counterparts SAMR1, as measured by the reduction in the time spent in the open area of the OFT. A clear cognitive and memory impairment was also evidenced in the SAMP8 mice by the MWM. In that study, SAMP8 animals showed neither learning skills during the acquisition phase (see Figure 4) nor memory during the retention phase (see Figure 5). Disappointingly, the administration of zein nanoparticles (200 mg/kg every two days, for 3 months, from the age of 7 months), either mucoadhesive or mucus-permeating, did not show any improvement in the anxiety or cognitive impairment of the mice. This might be explained because, at the age of 7 months, SAMP8 mice have already developed the typical histopathological lesions characterizing AD such as tau hyperphosphorylation and Aβ deposition (Bayod et al., 2015; Del Valle et al., 2010; Moreno et al., 2017; Zhang et al., 2019). Hence, by this time, even if the oral administration of zein nanoparticles could induce an increased production of insulin and incretins, it could not reverse the accumulation of hyperphosphorylated tau proteins nor the Aβ deposition. This phenomenon has been previously reported by Kamei and co-workers (Kamei et al., 2017). In this study, increased levels of insulin in the brain slowed the progression of memory loss of young SAMP8 mice. However, in older mice (more than 6 months), the administration of insulin did not induce a recovery of the cognitive dysfunction.
Regarding the locomotor activity of the animals, both the rotarod and the swimming velocity in the MWM, showed that SAMP8 had a significant reduction in the physical endurance, compared to SAMR1 mice (Figures 3 and 6, respectively). In contrast, during the OFT, both strains walked similar distances and at similar velocities, without statistical differences. These findings are in the line with those previously reported (Moreno et al., 2017). The administration of zein nanoparticles did not improve the physical performance of the mice in the rotarod nor in the OFT. However, animals treated with NP-PEG50 showed a surprising increase in their swimming velocity during the MWM.

The first step of our longevity study was to evaluate the effect of zein nanoparticles on the lifespan of *C. elegans*. For that purpose, worms were cultured under high glucose conditions, which simulate the hyperglycemic state of diabetic patients (Zhu et al.,

2016), in a medium supplemented with nanoparticles. We found that the addition to the medium of either NP or NP-PEG50 increased, very significantly ($p < 0.001$), the lifespan of the worms (Figure 1). It is worth noting that the increased lifespan of the worms is induced only by the nanoparticles, since the supplementation with PEG did not show any relevant difference, compared to controls. The reason for this may be the protein composition of the nanoparticles, whose digestion and eventual absorption of the peptides and amino acids, trigger metabolic pathways involved in the lifespan of the animal. The PEPT-1 peptide transporter, located in the enterocytes of the worm (Miguel-Aliaga, 2012), is tightly related to the lifespan of the worm (Schifano et al., 2019). In fact, a downregulation of PEPT-1 in *C. elegans* induces a significant reduction in their median lifespan (Dysarz et al., 2021). Thus, the uptake of peptides through this transporter may also be influencing the longevity of the worms. This suggestion would reinforce the results obtained in Chapter 4, where we hypothesized that the reduction in the fat accumulation observed in the worms could be PEPT-1-mediated. However, further studies should be addressed to verify the hypothesis of the implication of PEPT-1 in the reduced fat content and increased lifespan found in worms grown in media supplemented with nanoparticles.

When the evaluation of the longevity was carried out in the SAMP8 animal model, surprising results were found (Figure 7). PEG-coated nanoparticles (NP-PEG50) did not induce any expansion on the life expectancy of the animals while animals treated with bare nanoparticles (NP) displayed a significantly enhanced longevity ($p < 0.05$). The reason for the difference between both formulations may be a contrasting residence time within the gut of the animals. On the one hand, NP-PEG50 flow rapidly through the gastrointestinal tract due to its increased mucus-diffusivity (Reboredo et al., 2021) and reduced interaction with proteins and other components from the medium (Pozzi et al., 2014; Tobío et al., 2000). Moreover, PEGs have been described to have a laxative effect (Corsetti et al., 2021) caused by the draw of water into the lumen due to an osmotic action (Chen et al., 2013; Corsetti et al., 2021) that leads to the hydrogen bonding between water molecules and PEG (Leung, 2014). This increases the volume of the stools and leads to the stretching of the epithelium of the gut, what triggers peristaltic reflexes (Birrer, 2002). In studies conducted in humans, oral administration of PEG improved very significantly the symptoms of constipation, including a higher number of bowel contractions and less hardened stools, without causing diarrhea or any serious adverse effect (DiPalma et al., 2000; McGraw, 2016). Moreover, in these studies, the dose of PEG was more than 3-times greater than the one given to the mice and the polymer was of low molecular weight (3350 da), which is more toxic than high molecular weight PEGs (Leung, 2014). These might be the reason why no diarrhea episodes were observed in animals treated with PEG-coated nanoparticles. Thus, the increased peristalsis would accelerate the excretion rate of NP-PEG50, reducing its presence inside the small intestine of the mice, without causing diarrhea.

In any case, the effect over the longevity of NP observed in mice would be related to their hypoglycemic effect (Chapter 4). SAMP8 mice display, naturally, a hyperglycemic

state (Cuesta et al., 2013; Liu et al., 2015), condition that leads to an increased formation of ROS and AGES and, thus, an accelerated aging (Moldogazieva et al., 2019; Volpe et al., 2018). In this context, a growing number of studies have indicated that metformin (an oral antidiabetic drug), can potentially stall aging and delay the onset of age-related diseases in humans (Fang et al., 2018; Glossmann and Lutz, 2019; Martin-Montalvo et al., 2013). On the other hand, some authors have showed data that lead to suspect that an upregulation of fasting and postprandial production of GLP-1 would be responsible for the versatile health protection conferred by some agents employed in the treatment of type 2 diabetes (i.e., acarbose) (McCarty and DiNicolantonio, 2015). In fact, GLP-1 may act on the liver to modulate the production of fibroblast growth factor-21 (FGF21) and insulin-like growth factor (IGF-I) and, thus, promoting longevity (Liu et al., 2019; Yan et al., 2021).

In summary, oral administration of either NP or NP-PEG50 have demonstrated beneficial effects over the lifespan of *C. elegans*. However, when the same formulations were evaluated in a mouse model of accelerated aging (SAMP8 mice), only NP increased the life expectancy of the animals. This effect on the longevity of animals may be related to their capability as inductor of GLP-1 release when orally administered. In any case, other different pathways may be involved in the lifespan-expanding effects observed; thus, further research must be carried out in order the elucidate them. Nevertheless, none of the formulations improved the learning impairment of the mice, denoting that their beneficial effects are not enough to counteract the outcomes of an already-developed state of Alzheimer's Disease.

5.5. References

2017 Alzheimer's disease facts and figures, 2017. . Alzheimer's Dement. 13, 325–373. https://doi.org/10.1016/j.jalz.2017.02.001

Ahima, R.S., 2009. Connecting obesity, aging and diabetes. Nat. Med. 15, 996–997. https://doi.org/10.1038/nm0909-996

Alcántar-Fernández, J., Navarro, R.E., Salazar-Martínez, A.M., Pérez-Andrade, M.E., Miranda-Ríos, J., 2018. Caenorhabditis elegans respond to high-glucose diets through a network of stress-responsive transcription factors. PLoS One 13, e0199888. https://doi.org/10.1371/journal.pone.0199888

Anderberg, R.H., Richard, J.E., Hansson, C., Nissbrandt, H., Bergquist, F., Skibicka, K.P., 2016. GLP-1 is both anxiogenic and antidepressant; divergent effects of acute and chronic GLP-1 on emotionality. Psychoneuroendocrinology 65, 54–66. https://doi.org/10.1016/j.psyneuen.2015.11.021

Arbós, P., Arangoa, M.A., Campanero, M.A., Irache, J.M., 2002. Quantification of the bioadhesive properties of protein-coated PVM/MA nanoparticles. Int. J. Pharm. 242, 129–136. https://doi.org/10.1016/S0378-5173(02)00182-5

Baggio, L.L., Drucker, D.J., 2007. Biology of Incretins: GLP-1 and GIP. Gastroenterology 132, 2131–2157. https://doi.org/10.1053/j.gastro.2007.03.054

Bayod, S., Felice, P., Andrés, P., Rosa, P., Camins, A., Pallàs, M., Canudas, A.M., 2015. Downregulation of canonical Wnt signaling in hippocampus of SAMP8 mice. Neurobiol. Aging 36, 720–729. https://doi.org/10.1016/j.neurobiolaging.2014.09.017

Birrer, R.B., 2002. Irritable bowel syndrome, in: Disease-a-Month. Elsevier, pp. 101–143. https://doi.org/10.1067/mda.2002.122480

Blázquez, E., Velázquez, E., Hurtado-Carneiro, V., Ruiz-Albusac, J.M., 2014. Insulin in the brain: Its pathophysiological implications for states related with central insulin resistance, type 2 diabetes and alzheimer's disease. Front. Endocrinol. (Lausanne). https://doi.org/10.3389/fendo.2014.00161

Bullard, K.M., Cowie, C.C., Lessem, S.E., Saydah, S.H., Menke, A., Geiss, L.S., Orchard, T.J., Rolka, D.B., Imperatore, G., 2018. Prevalence of Diagnosed Diabetes in Adults by Diabetes Type — United States, 2016. MMWR. Morb. Mortal. Wkly. Rep. 67, 359–361. https://doi.org/10.15585/mmwr.mm6712a2

Burton, D.G.A., Faragher, R.G.A., 2018. Obesity and type-2 diabetes as inducers of premature cellular senescence and ageing. Biogerontology 19, 447–459. https://doi.org/10.1007/s10522-018-9763-7

Caspersen, C.J., Thomas, G.D., Boseman, L.A., Beckles, G.L.A., Albright, A.L., 2012. Aging, diabetes, and the public health system in the United States. Am. J. Public Health 102, 1482–1497. https://doi.org/10.2105/AJPH.2011.300616

Chen, M.L., Sadrieh, N., Yu, L., 2013. Impact of osmotically active excipients on bioavailability and bioequivalence of BCS class III drugs. AAPS J. 15, 1043–1050. https://doi.org/10.1208/s12248-013-9509-z

Corsetti, M., Thys, A., Harris, A., Pagliaro, G., Deloose, E., Demedts, I., Tack, J., 2021. High-resolution manometry reveals different effect of polyethylene glycol, bisacodyl, and prucalopride on colonic motility in healthy subjects: An acute, open label, randomized, crossover, reader-blinded study with potential clinical implications. Neurogastroenterol. Motil. 33, e14040. https://doi.org/10.1111/nmo.14040

Cuesta, S., Kireev, R., García, C., Rancan, L., Vara, E., Tresguerres, J.A.F., 2013. Melatonin can improve insulin resistance and aging-induced pancreas alterations in senescence-accelerated prone male mice (SAMP8). Age (Omaha). 35, 659–671. https://doi.org/10.1007/s11357-012-9397-7

Czech, M.P., 2017. Insulin action and resistance in obesity and type 2 diabetes. Nat. Med. 23, 804–814. https://doi.org/10.1038/nm.4350

De La Monte, S.M., Wands, J.R., 2008. Alzheimer's disease is type 3 diabetes-evidence reviewed. J. Diabetes Sci. Technol. https://doi.org/10.1177/193229680800200619

Del Valle, J., Duran-Vilaregut, J., Manich, G., Casadesús, G., Smith, M.A., Camins, A., Pallàs, M., Pelegrí, C., Vilaplana, J., 2010. Early amyloid accumulation in the hippocampus of SAMP8 mice. J. Alzheimer's Dis. 19, 1303–1315. https://doi.org/10.3233/JAD-2010-1321

Diaz-Perdigon, T., Belloch, F.B., Ricobaraza, A., Elboray, E.E., Suzuki, T., Tordera, R.M., Puerta, E., 2020. Early sirtuin 2 inhibition prevents age-related cognitive decline in a senescence-accelerated mouse model. Neuropsychopharmacology 45, 347–357. https://doi.org/10.1038/s41386-019-0503-8

DiPalma, J.A., DeRidder, P.H., Orlando, R.C., Kolts, B.E., Cleveland, M. vB, 2000. A Randomized, Placebo-Controlled, Multicenter Study of The Safety and Efficacy of A New Polyethylene Glycol Laxative. Am. J. Gastroenterol. 95, 446–450. https://doi.org/10.1111/j.1572-0241.2000.01765.x

Dysarz, J., Fuellen, G., Möller, S., Luyten, W., Schmitz-Linneweber, C., Saul, N., 2021. Genes implicated in Caenorhabditis elegans and human health regulate stress resistance and physical abilities in aged Caenorhabditis elegans. Biol. Lett. 17. https://doi.org/10.1098/rsbl.2020.0916

Fang, J., Yang, J., Wu, X., Zhang, G., Li, T., Wang, X., Zhang, H., Wang, C. chen, Liu, G.H., Wang, L., 2018. Metformin alleviates human cellular aging by upregulating the endoplasmic reticulum glutathione peroxidase 7. Aging Cell 17, e12765. https://doi.org/10.1111/acel.12765

Glossmann, H.H., Lutz, O.M.D., 2019. Metformin and Aging: A Review. Gerontology. https://doi.org/10.1159/000502257

Golay, A., Ybarra, J., 2005. Link between obesity and type 2 diabetes. Best Pract. Res. Clin. Endocrinol. Metab. 19, 649–663. https://doi.org/10.1016/j.beem.2005.07.010

Hallschmid, M., 2021. Intranasal Insulin for Alzheimer's Disease. CNS Drugs 35, 21–37. https://doi.org/10.1007/s40263-020-00781-x

Higuchi, N., Hira, T., Yamada, N., Hara, H., 2013. Oral administration of corn zein hydrolysate stimulates GLP-1 and GIP secretion and improves glucose tolerance in male normal rats and Goto-Kakizaki rats. Endocrinology 154, 3089–3098. https://doi.org/10.1210/en.2012-2275

Hölscher, C., 2014. The incretin hormones glucagonlike peptide 1 and glucose-dependent insulinotropic polypeptide are neuroprotective in mouse models of Alzheimer's disease. Alzheimer's Dement. 10. https://doi.org/10.1016/j.jalz.2013.12.009

Kamei, N., Tanaka, M., Choi, H., Okada, N., Ikeda, T., Itokazu, R., Takeda-Morishita, M., 2017. Effect of an Enhanced Nose-to-Brain Delivery of Insulin on Mild and Progressive Memory Loss in the Senescence-Accelerated Mouse. Mol. Pharm. 14, 916–927. https://doi.org/10.1021/acs.molpharmaceut.6b01134

Kandimalla, R., Thirumala, V., Reddy, P.H., 2017. Is Alzheimer's disease a Type 3 Diabetes? A critical appraisal. Biochim. Biophys. Acta - Mol. Basis Dis. https://doi.org/10.1016/j.bbadis.2016.08.018

Kinney, J.W., Bemiller, S.M., Murtishaw, A.S., Leisgang, A.M., Salazar, A.M., Lamb, B.T., 2018. Inflammation as a central mechanism in Alzheimer's disease. Alzheimer's Dement. Transl. Res. Clin. Interv. 4, 575–590. https://doi.org/10.1016/j.trci.2018.06.014

Lazzaro, B.P., Schneider, D.S., 2014. The genetics of immunity. Genetics 197, 467–470. https://doi.org/10.1534/genetics.114.165449

Leung, H.W., 2014. Polyethylene Glycol. Encycl. Toxicol. Third Ed. 1043–1044. https://doi.org/10.1016/B978-0-12-386454-3.00050-6

Liang, Q., Chalamaiah, M., Liao, W., Ren, X., Ma, H., Wu, J., 2020. Zein hydrolysate and its peptides exert anti-inflammatory activity on endothelial cells by preventing TNF-α-induced NF-κB activation. J. Funct. Foods 64, 103598. https://doi.org/10.1016/j.jff.2019.103598

Liu, B., Liu, J., Shi, J.-S., 2020. SAMP8 Mice as a Model of Age-Related Cognition Decline with Underlying Mechanisms in Alzheimer's Disease. J. Alzheimer's Dis. 75, 385–395. https://doi.org/10.3233/jad-200063

Liu, H.W., Chan, Y.C., Wang, M.F., Wei, C.C., Chang, S.J., 2015. Dietary (-)-Epigallocatechin-3-gallate Supplementation Counteracts Aging-Associated Skeletal Muscle Insulin Resistance and Fatty Liver in Senescence-Accelerated Mouse. J. Agric. Food Chem. 63, 8407–8417. https://doi.org/10.1021/acs.jafc.5b02501

Liu, H.W., Chan, Y.C., Wei, C.C., Chen, Y.A., Wang, M.F., Chang, S.J., 2017. An alternative model for studying age-associated metabolic complications: Senescence-accelerated mouse prone 8. Exp. Gerontol. 99, 61–68. https://doi.org/10.1016/j.exger.2017.08.023

Liu, J., Yang, K., Yang, J., Xiao, W., Le, Y., Yu, F., Gu, L., Lang, S., Tian, Q., Jin, T., Wei, R., Hong, T., 2019. Liver-derived fibroblast growth factor 21 mediates effects of glucagon-like peptide-1 in attenuating hepatic glucose output. EBioMedicine 41,

73–84. https://doi.org/10.1016/j.ebiom.2019.02.037

Liu, P., Liao, W., Qi, X., Yu, W., Wu, J., 2020. Identification of immunomodulatory peptides from zein hydrolysates. Eur. Food Res. Technol. 246, 931–937. https://doi.org/10.1007/s00217-020-03450-x

Mao, Y.F., Guo, Z., Zheng, T., Jiang, Y., Yan, Y., Yin, X., Chen, Y., Zhang, B., 2016. Intranasal insulin alleviates cognitive deficits and amyloid pathology in young adult APPswe/PS1dE9 mice. Aging Cell 15, 893–902. https://doi.org/10.1111/acel.12498

Martin-Montalvo, A., Mercken, E.M., Mitchell, S.J., Palacios, H.H., Mote, P.L., Scheibye-Knudsen, M., Gomes, A.P., Ward, T.M., Minor, R.K., Blouin, M.J., Schwab, M., Pollak, M., Zhang, Y., Yu, Y., Becker, K.G., Bohr, V.A., Ingram, D.K., Sinclair, D.A., Wolf, N.S., Spindler, S.R., Bernier, M., De Cabo, R., 2013. Metformin improves healthspan and lifespan in mice. Nat. Commun. 4. https://doi.org/10.1038/ncomms3192

Martínez-López, A.L., González-Navarro, C.J., Aranaz, P., Vizmanos, J.L., Irache, J.M., 2021a. In vivo testing of mucus-permeating nanoparticles for oral insulin delivery using Caenorhabditis elegans as a model under hyperglycemic conditions. Acta Pharm. Sin. B 11, 989–1002. https://doi.org/10.1016/j.apsb.2021.02.020

Martínez-López, A.L., González-Navarro, C.J., Vizmanos, J.L., Irache, J.M., 2021b. Zein-based nanocarriers for the oral delivery of insulin. In vivo evaluation in Caenorhabditis elegans. Drug Deliv. Transl. Res. 11, 647–658. https://doi.org/10.1007/s13346-021-00919-4

McCarty, M.F., DiNicolantonio, J.J., 2015. Acarbose, lente carbohydrate, and prebiotics promote metabolic health and longevity by stimulating intestinal production of GLP-1. Open Hear. 2, e000205. https://doi.org/10.1136/openhrt-2014-000205

McGraw, T., 2016. Polyethylene glycol 3350 in occasional constipation: A one-week, randomized, placebo-controlled, double-blind trial. World J. Gastrointest. Pharmacol. Ther. 7, 274. https://doi.org/10.4292/wjgpt.v7.i2.274

Miguel-Aliaga, I., 2012. Nerveless and gutsy: Intestinal nutrient sensing from invertebrates to humans. Semin. Cell Dev. Biol. 23, 614–620. https://doi.org/10.1016/j.semcdb.2012.01.002

Mittal, K., Mani, R.J., Katare, D.P., 2016. Type 3 Diabetes: Cross Talk between Differentially Regulated Proteins of Type 2 Diabetes Mellitus and Alzheimer's Disease. Sci. Rep. 6. https://doi.org/10.1038/srep25589

Mochida, T., Hira, T., Hara, H., 2010. The corn protein, zein hydrolysate, administered into the ileum attenuates hyperglycemia via its dual action on glucagon-like peptide-1 secretion and dipeptidyl peptidase-IV activity in rats. Endocrinology 151, 3095–3104. https://doi.org/10.1210/en.2009-1510

Moldogazieva, N.T., Mokhosoev, I.M., Mel'Nikova, T.I., Porozov, Y.B., Terentiev, A.A., 2019. Oxidative Stress and Advanced Lipoxidation and Glycation End Products (ALEs and AGEs) in Aging and Age-Related Diseases. Oxid. Med. Cell. Longev. 2019. https://doi.org/10.1155/2019/3085756

Moreno, L.C.G. e. I., Puerta, E., Suárez-Santiago, J.E., Santos-Magalhães, N.S., Ramirez,

M.J., Irache, J.M., 2017. Effect of the oral administration of nanoencapsulated quercetin on a mouse model of Alzheimer's disease. Int. J. Pharm. 517, 50–57. https://doi.org/10.1016/j.ijpharm.2016.11.061

Morley, J.E., 2008. Diabetes and Aging: Epidemiologic Overview. Clin. Geriatr. Med. 24, 395–405. https://doi.org/10.1016/j.cger.2008.03.005

Morley, J.E., Armbrecht, H.J., Farr, S.A., Kumar, V.B., 2012. The senescence accelerated mouse (SAMP8) as a model for oxidative stress and Alzheimer's disease. Biochim. Biophys. Acta - Mol. Basis Dis. 1822, 650–656. https://doi.org/10.1016/j.bbadis.2011.11.015

Müller, T.D., Finan, B., Bloom, S.R., D'Alessio, D., Drucker, D.J., Flatt, P.R., Fritsche, A., Gribble, F., Grill, H.J., Habener, J.F., Holst, J.J., Langhans, W., Meier, J.J., Nauck, M.A., Perez-Tilve, D., Pocai, A., Reimann, F., Sandoval, D.A., Schwartz, T.W., Seeley, R.J., Stemmer, K., Tang-Christensen, M., Woods, S.C., DiMarchi, R.D., Tschöp, M.H., 2019. Glucagon-like peptide 1 (GLP-1). Mol. Metab. https://doi.org/10.1016/j.molmet.2019.09.010

Nomura, Y., Okuma, Y., 1999. Age-related defects in lifespan and learning ability in SAMP8 mice. Neurobiol. Aging 20, 111–115. https://doi.org/10.1016/S0197-4580(99)00006-8

Nyberg, J., Anderson, M.F., Meister, B., Alborn, A.M., Ström, A.K., Brederlau, A., Illerskog, A.C., Nilsson, O., Kieffer, T.J., Hietala, M.A., Ricksten, A., Eriksson, P.S., 2005. Glucose-dependent insulinotropic polypeptide is expressed in adult hippocampus and induces progenitor cell proliferation. J. Neurosci. 25, 1816–1825. https://doi.org/10.1523/JNEUROSCI.4920-04.2005

Pallas, M., Camins, A., Smith, M.A., Perry, G., Lee, H.G., Casadesus, G., 2008. From aging to Alzheimer's disease: Unveiling "The switch" with the senescence-accelerated mouse model (SAMP8). J. Alzheimer's Dis. 15, 615–624. https://doi.org/10.3233/JAD-2008-15408

Pozzi, D., Colapicchioni, V., Caracciolo, G., Piovesana, S., Capriotti, A.L., Palchetti, S., De Grossi, S., Riccioli, A., Amenitsch, H., Laganà, A., 2014. Effect of polyethyleneglycol (PEG) chain length on the bio-nano- interactions between PEGylated lipid nanoparticles and biological fluids: From nanostructure to uptake in cancer cells. Nanoscale 6, 2782–2792. https://doi.org/10.1039/c3nr05559k

Qi, L., Ke, L., Liu, Xiaohong, Liao, L., Ke, S., Liu, Xiaoying, Wang, Y., Lin, X., Zhou, Y., Wu, L., Chen, Z., Liu, L., 2016. Subcutaneous administration of liraglutide ameliorates learning and memory impairment by modulating tau hyperphosphorylation via the glycogen synthase kinase-3β pathway in an amyloid β protein induced alzheimer disease mouse model. Eur. J. Pharmacol. 783, 23–32. https://doi.org/10.1016/j.ejphar.2016.04.052

Reboredo, C., González-Navarro, C.J., Martínez-Oharriz, C., Martínez-López, A.L., Irache, J.M., 2021. Preparation and evaluation of PEG-coated zein nanoparticles for oral drug delivery purposes. Int. J. Pharm. 597, 120287. https://doi.org/10.1016/j.ijpharm.2021.120287

Rowlands, J., Heng, J., Newsholme, P., Carlessi, R., 2018. Pleiotropic Effects of GLP-1 and Analogs on Cell Signaling, Metabolism, and Function. Front. Endocrinol. (Lausanne). 9, 672. https://doi.org/10.3389/fendo.2018.00672

Salvestrini, V., Sell, C., Lorenzini, A., 2019. Obesity may accelerate the aging process. Front. Endocrinol. (Lausanne). 10, 266. https://doi.org/10.3389/fendo.2019.00266

Schifano, E., Zinno, P., Guantario, B., Roselli, M., Marcoccia, S., Devirgiliis, C., Uccelletti, D., 2019. The foodborne strain lactobacillus fermentum mbc2 triggers pept-1-dependent pro-longevity effects in caenorhabditis elegans. Microorganisms 7, 45. https://doi.org/10.3390/microorganisms7020045

Schulz, T.J., Zarse, K., Voigt, A., Urban, N., Birringer, M., Ristow, M., 2007. Glucose Restriction Extends Caenorhabditis elegans Life Span by Inducing Mitochondrial Respiration and Increasing Oxidative Stress. Cell Metab. 6, 280–293. https://doi.org/10.1016/j.cmet.2007.08.011

Shieh, J.C.C., Huang, P.T., Lin, Y.F., 2020. Alzheimer's Disease and Diabetes: Insulin Signaling as the Bridge Linking Two Pathologies. Mol. Neurobiol. 57, 1966–1977. https://doi.org/10.1007/s12035-019-01858-5

Shukla, R., Cheryan, M., 2001. Zein: The industrial protein from corn. Ind. Crops Prod. 13, 171–192. https://doi.org/10.1016/S0926-6690(00)00064-9

Su, D., Li, W., She, X., Chen, X., Zhai, Q., Cui, B., Wang, R., 2018. Chronic noise exposure exacerbates AD-like neuropathology in SAMP8 mice in relation to Wnt signaling in the PFC and hippocampus. Sci. Rep. 8, 1–10. https://doi.org/10.1038/s41598-018-32948-4

Tang, X., He, Z., Dai, Y., Xiong, Y.L., Xie, M., Chen, J., 2010. Peptide fractionation and free radical scavenging activity of zein hydrolysate. J. Agric. Food Chem. 58, 587–593. https://doi.org/10.1021/jf9028656

Tobío, M., Sánchez, A., Vila, A., Soriano, I., Evora, C., Vila-Jato, J.L., Alonso, M.J., 2000. The role of PEG on the stability in digestive fluids and in vivo fate of PEG-PLA nanoparticles following oral administration. Colloids Surfaces B Biointerfaces 18, 315. https://doi.org/10.1016/s0927-7765(99)00157-5

Volpe, C.M.O., Villar-Delfino, P.H., Dos Anjos, P.M.F., Nogueira-Machado, J.A., 2018. Cellular death, reactive oxygen species (ROS) and diabetic complications review-Article. Cell Death Dis. 9, 1–9. https://doi.org/10.1038/s41419-017-0135-z

Wang, X., Wang, W., Li, L., Perry, G., Lee, H. gon, Zhu, X., 2014. Oxidative stress and mitochondrial dysfunction in Alzheimer's disease. Biochim. Biophys. Acta - Mol. Basis Dis. 1842, 1240–1247. https://doi.org/10.1016/j.bbadis.2013.10.015

Yan, J., Nie, Y., Cao, J., Luo, M., Yan, M., Chen, Z., He, B., 2021. The Roles and Pharmacological Effects of FGF21 in Preventing Aging-Associated Metabolic Diseases. Front. Cardiovasc. Med. 8. https://doi.org/10.3389/fcvm.2021.655575

Zhang, Z., Yang, J., Liu, C., Xie, J., Qiu, S., Yang, X., Wu, C., 2019. Pseudoginsenoside-F11 alleviates cognitive deficits and Alzheimer's disease-type pathologies in SAMP8 mice. Pharmacol. Res. 139, 512–523. https://doi.org/10.1016/j.phrs.2018.10.024

Zhu, G., Yin, F., Wang, L., Wei, W., Jiang, L., Qin, J., 2016. Modeling type 2 diabetes-like hyperglycemia in C. elegans on a microdevice. Integr. Biol. (United Kingdom) 8, 30–38. https://doi.org/10.1039/c5ib00243e

Chapter 6

Zein-based nanoparticles as oral carriers for insulin delivery

6. Zein-based nanoparticles as oral carriers for insulin delivery

Cristian Reboredo[1], Carlos Javier González-Navarro[2], Ana Luisa Martínez-López[1], María Cristina Martínez-Ohárriz[3], Bruno Sarmento[4,5] and Juan Manuel Irache[1]

[1]Department of Chemistry and Pharmaceutical Technology, University of Navarra, C/Irunlarrea 1, 31008 Pamplona, Spain
[2]Center for Nutrition Research, School of Pharmacy and Nutrition, University of Navarra, C/Irunlarrea 1, 31008 Pamplona, Spain
[3]Department of Chemistry, University of Navarra, C/Irunlarrea 1, 31008 Pamplona, Spain
[4]i3S, Instituto de Investigação e Inovação em Saúde, Alfredo Allen 208, 4200-180 Porto, Portugal
[5]CESPU—Instituto de Investigação e Formação Avançada em Ciências e Tecnologias da Saúde, 4585-116 Gandra, Portugal

Corresponding author:
Prof. Juan M. Irache
Dep. Chemistry and Pharmaceutical Technology
University of Navarra
C/ Irunlarrea, 1
31008 – Pamplona Spain
Phone: +34948425600
Fax: +34948425619
E-mail: jmirache@unav.es

Pharmaceutics (2022): 14, 39

DOI: https://doi.org/10.3390/pharmaceutics14010039

Abstract

Zein, the major storage protein from corn, has a GRAS (Generally Regarded as Safe) status and may be easily transformed into nanoparticles, offering significant payloads for protein materials without affecting their stability. In this work, bare zein nanoparticles (mucoadhesive) and nanoparticles coated with poly(ethylene glycol) (mucus-permeating) were evaluated as oral carriers of insulin (I-NP and I-NP-PEG, respectively). Both nanocarriers displayed sizes of around 270 nm, insulin payloads close to 80 μg/mg and did not induce cytotoxic effects in Caco-2 and HT29-MTX cell lines. In *Caenorhabditis elegans*, where insulin decreases fat storage, I-NP-PEG induced a higher reduction in the fat content than I-NP and slightly lower than the control (Orlistat®). In diabetic rats, nanoparticles induced a potent hypoglycemic effect and achieved an oral bioavailability of 4.2% for I-NP and 10.2% for I-NP-PEG. This superior effect observed for I-NP-PEG would be related to their capability to diffuse through the mucus layer and reach the surface of enterocytes (where insulin would be released), whereas the mucoadhesive I-NP would remain trapped in the mucus, far away from the absorptive epithelium. In summary, PEG-coated zein nanoparticles may be an interesting device for the effective delivery of proteins through the oral route.

6.1. Introduction

The oral route is the preferred way for drug administration due to its advantages for the patient but also for the manufacturer. For the patients, this route facilitates the administration of the drug and avoids the association of the medication with a painful act (as sometimes occur with parenteral administrations); increasing the compliance of the treatment (Mahmood and Bernkop-Schnürch, 2019; Sim et al., 2016). For the manufacturer, medications intended for the oral route have less demanding cleaning and sterility requirements than for parenteral drugs. However, the large majority of peptides and therapeutic proteins are formulated and administered as injections due to their very low bioavailability when orally administered (usually lower than 1%) (Brown et al., 2020). The reason for this low availability is the presence of several obstacles that hamper their access to the absorptive epithelium. These obstacles include the chemical and enzymatic barriers, as well as the protective mucus layer. The chemical barrier comprises the varying pH conditions all along the gastrointestinal tract, shifting from highly acidic in the stomach (pH ≈ 1.2) to slightly basic in the colon (pH ≈ 7.5). Under these conditions, many proteins undergo a loss of their activity due to hydrolysis, deamination, or pH-induced oxidation processes (Ahmad et al., 2012; Brown et al., 2020). The enzymatic barrier refers to the efficient degrading enzymes present in the lumen of the gastrointestinal tract and in the apical membrane of the enterocytes, including pepsin, trypsin, chymotrypsin, elastase, carboxypeptidases, aminopeptidases, etc. (Frizzell and Woodrow, 2020). Those proteases degrade around 94-98% of all the proteins administered orally (Langguth et al., 1997). Finally, the mucus layer is a hydrogel matrix that covers the whole gastrointestinal tract and acts as the first line of defense against epithelial damage by physical, chemical, or biological aggression. This protective layer is mainly composed of mucins (highly O-glycosylated proteins), which confer a negative charge to the gel (Li et al., 2013) and expose hydrophobic domains where proteins may bind and get retained (Johansson et al., 2011).

However, the intestinal epithelium itself acts as a selective fence, hindering the pass of molecules according to their molecular weight and chemical properties. The transport of macromolecules from the lumen to the bloodstream can occur through two different pathways: transcellular or paracellular (Hwang and Byun, 2014). The paracellular transport occurs by passive diffusion through the spaces between two adjacent cells, spaces occupied by tight junctions that bind both cells together and act as a selective barrier (Lee et al., 2018). However, peptides absorbed through this route must be hydrophilic, neutral, and with a low molecular weight (Xu et al., 2019). Thus, molecules larger than 700 Da would enter the cell via active transport (Hwang and Byun, 2014). The transcellular pathway (a type of active transport) involves the endocytic uptake at the apical site, intracellular vesicle traffic, and basolateral efflux of the content (Li et al., 2021). This phenomenon occurs both in the enterocytes and in the M cells of Peyer patches localized in the intestinal epithelium (Shakweh et al., 2004). Hence, due to the large molecular weight of insulin (5.8 kDa) (Vakilian et al., 2019), it would not be suitable to be absorbed through the paracellular route. Moreover, previous studies suggest that the transcellular transport through the enterocytes would be the main route for insulin

absorption (McGinn and Morrison, 2016). In fact, enterocytes present insulin receptors in both their apical and basolateral membranes (Ben Lulu et al., 2010). After binding to its membrane receptor, insulin would be internalized by endocytosis and, once in the intracellular space, released to the cytoplasm (Ben Lulu et al., 2010; Hall et al., 2020).

To minimize the negative effect of these drawbacks on the bioavailability of orally administered peptides and proteins, several strategies have been proposed. These strategies include the use of polymer-drug conjugates (Ibie et al., 2019; Marschütz and Bernkop-Schnürch, 2000), liposomes (Torchilin, 2005; Wong et al., 2018), SNEDDS (Irache et al., 2011; Li et al., 2014), and polymeric nanoparticles (Fonte et al., 2014; Hirlekar et al., 2017; Paques et al., 2014). Thus, in recent years, clinical trials with oral peptide and protein-based products have progressively increased. As a result of these research efforts, in 2019, the US-FDA approved semaglutide (Rybelsus®) as an oral medication against type 2 diabetes mellitus. Nevertheless, the possibility of using the oral route as a way for the administration of peptides and proteins requires the development of delivery systems adapted to the particularities of both the gut and the macromolecules.

In this context, a possible alternative may be the use of zein-based nanoparticles. Zein is a natural GRAS (Generally Recognized As Safe by the FDA) protein found in corn that has been widely used in the pharmaceutical industry, as well as for the development of polymeric nanocarriers, due to its safety, biodegradability, and low toxicity (Luo and Wang, 2014). Zein nanoparticles have already demonstrated an important potential to increase the oral bioavailability of both small (Penalva et al., 2015) and large molecules (Inchaurraga et al., 2020). Moreover, although zein nanoparticles display a mucoadhesive behavior (Peñalva et al., 2015), their surface properties can be easily modified with hydrophilic polymers (e.g., poly(ethylene glycol)); abolishing the possibility of developing adhesive interactions with the components of the mucus layer and, thus, facilitating the possibility of reaching the intestinal epithelium. Hence, the coating of zein nanoparticles with poly(ethylene glycol) 35,000 (PEG) permits to increase their mucus diffusivity (Reboredo et al., 2021), which could lead to an increased oral bioavailability of the loaded biologically active compound.

The objective of this work was to evaluate the capability of two different zein-based nanoparticles, with either mucoadhesive or mucus-permeating properties, for oral protein delivery, using insulin as a model. For this purpose, the capability of both formulations to reduce the fat accumulation in *C. elegans* (regulated by insulin pathways), as well as their effect in an animal model of diabetic rats was assessed.

6.2. Materials and methods

6.2.1. Materials

Zein, lysine, human recombinant insulin, Rose Bengal sodium salt, poly(ethylene glycol) 35,000, sodium hydroxide, Nile red, Orlistat®, glucose, isopropanol, Triton X-100, agarose, trypan blue, 3-(4,5-Dimethylthiazol-2-yl)-2,5-diphenyltetrazolium bromide (MTT), dimethyl sulfoxide, trypsin-EDTA, and monobasic sodium phosphate were

purchased from Sigma-Aldrich (St. Louis, MO, USA). Absolute ethanol was obtained from Scharlab (Sentmenat, Spain). 10% heat-inactivated FBS was obtained from Biochrom (Berlin, Germany). 1% penicillin/streptomycin 100X was from Biowest (Riverside, MO, USA). NEAA (non-essential amino acids) 100X were purchased from Gibco (Amarillo, TX, USA). DMEM with Ultraglutamin was from Lonza (Basilea, Switzerland). Human colon adenocarcinoma cells (Caco-2) were purchased from American Type Culture Collection (ATCC, United States). Mucus-producing cells (HT29-MTX) were kindly provided by Dr. T. Lesuffleur (INSERM U178, Villejuif, France). Isoflurane (IsoVet®) was from Braun (Kronberg, Germany). Sodium chloride, trifluoroacetic acid (TFA) and acetonitrile (HPLC grade) were from Merck (Darmstadt, Germany). Lumogen® F Red was provided by BASF (Ludwigshafen, Germany). European bacteriological agar and peptone were acquired from Laboratorios Conda (Madrid, Spain). 96-well plates and T75 flasks were purchased from Corning Inc., (Steuben County, NY, USA). "Insulin Enzyme Immunoassay Kit" was purchased from Arbor Assays (Ann Arbor, MI, USA).

6.2.2. Preparation of nanoparticles

6.2.2.1. Preparation of bare nanoparticles loaded with insulin (I-NP)

A desolvation procedure previously described (Reboredo et al., 2021) was followed to prepare zein nanoparticles, with minor modifications. Briefly, 20 mL of a hydroalcoholic solution (61% pure ethanol in water) was used to dissolve 200 mg zein and 30 mg lysine, under magnetic stirring during 10 min. In parallel, 20 mg insulin was dissolved in 2 mL of slightly acidulated water (HCl 10 mM). Both solutions were mixed and, after 10 min of incubation, the desolvation step of zein was induced by the addition of 20 mL purified water. Afterwards, ethanol was removed using a rotatory evaporator (Büchi Rotavapor R-144; Büchi, Postfach, Switzerland) and the suspension of nanoparticles was purified by tangential flow filtration using a membrane with a molecular weight cutoff of 500 kDa (Repligen, Rancho Dominguez, CA, USA). Finally, the suspension of nanoparticles was dried in a Büchi Mini Spray Dryer B-290 apparatus (Büchi Labortechnik AG, Switzerland). The drying conditions in the spray-dryer were as follows: (i) inlet temperature, 90 °C; (ii) outlet temperature, 45–50 °C; (iii) air pressure, 4–6 bar; (iv) pumping rate, 5 mL/min; (v) aspirator, 80%; and (vi) airflow, 400–500 L/h.

Empty nanoparticles (NP), used as controls for some experiments, were prepared in the same way but in the absence of insulin.

6.2.2.2. Preparation of insulin-loaded PEG-coated nanoparticles (I-NP-PEG)

The coating of the nanoparticles with poly(ethylene glycol) 35,000 was achieved by incubation of the just-formed nanoparticles, prior to the purification step. For this purpose, 100 mg/mL stock solution of PEG in water was prepared, and 1 mL of this stock was added to the suspension of nanoparticles. The mixture was incubated for 30 min under magnetic stirring at room temperature. Then, nanoparticles were purified and dried as described above.

Control PEG-coated nanoparticles (NP-PEG), in absence of insulin, were prepared in the same way as described above.

6.2.2.3. Preparation of nanoparticles fluorescently labeled with Lumogen® F Red 305
For the fluorescently labeling of nanoparticles, 2.6 mL of a solution of Lumogen® Red (0.4 mg/mL in ethanol) were added to the hydroalcoholic solution of zein and lysin and the mixture was magnetically agitated during 10 min at RT. Then, the desolvation and drying steps were conducted as aforementioned.

6.2.3. Characterization of the physico-chemical properties of the resulting nanoparticles

6.2.3.1. Mean size, PDI (polydispersity index), ζ-potential, and total process Yyield
The particle size, PDI and zeta potential of the resulting formulations were assessed in a Zetasizer analyzer system (Brookhaven Instruments Corporation, Holtsville, NY, USA), after dispersion of the dried powder of nanoparticles in water. The yield of the complete process was calculated by gravimetry (Arbós et al., 2002).

6.2.3.2. Morphology evaluation
The surface morphology and the shape of the nanoparticles were examined by scanning electron microscopy (SEM). 1.5 mg of dried nanoparticles were dispersed in 1 mL ultrapure water, mounted on SEM grids and allowed to dry overnight at room temperature. Then, the samples were coated with a gold layer using a Quorum Technologies Q150R S sputter-coated (Ontario, Canada) and images were obtained using a ZEISS Sigma 500 VP FE-SEM apparatus.

6.2.3.3. Assessment of the surface hydrophobicity of the nanoparticles
The evaluation of the surface hydrophobicity of the resulting nanoparticles was performed following the Rose Bengal method (Doktorovova et al., 2012) with minor modifications. In brief, 500 μL-aliquots of nanoparticle suspensions at different concentrations (ranging from 0.03 to 3 mg/mL) were mixed with 1 mL of an aqueous solution of Rose Bengal dye (100 μg/mL). Then, the mixtures were incubated for 30 min at 25 °C and 1500 rpm shaking in a Labnet VorTemp 56 EVC (Labnet International Inc., NJ, USA). Afterwards, samples were centrifuged for 30 min at 13,500× g in a centrifuge MIKRO 220 (Hettich, Germany) and the supernatants were collected. The amount of Rose Bengal (Rose Bengal unbound) was calculated by the measurement of the absorbance at 548 nm, using a PowerWave XS Microplate reader (BioTek Instruments Inc., Winooski, VT, USA). The calculations carried out for the determination of the surface hydrophobicity are as follows:

The total surface area (TSA) of the nanoparticles was calculated assuming that the nanoparticles were completely spherical in shape and monodisperse, whose diameter is equal to the mean size determined by DLS.

$$TSA = (SANP) \times (NTNP) \qquad \text{[Equation 1]}$$

In which SANP corresponds to the surface area of a single nanoparticle ($4\pi r^2$), and NTNP represents the total number of nanoparticles present in the dilution, calculated with Equation (2):

$$NTNP = mNP/(\rho zein \times VNP) \quad \text{[Equation 2]}$$

where mNP is the mass of nanoparticles present in the dilution, ρzein corresponds to the density of zein (1.41 g/mL) calculated by pycnometry (Martínez-López et al., 2021b) and VNP represents the volume of a single nanoparticle, calculated using as diameter value the mean size obtained in the Zetasizer.

The hydrophobicity of the formulation was determined by the slope of the line obtained by the representation of the TSA (X axis) against the partitioning quotient (PQ) (Y axis), where PQ is the quotient between the amount of Rose Bengal bound and unbound. The higher the slope of the line, the higher the hydrophobicity of the formulation.

6.2.3.4. Nanoparticles surface evaluation by fourier transform infrared resonance (FTIR)
The Fourier transform infrared spectroscopy (FTIR) spectra of the nanoparticles were obtained using a Fourier transform spectrophotometer IR Affinity-1S (Shimadzu, Japan) coupled to a Specac Golden Gate ATR. For that purpose, a small amount of powder of nanoparticles was placed over the diamond and the reflectance spectra were obtained scanning from 600 to 4000 cm^{-1} at 2 cm^{-1} of resolution, and 50 scans per spectrum. Then, the Labsolution IR software was used to analyze the spectra.

6.2.4. Insulin analysis

6.2.4.1. Insulin payload and encapsulation efficiency
The insulin loading of the resulting nanoparticles was quantified by ELISA. For this purpose, nanoparticles were dissolved in ethanol 70% and diluted with purified water until a theoretical concentration of 600 pg/mL insulin. Afterwards, the quantification was carried out following the specifications described by the manufacturer. The payload was expressed as the amount of insulin (µg) per milligram of nanoparticles and, the encapsulation efficiency (EE, expressed as a percentage), was calculated as the quotient between the amount of insulin quantified and the total amount of insulin added for the formulation of the nanoparticles.

6.2.4.2. In vitro release studies
Insulin release studies from the nanoparticles were performed in simulated gastric fluid (SGF; pH 1.2) and simulated intestinal fluid (SIF; pH 6.8). For this purpose, 5 mL of aqueous suspensions of nanoparticles (10 mg/mL) were placed into Float-A-lyzer® devices with a molecular weight cutoff of 300 kDa (Spectrum Labs, Breda, Netherlands). Then, the devices were placed in vessels containing 45 mL SGF and kept for 2 h under magnetic agitation. After 2 h of incubation in SGF, the devices were transferred to other vessels containing 45 mL SIF and incubated for 24 h. The whole experiment was carried out at 37 °C. At determined times, 200 µL were withdrawn and replaced with 200 µL fresh medium. Samples were analyzed by HPLC.

The amount of insulin was quantified in an Agilent model 1200 series (Agilent Technologies, Waldbronn, Germany), coupled with a photodiode array detection system at 240 nm. A Jupiter column (5 µm C18 300 A, 150 × 4.6 mm; Phenomenex, California, United States) was used as stationary phase, whereas the mobile phase was composed

of an isocratic mixture of acetonitrile and 0.1% trifluoroacetic acid in water (7:3 by vol.). The flow rate was 0.8 mL/min and the temperature of the column was set to 25 °C. The calibration curve was performed using 8 different insulin solutions with concentrations ranging from 7 to 1000 µg/mL (1000, 500, 250, 125, 62.5, 31.25, 15.62 and 7.8 µg/mL). Good linearity (R2 = 0.9994) was obtained in the studied range. Under these conditions, the detection limit for insulin quantification was found to be 7 µg/mL.

6.2.5. Cellular studies

6.2.5.1. Caco-2 cell culture

The human colon carcinoma cell line Caco-2 was used as a model of the intestinal epithelial cell due to its property of forming a monolayer of polarized cells with the phenotype of the small intestine (Lechanteur et al., 2017). Moreover, epithelial cells represent the most abundant type of cell in the gastrointestinal tract. Caco-2 cells were incubated at 37 °C in a 5% CO^2/95% O^2 atmosphere and 90% relative humidity in an incubator (ESCO CelCulture® CO^2 incubator, Singapore). Cells were cultured in Dulbecco's Modified Eagle Medium with Ultraglutamine (DMEM ATCC) supplemented with 10% heat-inactivated fetal bovine serum (FBS), 1% (v/v) penicillin/streptomycin (100 U/mL and 100 µg/mL, respectively) and 1% (v/v) non-essential amino acids (NEAA). Cell passages were performed once a week with trypsin-EDTA (0.25%, 0.05%) and seeded in 75 cm^2 flasks at a density of 4×10^5 cells/flask. The medium was changed every two days.

6.2.5.2. HT29-MTX cell culture

The mucus-secreting HT29-MTX cell line was used as model of intestinal goblet cells due to their phenotypical similarities. In addition, mucus-secreting cells correspond to the second most abundant population of cells in the gastrointestinal tract (Hilgendorf et al., 2000). HT29-MTX cells were maintained at 37 °C in a 5% CO^2/95% O^2 atmosphere and 90% relative humidity in an incubator (ESCO CelCulture® CO^2 incubator, Singapore). Cells were cultured in Dulbecco's Modified Eagle Medium (DMEM) supplemented with 10% FBS, 1% penicillin/streptomycin and 1% NEAA. The medium was changed every two days and cells were subcultured once a week with trypsin-EDTA at a density of 4×10^5 cells/75 cm^2 flask.

6.2.5.3. Cytotoxicity evaluation

The potential cytotoxic effect of insulin-loaded nanoparticles was assessed against Caco-2 (passage 70–75) and HT29-MTX (passage 45–50) cell lines using the MTT procedure. Both cell lines were separately grown in culture flasks with the complete medium, as described before. Cells were detached from the flask, seeded into 96-well plates at 20,000 cells/well for Caco-2 and 10,000 for HT29-MTX cell lines, and incubated for 24 h. Afterwards, the medium was removed, and cells were washed twice with phosphate-buffered saline (PBS) prior to the addition of different concentrations (1.7–70 µg/mL) of insulin loaded into nanoparticles dispersed in fresh medium without FBS supplementation. A positive control without nanoparticles, and a negative control of Triton X-100 (1%) were also added. After 24 h of incubation, the media were removed,

and cells were washed twice with PBS. Then, the MTT solution (0.5 mg/mL in cell-culture medium) was added to each well and incubated for 4 h in a dark environment. Subsequently, the MTT solution was removed and 200 µL DMSO was added to each well in order to solubilize formazan crystals. Plates with DMSO were shaken in an orbital shaker for 15 min at room temperature and covered from light. Then, the absorbances were measured in a plate reader (Biotek Synergy 2, Winooski, VT, USA) at 570 and 630 nm wavelength. The cell viability was calculated according to the following equation:

$$Cell\ viability\ (\%) = \frac{\text{sample value} - \text{negative control}}{\text{positive control} - \text{negative control}} \times 100 \qquad \text{[Equation 3]}$$

6.2.6. In vivo evaluation of insulin-loaded nanoparticles in an animal model of Caenorhabditis elegans

6.2.6.1. Strain and culture conditions

Caernoharbditis elegans (*C. elegans*) was chosen as an animal model for a first-step evaluation of the suitability of insulin-loaded zein nanoparticles. *C. elegans* is a nematode sensitive to human insulin in which the hormone binds to the DAF-2 receptor and modulates its downstream signaling cascade, including fat accumulation (Lazzaro and Schneider, 2014; Martínez-López et al., 2021b). For this purpose, *C. elegans* were maintained and cultured as described previously (Martínez-López et al., 2021b). The Wild-type N2 Bristol strain was obtained from the Caenorhabditis Genetics Center (CGC, University of Minnesota, MN), and was cultured at 20 °C on NGM (Nematode Growth Medium) agar, with Escherichia coli OP50 as a normal nematode diet. For all experiments, age-synchronized worms were obtained by bleaching with hypochlorite, a condition in which only eggs can survive. Recovered eggs were left to hatch overnight in an M9 buffer solution.

6.2.6.2. Nanoparticles intake

To evaluate the intake of nanoparticles by the worms, Lumogen® red-loaded nanoparticles were supplemented to the growth medium of *C. elegans*. After the preparation of the NGM plates, a suspension of fluorescent nanoparticles was added and let dry. Afterwards, 50 µL of a culture of OP50 were added over the solid NGM plates supplemented with the nanoparticles and let dry in darkness overnight. About 500 adult (L4 stage) worms were placed onto each plate and incubated for 2 h at 20 °C. After the incubation time, worms were collected and fixed with agarose over glass slides. Agarose was prepared at a 2% concentration (w/v) and supplemented with 1% sodium azide to kill the worms during fixation. Glass slides containing the fixed worms were observed with a Nikon eclipse 80i epi-fluorescent microscope. Two different filters were used to observe the glass slides: the rhodamine filter, to visualize the Lumogen®-loaded nanoparticles, and the DAPI filter to observe the whole body of the worms (*C. elegans* shows autofluorescence under the DAPI filter).

6.2.6.3. In vivo efficacy of the nanoparticles in C. elegans

The evaluation of the efficacy of insulin-loaded nanoparticles was performed by the quantification of the fat tissue inside the worm, as described previously (Lucio et al., 2017). The assays were carried out in triplicates in 6-well plates containing 4 mL glucose-supplemented NGM (0.5% w/v) per well. The insulin treatment (free or nanoencapsulated) was added at a concentration of 50 μg/mL in NGM. Treatments of empty nanoparticles (NP and NP-PEG) were also added to evaluate the effect of the vehicle itself. A positive control of Orlistat® (6 μg/mL), as a fat-reducing agent, was employed.

L1 larvae worms were transferred into the wells containing the NGM supplemented with treatments and were allowed to grow until the L4 larvae stage (approximately 46 h). Afterwards, worms were harvested and washed with 0.01% triton-X in phosphate-buffered saline (PBST). Washed worms were fixed with 40% isopropanol and stained by the addition of Nile Red solution (3 μg/mL) and incubation for 30 min at room temperature with soft rocking. Finally, stained worms were fixed in 2% agarose over glass slides. Images of the worms were obtained using a Nikon's SMZ18 stereomicroscope (Nikon Instruments Inc., Japan) attached to a DS-FI1C refrigerated color digital camera and an epi-fluorescence system. For the acquisition of the images, a GFP filter was used (Ex 480–500; DM 505; BA 535–550). The post-acquisition processing of the images and the fat quantification were carried out using the FIJI (image J) software.

6.2.7. In vivo evaluation of insulin-loaded nanoparticles in diabetic rats

6.2.7.1. Strain and housing conditions

Healthy male Wistar rats were purchased from Envigo (Indianapolis, USA) with a weight in the range of 180–220 g. They were housed with 12-h dark/light cycles under controlled temperature (23 ± 2 °C) and with free access to food and water. Upon arrival, animals were allowed to acclimate at least for one week before any manipulation. During the procedures, animals had free access to water but were deprived of food. All the manipulations were carried out following an approved protocol by the "Ethical and Biosafety Committee for Research on Animals" from the University of Navarra, following the European legislation on animal experimentation (protocol 063-20).

6.2.7.2. Induction of diabetes

Diabetes was induced by a single intraperitoneal injection of streptozotocin (80 mg/kg) to overnight fasted animals (Inchaurraga et al., 2020). For that purpose, streptozotocin was dissolved in 0.1 M citrate buffer (pH 4.5). After 5–8 days, rats with frequent urination and fasting blood glucose levels higher than 250 mg/dL were considered as diabetic and, thus, randomized for further studies.

6.2.7.3. Efficacy evaluation

The efficacy evaluation was carried out in diabetic rats fasted for 12 h prior to any administration. All the administrations were performed through oral gavage by using a stainless-steel cannula, except otherwise stated. Animals were divided into the

following four groups (n = 6): (i) control animals receiving 1 mL purified water; (ii) I-NP group, receiving a suspension of bare nanoparticles loaded with insulin, dispersed in purified water, at a dose of 50 IU/kg; (iii) I-NP-PEG group, receiving a suspension of insulin-loaded PEG-coated nanoparticles, dispersed in purified water, at a dose of 50 IU/kg; (iv) Ins sc group, receiving a subcutaneous administration of an aqueous solution of insulin at a dose of 5 IU/kg.

Blood samples were collected from the tail vein in isoflurane-anesthetized animals. Samples were collected prior to the administration of the treatments, to establish the glucose baselines, and at fixed times after the administration. At every extraction point, blood glucose levels were analyzed with an Accu-Check® Aviva glucometer (Roche Diagnostics, Basel, Switzerland). Insulin levels in blood were quantified using an ELISA kit.

6.2.7.4. Pharmacokinetic and pharmacodynamic analysis

The hypoglycemic effect was estimated by calculating the area above the curve (AAC_{0-6h}) from the blood glucose curves. The calculation was carried out by using the trapezoidal method, calculated using the PKsolver software (Zhang et al., 2010). The relative pharmacological availability (PA) was calculated as the percentage of the hypoglycemic effect induced by the formulations compared to the sc insulin (Equation 3) AAC_{oral}

$$\mathrm{PA} = \frac{\mathrm{AAC\ oral} \times \mathrm{Dose\ sc}}{\mathrm{AAC\ sc} \times \mathrm{Dose\ oral}} \times 100 \qquad \text{[Equation 4]}$$

The main pharmacokinetic parameters (C_{max}, T_{max} and area under the curve (AUC_{0-6h})) were calculated from the representation of the serum insulin levels vs time, again using the PKsolver software. The relative bioavailability of oral formulations (Fr) was calculated as the percentage of AUC of oral formulations compared to the subcutaneous injection.

6.2.8. Statistical analysis

For statistical analyses, the means and standard errors of each data set were calculated. The comparisons between groups were carried out using a one-way ANOVA test followed by a multiple comparison test (Tukey–Kramer test), except for pharmacokinetic and pharmacodynamic studies in which t-student was used to compare I-NP to I-NP-PEG. Significant differences are marked as follows: * $p < 0.05$, ** $p < 0.01$ or *** $p < 0.001$. All calculations were performed using GraphPad Prism v6 (GraphPad Software, San Diego, CA, USA) and the curves were plotted with the Origin 8 software (OriginLab Corp, Northampton, MA, USA).

6.3. Results

6.3.1. Characterization of nanoparticles

Table 1 summarizes the main physicochemical properties of empty and insulin-loaded nanoparticles. Zein nanoparticles, containing insulin, were obtained by desolvation and, eventually, “decorated” by incubation with PEG 35,000. Then, the nanoparticles were

purified and dried. The encapsulation of insulin increased the mean size of the resulting nanoparticles (from about 230 nm to 270 nm) and decreased the negative zeta potential (from −54 mV to −39 mV). In a similar way, the coating of nanoparticles with PEG 35,000 did not importantly affect the size or the zeta potential of the resulting nanoparticles, compared to bare ones (Table 1). The insulin loading was calculated to be close to 80 µg/mg nanoparticles. Again, the coating of nanoparticles with PEG 35,000 did not modify their insulin payload.

Table 1. Physico-chemical characteristics of empty (NP and NP-PEG) and insulin-loaded nanoparticles (I-NP and I-NP-PEG). Data expressed as mean ± S.D. (n ≥ 3).

Formulation	Size (nm)	PDI	Zeta Potential (mV)	Insulin Payload (µg/mg)	EE (%)
NP	239 ± 19	0.17 ± 0.07	−56.7 ± 3.4	-	-
NP-PEG	222 ± 19	0.14 ± 0.07	−51.2 ± 1.8	-	-
I-NP	277 ± 14	0.17 ± 0.06	−39.4 ± 0.2	76.1 ± 2	77.3 ± 3
I-NP-PEG	263 ± 19	0.15 ± 0.05	−38.9 ± 2.3	81.1 ± 6	84.8 ± 3

The surface morphology and shape of insulin-loaded nanoparticles, evaluated by SEM, are shown in Figure 1. Both types of nanoparticles were spherical in shape but with differences in surface morphology. While bare nanoparticles (I-NP) showed a rough surface, PEG-coated nanoparticles showed a smooth surface, without perceptible irregularities.

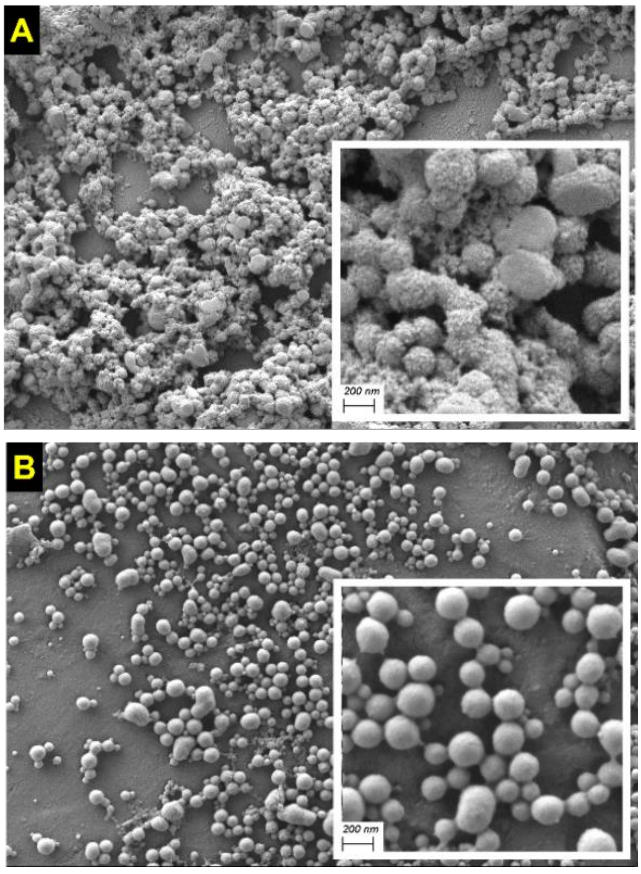

Figure 1. SEM microphotographs of insulin-loaded nanoparticles. A: bare nanoparticles (I-NP); B: PEG-coated nanoparticles (I-NP-PEG). White squares are magnifications of the nanoparticles, in which the scale bar corresponds to 200 nm.

The surface hydrophobicity of the nanoparticles, calculated by the Rose Bengal test, is shown in Figure 2. Interestingly, the encapsulation of insulin in bare nanoparticles increased the hydrophobicity of the resulting nanoparticles (Figure 2; $p < 0.05$). On the contrary, the incorporation of insulin in PEG-coated nanoparticles did not significantly modify their hydrophobicity, when compared to empty NP-PEG.

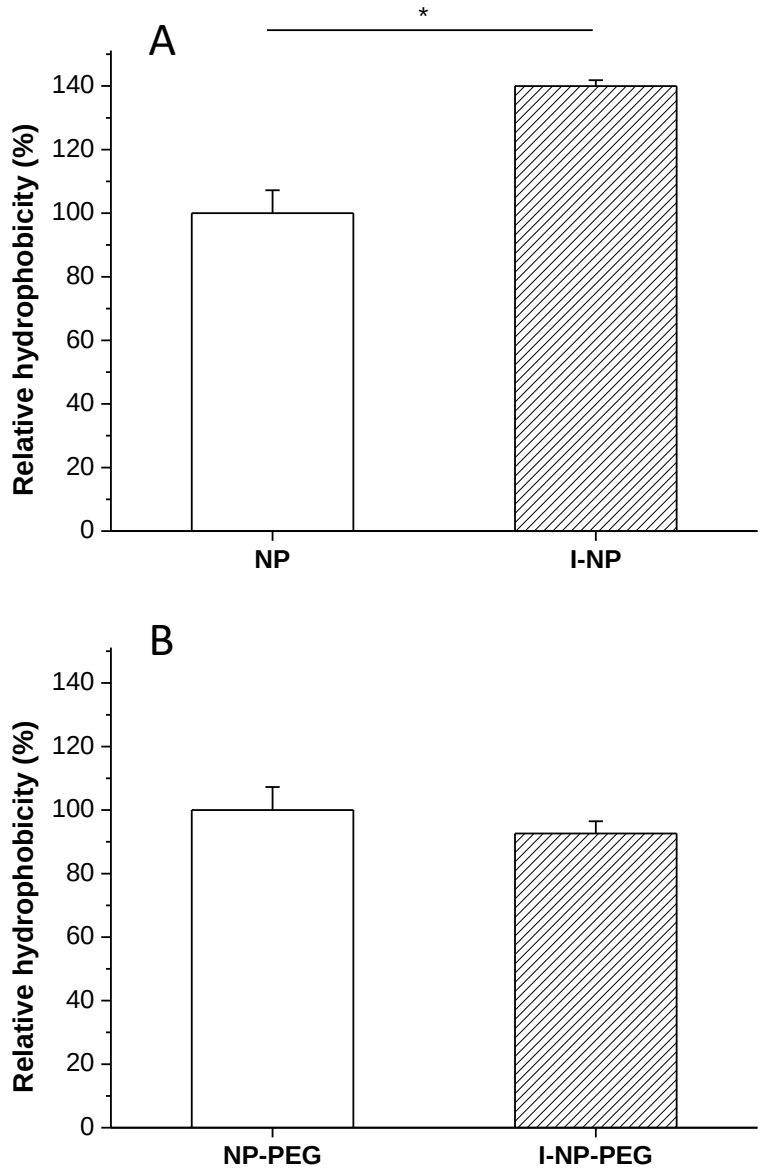

Figure 2. Surface hydrophobicity of A: empty and insulin-loaded bare nanoparticles (NP and I-NP); B: empty and insulin-loaded PEG-coated nanoparticles (NP-PEG and I-NP-PEG). Values are normalized to the hydrophobicity of the empty formulation (NP or NP-PEG). Data expressed as mean ± S.D. (n = 3). *: $p < 0.05$.

Figure 3 shows the FTIR spectra of the different formulations, as well as the raw materials employed for the formulation of the nanoparticles. Both proteins (zein and

insulin) displayed characteristic absorption bands corresponding to amide I, and II groups. In free zein, as well as in zein nanoparticles, a band centered at about 1647 cm^{-1} (mainly attributed to the C=O stretching vibration of amide I) was detected. In addition, the –N-H bending coupled to –C-N stretching vibration (amide II) was observed as a broad band at 1517cm^{-1}. However, in the insulin spectrum, both signals appeared as multi- shouldered broad bands centered at 1639 cm^{-1} for amide I and 1512 cm^{-1} for amide II. Regarding the amide III (combination of N-H in-plane bending and C-N vibrations), also characteristic of proteins, was observed as multiple signals (1247–1352 cm^{-1}) in the spectrum of zein nanoparticles. For insulin, the amide II band appeared as a broad band centered at 1236 cm^{-1}. It is worth noting that the spectrum of I-NP clearly showed the characteristic vibration band corresponding to insulin amide I (1639 cm^{-1}) together with the superposition of signals corresponding to insulin and zein amide II. Moreover, the appearance of multiple signals in the amide III vibration region was associated with an overlapping of signals from both proteins (insulin and zein). The slight displacement of insulin vibration bands of 1236 to 1240 cm^{-1} (among others) could be attributed to a weak interaction between insulin and zein as a result of the hormone encapsulation. In the spectrum of I-NP-PEG, insulin bands previously mentioned (mainly amide I and II) together with multiple PEG signals (1465, 1338, 1276, 1240, 1145, 1101 cm^{-1}) and those corresponding to the polymer fingerprint region (1060, 960 and 840 cm^{-1}) were presented. In addition, the displacement of some of them (e.g., 1093 cm^{-1} to 1101 cm^{-1} corresponding to PEG alcoholic group) confirmed the interaction between zein and PEG.

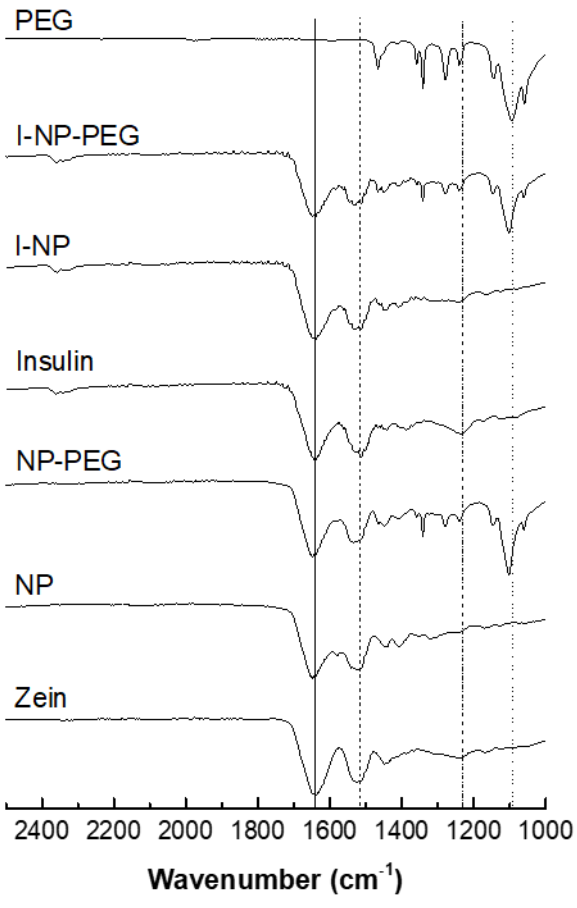

Figure 3. FTIR spectra of PEG 35,000, zein, insulin, empty zein nanoparticles uncoated (NP) and coated with PEG (NP-PEG), and insulin-loaded nanoparticles with (I-NP-PEG) and without PEG coating (I-NP). Straight line corresponds to the 1647 cm^{-1} band belonging to the amide I group; dashed line corresponds to the 1517 cm^{-1} band belonging to the amide II group; dashed-dotted line corresponds to the 1236 cm^{-1} band belonging to the amide III group; dotted line corresponds to the 1096 cm^{-1} band belonging to the alcoholic group of PEG.

6.3.2. In vitro release behavior of insulin-loaded nanoparticles

The release behavior of the formulations during their incubation in SGF and SIF is shown in Figure 4. Both formulations (I-NP and I-NP-PEG) displayed a similar release profile; although, the coating of zein nanoparticles with PEG 35,000 induced a slightly slower release rate, compared to bare nanoparticles. In SGF, after 2 h of incubation, the amount of insulin released from I-NP represented about 37% of the payload. For I-NP-PEG50, only 30% of the insulin loading was released in 2 h of incubation. When nanoparticles were transferred to the SIF, the release rate for both formulations appeared to be similar to that observed in SGF, evidencing the null effect of the pH on the release of insulin from the nanoparticles. After 22h in SIF, both formulations of nanoparticles had released the total content of the initial payload.

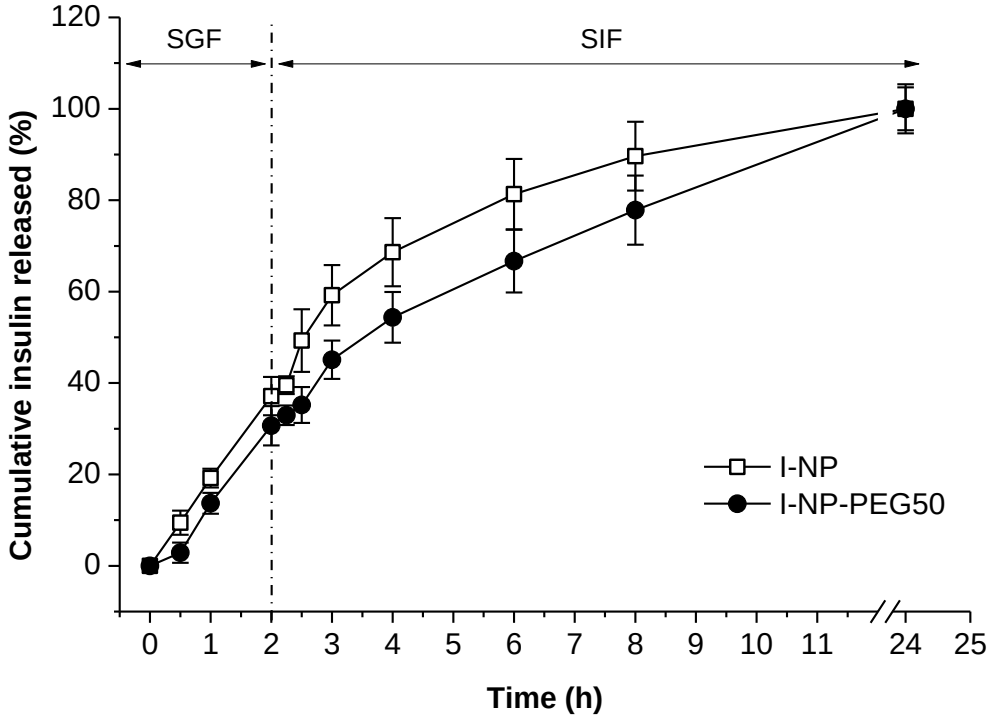

Figure 4. *In vitro* release behavior of insulin from I-NP and I-NP-PEG50 in SGF and SIF at 37 °C. Data presented as mean ± S.D. (n = 3).

6.3.3. Cytotoxicity evaluation of insulin-loaded nanoparticles

The cytotoxic effect of insulin-loaded nanoparticles (I-NP and I-NP-PEG50) over two cell lines that mimic the most predominant cell types in the intestines, Caco-2 cells (epithelial cells) and HT29-MTX cells (mucus-secreting cells), were quantified by the MTT

assay. Figure 5 displays the results of the cell viability after 24 h of incubation of the cells with either bare or PEG-coated insulin-loaded nanoparticles. After 24 h of incubation of the cell lines with the treatments, none of the formulations showed a cytotoxic effect at any of the concentrations tested, ranging from 1.7 to 70 µg/mL of insulin.

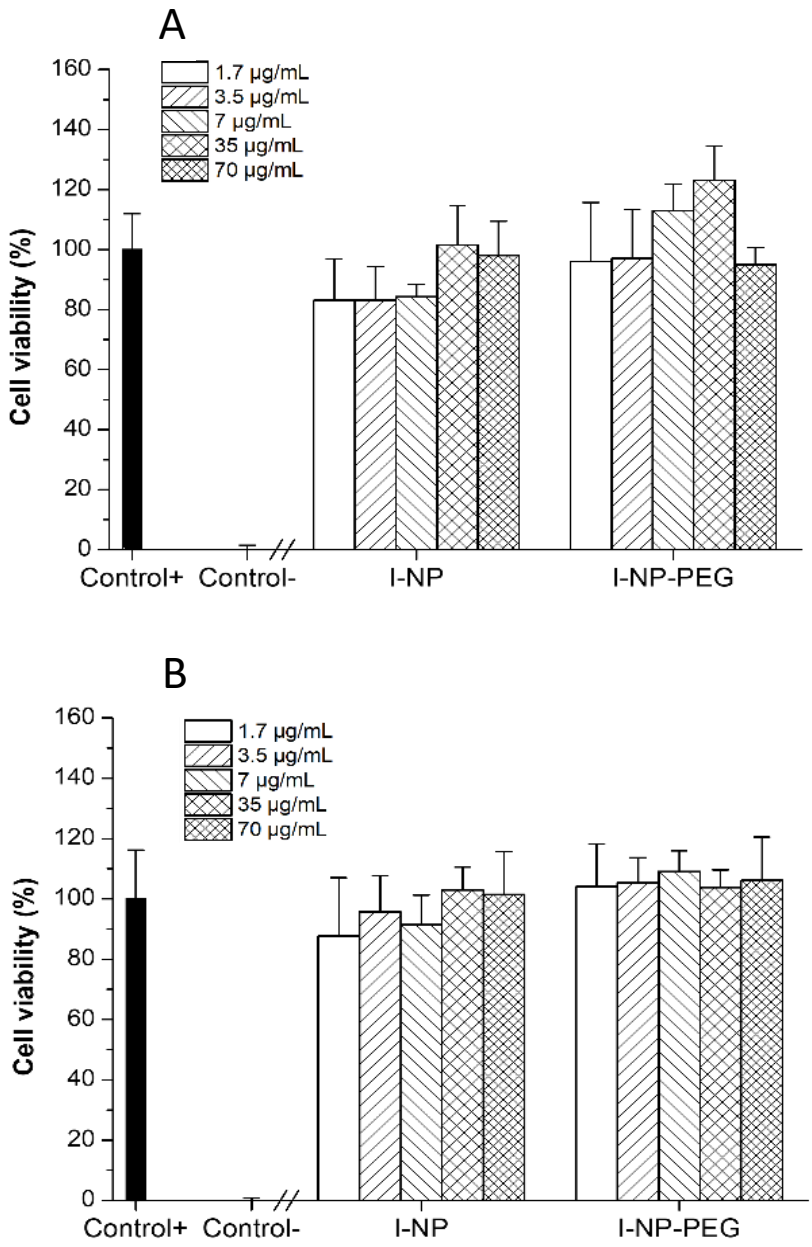

Figure 5. Effect of insulin-loaded nanoparticles (I-NP and I-NP-PEG50) on the viability of A: Caco-2 cells; B: HT29-MTX cell lines. Data presented as mean ± S.D. (n = 6).

6.3.4. Effect of insulin-loaded nanoparticles in C. elegans

The effect of insulin (free or loaded in zein nanoparticles) on the fat content of *C. elegans* grown in a medium (NGM) supplemented with glucose is presented in Figure 6. As expected, the incorporation of free insulin (50 µg/mL) to the medium induced a reduction in the fat accumulated by the worms ($p < 0.01$). This reduction was calculated to be about 15%, in comparison with control animals.

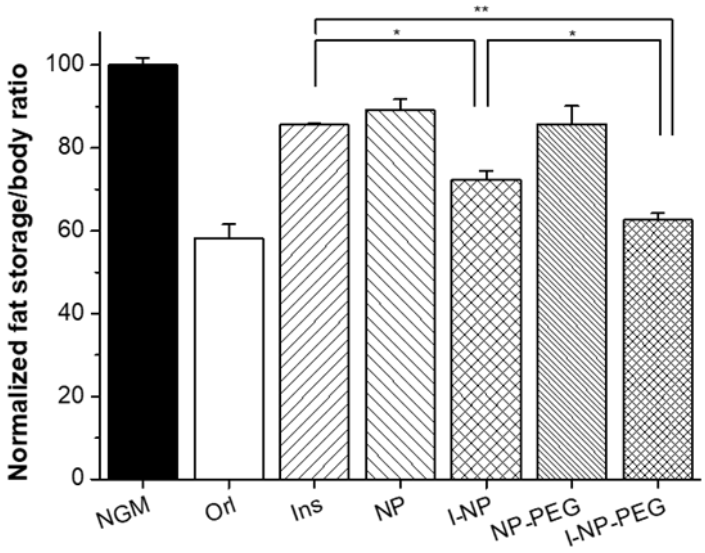

Figure 6. Effect over the fat storage of *C. elegans* cultured under high-glucose conditions of empty and insulin-loaded zein nanoparticles (coated with PEG and uncoated), as well as a solution of free insulin. Data presented as mean ± S.D. ($n \geq 75$ worms). * $p < 0.05$; ** $p < 0.01$. Orl: Orlistat®; Ins: free insulin; NP: empty bare zein nanoparticles; I-NP: insulin-loaded bare nanoparticles; NP-PEG50: empty PEG-coated nanoparticles; I-NP-PEG50: insulin-loaded PEG-coated nanoparticles.

Regarding the effect of nanoparticles, the first step was to confirm if the worms ate the nanoparticles. As presented in Figure 7, the fluorescence caused by the presence of lumogen® red in nanoparticles (incorporated in the medium in which the worms were grown) is observed all along the gastrointestinal tract of the animal. For I-NP-treated worms, the amount of fat accumulated in these animals was calculated to be about 30% lower than for control worms (NGM group in Figure 6). In a similar way, animals treated with I-NP-PEG50 displayed a reduction in their fat content close to 40%; slightly lower than the effect produced by Orlistat® (6 µg/mL; employed as positive control), which was quantified to be 42%. Another interesting fact was to evidence that empty zein nanoparticles (both bare and PEG-coated) also induced a decrease in the fat content of the worms (about 11% for NP and 14% for NP-PEG50).

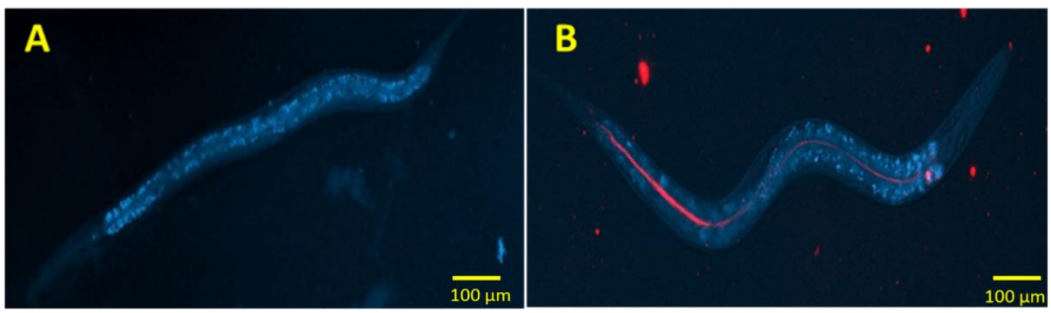

Figure 7. Fluorescence micrographs of *C. elegans*. A: self-fluorescence of a worm under DAPI filter. B: Worm fed with fluorescently-tagged nanoparticles.

6.3.5. Evaluation of the hypoglycemic activity in diabetic rats

Figure 8 shows the evolution of glycemia in animals as a function of the treatment. Animals receiving a subcutaneous injection of insulin solution (5 IU/kg) displayed a rapid decrease in blood glucose levels. Thus, 2 h post-administration, the glycemia of these animals represented 22% of the initial blood glucose levels, reaching blood glucose levels below 120 mg/dL. These low blood glucose values were maintained for at least four more hours. On the other hand, animals treated with insulin-loaded nanoparticles exhibited a slower and more sustained decrease in glycemia. Hence, one hour after the administration of I-NP and I-NP-PEG50, both groups of animals presented similar values of glucose in the blood. For later extraction points, on the one hand, animals treated with I-NP showed the same glycemic values without any relevant further reduction. This group of animals achieved a maximum decrease in the blood glucose levels of 57%, compared to initial values, displaying glycemic values close to 280 mg/dL. On the other hand, rats treated orally with I-NP-PEG50 exposed decreasing values of glycemia with time, reaching the highest decrease 6 h after the administration, with 32% of the initial values, corresponding to blood glucose levels around 170 mg/dL. Moreover, at this extraction point, the glycemic values of animals treated with I-NP-PEG50 matched the values of those treated with the subcutaneous injection of insulin.

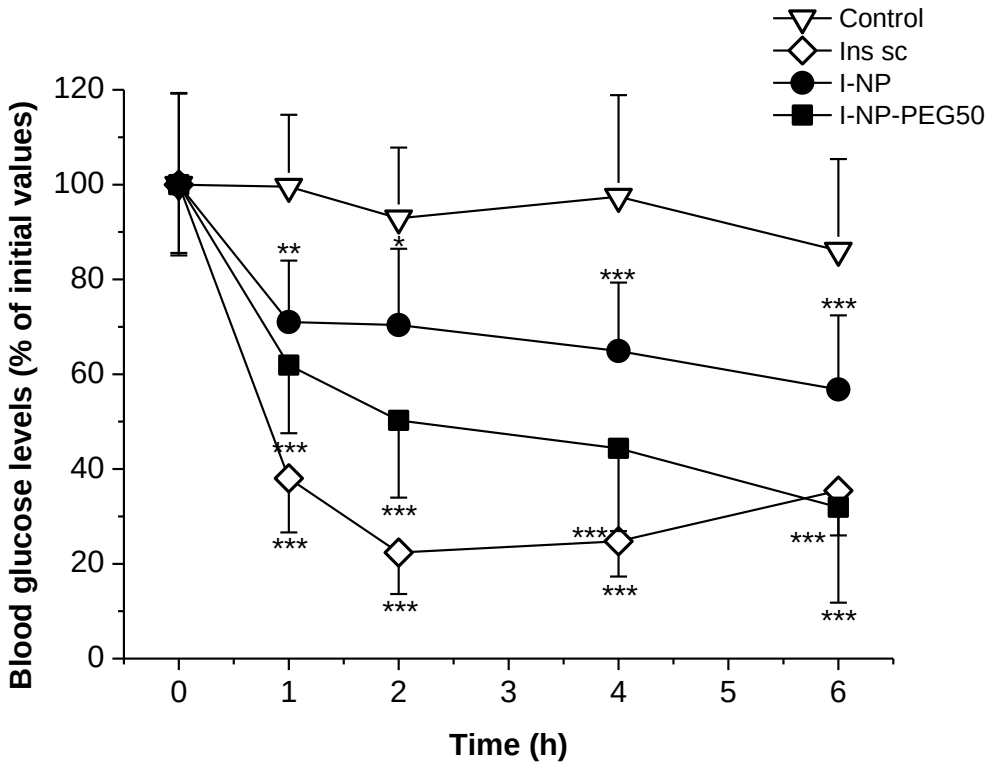

Figure 8. Blood glucose levels (% of initial values) of streptozotocin-induced diabetic rats after administration of subcutaneous solution of insulin (Ins sc; 5 IU/Kg) or oral administration of water (control), insulin-loaded bare nanoparticles (I-NP; 50 IU/Kg), or insulin-loaded PEG-coated nanoparticles (I-NP-PEG50; 50 IU/Kg). Data expressed as mean ± S.D. ($n \geq 6$). * $p < 0.05$; ** $p < 0.01$; *** $p < 0.001$, compared to control.

From the curves of glycemia over time, the main pharmacodynamic parameters were calculated (Table 2). The most remarkable finding is that the oral administration of I-NP-PEG50 decreased the blood glucose levels (C_{min}) to almost the same values as the subcutaneous injection of insulin. Furthermore, this formulation needed 2 h more to induce the maximum decrease in glycemia (T_{max}) than for animals treated with either subcutaneous insulin or with oral nanoparticles (5 h vs. 3 h, respectively). It is also important to highlight that the coating of the nanoparticles with PEG increased more than 3-fold the pharmacological availability (PA) of insulin administered in bare nanoparticles. The PA of I-NP was calculated to be 4.7% compared to the control (subcutaneous insulin) while, for I-NP-PEG50, the PA was calculated to be close to 15%.

Table 2. Main pharmacodynamic parameters after a subcutaneous administration of insulin (5 IU/kg) or after oral administration of bare nanoparticles loaded with insulin (I-NP; 50 IU/kg) or PEG-coated nanoparticles loaded with insulin (I-NP-PEG50; 50 IU/kg). AAC corresponds to the area above the glycemic curve; T_{max} corresponds to the time when the maximum effect was achieved; C_{min} corresponds to the minimum levels of glucose (as a % of the initial values) achieved; PA corresponds to the pharmacological activity. Data represent the mean ± SD ($n \geq 6$). ***: $p < 0.001$, compared to I-NP.

Treatment	Dose (IU/kg)	AAC (µg/hmL)	T_{max} (h)	C_{min} (% of Initial Values)	PA (%)
Ins sc	5	1789.8 ± 155.5	3.1 ± 0.9	22.4 ± 8.7	100
I-NP	50	845.9 ± 357.6	5.1 ± 0.9	56.7 ± 15.6	4.7 ± 1.9
I-NP-PEG50	50	1267.3 ± 297.0	5.6 ± 0.7	31.9 ± 20.1	14.9 ± 1.6 ***

Figure 9 shows the plasma levels of human insulin in rats receiving a subcutaneous administration of insulin (Ins sc; 5 IU/kg) or an oral administration of nanoencapsulated insulin (I-NP or I-NP-PEG50; 50 IU/kg). The main pharmacodynamic parameters, calculated from the insulin plasma levels, are summarized in Table 3. Animals treated with a subcutaneous dose of insulin showed the typical profile characterized by a fast rise, reaching the C_{max} during the first 2 h post-administration, achieving insulinemic values of almost 6 ng/mL. Afterwards, plasma levels of insulin decreased to almost undetectable levels after 4 h. For oral nanoencapsulated insulin, both formulations showed the same pattern, characterized by a rapid increase in the blood levels of insulin 1 h post-administration, when the insulin levels in blood were found to be around 1 ng/mL for I-NP and 2.5 ng/mL for I-NP-PEG50. The fast rise observed 1 h after the oral administration of I-NP and I-NP-PEG50 was followed by a plateau state that lasted several hours. Despite both formulations showed the same profile, PEG-coated nanoparticles produced blood levels of insulin which were about two-fold than those obtained with bare nanoparticles. As a result, the relative oral bioavailability of insulin formulated in bare nanoparticles was calculated to be 4.2%, whereas, for I-NP-PEG50, this value increased almost 2.5 times (10.2%).

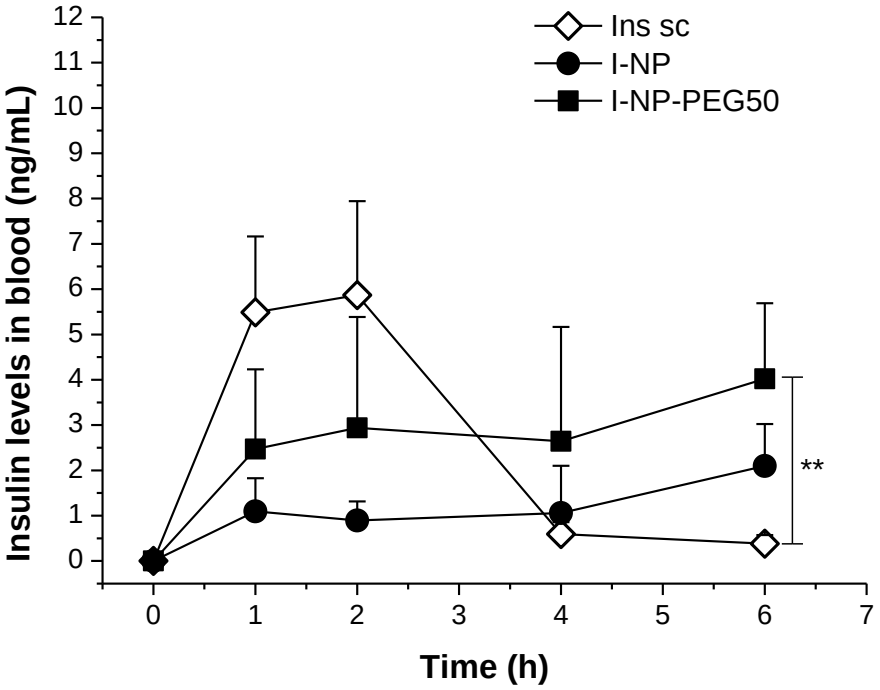

Figure 9. Serum insulin levels vs time after the subcutaneous administration of an insulin solution (Ins sc; 5 IU/Kg) or oral administration insulin-loaded bare nanoparticles (I-NP; 50 IU/Kg), or insulin-loaded PEG-coated nanoparticles (I-NP-PEG50; 50 IU/Kg). Data expressed as mean ± S.D. (n ≥ 6). **: $p < 0.01$.

Table 3. Pharmacokinetic parameters of insulin administered either subcutaneously or orally. Ins sc: subcutaneous insulin (5 IU/kg); I-NP: insulin-loaded bare nanoparticles (50 IU/kg); I-NP-PEG50: insulin-loaded PEG-coated nanoparticles (50 IU/kg); C_{max}: maximum plasma concentration; T_{max}: time when the maximum plasma levels of insulin were achieved; AUC: area under the curve; Fr%: oral bioavailability relative to subcutaneous administrations. Data expressed as mean ± SD (n = 6). *: $p < 0.05$ compared to Ins sc. **: $p < 0.01$ compared to Ins sc.

Treatment	Dose (IU/kg)	C_{max} (ng/mL)	T_{max} (h)	AUC (ng/hmL)	Fr (%)
Ins sc	5	5.87 ± 2.07	1.37 ± 0.48	15.86 ± 4.13	100
I-NP	50	2.10 ± 0.93 **	6.00 ± 0.00	6.65 ± 2.74 *	4.2
I-NP-PEG50	50	4.02 ± 1.67	5.49 ± 0.90	16.18 ± 9.76	10.2

6.4. Discussion

Orally administered therapeutic proteins and peptides need to face several biological barriers that make the oral bioavailability of the drug almost negligible. In principle, the use of nanoparticles for the oral delivery of such compounds may be an adequate approach to protect the loaded cargo against premature degradation, including the acidic conditions of the stomach, the presence of enzymes, as well as the mechanical stress in the lumen (e.g., osmotic pressure and peristalsis) (Homayun et al., 2019; Wu et al., 2019). On the other hand, the design of nanoparticles with either mucoadhesive or mucus-permeating properties may be of interest to increase the residence time of the

drug delivery system in close contact with the epithelium, improving the probabilities for insulin absorption and/or interaction with its receptor (Hall et al., 2020).
From a general point of view, protein-based nanoparticles offer some advantages for drug delivery purposes, including their biodegradability and capability to accommodate a high variety of compounds in a non-specific way (Jain et al., 2018). In this context, zein possesses some peculiarities that provide additional advantages for the formulation of nanoparticles. First, an optimal regulatory status. Second, its lipophilic character that facilitate both the preparation of stable nanoparticles, without the need for stabilization or cross-linking procedures (Inchaurraga et al., 2020), and the modification of their surface with different coating agents by simple non-covalent based procedures (Pascoli et al., 2018; Reboredo et al., 2021). Third, its lower allergenicity (Reddy and Rapisarda, 2021) and slower digestion than other proteins (Calvez et al., 2019).

In this work, zein-based nanoparticles with either mucoadhesive (NP) or mucus-permeating properties (NP-PEG50) were selected to evaluate and compare their capability to deliver insulin orally. Both types of nanoparticles (bare and PEG-coated) displayed a mean size of around 270 nm and negative zeta potential (Table 1). Noteworthy, the surface zeta potential of insulin-loaded nanoparticles was markedly less negative than empty nanoparticles, suggesting that, in the formation of insulin-loaded nanoparticles, some structural changes may happen during the insulin encapsulation. The insulin payload of the nanoparticles was calculated to be around 8%. However, the insulin release profile of PEG-coated nanoparticles has been demonstrated to be slightly slower and more sustained than for bare nanoparticles. This may be caused by the presence of the PEG coating, which generates a shell that surrounds the nanoparticle and delays the release of insulin to the outer medium. It is worth noting that the pH conditions of the SGF and SIF seemed not to affect the insulin release profiles, denoting stability of the system in both incubation media.

FTIR analysis was employed to put in evidence the presence of both insulin and PEG in their corresponding formulations. Likely, the encapsulation of inulin did not affect the coating of nanoparticles, since the displacement of the PEG bands was similar for both empty and insulin-loaded formulations (Figure 3). Zein nanoparticles do not display a shell-core structure, but a fractal-like conformation composed of 20 nm spherical blocks of zein that, during the desolvation, collide to form the nanoparticle (Lucio et al., 2017). Thus, during the formation of nanoparticles, some insulin molecules may get adhered to the surface of the nanoparticle and, hence, induce the changes in the surface hydrophobicity for I-NP observed in Figure 2.

The safety of the formulations has been evidenced by the cytotoxicity evaluation carried out in Caco-2 and HT29-MTX cells. Since our formulations are intended for oral delivery purposes, these two cell lines were selected for being widely used as a model for intestinal epithelial cells (Caco-2) (Ye et al., 2017) and intestinal goblet cells (HT29-MTX) (Reale et al., 2021). The cell viability of both cell lines has been demonstrated not to be affected by the incubation with insulin-loaded nanoparticles, either uncoated or PEG-coated. Thus, since no toxicity was observed in these cellular models, no toxic effects

would be expectable in greater animal models such as *C. elegans* or rodents receiving insulin-loaded zein nanoparticles through the oral route.

C. elegans is an animal with insulin signaling pathways highly conserved with humans. Under high-glucose conditions, these nematodes experience an expansion of the adipose tissue caused by the activation of the DAF-2 receptor (Martínez-López et al., 2021b). Likely, human insulin exerts an antagonistic effect over this receptor, blocking the metabolic pathways that lead to increased fat storage (Martínez-López et al., 2021a; Pierce et al., 2001). On the other hand, the intestine of *C. elegans* has some homologies with that of mammals (Cohen and Sundaram, 2020), including the presence of an absorptive layer of ciliated cells covered by a glycocalyx. These characteristics make this animal model an interesting instrument for the evaluation of insulin-loaded nanoparticles intended for oral administration. When the worms were treated with insulin, as expected, a decrease in the fat accumulation was observed (Figure 6). This decrease in the fat content of worms was significantly higher when insulin was administered into nanoparticles; particularly when insulin was formulated in PEG-coated nanoparticles. This observation may rely on the protection conferred by the nanoparticles against the physical and chemical digestion in the gastrointestinal tract of the worms. The superior capability of PEG-coated nanoparticles to decrease the accumulation of fat, when compared with bare nanoparticles, would be related to the increased diffusivity of the nanoparticles in mucus, facilitating their arrival to the epithelium surface (Reboredo et al., 2021).

In rats with streptozotocin-induced diabetes, the administration of a subcutaneous injection of insulin showed a fast decrease in the glycemia, reaching the lowest values at around 2–3 h post-administration. This result is in the line with others previously reported (Jin et al., 2012; Mumuni et al., 2020; Sarmento et al., 2007; Sonaje et al., 2009). On the other hand, administration of insulin-loaded nanoparticles induced a hypoglycemic effect that started 1 h post-administration and lasted for at least 5 h more, being I-NP-PEG50 significantly more potent I-NP ($p < 0.001$). This fact suggests that the capability of zein nanoparticles to effectively deliver insulin through the oral route would be directly determined by their biodistribution within the gut. While bare nanoparticles, with a mucoadhesive behavior (Martínez-López et al., 2021b), are mainly trapped in the protective mucus layer (remaining away from the absorptive epithelium), PEG-coated nanoparticles are able to diffuse through the mucus layer and reach the surface of enterocytes (Reboredo et al., 2021). Moreover, PEG-coated nanoparticles have shown the capability of reaching the cecum more rapidly than bare nanoparticles and, despite the cecum function is mainly to absorb water and small molecules, insulin can also be absorbed in this section of the gut (Chen et al., 2017; Guo et al., 2016). The arrival of nanoparticles close to the surface of the intestinal epithelium, and onsite release of the loaded hormone, would facilitate the interaction of insulin with its receptor and, thus, the absorption of the peptide through the receptor-mediated endocytosis (Hall et al., 2020). The sustained release of insulin from the nanoparticles (as observed in Figure 4) is reflected in the sustained levels of insulin in the rats' blood.

In our work, the relative oral bioavailability of insulin formulated in PEG-coated nanoparticles was calculated to be close to 10%, 2.5-fold higher than for bare nanoparticles. This oral bioavailability is higher than other values previously published with PLGA-chitosan composite nanocarriers (about 8%; (Xu et al., 2017)) or SNEDDS (about 1.8%; (Bravo-Alfaro et al., 2020)); although, it is lower (about 2-times) when compared with other previous results obtained with liposomes decorated with PEG and folic acid (19.08%; (Yazdi et al., 2020)), folate-chitosan nanoparticles (17.04%; (El Leithy et al., 2019)), or zein/caseinate-based nanoparticles co-encapsulating insulin and cholic acid (20.5%; (Bao et al., 2021)). In spite of the lower capability to promote the oral absorption of insulin, our formulation offers some interesting advantages that may facilitate a translational approach; particularly in those aspects related to the scale-up of a reproducible process (including the drying step) and the simplification of non-clinical toxicity assessments of the regulatory dossier. Among others, PEG-coated zein nanoparticles may be obtained in a simple and scalable preparative process that only requires the use of pharmaceutical acceptable reagents and solvents (ethanol and water) and allows the generation of a powder formulation, easily dispersible in water, with a high insulin payload. Furthermore, as described previously (Reboredo et al., 2021), PEG-coated zein nanoparticles do not enter the systemic circulation minimizing a possible accumulation in the body and toxicological issues.

In summary, zein nanoparticles can be used to encapsulate insulin and produce (through a simple and reliable method) cheap, safe, and efficient nanocarriers for oral delivery purposes that would protect the cargo in the harsh conditions of the gut after an oral administration. The resulting nanoparticles display an appropriate size and surface zeta potential, with high entrapment efficiencies. Moreover, the coating of insulin-loaded nanoparticles with a hydrophilic polymer (PEG) did not alter the physicochemical properties of the nanoparticles and led to a significant increase in the oral bioavailability of insulin and a more potent hypoglycemic effect. Thus, this type of nanocarrier might be a suitable tool for the effective delivery of insulin through the oral route.

6.5. References

Ahmad, A., Othman, I., Zaini, A., Chowdhury, E.H., 2012. Oral Nano-Insulin Therapy: Current Progress on Nanoparticle-Based Devices for Intestinal Epithelium-Targeted Insulin Delivery. J. Nanomed. Nanotechnol. s4. https://doi.org/10.4172/2157-7439.s4-007

Arbós, P., Arangoa, M.A., Campanero, M.A., Irache, J.M., 2002. Quantification of the bioadhesive properties of protein-coated PVM/MA nanoparticles. Int. J. Pharm. 242, 129–136. https://doi.org/10.1016/S0378-5173(02)00182-5

Bao, X., Qian, K., Yao, P., 2021. Insulin- And cholic acid-loaded zein/casein-dextran nanoparticles enhance the oral absorption and hypoglycemic effect of insulin. J. Mater. Chem. B 9, 6234–6245. https://doi.org/10.1039/d1tb00806d

Ben Lulu, S., Coran, A.G., Mogilner, J.G., Shaoul, R., Shamir, R., Shehadeh, N., Sukhotnik, I., 2010. Oral insulin stimulates intestinal epithelial cell turnover in correlation with insulin-receptor expression along the villus-crypt axis in a rat model of short bowel syndrome. Pediatr. Surg. Int. 26, 37–44. https://doi.org/10.1007/s00383-009-2520-x

Bravo-Alfaro, D.A., Muñoz-Correa, M.O.F., Santos-Luna, D., Toro-Vazquez, J.F., Cano-Sarmiento, C., García-Varela, R., García, H.S., 2020. Encapsulation of an insulin-modified phosphatidylcholine complex in a self-nanoemulsifying drug delivery system (SNEDDS) for oral insulin delivery. J. Drug Deliv. Sci. Technol. 57, 101622. https://doi.org/10.1016/j.jddst.2020.101622

Brown, T.D., Whitehead, K.A., Mitragotri, S., 2020. Materials for oral delivery of proteins and peptides. Nat. Rev. Mater. 5, 127–148. https://doi.org/10.1038/s41578-019-0156-6

Calvez, J., Benoit, S., Fleury, L., Khodorova, N., Piedcoq, J., Tomé, D., Airinei, G., Ben-Amouzig, R., Gaudichon, C., 2019. True Ileal Protein Digestibility of Zein and Whey Protein Isolate in Healthy Humans (OR27-06-19). Curr. Dev. Nutr. 3. https://doi.org/10.1093/CDN/NZZ046.OR27-06-19

Chen, S., Guo, F., Deng, T., Zhu, S., Liu, W., Zhong, H., Yu, H., Luo, R., Deng, Z., 2017. Eudragit S100-Coated Chitosan Nanoparticles Co-loading Tat for Enhanced Oral Colon Absorption of Insulin. AAPS PharmSciTech 18, 1277–1287. https://doi.org/10.1208/s12249-016-0594-z

Cohen, J.D., Sundaram, M. V., 2020. C. Elegans apical extracellular matrices shape epithelia. J. Dev. Biol. 8, 1–26. https://doi.org/10.3390/jdb8040023

Doktorovova, S., Shegokar, R., Martins-Lopes, P., Silva, A.M., Lopes, C.M., Müller, R.H., Souto, E.B., 2012. Modified Rose Bengal assay for surface hydrophobicity evaluation of cationic solid lipid nanoparticles (cSLN). Eur. J. Pharm. Sci. 45, 606–612. https://doi.org/10.1016/j.ejps.2011.12.016

El Leithy, E.S., Abdel-Bar, H.M., Ali, R.A.M., 2019. Folate-chitosan nanoparticles triggered insulin cellular uptake and improved in vivo hypoglycemic activity. Int. J. Pharm. 571, 118708. https://doi.org/10.1016/j.ijpharm.2019.118708

Fonte, P., Araújo, F., Silva, C., Pereira, C., Reis, S., Santos, H.A., Sarmento, B., 2014. Polymer-based nanoparticles for oral insulin delivery: Revisited approaches. Biotechnol. Adv. 33, 1342–1354. https://doi.org/10.1016/j.biotechadv.2015.02.010

Frizzell, H., Woodrow, K.A., 2020. Biomaterial Approaches for Understanding and Overcoming Immunological Barriers to Effective Oral Vaccinations. Adv. Funct. Mater. 30, 1907170. https://doi.org/10.1002/adfm.201907170

Guo, F., Zhang, M., Gao, Y., Zhu, S., Chen, S., Liu, W., Zhong, H., Liu, J., 2016. Modified nanoparticles with cell-penetrating peptide and amphipathic chitosan derivative for enhanced oral colon absorption of insulin: preparation and evaluation. Drug Deliv. 23, 2003–2014. https://doi.org/10.3109/10717544.2015.1048489

Hall, C., Yu, H., Choi, E., 2020. Insulin receptor endocytosis in the pathophysiology of insulin resistance. Exp. Mol. Med. 52, 911–920. https://doi.org/10.1038/s12276-020-0456-3

Hilgendorf, C., Spahn-Langguth, H., Regårdh, C.G., Lipka, E., Amidon, G.L., Langguth, P., 2000. Caco-2 versus Caco-2/HT29-MTX co-cultured cell lines: Permeabilities via diffusion, inside- and outside-directed carrier-mediated transport. J. Pharm. Sci. 89, 63–75. https://doi.org/10.1002/(SICI)1520-6017(200001)89:1<63::AID-JPS7>3.0.CO;2-6

Hirlekar, R.S., Patil, E.J., Bhairy, S.R., 2017. Oral insulin delivery: Novel strategies. Asian J. Pharm. 11, S434–S443.

Homayun, B., Lin, X., Choi, H.J., 2019. Challenges and recent progress in oral drug delivery systems for biopharmaceuticals. Pharmaceutics 11. https://doi.org/10.3390/pharmaceutics11030129

Hwang, S.R., Byun, Y., 2014. Advances in oral macromolecular drug delivery. Expert Opin. Drug Deliv. 11, 1955–1967. https://doi.org/10.1517/17425247.2014.945420

Ibie, C.O., Knott, R.M., Thompson, C.J., 2019. Complexation of novel thiomers and insulin to protect against in vitro enzymatic degradation–towards oral insulin delivery. Drug Dev. Ind. Pharm. 45, 67–75. https://doi.org/10.1080/03639045.2018.1517776

Inchaurraga, L., Martínez-López, A.L., Martin-Arbella, N., Irache, J.M., 2020. Zein-based nanoparticles for the oral delivery of insulin. Drug Deliv. Transl. Res. 10, 1601–1611. https://doi.org/10.1007/s13346-020-00796-3

Irache, J.M., Esparza, I., Gamazo, C., Agüeros, M., Espuelas, S., 2011. Nanomedicine: Novel approaches in human and veterinary therapeutics. Vet. Parasitol. 180, 47–71. https://doi.org/10.1016/j.vetpar.2011.05.028

Jain, A., Singh, S.K., Arya, S.K., Kundu, S.C., Kapoor, S., 2018. Protein Nanoparticles: Promising Platforms for Drug Delivery Applications. ACS Biomater. Sci. Eng. https://doi.org/10.1021/acsbiomaterials.8b01098

Jin, Y., Song, Y., Zhu, X., Zhou, D., Chen, C., Zhang, Z., Huang, Y., 2012. Goblet cell-targeting nanoparticles for oral insulin delivery and the influence of mucus on

insulin transport. Biomaterials 33, 1573–1582. https://doi.org/10.1016/j.biomaterials.2011.10.075

Johansson, M.E.V., Ambort, D., Pelaseyed, T., Schütte, A., Gustafsson, J.K., Ermund, A., Subramani, D.B., Holmén-Larsson, J.M., Thomsson, K.A., Bergström, J.H., Van Der Post, S., Rodriguez-Piñeiro, A.M., Sjövall, H., Bäckström, M., Hansson, G.C., 2011. Composition and functional role of the mucus layers in the intestine. Cell. Mol. Life Sci. 68, 3635–3641. https://doi.org/10.1007/s00018-011-0822-3

Langguth, P., Bohner, V., Heizmann, J., Merkle, H.P., Wolffram, S., Amidon, G.L., Yamashita, S., 1997. The challenge of proteolysis enzymes in intestinal peptide delivery. J. Control. Release 46, 39–57. https://doi.org/10.1016/S0168-3659(96)01586-6

Lazzaro, B.P., Schneider, D.S., 2014. The genetics of immunity. Genetics 197, 467–470. https://doi.org/10.1534/genetics.114.165449

Lechanteur, A., Almeida, A., Sarmento, B., 2017. Elucidation of the impact of cell culture conditions of Caco-2 cell monolayer on barrier integrity and intestinal permeability. Eur. J. Pharm. Biopharm. 119, 137–141. https://doi.org/10.1016/j.ejpb.2017.06.013

Lee, B., Moon, K.M., Kim, C.Y., 2018. Tight junction in the intestinal epithelium: Its association with diseases and regulation by phytochemicals. J. Immunol. Res. 2018, 2645465. https://doi.org/10.1155/2018/2645465

Li, L.D., Crouzier, T., Sarkar, A., Dunphy, L., Han, J., Ribbeck, K., 2013. Spatial configuration and composition of charge modulates transport into a mucin hydrogel barrier. Biophys. J. 105, 1357–1365. https://doi.org/10.1016/j.bpj.2013.07.050

Li, P., Tan, A., Prestidge, C.A., Nielsen, H.M., Müllertz, A., 2014. Self-nanoemulsifying drug delivery systems for oral insulin delivery: In vitro and in vivo evaluations of enteric coating and drug loading. Int. J. Pharm. 477, 390–398. https://doi.org/10.1016/j.ijpharm.2014.10.039

Li, R., Laurent, F., Taverner, A., Mackay, J., De Bank, P.A., Mrsny, R.J., 2021. Intestinal transcytosis of a protein cargo and nanoparticles mediated by a non-toxic form of pseudomonas aeruginosa exotoxin a. Pharmaceutics 13, 1171. https://doi.org/10.3390/pharmaceutics13081171

Lucio, D., Martínez-Ohárriz, M.C., Jaras, G., Aranaz, P., González-Navarro, C.J., Radulescu, A., Irache, J.M., 2017. Optimization and evaluation of zein nanoparticles to improve the oral delivery of glibenclamide. In vivo study using C. elegans. Eur. J. Pharm. Biopharm. 121, 104–112. https://doi.org/10.1016/j.ejpb.2017.09.018

Luo, Y., Wang, Q., 2014. Zein-based micro- and nano-particles for drug and nutrient delivery: A review. J. Appl. Polym. Sci. https://doi.org/10.1002/app.40696

Mahmood, A., Bernkop-Schnürch, A., 2019. SEDDS: A game changing approach for the oral administration of hydrophilic macromolecular drugs. Adv. Drug Deliv. Rev. 142, 91–101. https://doi.org/10.1016/j.addr.2018.07.001

Marschütz, M.K., Bernkop-Schnürch, A., 2000. Oral peptide drug delivery: Polymer-inhibitor conjugates protecting insulin from enzymatic degradation in vitro. Biomaterials 21, 1499–1507. https://doi.org/10.1016/S0142-9612(00)00039-9

Martínez-López, A.L., González-Navarro, C.J., Aranaz, P., Vizmanos, J.L., Irache, J.M., 2021a. In vivo testing of mucus-permeating nanoparticles for oral insulin delivery using Caenorhabditis elegans as a model under hyperglycemic conditions. Acta Pharm. Sin. B 11, 989–1002. https://doi.org/10.1016/j.apsb.2021.02.020

Martínez-López, A.L., González-Navarro, C.J., Vizmanos, J.L., Irache, J.M., 2021b. Zein-based nanocarriers for the oral delivery of insulin. In vivo evaluation in Caenorhabditis elegans. Drug Deliv. Transl. Res. 11, 647–658. https://doi.org/10.1007/s13346-021-00919-4

McGinn, B.J., Morrison, J.D., 2016. Investigations into the absorption of insulin and insulin derivatives from the small intestine of the anaesthetised rat. J. Control. Release 232, 120–130. https://doi.org/10.1016/j.jconrel.2016.04.002

Mumuni, M.A., Kenechukwu, F.C., Ofokansi, K.C., Attama, A.A., Díaz, D.D., 2020. Insulin-loaded mucoadhesive nanoparticles based on mucin-chitosan complexes for oral delivery and diabetes treatment. Carbohydr. Polym. 229, 115506. https://doi.org/10.1016/j.carbpol.2019.115506

Paques, J.P., Van Der Linden, E., Van Rijn, C.J.M., Sagis, L.M.C., 2014. Preparation methods of alginate nanoparticles. Adv. Colloid Interface Sci. https://doi.org/10.1016/j.cis.2014.03.009

Pascoli, M., de Lima, R., Fraceto, L.F., 2018. Zein nanoparticles and strategies to improve colloidal stability: A mini-review. Front. Chem. 6. https://doi.org/10.3389/fchem.2018.00006

Peñalva, R., Esparza, I., González-Navarro, C.J., Quincoces, G., Peñuelas, I., Irache, J.M., 2015. Zein nanoparticles for oral folic acid delivery. J. Drug Deliv. Sci. Technol. 30, 450–457. https://doi.org/10.1016/j.jddst.2015.06.012

Penalva, R., Esparza, I., Larraneta, E., González-Navarro, C.J., Gamazo, C., Irache, J.M., 2015. Zein-Based Nanoparticles Improve the Oral Bioavailability of Resveratrol and Its Anti-inflammatory Effects in a Mouse Model of Endotoxic Shock. J. Agric. Food Chem. 63, 5603–5611. https://doi.org/10.1021/jf505694e

Pierce, S.B., Costa, M., Wisotzkey, R., Devadhar, S., Homburger, S.A., Buchman, A.R., Ferguson, K.C., Heller, J., Platt, D.M., Pasquinelli, A.A., Liu, L.X., Doberstein, S.K., Ruvkun, G., 2001. Regulation of DAF-2 receptor signaling by human insulin and ins-1, a member of the unusually large and diverse C. elegans insulin gene family. Genes Dev. 15, 672–686. https://doi.org/10.1101/gad.867301

Reale, O., Huguet, A., Fessard, V., 2021. Co-culture model of Caco-2/HT29-MTX cells: A promising tool for investigation of phycotoxins toxicity on the intestinal barrier. Chemosphere 273, 128497. https://doi.org/10.1016/J.CHEMOSPHERE.2020.128497

Reboredo, C., González-Navarro, C.J., Martínez-Oharriz, C., Martínez-López, A.L., Irache,

J.M., 2021. Preparation and evaluation of PEG-coated zein nanoparticles for oral drug delivery purposes. Int. J. Pharm. 597, 120287. https://doi.org/10.1016/j.ijpharm.2021.120287

Reddy, N., Rapisarda, M., 2021. Properties and applications of nanoparticles from plant proteins. Materials (Basel). https://doi.org/10.3390/ma14133607

Sarmento, B., Ribeiro, A., Veiga, F., Sampaio, P., Neufeld, R., Ferreira, D., 2007. Alginate/chitosan nanoparticles are effective for oral insulin delivery. Pharm. Res. 24, 2198–2206. https://doi.org/10.1007/s11095-007-9367-4

Shakweh, M., Ponchel, G., Fattal, E., 2004. Particle uptake by Peyer's patches: A pathway for drug and vaccine delivery. Expert Opin. Drug Deliv. 1, 141–163. https://doi.org/10.1517/17425247.1.1.141

Sim, T., Lim, C., Hoang, N.H., Joo, H., Lee, J.W., Kim, D. won, Lee, E.S., Youn, Y.S., Kim, J.O., Oh, K.T., 2016. Nanomedicines for oral administration based on diverse nanoplatform. J. Pharm. Investig. 46, 351–362. https://doi.org/10.1007/s40005-016-0255-y

Sonaje, K., Lin, Y.H., Juang, J.H., Wey, S.P., Chen, C.T., Sung, H.W., 2009. In vivo evaluation of safety and efficacy of self-assembled nanoparticles for oral insulin delivery. Biomaterials 30, 2329–2339. https://doi.org/10.1016/j.biomaterials.2008.12.066

Torchilin, V.P., 2005. Recent advances with liposomes as pharmaceutical carriers. Nat. Rev. Drug Discov. 4, 145–160. https://doi.org/10.1038/nrd1632

Vakilian, M., Tahamtani, Y., Ghaedi, K., 2019. A review on insulin trafficking and exocytosis. Gene. https://doi.org/10.1016/j.gene.2019.04.063

Wong, C.Y., Al-Salami, H., Dass, C.R., 2018. Recent advancements in oral administration of insulin-loaded liposomal drug delivery systems for diabetes mellitus. Int. J. Pharm. 549, 201–217. https://doi.org/10.1016/j.ijpharm.2018.07.041

Wu, S., Bin, W., Tu, B., Li, X., Wang, W., Liao, S., Sun, C., 2019. A Delivery System for Oral Administration of Proteins/Peptides Through Bile Acid Transport Channels. J. Pharm. Sci. 108, 2143–2152. https://doi.org/10.1016/j.xphs.2019.01.027

Xu, B., Jiang, G., Yu, W., Liu, D., Liu, Y., Kong, X., Yao, J., 2017. Preparation of poly(lactic-co-glycolic acid) and chitosan composite nanocarriers via electrostatic self assembly for oral delivery of insulin. Mater. Sci. Eng. C 78, 420–428. https://doi.org/10.1016/j.msec.2017.04.113

Xu, Q., Hong, H., Wu, J., Yan, X., 2019. Bioavailability of bioactive peptides derived from food proteins across the intestinal epithelial membrane: A review. Trends Food Sci. Technol. 86, 399–411. https://doi.org/10.1016/j.tifs.2019.02.050

Yazdi, J.R., Tafaghodi, M., Sadri, K., Mashreghi, M., Nikpoor, A.R., Nikoofal-Sahlabadi, S., Chamani, J., Vakili, R., Moosavian, S.A., Jaafari, M.R., 2020. Folate targeted PEGylated liposomes for the oral delivery of insulin: In vitro and in vivo studies. Colloids Surfaces B Biointerfaces 194, 111203. https://doi.org/10.1016/j.colsurfb.2020.111203

Ye, D., Bramini, M., Hristov, D.R., Wan, S., Salvati, A., Åberg, C., Dawson, K.A., 2017. Low uptake of silica nanoparticles in Caco-2 intestinal epithelial barriers. Beilstein J. Nanotechnol. 8, 1396–1406. https://doi.org/10.3762/bjnano.8.141

Zhang, Y., Huo, M., Zhou, J., Xie, S., 2010. PKSolver: An add-in program for pharmacokinetic and pharmacodynamic data analysis in Microsoft Excel. Comput. Methods Programs Biomed. 99, 306–314. https://doi.org/10.1016/j.cmpb.2010.01.007

Chapter 7

General discussion

7. General discussion

7.1. General discussion

7.1.1. Why zein nanoparticles?

Zein presents several properties that makes it an interesting biomaterial for the development of new nanometric devices for drug delivery purposes. On the one hand, zein is the major storage protein of maize, comprising around the 80% of the total content of corn (Corradini et al., 2014). Moreover, due to its regulatory status (Generally Recognized As Safe by the FDA), this protein has been widely used in the pharmaceutical and food industries (Berardi et al., 2018; Luo and Wang, 2014), as well as in other sectors (Rastogi and Samyn, 2015). On the other hand, due to the physicochemical properties of the protein, it can be used to form stable nanoparticles in a fast, reliable, and scalable way without the needing of using crosslinkers or other reactive agents (Martínez-López et al., 2020; Reboredo et al., 2021).

Zein nanoparticles have been demonstrated to effectively entrap, and orally deliver, both hydrophobic (Brotons-Canto et al., 2021; Penalva et al., 2017) and hydrophilic (Inchaurraga et al., 2020) molecules. Moreover, the promising results acquired in laboratory animals have led to the evaluation of zein nanoparticles in humans, where the oral administration of resveratrol loaded into zein nanoparticles showed great pharmacokinetic values, with a more than 3-fold increase in the $t_{1/2}$, compared to free resveratrol (Brotons-Canto et al., 2020). Another interesting property of zein nanoparticles is that their surface properties can be easily modified by the coating with different polymers, such as poly(ethylene glycol) (Inchaurraga et al., 2019), Gantrez®-based conjugates (Martínez-López et al., 2021b), soluble soybean polysaccharide (Li et al., 2019) or alginate/chitosan complexes (Khan et al., 2019).

Another important aspect to highlight is the fact that zein hydrolysates (obtained from enzymatic digestion of the native protein) appear to possess antioxidant (Shukla and Cheryan, 2001; Tang et al., 2010), immunomodulatory (Liang et al., 2020; P. Liu et al., 2020), and hypoglycemic properties (Higuchi et al., 2013; Mochida et al., 2010).

7.1.2. Why mucus-diffusive (or mucus-permeating) rather than mucoadhesive nanoparticles?

Mucoadhesion may be defined as the adhesive interaction (adhesion) between two materials, at least one of which is a mucosal surface (Ponchel and Irache, 1998). This phenomenon involves an effective trap of the mucoadhesive material in the proactive mucus layer lining the mucosal surface. On the contrary, mucus-permeation involves certain degree of diffusion and movement across the protective mucus layer and the capability for the mucus-permeating material of reaching the epithelium surface (Pangua et al., 2021). Thus, for some administration routes, such as buccal, bladder, and vagina, mucoadhesiveness is an asset due to the increased residence time (Netsomboon and Bernkop-Schnürch, 2016; Serra et al., 2009). However, mucus-permeating nanocarriers have been demonstrated to be more effective than mucoadhesive ones for

drug administration through the nasal (Porfiryeva et al., 2021), ocular (Popov, 2020), pulmonary (Dong et al., 2020; Popov et al., 2016b) and oral administration routes (Chen et al., 2013; Yamazoe et al., 2021).

Different approaches can be chosen to confer mucus-diffusive properties to the nanoparticles, what would allow them to cross the mucus layer and reach the absorptive epithelium (Pangua et al., 2021). Facilitating the close contact between the nanocarrier and the enterocyte would reduce the exposure of the loaded drug against the harsh conditions of the gastrointestinal tract and, thus, increase its oral bioavailability. A schematic representation of the behavior of mucoadhesive and mucus-penetrating nanoparticles in the gastrointestinal tract is shown in Figure 1.

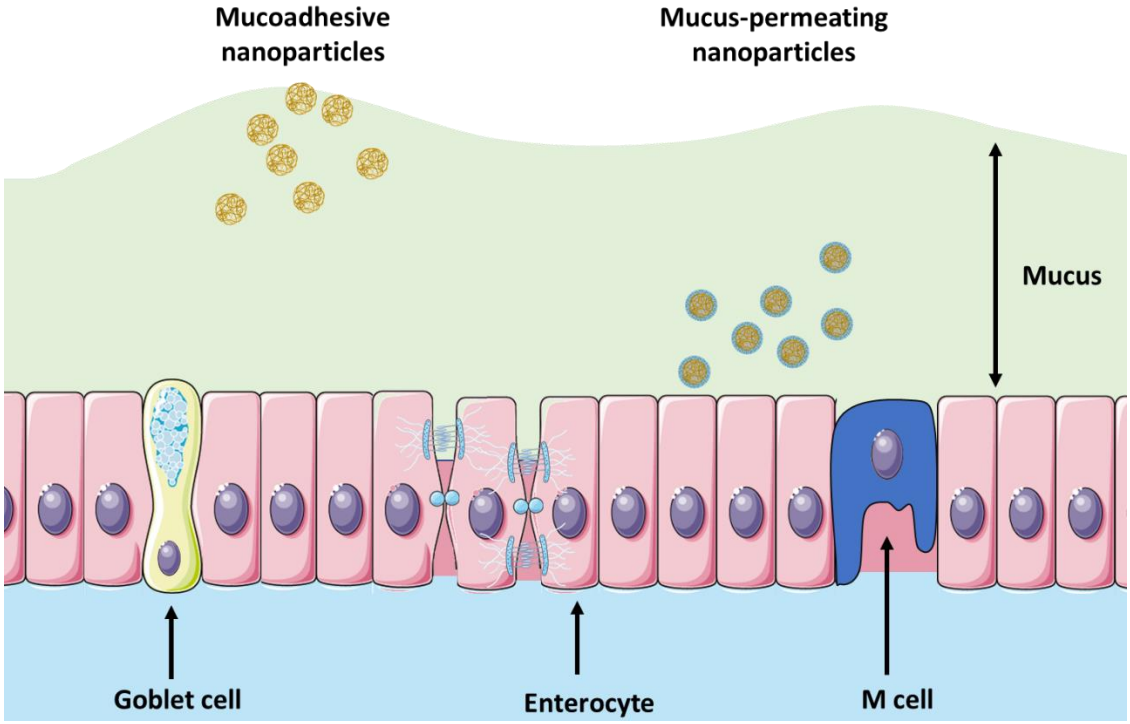

Figure 1. Schematic representation of the behavior of mucoadhesive and mucus-permeating nanoparticles in the gastrointestinal tract. Figure produced using Servier Medical Art pre-made icons and templates (http://smart.servier.com/).

7.1.3. Why to use PEG to produce mucus-diffusive nanocarriers?

Several strategies can be addresses in order to increase the mucus diffusivity of a nanoparticulated device. Depending on the way of action, mucus-penetrating nanoparticles can be classified as active or passive systems (Menzel and Bernkop-Schnürch, 2018). Active systems modify the structure of the mucus, making it leakier (Dünnhaupt et al., 2015). The functionalization of the nanocarrier with thiol groups leads to the cleavage of the disulfide bonds between mucins, conferring a more mucus-diffusive behavior (Dünnhaupt et al., 2015; Rohrer et al., 2016). The decoration of nanoparticles with proteolytic enzymes, such as bromelain (Wilcox et al., 2015) or papain (Müller et al., 2014), has demonstrated to increase the capability of the system to diffuse in the mucus. However, the alteration of the structure of the mucus may be

risky because reducing its rheological properties could compromise its protecting function over the epithelium (Chater et al., 2018).
On the other hand, passive systems intend to avoid interactions between the nanoparticle and the mucus components (Menzel and Bernkop-Schnürch, 2018). Depending on the surface properties of the nanoparticle (mainly hydrophobicity and surface charge), its behavior can be mucoadhesive or mucus-diffusive. For instance, nanoparticles with positive surface zeta potential have increased electrostatic interactions with the negatively-charged mucins (main component of the mucus conferring the gel-forming properties), thus, displaying a mucoadhesive behavior (Cheng et al., 2021; Vieira et al., 2018). Regarding the surface hydrophobicity of the nanoparticle, an increase in the hydrophilicity leads to a reduced interaction between the hydrophobic components of the mucus and the system, what is translated into an increased mucus diffusion (Pangua et al., 2021). For this purpose, the surface properties of the nanoparticles can be modified by the coating with different polymers, such as poly(ethylene glycol) (PEG) (Inchaurraga et al., 2015), poly(vinyl alcohol) (PVA) (Popov et al., 2016a), N-(2-hydroxypropyl) methacrylamide (HPMA) (Cui et al., 2017), conjugates between poly(acrylic acid) and poly(allylamine) (Laffleur et al., 2014), conjugates between Gantrez® AN and manosamine (Matías et al., 2020), dextrans (Iglesias et al., 2017), or zwitterionic polymers (Gao et al., 2021)

The “decoration” of nanoparticles with PEG or pegylation is one of the most popular strategies to confer mucus-diffusive properties (Abdulkarim et al., 2015). PEGs are widely employed in the pharmaceutical industry as excipients in many pharmaceutical dosage forms. These hydrophilic and neutral compounds are not absorbed when orally administered (Chen et al., 2013). In principle, PEG coating may be achieved by simple adsorption (Luis de Redín et al., 2019; Yoncheva et al., 2007) or by covalent binding through functional groups located on the surface of just formed nanoparticles (Ruiz et al., 2013). Another possibility to decorate nanoparticles with PEG may be the synthesis of conjugates between PEG and a polymer (Tobío et al., 2000) or a protein (Lee et al., 2018) before the formation of nanoparticles. Finally, the coating of nanoparticles with PEG considerably reduces their interaction with digestive enzymes (Tobío et al., 2000).

7.1.4. Why to use C. elegans as a model to evaluate oral nanocarriers?

C. elegans is an animal model that has been widely used in research because of its several advantages, which include optical transparency, genetic manipulability, low cost, ease of manipulation, non-hazardous, conserved metabolic pathways with humans, and a short life cycle (DasGupta et al., 2020; Hunt, 2017; Yu et al., 2020). Moreover, the intestinal tract of this animal model shares some similarities with that of mammals, such as acidic environment, secretion of degrading enzymes, intestinal cells with microvilli, and peristalsis (Hunt, 2017). Nevertheless, the surface of the absorptive intestinal cells of *C. elegans* is also covered by a glycocalyx-like layer composed by mucins, among other compounds (Cohen and Sundaram, 2020). Hence, this animal model seems to be an excellent candidate to evaluate the toxicity and viability of orally administered nanoparticles by the simple evaluation of its motility, offspring, quantification of

reactive oxygen species, gonad morphology, accumulation of autofluorescence, and lifespan (Hunt, 2017).

In addition, this animal model is particularly interesting for the evaluation of oral delivery of insulin due to its conserved insulin/IGF-1 metabolic pathway with humans (Ayuda-Durán et al., 2019). Insulin binds to the DAF-2 receptor and trigger signaling pathways that are involved in aging, development, oxidative stress, thermal stress, and lipid metabolism (Ayuda-Durán et al., 2019; Bai et al., 2020; Zheng et al., 2019). When worms are cultured under high glucose conditions, they display increased values of oxidative stress (Yan et al., 2017), which causes, in last term, an increase in the fat accumulation and a reduction in the lifespan (Wang et al., 2018; Yan et al., 2017). In this hyperglycemic state, the binding of human insulin to DAF-2 leads to a decrease in the fat accumulation within the worm (Martínez-López et al., 2021a; Pierce et al., 2001). Thus, the amount of lipidic droplets can be easily quantified and used as marker to assess the efficacy of orally delivered insulin.

7.1.5. Which is the mechanism underlying the hypoglycemic effect exerted by the oral administration of zein nanoparticles?

The gastrointestinal tract plays a key role in the glucose homeostasis via the secretion of incretin hormones (GLP-1 and GIP) from the enteroendocrine L and K cells, respectively. The effect of the incretins over the glucose management is so huge that their influence accounts for above 50% of the total insulin release in the body (Bugliani et al., 2018; Röhrborn et al., 2015; Vilsbøll and Holst, 2004; Wu et al., 2015). These enteroendocrine cells act as sensors of the composition of the chyme and, in response, they release the hormones. Both K and L cells sense saccharides, fats, and proteins (Chai et al., 2012; Nadkarni et al., 2014; Seino et al., 2010), although carbohydrates and lipids are the most potent incretin secretion inductors (Lim and Brubaker, 2006; McIntosh et al., 2009). Regarding the protein-mediated stimulation, L cells seem to be more sensitive to oligo- or large peptides than to free amino acids (Ishikawa et al., 2015), although some of them (e.g., L-glutamine, glycine, alanine, phenylalanine, and arginine) have demonstrated to induce GLP-1 secretion (Clemmensen et al., 2013; Pais et al., 2016a, 2016b). From both incretins, GLP-1 is the most relevant on glucose homeostasis (Holst, 2019). Despite GLP-1 has effects over several tissues throughout the body, regarding glucose homeostasis, the main targets are pancreas, liver, muscle, and heart. It stimulates the glucose uptake from heart, muscle, and liver, as well as increases the hepatic glucose clearance (Ayala et al., 2009; Nikolaidis et al., 2004). Moreover, it also upregulates the inulin production and release from the pancreas (Nadkarni et al., 2014; Rowlands et al., 2018), even in healthy humans (Aulinger et al., 2015). Nevertheless, GLP-1 also inhibits glucagon release, leading to a hypoglycemic effect (Müller et al., 2019). In addition, GIP has homologous effects to GLP-1 over the pancreas (Baggio and Drucker, 2007; Kim and Egan, 2008). All these factors lead to a decrease in the circulating levels of glucose (Chapter 4, Figure 3) and in a better tolerance to a glucose overload

(Chapter 4, Figure 8). A schematic representation of how zein nanoparticles would achieve they hypoglycemic effect is shown in Figure 2.

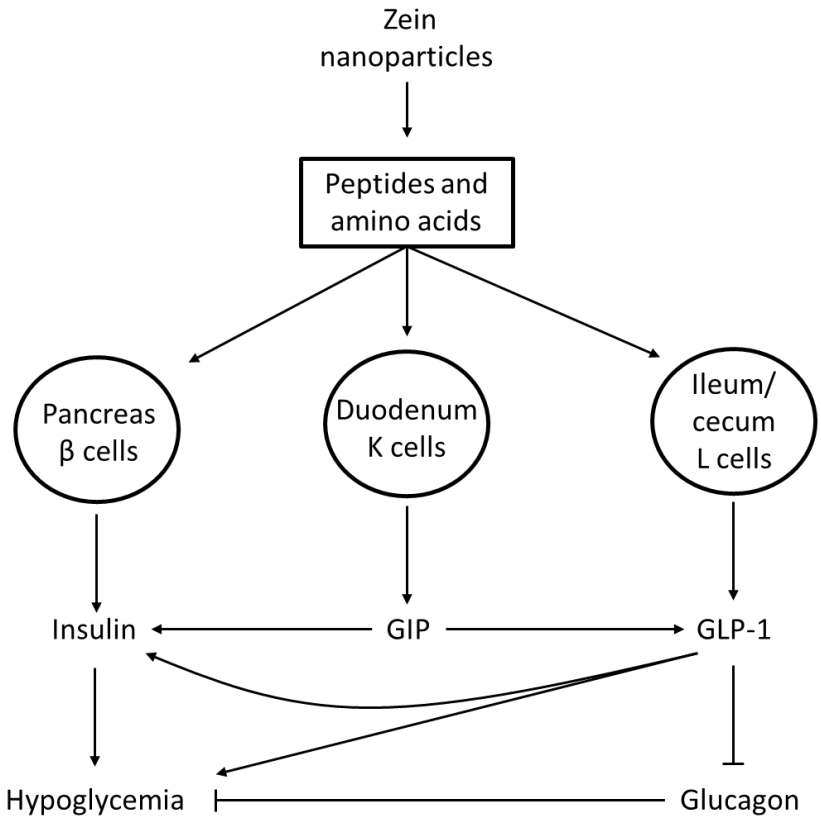

Figure 2. Schematic representation of the mechanisms underlying the hypoglycemic and incretin-release inductor effect observed for orally administered zein nanoparticles. Arrows represent stimulation; T-bars indicate inhibition.

7.1.6. Why zein nanoparticles induced a hypoglycemic effect but the free protein did not?

In principle, the differences observed in the capability to induce hypoglycemic effects in rats between the free protein and zein nanoparticles would be mainly due to their physico-chemical behavior and different biodistribution in the gut. The total proteolytic activity of digestive enzymes varies in different regions of the intestine, being markedly greater in the proximal than in the distal portions (Oleinik, 1995)

The free protein is highly hydrophobic, what makes it to aggregate upon resuspension in water. Furthermore, the aggregates formed by the aqueous resuspension harden very quickly when the temperature is below 40 ºC (Zhang et al., 2022), leading to a plastic-like structure. These hard and highly hydrophobic aggregates will get retained in the stomach and upper regions of the gut, where will be digested. It has been demonstrated that even before the digestion starts, some amino acids are released from zein (leucine > phenylalanine > isoleucine > valine >methionine); and, after enzymatic digestion, the most abundant amino acid released is leucine (Matthews et al., 2011). Leucine is known to be one of the amino acids with most potent insulinogogue activity (Newsholme et al., 2006; Yang et al., 2010), and is particularly abundant in zein (Gianazza et al., 1977;

Rosentrater and Evers, 2018). Moreover, the digestibility of zein in distal regions of the gut (ileum) has been demonstrated to be very poor (Calvez et al., 2021). On the other hand, nanoparticulated zein redisperses much better in water than the free protein, avoiding the generation of such hard and hydrophobic aggregates. Thus, they reach further regions of the gastrointestinal tract in a faster way, especially for PEG-coated nanoparticles. Nevertheless, zein nanoparticles are very resistant to the digestion in gastric conditions, however, in the intestines, they are digested into peptides (Cheng et al., 2019).

Hence, a feasible hypothesis is that orally administered zein nanoparticles display a reduced degradation in the upper regions of the gastrointestinal tract and, once reached distal zones, is degraded. The degradation of the nanoparticles would lead to the release of peptides (and eventually amino acids) that would be sensed by the enteroendocrine cells from the mucosa, leading to the release of incretins (Clemmensen et al., 2013; Pais et al., 2016a). Then, GLP-1 stimulates the glucose uptake in several tissues, as well as increases the hepatic glucose clearance and pancreatic insulin secretion (Ayala et al., 2009; Nadkarni et al., 2014; Nikolaidis et al., 2004; Rowlands et al., 2018). Thus, the hypoglycemic effect observed seems to be driven directly by the action of GLP-1 on increasing glucose uptake from tissues, and indirectly by the increased secretion of insulin. Moreover, some amino acids released are able of reaching the pancreas through the bloodstream and directly stimulate the β cells (Deeney et al., 2000; Fu et al., 2012; Newsholme et al., 2006), what might be potentiating the release of insulin. On the contrary, following oral administration, the free protein would start being digested in the stomach, releasing peptides and amino acids with potential insulinogogue effect. Thus, the release and absorption of leucine and other amino acids in the upper regions of the gut may be involved in the development of the hyperinsulinemia observed (Chapter 4, Figure 4). However, this increased levels of insulin are not translated into a glycemic decrease because when the levels of some amino acids in blood rise, the glucose metabolism is inhibited and the protein metabolism is potentiated (James et al., 2017), even in hyperinsulinemic conditions (Pisters et al., 1991). Afterwards, the remaining zein reaches further regions of the gut, where its digestibility is very poor, leading to the absence of effect observed over GLP-1 secretion.

Figure 3 shows a schematic representation of the observed results in animals after oral administration of nanoparticulated (NP and NP-PEG50) or free zein, according to their biodistribution and digestibility in the gastrointestinal tract.

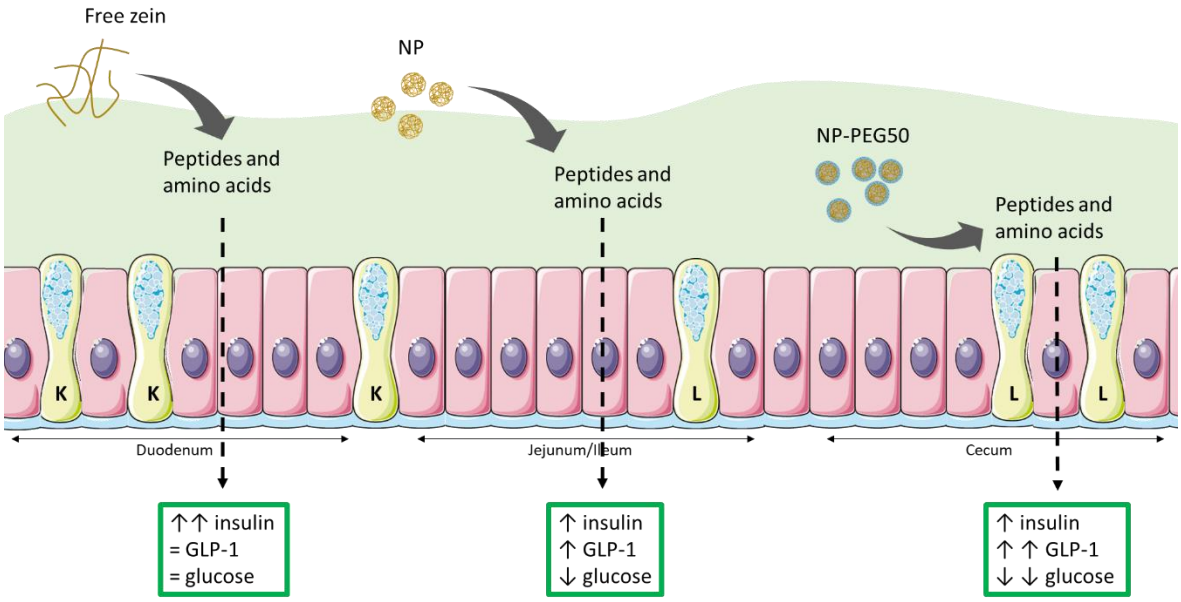

Figure 3. Schematic representation of the fate of orally administered zein nanoparticles (NP and NP-PEG50) and the free protein, and the biological effects observed. NP: bare zein nanoparticles; NP-PEG50: PEG-coated zein nanoparticles; K: K cell of the intestinal epithelium; L: L cell of the intestinal epithelium; GLP-1: glucagon-like peptide 1. Figure produced using Servier Medical Art pre-made icons and templates (http://smart.servier.com/).

7.1.7. Why PEG-coated nanoparticles (NP-PEG50) displayed a more potent effect than bare nanoparticles?

Again, the difference remains on the biodistribution of the nanoparticles within the gastrointestinal tract. PEG-coated nanoparticles show a more mucus-diffusive behavior than bare nanoparticles, thus, they are able of getting closer to the intestinal epithelium and reaching further regions of the gut in the same timeframe (Reboredo et al., 2021). These, combined with the larger amount of L cells present in the distal zones of the intestines (Mortensen et al., 2003; Pais et al., 2016a), lead to the greater GLP-1 release observed in animals receiving NP-PEG50 (Chapter 4, Figure 5). Therefore, this group of animals also showed an increased secretion of insulin (Chapter 4, Figure 4) and a more potent hypoglycemic effect (Chapter 4, Figure 3).

7.1.8. Would the administration of empty zein nanoparticles be useful for the management of T1D?

No. Oral administration of zein nanoparticles has demonstrated to improve the glycemic control through incretins and insulin signaling (Chapter 4). However, in the case of T1D, the basis of the pathological condition is a destruction of the β cells of the pancreas, what leads to an insulin deficiency (Katsarou et al., 2017; Tan et al., 2019). Thus, despite of the insulinogogue effect of the nanoparticles, no increase in the insulinemic values of a T1D individual would be expected. However, the administration of insulin into zein nanoparticles could be beneficial for the patient due to the synergistic effect of GLP-1/GIP combined with insulin. Actually, it has been reported that patients receiving GLP-

1R agonists in combination with subcutaneous insulin displayed a better control of the glycemia, as well as reduced daily insulin doses and a decrease in the glycated hemoglobin levels (Liu et al., 2019). Moreover, the administration of insulin into zein nanoparticles could also be beneficial not only for the glucose management but also to improve other outcomes of T1D such as bone deterioration thanks to the effects of GLP-1 and GIP (Mansur et al., 2015).

7.1.9. Why would the hypoglycemic effect of the nanoparticles be beneficial for the management of Alzheimer's Disease?

Alzheimer's Disease (AD) is the most common type of dementia (Hodson, 2018; Soria Lopez et al., 2019), although the etiology of the illness is still not well understood. However, new understandings regarding its pathogenesis brought to light a close relationship between AD and diabetes (De la Monte, 2014). Actually, the relationship seems to be so close that some authors refer to AD as type 3 diabetes (De La Monte and Wands, 2008; Kandimalla et al., 2017; Mittal et al., 2016). A reduced insulin signaling in the brain (De la Monte, 2014; Kandimalla et al., 2017; Rorbach-Dolata and Piwowar, 2019) and increased blood glucose levels (Crane et al., 2013) are associated to the development of dementia. In fact, the treatment of AD animal models with insulin (Mao et al., 2016; Salameh et al., 2015; Vandal et al., 2014) or GLP-1 analogues (Batista et al., 2018; Hansen et al., 2015) have demonstrated to alleviate the symptoms of the pathology. Thus, Mao and coworkers, found that the intranasal administration of insulin improved the brain insulin signaling, leading to an increase in hippocampal neurogenesis and reduction in β-amyloid production and cognitive impairment in mice. In addition, Batista and coworkers, demonstrated that administration of liraglutide (GLP-1 analogue) reduced the symptoms of insulin resistance in the brain, protected against a chemical induction of AD (based on a loss of insulin receptors), and led to a cognitive improvement in mice and primates.

Therefore, the hypoglycemic, insulinogogue, and GLP-1-secretion inductor effects observed for orally administered zein nanoparticles may improve the development, and outcomes, of Alzheimer's Disease.

7.1.10. Why the administration of zein nanoparticles did not improve the outcomes of the animal model of AD?

In our study, the animal model of choice was the SAMP8 mice, which starts developing memory and learning impairments at the age of 6 months (Liu et al., 2020; Moreno et al., 2017). The age of the mice at the beginning of the experiment was 7-month-old, time by when the animals already show tau hyperphosphorylation and Aβ deposition (Bayod et al., 2015; Del Valle et al., 2010; Moreno et al., 2017; Zhang et al., 2019). Hence, the time when the administration of the treatments started could be too late to reverse the development of the histopathological lesions that lead to the cognitive impairment in AD, even if the treatments induces insulin and GLP-1 secretion. These findings would fit with a previous report in which the administration of insulin was able of slowing the progression of young, but not older (more than 6 months old), SAMP8 mice (Kamei et

al., 2017). Another reason for the lack of beneficial effects observed could be the dose or posology chosen (200 mg/kg every two days). Maybe, the followed administration schedule was not enough to achieve a good effect and, a daily dose of nanoparticles could have been more effective.

7.1.11. Which could be the underlaying mechanism involved in the increased life expectancy observed in animals receiving zein nanoparticles?

The lifespan-increasing effect observed in animals receiving NP may rely on a combination of the properties of the nanoparticles and its degradation products (peptides and amino acids). First, zein nanoparticles have demonstrated to induce an hypoglycemic effect (Chapter 4, Figure 3), which could counteract the physiological hyperglycemic state of SAMP8 mice (Cuesta et al., 2013; Liu et al., 2015). The reduction in circulating glucose levels would lead to a reduction in the formation of AGES and ROS that cause accelerated aging (Moldogazieva et al., 2019; Volpe et al., 2018). Second, the increased GLP-1 secretion-inductor effect of nanoparticles (Chapter 4, Figure 5) could be leading to a rise in the production of two factors with longevity-promoting effects: fibroblast growth factor-21 (FGF21) and insulin-like growth factor (IGF-I) (J. Liu et al., 2019; Yan et al., 2021). Third, the composition of zein is particularly rich in leucine, a branched-chain amino acid that induces mitochondrial biogenesis, what is translated into a reduced accumulation of ROS and increased longevity in animals (D'Antona et al., 2010; Duan et al., 2016; Valerio et al., 2011). Thus, a combination of all these 3 phenomena may be driving the lifespan expansion observed in animals receiving a suspension of bare zein nanoparticles through the oral route.

7.1.12. Why PEG-coated nanoparticles did not induce the same lifespan-expanding effect than bare nanoparticles?

Although PEG-coated zein nanoparticles (NP-PEG50) displayed the most potent hypoglycemic (Chapter 4, Figure 3) and GLP-1-inductor effects (Chapter 4, Figure 5), SAMP8 mice receiving a suspension of this type of nanoparticles did not show an increase in the longevity (Chapter 5, Figure 7). The reason for this may be a reduced residence time within the gastrointestinal tract of the animals. NP-PEG50 have demonstrated to move rapidly through the gut, reaching the cecum of rats 2 hours post-administration (Reboredo et al., 2021). In addition, in the experiment carried out in SAMP8 mice, the dose of nanoparticles was 200 mg/kg nanoparticles while in the experiment developed to evaluate the capability of nanoparticles to reduce the glycemia and increase GLP-1, the dose was 50 mg/kg nanoparticles. Hence, the higher dose of NP-PEG50 carries with higher amounts of PEG. PEGs are polymers with a laxative function caused by the osmotic draw of water molecules (Chen et al., 2013; Corsetti et al., 2021) that generate hydrogen bond with the polymer (Leung, 2014). This retention of water in the lumen leads to an increase in the size of the stools, what stimulates peristaltic reflexes (Birrer, 2002). Therefore, the combination of these two factors (increased flow through the gut and laxative effect from PEG) may lead to a faster excretion of the nanoparticles, which would not have time enough to be degraded and release the biologically active peptides and amino acids.

7.1.13. Would you expect the administration of free zein to induce a similar effect as NP on the lifespan of mice?

No. As already discussed, the fate of the orally administered free zein is not the same as the ones of NP and NP-PEG50. A suspension of free zein would form hard and highly hydrophobic aggregates that would alter the biodistribution and digestibility of the protein. This would lead to the null effect over the glycemia and GLP-1 release and, as consequence, no effect over the lifespan of the animals would be expectable either.

7.1.14. What are the main advantages and limitations of the process employed for the preparation of insulin-loaded nanoparticles?

The preparative process of zein nanoparticles, either bare or PEG-coated, is a simple and reproducible technique that does not need for the use of crosslinkers or other reactive compounds to obtain formulations displaying homogeneous sizes between batches. Moreover, resulting nanoparticles have a high encapsulation efficiency of insulin (around 80%) and the procedure does not alter or degrade the proteins. Nevertheless, the process is scalable, and the end-product is a dry powder ready to be dispersed in water. On the other hand, the disadvantages of the system are the high hygroscopicity of the powder and the presence of insulin molecules in the surface of the resulting nanoparticles.

7.1.15. How could the presence of insulin on the surface of the nanoparticles be minimized?

Due to the formulation process of the nanoparticles (desolvation) and the structure of the resulting zein nanocarriers, some insulin seems to be present in the surface of the system. Zein nanoparticles are formed by around 25 nm blocks that, during the desolvation step, collapse to form the 200 nm matrix nanoparticle (Martínez-López et al., 2020). During this process, the insulin that is present in the hydroalcoholic medium gets entrapped in the zein matrix, thus, some insulin molecules may get retained in the surface of the nanoparticle. One approach to reduce the presence of insulin in the surface of the nanoparticles would be to conjugate the insulin with a hydrophobic compound (e.g., bile salts, phospholipids, or fatty acids). Hence, after the addition of the insulin conjugates to the medium, and prior to the desolvation step, the conjugates would form droplets that upon desolvation would get covered by the zein blocks (Elzoghby et al., 2017). However, this would change the structure of the matrix nanoparticle to a nanocapsule with an oily core (Elzoghby et al., 2017; Sallam and Elzoghby, 2018). This would be an interesting approach because it would confer two benefits at once. On the one hand, the encapsulation of insulin-bile acid conjugates would reduce the presence of insulin molecules in the surface of the nanoparticle, leading to a reduced initial release of the hormone during incubation in gastric or intestinal fluids. On the other hand, the presence of bile salts could increase the uptake of insulin across the intestinal epithelium.

7.1.16. Is the encapsulation of insulin into zein nanoparticles enough to achieve a good oral bioavailability?

No. The use of zein nanoparticles is a good strategy to protect the hormone during its pass through the gastrointestinal tract and, the coating with PEG, confers a muco-diffusive behavior that led to an almost 2.5-fold increase in the oral bioavailability of insulin, compared to bare nanoparticles. However, the relative oral bioavailability achieved was still a 10.2%. Despite this value is slightly greater than others obtained with different nanocarriers such as SNEDDS (7.15%; (Zhang et al., 2012)) or PLGA-chitosan composite nanocarriers (7.77%; (Xu et al., 2017)), it is lower than others reported for liposomes (15.7%; (Koland et al., 2021)) or other polymeric nanoparticles with mucus-penetrating properties (16.2%; (Zhou et al., 2020). Due to the fact that zein nanoparticles do not pass to the bloodstream (Irache and González-Navarro, 2017), their function is to transport intact insulin to the surface of the epithelium, where it will be released and absorbed by the enterocytes or M cells (Shakweh et al., 2004). However, the absorption of insulin is still very poor since the uptake is receptor-mediated (Hall et al., 2020) and most of the internalized insulin would suffer from endosomal degradation (McClain, 1992; Wu et al., 2019).

7.1.17. How could the absorption of insulin through the intestinal epithelium be increased?

To increase the uptake of insulin through the absorptive barrier different approaches could be addressed, which are schematically represented in Figure 4. One strategy could be the encapsulation of a fusion protein consisting on insulin and the Fc (fragment crystallizable) of immunoglobulins (Faust et al., 2020). The reason for this is the presence of Fc receptors (FcRn) in the apical membrane of enterocytes, what allows the internalization and trafficking of immunoglobulins through the intestinal epithelium (Date et al., 2016). This strategy has demonstrated to promote intestinal uptake of other molecules functionalized with Fc (Lawrence et al., 2021). Likely, similar results could be achieved with the insulin-Fc fusion protein. Another feasible strategy is the co-encapsulation of insulin with bile salts (e.g., glycodeoxycholate, sodium deoxycholate or taurocholate), which are known to have absorption-enhancing effects by improving the solubilization of drugs through hydrophobic barriers, increasing the fluidity of the cell membrane (Moghimipour et al., 2015) and enhancing the paracellular permeability (Brayden and Stuettgen, 2021). Previous works have demonstrated that the encapsulation of insulin-sodium deoxycholate complexes into PLGA nanoparticles have a great hypoglycemic effect, inducing about 70% reduction in the glycemic values and lasting more than 24 hours (Sun et al., 2011). Moreover, an interesting feature of bile acids is their capability of inducing GLP-1 release (Bala et al., 2014). Thus, the co-encapsulation of insulin with bile acids into zein nanoparticles could increase, synergistically, the efficacy achieved. The use of cell-penetrating peptides (CPP), as permeation enhancers, is another strategy that can be used to increase the internalization of insulin into enterocytes. CPPs are peptides of less than 20 amino acids that are efficiently internalized into the cells, and can be divided into cationic peptides (e.g., TAT peptide and oligoarginine) and amphiphilic peptides (e.g., penetratin) (Kamei

et al., 2013). The ways by which CPPs pass through the cell membrane depend on their composition and physicochemical properties (Gräslund et al., 2011). For instance, penetratin changes in secondary structure upon contact with the cell membrane and, due to its amphiphilic behavior, it passes through the membrane (Gräslund et al., 2011). Coadministration of insulin with different CPPs has demonstrated to increase intestinal absorption of the hormone in the ileum of rats (Kamei et al., 2008). Thus, the encapsulation of insulin-penetratin nanocomplexes (Kaklotar et al., 2016; Kristensen et al., 2015), into zein nanoparticles could increase the oral bioavailability of the drug. Finally, another strategy that could be addressed is the functionalization of insulin with endosomal scaping signals to avoid the degradation of the endosomal content. In this case, once the insulin-containing endosome would be internalized, the breakdown of its content could be evaded by different mechanisms, such as membrane fusion, pore formation, flip-flop phenomenon, or proton sponge effects, among others (Shete et al., 2014; Varkouhi et al., 2011). Interestingly, some histidine-rich CPPs can also act as inductors of endosome escape by absorbing protons from inside the vesicle and swelling, leading to the alteration of the membrane of the vesicle (Shete et al., 2014). Thus, the conjugation of insulin with histidine-rich CPPs and further encapsulation into zein nanoparticles could be an interesting approach for increasing the oral bioavailability of the hormone.

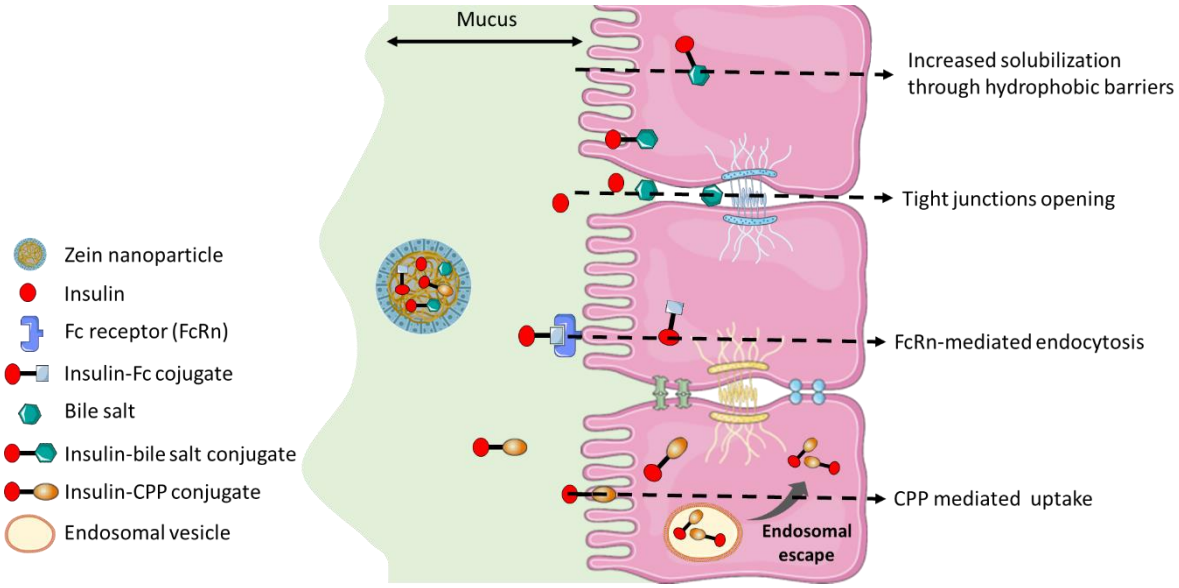

Figure 4. Schematic representation of different approaches that could increase the uptake of insulin across the intestinal epithelium. Fc: fraction crystallizable; FcRn: Fraction crystallizable receptor neonatal; CPP: cell-penetrating peptide. Figure produced using Servier Medical Art pre-made icons and templates (http://smart.servier.com/).

7.2. References

Abdulkarim, M., Agulló, N., Cattoz, B., Griffiths, P., Bernkop-Schnürch, A., Gómez Borros, S., Gumbleton, M., 2015. Nanoparticle diffusion within intestinal mucus: Three-dimensional response analysis dissecting the impact of particle surface charge, size and heterogeneity across polyelectrolyte, pegylated and viral particles. Eur. J. Pharm. Biopharm. 97, 230–238. https://doi.org/10.1016/j.ejpb.2015.01.023

Aulinger, B.A., Vahl, T.P., Wilson-Pérez, H.E., Prigeon, R.L., D'Alessio, D.A., 2015. β-cell sensitivity to GLP-1 in healthy humans is variable and proportional to insulin sensitivity. J. Clin. Endocrinol. Metab. 100, 2489–2496. https://doi.org/10.1210/jc.2014-4009

Ayala, J.E., Bracy, D.P., James, F.D., Julien, B.M., Wasserman, D.H., Drucker, D.J., 2009. The glucagon-like peptide-1 receptor regulates endogenous glucose production and muscle glucose uptake independent of its incretin action. Endocrinology 150, 1155–1164. https://doi.org/10.1210/en.2008-0945

Ayuda-Durán, B., González-Manzano, S., Miranda-Vizuete, A., Dueñas, M., Santos-Buelga, C., González-Paramás, A.M., 2019. Epicatechin modulates stress-resistance in C. Elegans via insulin/IGF-1 signaling pathway. PLoS One 14, e0199483. https://doi.org/10.1371/journal.pone.0199483

Baggio, L.L., Drucker, D.J., 2007. Biology of Incretins: GLP-1 and GIP. Gastroenterology 132, 2131–2157. https://doi.org/10.1053/j.gastro.2007.03.054

Bai, J., Farias-Pereira, R., Zhang, Y., Jang, M., Park, Y., Kim, K.H., 2020. C. elegans ACAT regulates lipolysis and its related lifespan in fasting through modulation of the genes in lipolysis and insulin/IGF-1 signaling. BioFactors 46, 754–765. https://doi.org/10.1002/biof.1666

Bala, V., Rajagopal, S., Kumar, D.P., Nalli, A.D., Mahavadi, S., Sanyal, A.J., Grider, J.R., Murthy, K.S., 2014. Release of GLP-1 and PYY in response to the activation of G protein-coupled bile acid receptor TGR5 is mediated by Epac/PLC-ε pathway and modulated by endogenous H2S. Front. Physiol. 5, 420. https://doi.org/10.3389/fphys.2014.00420

Batista, A.F., Forny-Germano, L., Clarke, J.R., Lyra e Silva, N.M., Brito-Moreira, J., Boehnke, S.E., Winterborn, A., Coe, B.C., Lablans, A., Vital, J.F., Marques, S.A., Martinez, A.M.B., Gralle, M., Holscher, C., Klein, W.L., Houzel, J.C., Ferreira, S.T., Munoz, D.P., De Felice, F.G., 2018. The diabetes drug liraglutide reverses cognitive impairment in mice and attenuates insulin receptor and synaptic pathology in a non-human primate model of Alzheimer's disease. J. Pathol. 245, 85–100. https://doi.org/10.1002/path.5056

Bayod, S., Felice, P., Andrés, P., Rosa, P., Camins, A., Pallàs, M., Canudas, A.M., 2015. Downregulation of canonical Wnt signaling in hippocampus of SAMP8 mice. Neurobiol. Aging 36, 720–729. https://doi.org/10.1016/j.neurobiolaging.2014.09.017

Berardi, A., Bisharat, L., AlKhatib, H.S., Cespi, M., 2018. Zein as a Pharmaceutical Excipient in Oral Solid Dosage Forms: State of the Art and Future Perspectives. AAPS

PharmSciTech. https://doi.org/10.1208/s12249-018-1035-y

Birrer, R.B., 2002. Irritable bowel syndrome, in: Disease-a-Month. Elsevier, pp. 101–143. https://doi.org/10.1067/mda.2002.122480

Brayden, D.J., Stuettgen, V., 2021. Sodium glycodeoxycholate and sodium deoxycholate as epithelial permeation enhancers: in vitro and ex vivo intestinal and buccal bioassays. Eur. J. Pharm. Sci. 159, 105737. https://doi.org/10.1016/j.ejps.2021.105737

Brotons-Canto, A., González-Navarro, C.J., Gil, A.G., Asin-Prieto, E., Saiz, M.J., Llabrés, J.M., 2021. Zein nanoparticles improve the oral bioavailability of curcumin in wistar rats. Pharmaceutics 13. https://doi.org/10.3390/pharmaceutics13030361

Brotons-Canto, A., Gonzalez-Navarro, C.J., Gurrea, J., González-Ferrero, C., Irache, J.M., 2020. Zein nanoparticles improve the oral bioavailability of resveratrol in humans. J. Drug Deliv. Sci. Technol. 57, 101704. https://doi.org/10.1016/j.jddst.2020.101704

Bugliani, M., Syed, F., Paula, F.M.M., Omar, B.A., Suleiman, M., Mossuto, S., Grano, F., Cardarelli, F., Boggi, U., Vistoli, F., Filipponi, F., De Simone, P., Marselli, L., De Tata, V., Ahren, B., Eizirik, D.L., Marchetti, P., 2018. DPP-4 is expressed in human pancreatic beta cells and its direct inhibition improves beta cell function and survival in type 2 diabetes. Mol. Cell. Endocrinol. 473, 186–193. https://doi.org/10.1016/j.mce.2018.01.019

Calvez, J., Benoit, S., Piedcoq, J., Khodorova, N., Azzout-Marniche, D., Tomé, D., Benamouzig, R., Airinei, G., Gaudichon, C., 2021. Very low ileal nitrogen and amino acid digestibility of zein compared to whey protein isolate in healthy volunteers. Am. J. Clin. Nutr. 113, 70–82. https://doi.org/10.1093/ajcn/nqaa274

Chai, W., Dong, Z., Wang, N., Wang, W., Tao, L., Cao, W., Liu, Z., 2012. Glucagon-like peptide 1 recruits microvasculature and increases glucose use in muscle via a nitric oxide-dependent mechanism. Diabetes 61, 888–896. https://doi.org/10.2337/db11-1073

Chater, P.I., Wilcox, M.D., Pearson, J.P., 2018. Efficacy and safety concerns over the use of mucus modulating agents for drug delivery using nanoscale systems. Adv. Drug Deliv. Rev. 124, 184–192. https://doi.org/10.1016/j.addr.2017.12.006

Chen, D., Xia, D., Li, X., Zhu, Q., Yu, H., Zhu, C., Gan, Y., 2013. Comparative study of Pluronic® F127-modified liposomes and chitosan-modified liposomes for mucus penetration and oral absorption of cyclosporine A in rats. Int. J. Pharm. 449, 1–9. https://doi.org/10.1016/j.ijpharm.2013.04.002

Chen, M.L., Sadrieh, N., Yu, L., 2013. Impact of osmotically active excipients on bioavailability and bioequivalence of BCS class III drugs. AAPS J. 15, 1043–1050. https://doi.org/10.1208/s12248-013-9509-z

Cheng, C.J., Ferruzzi, M., Jones, O.G., 2019. Fate of lutein-containing zein nanoparticles following simulated gastric and intestinal digestion. Food Hydrocoll. 87, 229–236. https://doi.org/10.1016/j.foodhyd.2018.08.013

Cheng, H., Cui, Z., Guo, S., Zhang, X., Huo, Y., Mao, S., 2021. Mucoadhesive versus mucopenetrating nanoparticles for oral delivery of insulin. Acta Biomater. https://doi.org/10.1016/j.actbio.2021.08.046

Clemmensen, C., Smajilovic, S., Smith, E.P., Woods, S.C., Bräuner-Osborne, H., Seeley, R.J., D'Alessio, D.A., Ryan, K.K., 2013. Oral L-arginine stimulates GLP-1 secretion to improve glucose tolerance in male mice. Endocrinology 154, 3978–3983. https://doi.org/10.1210/en.2013-1529

Cohen, J.D., Sundaram, M. V., 2020. C. Elegans apical extracellular matrices shape epithelia. J. Dev. Biol. 8, 1–26. https://doi.org/10.3390/jdb8040023

Corradini, E., Curti, P.S., Meniqueti, A.B., Martins, A.F., Rubira, A.F., Muniz, E.C., 2014. Recent advances in food-packing, pharmaceutical and biomedical applications of zein and zein-based materials. Int. J. Mol. Sci. 15, 22438–22470. https://doi.org/10.3390/ijms151222438

Corsetti, M., Thys, A., Harris, A., Pagliaro, G., Deloose, E., Demedts, I., Tack, J., 2021. High-resolution manometry reveals different effect of polyethylene glycol, bisacodyl, and prucalopride on colonic motility in healthy subjects: An acute, open label, randomized, crossover, reader-blinded study with potential clinical implications. Neurogastroenterol. Motil. 33, e14040. https://doi.org/10.1111/nmo.14040

Crane, P.K., Walker, R., Hubbard, R.A., Li, G., Nathan, D.M., Zheng, H., Haneuse, S., Craft, S., Montine, T.J., Kahn, S.E., McCormick, W., McCurry, S.M., Bowen, J.D., Larson, E.B., 2013. Glucose levels and risk of dementia. Forsch. Komplementarmed. 20, 386–387. https://doi.org/10.1056/nejmoa1215740

Cuesta, S., Kireev, R., García, C., Rancan, L., Vara, E., Tresguerres, J.A.F., 2013. Melatonin can improve insulin resistance and aging-induced pancreas alterations in senescence-accelerated prone male mice (SAMP8). Age (Omaha). 35, 659–671. https://doi.org/10.1007/s11357-012-9397-7

Cui, Y., Shan, W., Liu, M., Wu, L., Huang, Y., 2017. A strategy for developing effective orally-delivered nanoparticles through modulation of the surface "hydrophilicity/hydrophobicity balance." J. Mater. Chem. B 5, 1302–1314. https://doi.org/10.1039/c6tb02475k

D'Antona, G., Ragni, M., Cardile, A., Tedesco, L., Dossena, M., Bruttini, F., Caliaro, F., Corsetti, G., Bottinelli, R., Carruba, M.O., Valerio, A., Nisoli, E., 2010. Branched-chain amino acid supplementation promotes survival and supports cardiac and skeletal muscle mitochondrial biogenesis in middle-aged mice. Cell Metab. 12, 362–372. https://doi.org/10.1016/j.cmet.2010.08.016

DasGupta, A., Lee, T.L., Li, C., Saltzman, A.L., 2020. Emerging Roles for Chromo Domain Proteins in Genome Organization and Cell Fate in C. elegans. Front. Cell Dev. Biol. 8, 1027. https://doi.org/10.3389/fcell.2020.590195

Date, A.A., Hanes, J., Ensign, L.M., 2016. Nanoparticles for oral delivery: Design, evaluation and state-of-the-art. J. Control. Release 240, 504–526. https://doi.org/10.1016/j.jconrel.2016.06.016

De la Monte, S.M., 2014. Type 3 diabetes is sporadic Alzheimer-s disease: Mini-review. Eur. Neuropsychopharmacol. 24, 1954–1960. https://doi.org/10.1016/j.euroneuro.2014.06.008

De La Monte, S.M., Wands, J.R., 2008. Alzheimer's disease is type 3 diabetes-evidence reviewed. J. Diabetes Sci. Technol. https://doi.org/10.1177/193229680800200619

Deeney, J.T., Prentki, M., Corkey, B.E., 2000. Metabolic control of β-cell function. Semin. Cell Dev. Biol. 11, 267–275. https://doi.org/10.1006/scdb.2000.0175

Del Valle, J., Duran-Vilaregut, J., Manich, G., Casadesús, G., Smith, M.A., Camins, A., Pallàs, M., Pelegrí, C., Vilaplana, J., 2010. Early amyloid accumulation in the hippocampus of SAMP8 mice. J. Alzheimer's Dis. 19, 1303–1315. https://doi.org/10.3233/JAD-2010-1321

Dong, W., Ye, J., Zhou, J., Wang, W., Wang, H., Zheng, X., Yang, Y., Xia, X., Liu, Y., 2020. Comparative study of mucoadhesive and mucus-penetrative nanoparticles based on phospholipid complex to overcome the mucus barrier for inhaled delivery of baicalein. Acta Pharm. Sin. B 10, 1576–1585. https://doi.org/10.1016/j.apsb.2019.10.002

Duan, Y., Li, F., Li, Y., Tang, Y., Kong, X., Feng, Z., Anthony, T.G., Watford, M., Hou, Y., Wu, G., Yin, Y., 2016. The role of leucine and its metabolites in protein and energy metabolism. Amino Acids 48, 41–51. https://doi.org/10.1007/s00726-015-2067-1

Dünnhaupt, S., Kammona, O., Waldner, C., Kiparissides, C., Bernkop-Schnürch, A., 2015. Nano-carrier systems: Strategies to overcome the mucus gel barrier. Eur. J. Pharm. Biopharm. 96, 447–453. https://doi.org/10.1016/j.ejpb.2015.01.022

Elzoghby, A.O., El-Lakany, S.A., Helmy, M.W., Abu-Serie, M.M., Elgindy, N.A., 2017. Shell-crosslinked zein nanocapsules for oral codelivery of exemestane and resveratrol in breast cancer therapy. Nanomedicine 12, 2785–2805. https://doi.org/10.2217/nnm-2017-0247

Faust, C., Ochs, C., Korn, M., Werner, U., Jung, J., Dittrich, W., Schiebler, W., Schauder, R., Rao, E., Langer, T., 2020. Production of a novel heterodimeric two-chain insulin-Fc fusion protein. Protein Eng. Des. Sel. 33, 1–9. https://doi.org/10.1093/PROTEIN/GZAA026

Fu, Z., R. Gilbert, E., Liu, D., 2012. Regulation of Insulin Synthesis and Secretion and Pancreatic Beta-Cell Dysfunction in Diabetes. Curr. Diabetes Rev. 9, 25–53. https://doi.org/10.2174/15733998130104

Gao, Y., He, Y., Zhang, H., Zhang, Y., Gao, T., Wang, J.H., Wang, S., 2021. Zwitterion-functionalized mesoporous silica nanoparticles for enhancing oral delivery of protein drugs by overcoming multiple gastrointestinal barriers. J. Colloid Interface Sci. 582, 364–375. https://doi.org/10.1016/j.jcis.2020.08.010

Gianazza, E., Viglienghi, V., Righetti, P.G., Salamini, F., Soave, C., 1977. Amino acid composition of zein molecular components. Phytochemistry 16, 315–317. https://doi.org/10.1016/0031-9422(77)80054-X

Gräslund, A., Madani, F., Lindberg, S., Langel, Ü., Futaki, S., 2011. Mechanisms of cellular

uptake of cell-penetrating peptides. J. Biophys. 2011. https://doi.org/10.1155/2011/414729

Hall, C., Yu, H., Choi, E., 2020. Insulin receptor endocytosis in the pathophysiology of insulin resistance. Exp. Mol. Med. 52, 911–920. https://doi.org/10.1038/s12276-020-0456-3

Hansen, H.H., Fabricius, K., Barkholt, P., Niehoff, M.L., Morley, J.E., Jelsing, J., Pyke, C., Knudsen, L.B., Farr, S.A., Vrang, N., 2015. The GLP-1 Receptor Agonist Liraglutide Improves Memory Function and Increases Hippocampal CA1 Neuronal Numbers in a Senescence-Accelerated Mouse Model of Alzheimer's Disease. J. Alzheimer's Dis. 46, 877–888. https://doi.org/10.3233/JAD-143090

Higuchi, N., Hira, T., Yamada, N., Hara, H., 2013. Oral administration of corn zein hydrolysate stimulates GLP-1 and GIP secretion and improves glucose tolerance in male normal rats and Goto-Kakizaki rats. Endocrinology 154, 3089–3098. https://doi.org/10.1210/en.2012-2275

Hodson, R., 2018. Alzheimer's disease. Nature. https://doi.org/10.1038/d41586-018-05717-6

Holst, J.J., 2019. The incretin system in healthy humans: The role of GIP and GLP-1. Metabolism. 96, 46–55. https://doi.org/10.1016/j.metabol.2019.04.014

Hunt, P.R., 2017. The C. elegans model in toxicity testing. J. Appl. Toxicol. 37, 50–59. https://doi.org/10.1002/jat.3357

Iglesias, T., López de Cerain, A., Irache, J.M., Martín-Arbella, N., Wilcox, M., Pearson, J., Azqueta, A., 2017. Evaluation of the cytotoxicity, genotoxicity and mucus permeation capacity of several surface modified poly(anhydride) nanoparticles designed for oral drug delivery. Int. J. Pharm. 517, 67–79. https://doi.org/10.1016/j.ijpharm.2016.11.059

Inchaurraga, L., Martín-Arbella, N., Zabaleta, V., Quincoces, G., Peñuelas, I., Irache, J.M., 2015. In vivo study of the mucus-permeating properties of PEG-coated nanoparticles following oral administration. Eur. J. Pharm. Biopharm. 97, 280–289. https://doi.org/10.1016/j.ejpb.2014.12.021

Inchaurraga, L., Martínez-López, A.L., Abdulkarim, M., Gumbleton, M., Quincoces, G., Peñuelas, I., Martin-Arbella, N., Irache, J.M., 2019. Modulation of the fate of zein nanoparticles by their coating with a Gantrez® AN-thiamine polymer conjugate. Int. J. Pharm. X 1, 100006. https://doi.org/10.1016/j.ijpx.2019.100006

Inchaurraga, L., Martínez-López, A.L., Martin-Arbella, N., Irache, J.M., 2020. Zein-based nanoparticles for the oral delivery of insulin. Drug Deliv. Transl. Res. 10, 1601–1611. https://doi.org/10.1007/s13346-020-00796-3

Irache, J.M., González-Navarro, C.J., 2017. Zein nanoparticles as vehicles for oral delivery purposes. Nanomedicine 12, 1209–1211. https://doi.org/10.2217/nnm-2017-0075

Ishikawa, Y., Hira, T., Inoue, D., Harada, Y., Hashimoto, H., Fujii, M., Kadowaki, M., Hara, H., 2015. Rice protein hydrolysates stimulate GLP-1 secretion, reduce GLP-1 degradation, and lower the glycemic response in rats. Food Funct. 6, 2525–2534.

https://doi.org/10.1039/c4fo01054j

James, H.A., O'Neill, B.T., Nair, K.S., 2017. Insulin Regulation of Proteostasis and Clinical Implications. Cell Metab. https://doi.org/10.1016/j.cmet.2017.06.010

Kaklotar, D., Agrawal, P., Abdulla, A., Singh, R.P., Sonali, Mehata, A.K., Singh, S., Mishra, B., Pandey, B.L., Trigunayat, A., Muthu, M.S., 2016. Transition from passive to active targeting of oral insulin nanomedicines: Enhancement in bioavailability and glycemic control in diabetes. Nanomedicine 11, 1465–1486. https://doi.org/10.2217/nnm.16.43

Kamei, N., Morishita, M., Eda, Y., Ida, N., Nishio, R., Takayama, K., 2008. Usefulness of cell-penetrating peptides to improve intestinal insulin absorption. J. Control. Release 132, 21–25. https://doi.org/10.1016/j.jconrel.2008.08.001

Kamei, N., Nielsen, E.J.B., Khafagy, E.S., Takeda-Morishita, M., 2013. Noninvasive insulin delivery: The great potential of cell-penetrating peptides. Ther. Deliv. 4, 315–326. https://doi.org/10.4155/tde.12.164

Kamei, N., Tanaka, M., Choi, H., Okada, N., Ikeda, T., Itokazu, R., Takeda-Morishita, M., 2017. Effect of an Enhanced Nose-to-Brain Delivery of Insulin on Mild and Progressive Memory Loss in the Senescence-Accelerated Mouse. Mol. Pharm. 14, 916–927. https://doi.org/10.1021/acs.molpharmaceut.6b01134

Kandimalla, R., Thirumala, V., Reddy, P.H., 2017. Is Alzheimer's disease a Type 3 Diabetes? A critical appraisal. Biochim. Biophys. Acta - Mol. Basis Dis. https://doi.org/10.1016/j.bbadis.2016.08.018

Katsarou, A., Gudbjörnsdottir, S., Rawshani, A., Dabelea, D., Bonifacio, E., Anderson, B.J., Jacobsen, L.M., Schatz, D.A., Lernmark, A., 2017. Type 1 diabetes mellitus. Nat. Rev. Dis. Prim. 3, 1–17. https://doi.org/10.1038/nrdp.2017.16

Khan, M.A., Yue, C., Fang, Z., Hu, S., Cheng, H., Bakry, A.M., Liang, L., 2019. Alginate/chitosan-coated zein nanoparticles for the delivery of resveratrol. J. Food Eng. 258, 45–53. https://doi.org/10.1016/j.jfoodeng.2019.04.010

Kim, W., Egan, J.M., 2008. The role of incretins in glucose homeostasis and diabetes treatment. Pharmacol. Rev. 60, 470–512. https://doi.org/10.1124/pr.108.000604

Koland, M., Anchan, R.B., Mukund, S.G., Sindhoor, S.M., 2021. Design and investigation of alginate coated solid lipid nanoparticles for oral insulin delivery. Indian J. Pharm. Educ. Res. 55, 383–394. https://doi.org/10.5530/ijper.55.2.76

Kristensen, M., Franzyk, H., Klausen, M.T., Iversen, A., Bahnsen, J.S., Skyggebjerg, R.B., Foderà, V., Nielsen, H.M., 2015. Penetratin-Mediated Transepithelial Insulin Permeation: Importance of Cationic Residues and pH for Complexation and Permeation. AAPS J. 17, 1200–1209. https://doi.org/10.1208/s12248-015-9747-3

Laffleur, F., Hintzen, F., Shahnaz, G., Rahmat, D., Leithner, K., Bernkop-Schnürch, A., 2014. Development and in vitro evaluation of slippery nanoparticles for enhanced diffusion through native mucus. Nanomedicine 9, 387–396. https://doi.org/10.2217/nnm.13.26

Lawrence, S.A., Blankenship, R., Brown, R., Estwick, S., Ellis, B., Thangaraju, A., Datta-Mannan, A., 2021. Influence of FcRn binding properties on the gastrointestinal absorption and exposure profile of Fc molecules. Bioorganic Med. Chem. 32, 115942. https://doi.org/10.1016/j.bmc.2020.115942

Lee, J.E., Kim, M.G., Jang, Y.L., Lee, M.S., Kim, N.W., Yin, Y., Lee, J.H., Lim, S.Y., Park, J.W., Kim, J., Lee, D.S., Kim, S.H., Jeong, J.H., 2018. Self-assembled pegylated albumin nanoparticles (Span) as a platform for cancer chemotherapy and imaging. Drug Deliv. 25, 1570–1578. https://doi.org/10.1080/10717544.2018.1489430

Leung, H.W., 2014. Polyethylene Glycol. Encycl. Toxicol. Third Ed. 1043–1044. https://doi.org/10.1016/B978-0-12-386454-3.00050-6

Li, H., Wang, D., Liu, C., Zhu, J., Fan, M., Sun, X., Wang, T., Xu, Y., Cao, Y., 2019. Fabrication of stable zein nanoparticles coated with soluble soybean polysaccharide for encapsulation of quercetin. Food Hydrocoll. 87, 342–351. https://doi.org/10.1016/j.foodhyd.2018.08.002

Liang, Q., Chalamaiah, M., Liao, W., Ren, X., Ma, H., Wu, J., 2020. Zein hydrolysate and its peptides exert anti-inflammatory activity on endothelial cells by preventing TNF-α-induced NF-κB activation. J. Funct. Foods 64, 103598. https://doi.org/10.1016/j.jff.2019.103598

Lim, G.E., Brubaker, P.L., 2006. Glucagon-like peptide 1 secretion by the L-cell: The view from within. Diabetes 55, S70–S77. https://doi.org/10.2337/db06-S020

Liu, B., Liu, J., Shi, J.-S., 2020. SAMP8 Mice as a Model of Age-Related Cognition Decline with Underlying Mechanisms in Alzheimer's Disease. J. Alzheimer's Dis. 75, 385–395. https://doi.org/10.3233/jad-200063

Liu, H.W., Chan, Y.C., Wang, M.F., Wei, C.C., Chang, S.J., 2015. Dietary (-)-Epigallocatechin-3-gallate Supplementation Counteracts Aging-Associated Skeletal Muscle Insulin Resistance and Fatty Liver in Senescence-Accelerated Mouse. J. Agric. Food Chem. 63, 8407–8417. https://doi.org/10.1021/acs.jafc.5b02501

Liu, J., Yang, K., Yang, J., Xiao, W., Le, Y., Yu, F., Gu, L., Lang, S., Tian, Q., Jin, T., Wei, R., Hong, T., 2019. Liver-derived fibroblast growth factor 21 mediates effects of glucagon-like peptide-1 in attenuating hepatic glucose output. EBioMedicine 41, 73–84. https://doi.org/10.1016/j.ebiom.2019.02.037

Liu, L., Shao, Z., Xia, Y., Qin, J., Xiao, Y., Zhou, Z., Mei, Z., 2019. Incretin-based therapies for patients with type 1 diabetes: A meta-analysis. Endocr. Connect. 8, 277–288. https://doi.org/10.1530/EC-18-0546

Liu, P., Liao, W., Qi, X., Yu, W., Wu, J., 2020. Identification of immunomodulatory peptides from zein hydrolysates. Eur. Food Res. Technol. 246, 931–937. https://doi.org/10.1007/s00217-020-03450-x

Luis de Redín, I., Boiero, C., Recalde, S., Agüeros, M., Allemandi, D., Llabot, J.M., García-Layana, A., Irache, J.M., 2019. In vivo effect of bevacizumab-loaded albumin nanoparticles in the treatment of corneal neovascularization. Exp. Eye Res. 185, 107697. https://doi.org/10.1016/j.exer.2019.107697

Luo, Y., Wang, Q., 2014. Zein-based micro- and nano-particles for drug and nutrient delivery: A review. J. Appl. Polym. Sci. https://doi.org/10.1002/app.40696

Mansur, S.A., Mieczkowska, A., Bouvard, B., Flatt, P.R., Chappard, D., Irwin, N., Mabilleau, G., 2015. Stable Incretin Mimetics Counter Rapid Deterioration of Bone Quality in Type 1 Diabetes Mellitus. J. Cell. Physiol. 230, 3009–3018. https://doi.org/10.1002/jcp.25033

Mao, Y.F., Guo, Z., Zheng, T., Jiang, Y., Yan, Y., Yin, X., Chen, Y., Zhang, B., 2016. Intranasal insulin alleviates cognitive deficits and amyloid pathology in young adult APPswe/PS1dE9 mice. Aging Cell 15, 893–902. https://doi.org/10.1111/acel.12498

Martínez-López, A.L., González-Navarro, C.J., Aranaz, P., Vizmanos, J.L., Irache, J.M., 2021a. In vivo testing of mucus-permeating nanoparticles for oral insulin delivery using Caenorhabditis elegans as a model under hyperglycemic conditions. Acta Pharm. Sin. B 11, 989–1002. https://doi.org/10.1016/j.apsb.2021.02.020

Martínez-López, A.L., González-Navarro, C.J., Vizmanos, J.L., Irache, J.M., 2021b. Zein-based nanocarriers for the oral delivery of insulin. In vivo evaluation in Caenorhabditis elegans. Drug Deliv. Transl. Res. 11, 647–658. https://doi.org/10.1007/s13346-021-00919-4

Martínez-López, A.L., Pangua, C., Reboredo, C., Campión, R., Morales-Gracia, J., Irache, J.M., 2020. Protein-based nanoparticles for drug delivery purposes. Int. J. Pharm. 581, 119289. https://doi.org/10.1016/j.ijpharm.2020.119289

Matías, J., Brotons, A., Cenoz, S., Pérez, I., Abdulkarim, M., Gumbleton, M., Irache, J.M., Gamazo, C., 2020. Oral immunogenicity in mice and sows of enterotoxigenic escherichia coli outer-membrane vesicles incorporated into zein-based nanoparticles. Vaccines 8, 11. https://doi.org/10.3390/vaccines8010011

Matthews, L.B., Kunkel, M.E., Acton, J.C., Ogale, A.A., Dawson, P.L., 2011. Bioavailability of Soy Protein and Corn Zein Films. Food Nutr. Sci. 02, 1105–1113. https://doi.org/10.4236/fns.2011.210148

McClain, D.A., 1992. Mechanism and role of insulin receptor endocytosis. Am. J. Med. Sci. 304, 192–201. https://doi.org/10.1097/00000441-199209000-00009

McIntosh, C.H.S., Widenmaier, S., Kim, S.J., 2009. Chapter 15 Glucose-Dependent Insulinotropic Polypeptide (Gastric Inhibitory Polypeptide; GIP). Vitam. Horm. 80, 409–471. https://doi.org/10.1016/S0083-6729(08)00615-8

Menzel, C., Bernkop-Schnürch, A., 2018. Enzyme decorated drug carriers: Targeted swords to cleave and overcome the mucus barrier. Adv. Drug Deliv. Rev. 124, 164–174. https://doi.org/10.1016/j.addr.2017.10.004

Mittal, K., Mani, R.J., Katare, D.P., 2016. Type 3 Diabetes: Cross Talk between Differentially Regulated Proteins of Type 2 Diabetes Mellitus and Alzheimer's Disease. Sci. Rep. 6. https://doi.org/10.1038/srep25589

Mochida, T., Hira, T., Hara, H., 2010. The corn protein, zein hydrolysate, administered into the ileum attenuates hyperglycemia via its dual action on glucagon-like peptide-1 secretion and dipeptidyl peptidase-IV activity in rats. Endocrinology 151,

3095–3104. https://doi.org/10.1210/en.2009-1510

Moghimipour, E., Ameri, A., Handali, S., 2015. Absorption-Enhancing Effects of Bile Salts. Molecules 20, 14451–14473. https://doi.org/10.3390/molecules200814451

Moldogazieva, N.T., Mokhosoev, I.M., Mel'Nikova, T.I., Porozov, Y.B., Terentiev, A.A., 2019. Oxidative Stress and Advanced Lipoxidation and Glycation End Products (ALEs and AGEs) in Aging and Age-Related Diseases. Oxid. Med. Cell. Longev. 2019. https://doi.org/10.1155/2019/3085756

Moreno, L.C.G. e. I., Puerta, E., Suárez-Santiago, J.E., Santos-Magalhães, N.S., Ramirez, M.J., Irache, J.M., 2017. Effect of the oral administration of nanoencapsulated quercetin on a mouse model of Alzheimer's disease. Int. J. Pharm. 517, 50–57. https://doi.org/10.1016/j.ijpharm.2016.11.061

Mortensen, K., Christensen, L.L., Holst, J.J., Orskov, C., 2003. GLP-1 and GIP are colocalized in a subset of endocrine cells in the small intestine. Regul. Pept. 114, 189–196. https://doi.org/10.1016/S0167-0115(03)00125-3

Müller, C., Perera, G., König, V., Bernkop-Schnürch, A., 2014. Development and in vivo evaluation of papain-functionalized nanoparticles. Eur. J. Pharm. Biopharm. 87, 125–131. https://doi.org/10.1016/j.ejpb.2013.12.012

Müller, T.D., Finan, B., Bloom, S.R., D'Alessio, D., Drucker, D.J., Flatt, P.R., Fritsche, A., Gribble, F., Grill, H.J., Habener, J.F., Holst, J.J., Langhans, W., Meier, J.J., Nauck, M.A., Perez-Tilve, D., Pocai, A., Reimann, F., Sandoval, D.A., Schwartz, T.W., Seeley, R.J., Stemmer, K., Tang-Christensen, M., Woods, S.C., DiMarchi, R.D., Tschöp, M.H., 2019. Glucagon-like peptide 1 (GLP-1). Mol. Metab. https://doi.org/10.1016/j.molmet.2019.09.010

Nadkarni, P., Chepurny, O.G., Holz, G.G., 2014. Regulation of glucose homeostasis by GLP-1, in: Progress in Molecular Biology and Translational Science. Elsevier B.V., pp. 23–65. https://doi.org/10.1016/B978-0-12-800101-1.00002-8

Netsomboon, K., Bernkop-Schnürch, A., 2016. Mucoadhesive vs. mucopenetrating particulate drug delivery. Eur. J. Pharm. Biopharm. 98, 76–89. https://doi.org/10.1016/j.ejpb.2015.11.003

Newsholme, P., Brennan, L., Bender, K., 2006. Amino acid metabolism, β-cell function, and diabetes. Diabetes 55, S39–S47. https://doi.org/10.2337/db06-S006

Nikolaidis, L.A., Elahi, D., Hentosz, T., Doverspike, A., Huerbin, R., Zourelias, L., Stolarski, C., Shen, Y.T., Shannon, R.P., 2004. Recombinant glucagon-like peptide-1 increases myocardial glucose uptake and improves left ventricular performance in conscious dogs with pacing-induced dilated cardiomyopathy. Circulation 110, 955–961. https://doi.org/10.1161/01.CIR.0000139339.85840.DD

Oleinik, V.M., 1995. Distribution of digestive enzyme activities along intestine in blue fox, mink, ferret and rat. Comp. Biochem. Physiol. -- Part A Physiol. 112, 55–58. https://doi.org/10.1016/0300-9629(95)00090-T

Pais, R., Gribble, F.M., Reimann, F., 2016a. Stimulation of incretin secreting cells. Ther. Adv. Endocrinol. Metab. https://doi.org/10.1177/2042018815618177

Pais, R., Gribble, F.M., Reimann, F., 2016b. Signalling pathways involved in the detection of peptones by murine small intestinal enteroendocrine L-cells. Peptides 77, 9–15. https://doi.org/10.1016/j.peptides.2015.07.019

Pangua, C., Reboredo, C., Campión, R., Gracia, J.M., Martínez-López, A.L., Irache, J.M., 2021. Mucus-penetrating nanocarriers, in: Theory and Applications of Nonparenteral Nanomedicines. Elsevier, pp. 137–152. https://doi.org/10.1016/b978-0-12-820466-5.00007-7

Penalva, R., González-Navarro, C.J., Gamazo, C., Esparza, I., Irache, J.M., 2017. Zein nanoparticles for oral delivery of quercetin: Pharmacokinetic studies and preventive anti-inflammatory effects in a mouse model of endotoxemia. Nanomedicine Nanotechnology, Biol. Med. 13, 103–110. https://doi.org/10.1016/j.nano.2016.08.033

Pierce, S.B., Costa, M., Wisotzkey, R., Devadhar, S., Homburger, S.A., Buchman, A.R., Ferguson, K.C., Heller, J., Platt, D.M., Pasquinelli, A.A., Liu, L.X., Doberstein, S.K., Ruvkun, G., 2001. Regulation of DAF-2 receptor signaling by human insulin and ins-1, a member of the unusually large and diverse C. elegans insulin gene family. Genes Dev. 15, 672–686. https://doi.org/10.1101/gad.867301

Pisters, P.W.T., Restifo, N.P., Cersosimo, E., Brennan, M.F., 1991. The effects of euglycemic hyperinsulinemia and amino acid infusion on regional and whole body glucose disposal in man. Metabolism 40, 59–65. https://doi.org/10.1016/0026-0495(91)90193-Z

Ponchel, G., Irache, J.M., 1998. Specific and non-specific bioadhesive particulate systems for oral delivery to the gastrointestinal tract. Adv. Drug Deliv. Rev. https://doi.org/10.1016/S0169-409X(98)00040-4

Popov, A., 2020. Mucus-Penetrating Particles and the Role of Ocular Mucus as a Barrier to Micro- And Nanosuspensions. J. Ocul. Pharmacol. Ther. 36, 366–375. https://doi.org/10.1089/jop.2020.0022

Popov, A., Enlow, E., Bourassa, J., Chen, H., 2016a. Mucus-penetrating nanoparticles made with “mucoadhesive” poly(vinyl alcohol). Nanomedicine Nanotechnology, Biol. Med. 12, 1863–1871. https://doi.org/10.1016/j.nano.2016.04.006

Popov, A., Schopf, L., Bourassa, J., Chen, H., 2016b. Enhanced pulmonary delivery of fluticasone propionate in rodents by mucus-penetrating nanoparticles. Int. J. Pharm. 502, 188–197. https://doi.org/10.1016/j.ijpharm.2016.02.031

Porfiryeva, N.N., Semina, I.I., Salakhov, I.A., Moustafine, R.I., Khutoryanskiy, V. V., 2021. Mucoadhesive and mucus-penetrating interpolyelectrolyte complexes for nose-to-brain drug delivery. Nanomedicine Nanotechnology, Biol. Med. 37, 102432. https://doi.org/10.1016/j.nano.2021.102432

Rastogi, V.K., Samyn, P., 2015. Bio-based coatings for paper applications. Coatings 5, 887–930. https://doi.org/10.3390/coatings5040887

Reboredo, C., González-Navarro, C.J., Martínez-Oharriz, C., Martínez-López, A.L., Irache, J.M., 2021. Preparation and evaluation of PEG-coated zein nanoparticles for oral

drug delivery purposes. Int. J. Pharm. 597, 120287. https://doi.org/10.1016/j.ijpharm.2021.120287

Röhrborn, D., Wronkowitz, N., Eckel, J., 2015. DPP4 in diabetes. Front. Immunol. 6, 386. https://doi.org/10.3389/fimmu.2015.00386

Rohrer, J., Partenhauser, A., Hauptstein, S., Gallati, C.M., Matuszczak, B., Abdulkarim, M., Gumbleton, M., Bernkop-Schnürch, A., 2016. Mucus permeating thiolated self-emulsifying drug delivery systems. Eur. J. Pharm. Biopharm. 98, 90–97. https://doi.org/10.1016/j.ejpb.2015.11.004

Rorbach-Dolata, A., Piwowar, A., 2019. Neurometabolic Evidence Supporting the Hypothesis of Increased Incidence of Type 3 Diabetes Mellitus in the 21st Century. Biomed Res. Int. https://doi.org/10.1155/2019/1435276

Rosentrater, K.A., Evers, A.D., 2018. Chemical components and nutrition. Kent's Technol. Cereal. 267–368. https://doi.org/10.1016/b978-0-08-100529-3.00004-9

Rowlands, J., Heng, J., Newsholme, P., Carlessi, R., 2018. Pleiotropic Effects of GLP-1 and Analogs on Cell Signaling, Metabolism, and Function. Front. Endocrinol. (Lausanne). 9, 672. https://doi.org/10.3389/fendo.2018.00672

Ruiz, A., Salas, G., Calero, M., Hernández, Y., Villanueva, A., Herranz, F., Veintemillas-Verdaguer, S., Martínez, E., Barber, D.F., Morales, M.P., 2013. Short-chain PEG molecules strongly bound to magnetic nanoparticle for MRI long circulating agents. Acta Biomater. 9, 6421–6430. https://doi.org/10.1016/j.actbio.2012.12.032

Salameh, T.S., Bullock, K.M., Hujoel, I.A., Niehoff, M.L., Wolden-Hanson, T., Kim, J., Morley, J.E., Farr, S.A., Banks, W.A., 2015. Central Nervous System Delivery of Intranasal Insulin: Mechanisms of Uptake and Effects on Cognition. J. Alzheimer's Dis. 47, 715–728. https://doi.org/10.3233/JAD-150307

Sallam, M.A., Elzoghby, A.O., 2018. Flutamide-Loaded Zein Nanocapsule Hydrogel, a Promising Dermal Delivery System for Pilosebaceous Unit Disorders. AAPS PharmSciTech 19, 2370–2382. https://doi.org/10.1208/s12249-018-1087-z

Seino, Y., Fukushima, M., Yabe, D., 2010. GIP and GLP-1, the two incretin hormones: Similarities and differences. J. Diabetes Investig. https://doi.org/10.1111/j.2040-1124.2010.00022.x

Serra, L., Doménech, J., Peppas, N.A., 2009. Engineering design and molecular dynamics of mucoadhesive drug delivery systems as targeting agents. Eur. J. Pharm. Biopharm. 71, 519–528. https://doi.org/10.1016/j.ejpb.2008.09.022

Shakweh, M., Ponchel, G., Fattal, E., 2004. Particle uptake by Peyer's patches: A pathway for drug and vaccine delivery. Expert Opin. Drug Deliv. 1, 141–163. https://doi.org/10.1517/17425247.1.1.141

Shete, H.K., Prabhu, R.H., Patravale, V.B., 2014. Endosomal escape: A bottleneck in intracellular delivery. J. Nanosci. Nanotechnol. 14, 460–474. https://doi.org/10.1166/jnn.2014.9082

Shukla, R., Cheryan, M., 2001. Zein: The industrial protein from corn. Ind. Crops Prod.

13, 171–192. https://doi.org/10.1016/S0926-6690(00)00064-9

Soria Lopez, J.A., González, H.M., Léger, G.C., 2019. Alzheimer's disease, in: Handbook of Clinical Neurology. Elsevier B.V., pp. 231–255. https://doi.org/10.1016/B978-0-12-804766-8.00013-3

Sun, S., Liang, N., Kawashima, Y., Xia, D., Cui, F., 2011. Hydrophobic ion pairing of an insulin-sodium deoxycholate complex for oral delivery of insulin. Int. J. Nanomedicine 6, 3049–3056. https://doi.org/10.2147/ijn.s26450

Tan, S.Y., Mei Wong, J.L., Sim, Y.J., Wong, S.S., Mohamed Elhassan, S.A., Tan, S.H., Ling Lim, G.P., Rong Tay, N.W., Annan, N.C., Bhattamisra, S.K., Candasamy, M., 2019. Type 1 and 2 diabetes mellitus: A review on current treatment approach and gene therapy as potential intervention. Diabetes Metab. Syndr. Clin. Res. Rev. 13, 364–372. https://doi.org/10.1016/j.dsx.2018.10.008

Tang, X., He, Z., Dai, Y., Xiong, Y.L., Xie, M., Chen, J., 2010. Peptide fractionation and free radical scavenging activity of zein hydrolysate. J. Agric. Food Chem. 58, 587–593. https://doi.org/10.1021/jf9028656

Tobío, M., Sánchez, A., Vila, A., Soriano, I., Evora, C., Vila-Jato, J.L., Alonso, M.J., 2000. The role of PEG on the stability in digestive fluids and in vivo fate of PEG-PLA nanoparticles following oral administration. Colloids Surfaces B Biointerfaces 18, 315. https://doi.org/10.1016/s0927-7765(99)00157-5

Valerio, A., D'Antona, G., Nisoli, E., 2011. Branched-chain amino acids, mitochondrial biogenesis, and healthspan: An evolutionary perspective. Aging (Albany. NY). 3, 464–478. https://doi.org/10.18632/aging.100322

Vandal, M., White, P.J., Tremblay, C., St-Amour, I., Chevrier, G., Emond, V., Lefrançois, D., Virgili, J., Planel, E., Giguere, Y., Marette, A., Calon, F., 2014. Insulin reverses the high-fat diet-induced increase in brain Aβ and improves memory in an animal model of Alzheimer disease. Diabetes 63, 4291–4301. https://doi.org/10.2337/db14-0375

Varkouhi, A.K., Scholte, M., Storm, G., Haisma, H.J., 2011. Endosomal escape pathways for delivery of biologicals. J. Control. Release 151, 220–228. https://doi.org/10.1016/j.jconrel.2010.11.004

Vieira, A.C.C., Chaves, L.L., Pinheiro, S., Pinto, S., Pinheiro, M., Lima, S.C., Ferreira, D., Sarmento, B., Reis, S., 2018. Mucoadhesive chitosan-coated solid lipid nanoparticles for better management of tuberculosis. Int. J. Pharm. 536, 478–485. https://doi.org/10.1016/j.ijpharm.2017.11.071

Vilsbøll, T., Holst, J.J., 2004. Incretins, insulin secretion and Type 2 diabetes mellitus. Diabetologia 47, 357–366. https://doi.org/10.1007/s00125-004-1342-6

Volpe, C.M.O., Villar-Delfino, P.H., Dos Anjos, P.M.F., Nogueira-Machado, J.A., 2018. Cellular death, reactive oxygen species (ROS) and diabetic complications review-Article. Cell Death Dis. 9, 1–9. https://doi.org/10.1038/s41419-017-0135-z

Wang, K., Chen, S., Zhang, C., Huang, J., Wu, J., Zhou, H., Jin, L., Qian, X., Jin, J., Lyu, J., 2018. Enhanced ROS production leads to excessive fat accumulation through DAF-

16 in Caenorhabditis elegans. Exp. Gerontol. 112, 20–29. https://doi.org/10.1016/j.exger.2018.07.017

Wilcox, M.D., Van Rooij, L.K., Chater, P.I., Pereira De Sousa, I., Pearson, J.P., 2015. The effect of nanoparticle permeation on the bulk rheological properties of mucus from the small intestine. Eur. J. Pharm. Biopharm. 96, 484–487. https://doi.org/10.1016/j.ejpb.2015.02.029

Wu, S., Bin, W., Tu, B., Li, X., Wang, W., Liao, S., Sun, C., 2019. A Delivery System for Oral Administration of Proteins/Peptides Through Bile Acid Transport Channels. J. Pharm. Sci. 108, 2143–2152. https://doi.org/10.1016/j.xphs.2019.01.027

Wu, T., Rayner, C.K., Horowitz, M., 2015. Incretins. Handb. Exp. Pharmacol. 233, 137–171. https://doi.org/10.1007/164_2015_9

Xu, B., Jiang, G., Yu, W., Liu, D., Liu, Y., Kong, X., Yao, J., 2017. Preparation of poly(lactic-co-glycolic acid) and chitosan composite nanocarriers via electrostatic self assembly for oral delivery of insulin. Mater. Sci. Eng. C 78, 420–428. https://doi.org/10.1016/j.msec.2017.04.113

Yamazoe, E., Fang, J.Y., Tahara, K., 2021. Oral mucus-penetrating PEGylated liposomes to improve drug absorption: Differences in the interaction mechanisms of a mucoadhesive liposome. Int. J. Pharm. 593, 120148. https://doi.org/10.1016/j.ijpharm.2020.120148

Yan, F., Chen, X., Zheng, X., 2017. Protective effect of mulberry fruit anthocyanin on human hepatocyte cells (LO2) and Caenorhabditis elegans under hyperglycemic conditions. Food Res. Int. 102, 213–224. https://doi.org/10.1016/j.foodres.2017.10.009

Yan, J., Nie, Y., Cao, J., Luo, M., Yan, M., Chen, Z., He, B., 2021. The Roles and Pharmacological Effects of FGF21 in Preventing Aging-Associated Metabolic Diseases. Front. Cardiovasc. Med. 8. https://doi.org/10.3389/fcvm.2021.655575

Yang, J., Chi, Y., Burkhardt, B.R., Guan, Y., Wolf, B.A., 2010. Leucine metabolism in regulation of insulin secretion from pancreatic beta cells. Nutr. Rev. 68, 270–279. https://doi.org/10.1111/j.1753-4887.2010.00282.x

Yoncheva, K., Guembe, L., Campanero, M.A., Irache, J.M., 2007. Evaluation of bioadhesive potential and intestinal transport of pegylated poly(anhydride) nanoparticles. Int. J. Pharm. 334, 156–165. https://doi.org/10.1016/j.ijpharm.2006.10.016

Yu, C.C., Barry, N.C., Wassie, A.T., Sinha, A., Bhattacharya, A., Asano, S., Zhang, C., Chen, F., Hobert, O., Goodman, M.B., Haspel, G., Boyden, E.S., 2020. Expansion microscopy of c. Elegans. Elife 9, 1–78. https://doi.org/10.7554/eLife.46249

Zhang, Qianyu, He, N., Zhang, L., Zhu, F., Chen, Q., Qin, Y., Zhang, Z., Zhang, Qiang, Wang, S., He, Q., 2012. The in vitro and in vivo study on Self-Nanoemulsifying Drug Delivery System (SNEDDS) based on insulin-phospholipid complex. J. Biomed. Nanotechnol. 8, 90–97. https://doi.org/10.1166/jbn.2012.1371

Zhang, X., Gao, M., Zhang, Y., Dong, C., Xu, M., Hu, Y., Luan, G., 2022. Effect of plasticizer

and zein subunit on rheology and texture of zein network. Food Hydrocoll. 123, 107140. https://doi.org/10.1016/j.foodhyd.2021.107140

Zhang, Z., Yang, J., Liu, C., Xie, J., Qiu, S., Yang, X., Wu, C., 2019. Pseudoginsenoside-F11 alleviates cognitive deficits and Alzheimer's disease-type pathologies in SAMP8 mice. Pharmacol. Res. 139, 512–523. https://doi.org/10.1016/j.phrs.2018.10.024

Zheng, S., Chiu, H., Boudreau, J., Papanicolaou, T., Bendena, W., Chin-Sang, I., 2019. A functional study of all 40 Caenorhabditis elegans insulin-like peptides. J. Biol. Chem. 293, 16912–16922. https://doi.org/10.1074/jbc.RA118.004542

Zhou, S., Deng, H., Zhang, Y., Wu, P., He, B., Dai, W., Zhang, H., Zhang, Q., Zhao, R., Wang, X., 2020. Thiolated Nanoparticles Overcome the Mucus Barrier and Epithelial Barrier for Oral Delivery of Insulin. Mol. Pharm. 17, 239–250. https://doi.org/10.1021/acs.molpharmaceut.9b00971

Chapter 8

Conclusions

8. Conclusions

1. The coating of zein nanoparticles with poly(ethylene glycol) 35,000 can be carried out by incubating the excipient with the just formed nanoparticles in an aqueous environment, prior to the purification and drying in a spray-drier. The PEG layer confers a hydrophilic corona that significantly improve the capability of zein nanoparticles to diffuse in pig intestinal mucus. In vivo, PEG-coated nanoparticles (prepared at a PEG-to-zein ratio of 0.5) displayed mucus-permeating properties and moved rapidly along the gut, reaching the cecum two hours post-administration.

2. Zein-based nanoparticles, orally administered to healthy rats, induced a hypoglycemic response and improved the glycemic control against an ipGTT. These responses would be mediated by the ability of zein nanoparticles to induce the secretion of GLP-1. This effect was higher for PEG-coated than for bare nanoparticles, probably due to their mucus-permeating properties and their capability to reach rapidly distal areas of the ileum, where L cells are primarily found.

3. In a mouse model of accelerated senescence (SAMP8), the oral administration of zein-based nanoparticles at the age of 7 months did not induce any beneficial effect on the learning impairment and memory disorders of this model, similar to those observed in AD, probably due to the already-developed state of the pathology when the treatment started.

4. Supplementation of the glucose-enriched growth medium of *C. elegans* with either NP or NP-PEG50 reduced the fat accumulation and increased the lifespan of the worms (more than 50%), without differences between bare and PEG-coated nanoparticles. Nevertheless, the addition of a solution of PEG to the culture medium did not affect the lifespan of the worms.

5. SAMP8 mice receiving orally bare zein nanoparticles every two days from 7 months of age, displayed a median life expectancy significantly higher than control animals (about 30%). This increased lifespan was not found in animals treated with PEG-coated nanoparticles, probably due to the reduced intestinal retention caused by their increased movement within the gut combined with increased peristaltic reflexes caused by PEG.

6. Zein nanoparticles can be loaded with insulin, achieving an insulin payload of around 80 µg per mg nanoparticles. The encapsulation of the hormone did not alter the capability of the resulting nanoparticles to be coated with PEG.

7. Supplementation of the glucose-enriched growth medium of *C. elegans* with insulin-loaded nanoparticles significantly decreased the fat accumulation in the nematodes. This effect was significantly higher for insulin loaded in PEG-coated nanoparticles than

for bare ones. The reduction in the accumulation of fat in worms treated with I-NP-PEG50 was similar to that provided by the positive control (Orlistat®).

8. In diabetic rats, insulin-loaded nanoparticles enhanced intestinal absorption of insulin when orally administered. Both formulations showed a hypoglycemic effect that lasted for at least 6 hours. Moreover, the increased mucus-diffusivity of PEG-coated nanoparticles increased the main pharmacological and pharmacokinetic parameters, leading to a 14.9% pharmacological activity (PA) and a 10.2% relative oral bioavailability (Fr) compared to a subcutaneous injection of the protein.